

Dissertation  
submitted to the  
Combined Faculty of Natural Sciences and Mathematics  
of the Ruperto Carola University Heidelberg, Germany  
for the degree of  
Doctor of Natural Sciences

Presented by

**Tiago Ferreira, M. Sc.**

Born in Leiria, Portugal

Oral examination: 22/07/2021



# **Characterisation of Oncolytic H-1 Parvovirus Cell Entry Pathways**

Referees:

Prof. Dr. Ralf Bartenschlager

Priv. Doz. Dr. Antonio Marchini

The present dissertation was conducted in the lab of Priv. Doz. Dr. Antonio Marchini - the Laboratory of Oncolytic Virus Immuno-Therapeutics (LOVIT) between September 2017 and April 2021. The scholarship was awarded by the International PhD Program of the German Cancer Research Centre (DKFZ) in Heidelberg, Germany.

Under the guidance of my supervisor Priv. Doz. Dr. Antonio Marchini, I designed and performed all experiments, quantification and analysis, of all data presented in this thesis, except stated otherwise.



## Acknowledgements

I would like to thank everyone who contributed in some way to the work described in this dissertation. First of all, I would like to show my gratitude to my supervisor, Dr. Antonio Marchini, for all of his support and guidance throughout my time in his laboratory and for allowing me to grow as a scientist. Thank you for giving your very best at all times, in particular in the preparation of our manuscripts and this thesis. I would also like to thank my TAC committee, Prof. Dr. Ralf Bartenschlager, Dr. Francesca Ciccolini, and Dr. Richard Harbottle for their helpful feedback and constructive criticism over the course of the thesis. Furthermore, I am grateful for the financial support provided by the DKFZ International PhD Program.

I want to show my great appreciation for the assistance and helpful discussions Dr. Clemens Bretscher provided me throughout the time he was in the group. The same goes for Dr. Amit Kulkarni – thanks for the helpful feedback, guidance and contributions that made this work undoubtedly richer. I would like to extend my gratitude to Dr. Gian Mario for helping me kick start my Ph.D., and Dr. Valérie Palissot for collaborative work and organising the annual get-together between Germany and Luxembourg. I greatly thank Tiina Martilla and Annabel Grewenig for their great companionship and precious help in the laboratory. You made the time in the lab easier and more fun! I would also like to express my warm thanks to my fellow PhD students Gayatri Kavishwar, Anna Hartley and Ilaria Salvato for the unconditional support and unforgettable moments that we shared – you are very special! Likewise, Akash Ramakrishnan, my very first master student, I enjoyed and learned a lot from and with you.

I would also like to show my gratitude to the Parvovirus division, particularly to Dr. Jean Rommelaere for the great inspiration and Dr. Assia Angelova for collaborative work. And equally important to the fun leisure time that we all got to spend together. I also thank Barbara Leuchs for providing me with H-1PV capsid antibody as well as to Dr. Jürg Nüesch for his supervision on my IIC Journal Club.

At the DKFZ Electron Microscopy core facility, I would like to thank Dr. Karsten Richter and Dr. Michelle Neßling for their substantial help with the electron microscopy work which considerably enriched this thesis. I also show my appreciation to the collaborators in the University of Bergen, Norway, namely Dr. Jubayer Hossain

and the group leader Dr. Hrvoje Miletic who contributed with the screening of glioblastoma biopsies. Likewise, gratitude to Dr. Francisco Azuaje who performed the bioinformatic analysis.

Last but not least, I will be ever grateful to my family for supporting me emotionally and financially to fulfil my dreams since day one – this thesis is also theirs. My deepest gratitude also to those who are so important in my life that are considered as an extension of my family. They made this achievement possible by simply accepting me in their lives exactly as I am.





## Abstract

H-1 protoparvovirus (H-1PV) is a self-propagating virus, non-pathogenic in humans, endowed with oncolytic and oncosuppressive activities. H-1PV is the only member of the *Parvoviridae* family to be tested as an anticancer agent in a clinical setting. Results from clinical trials in patients with glioblastoma or pancreatic carcinoma showed that virus treatment is safe and well-tolerated. Virus treatment was associated with first signs of efficacy, including immune conversion of tumour microenvironment, good virus distribution in the tumour bed, as well as improved patient overall survival compared with historical controls. However, monotherapeutic use of the virus was not sufficient to eradicate the tumours. In this manner, my approach consists of further understanding the virus life cycle in order to improve H-1PV-based anticancer therapies. This knowledge can provide hints on which drugs or treatment modalities could be combined with the virus in order to enhance its oncotoxicity. In addition, a deeper understanding of H-1PV life cycle can help to identify biomarkers capable of predicting which patients would most likely benefit from virus treatment. To achieve this goal, previous members of the laboratory performed a druggable genome-wide siRNA library screening to identify putative modulators of H-1PV infection. Focusing on cellular factors potentially involved at the early steps of H-1PV infection, three top activators were identified: *LAMC1*, *LGALS1* and *AP2M1*. (i) Laminin containing the  $\gamma 1$  chain, encoded by *LAMC1*, had previously been demonstrated to play a pivotal role at the level of binding and entry into cancer cells. Building on these results, I provide direct evidence that H-1PV binds to laminins through the sialic acid moieties present in these molecules. (ii) Galectin-1, encoded by *LGALS1*, is here shown to interact directly with H-1PV at the cell surface and promote the efficient virus internalisation into cancer cells. Knock-down/out of *LGALS1* strongly decreases the ability of H-1PV to infect and kill cancer cells. These properties are rescued by the re-introduction of *LGALS1* into cancer cells. The *in silico* analysis reveals that *LGALS1* is overexpressed in glioblastoma and pancreatic carcinoma. In collaboration with Dr. Miletic (University of Bergen, Norway), we also show by immunohistochemistry analysis on 122 glioblastoma biopsies that galectin-1 protein levels vary across the different tumours with higher levels detected in glioblastoma than normal tissues, and higher in recurrent in comparison with primary glioblastoma tumours. We also found a direct correlation between *LGALS1* transcript levels and H-1PV oncolytic activity in 59 cancer cell lines from different tumour origins. Together these results suggest that tumours with higher galectin-1 content may be a more suitable target for H-1PV. Strikingly, the addition of purified galectin-1 sensitises poorly susceptible glioma cell lines to H-1PV killing activity by rescuing virus cell entry. (iii) AP2 $\mu$ 1, encoded by *AP2M1*, is a subunit from the adaptor 2, a key regulator of clathrin-mediated endocytosis. Indeed, siRNA-mediated knockdown of *AP2M1* or chemical inhibition of clathrin-mediated endocytosis strongly decreased H-1PV entry. Using electron and confocal microscopy, H-1PV particles were detected within clathrin-coated pits and vesicles, further corroborating that H-1PV uses clathrin-mediated endocytosis for cell

entry. In contrast, I observed no evidence of viral entry through caveolae-mediated endocytosis. I also show that H-1PV internalisation depends on dynamin activity, and that viral trafficking occurs from early to late endosomes, with low endosomal pH required for a successful infection. Based on the body of evidence gathered during this dissertation, I propose a model where H-1PV binds to the sialic acid present in laminins containing  $\gamma 1$  chains, and then galectin-1 promotes the efficient internalisation of virus particles through clathrin-mediated endocytosis. For the first time, this dissertation describes the cell entry pathways of oncolytic H-1PV.

## Zusammenfassung

Das H-1-Protoparvovirus (H-1PV) ist ein sich selbst vermehrendes Virus, das für den Menschen nicht pathogen ist und über onkolytische und onkosuppressive Aktivitäten verfügt. H-1PV ist das einzige Mitglied der Familie *Parvoviridae*, das in einem klinischen Umfeld als Antikrebsmittel getestet wurde. Ergebnisse aus klinischen Studien bei Patienten mit Glioblastom oder Pankreaskarzinom zeigten, dass die Virusbehandlung sicher und gut verträglich ist. Die Virusbehandlung zeigte erste Anzeichen einer Wirksamkeit, einschließlich einer Immunumwandlung der Tumormikroumgebung, einer guten Virusverteilung im Tumorbett sowie einer Verbesserung der Gesamtüberlebenszeit der Patienten im Vergleich zu historischen Kontrollen. Die alleinige Anwendung des Virus als Therapie reichte jedoch nicht aus, um die Tumore zu eliminieren. Dahingehend möchte ich versuchen, den Lebenszyklus des Virus besser zu verstehen, um die auf H-1PV-basierenden Krebstherapien zu verbessern. Dieses Wissen kann Hinweise darauf geben, welche Medikamente oder Behandlungsmodalitäten mit dem Virus kombiniert werden können, um dessen Onkotoxizität zu erhöhen. Darüber hinaus kann ein tieferes Verständnis des H-1PV-Lebenszyklus dazu beitragen, Biomarker zu identifizieren, die vorhersagen können, welche Patienten am wahrscheinlichsten von einer Virusbehandlung profitieren würden. Um dieses Ziel zu erreichen, hatten ehemalige Mitglieder des Labors ein medikamentöses genomweites Screening einer siRNA-Bibliothek durchgeführt, um mutmaßliche Modulatoren der H-1PV-Infektion zu identifizieren. Mit einem Schwerpunkt auf zelluläre Faktoren, die möglicherweise an der frühen Phase der H-1PV-Infektion beteiligt sind, wurden drei Top-Aktivatoren identifiziert: *LAMC1*, *LGALS1* und *AP2M1*. (i) Es wurde zuvor gezeigt, dass Laminin, das eine  $\gamma 1$ -Kette enthält (codiert durch *LAMC1*), eine entscheidende Rolle beim Andocken und Eintreten des Virus an und in die Krebszellen spielt. Aufbauend auf diesen Ergebnissen zeige ich, dass H-1PV über Sialinsäuren, die in diesen Molekülen vorhanden sind, an Laminine bindet. (ii) Es wird hier gezeigt, dass Galectin-1, das von *LGALS1* codiert wird, direkt mit H-1PV an der Zelloberfläche interagiert und die effiziente Virusinternalisierung in Krebszellen unterstützt. Durch den Knockout/Knockdown von *LGALS1* wird die Fähigkeit von H-1PV, Krebszellen zu infizieren und abzutöten, stark verringert. Diese Eigenschaften werden durch die Wiedereinführung von *LGALS1* in Krebszellen wiederhergestellt. Eine *in silico* Analyse zeigt, dass *LGALS1* beim Glioblastom und Bauchspeicheldrüsenkarzinom überexprimiert wird. Zudem zeigen wir in Zusammenarbeit mit Dr. Miletic (Universität Bergen, Norwegen) durch immunhistochemische Analyse von 122 Glioblastom-Biopsien, dass die Proteinspiegel von Galectin-1 in den verschiedenen Tumoren variieren, wobei im Glioblastom ein höherer Gehalt an Galectin-1 als in normalen Geweben nachgewiesen wurde und die Expression von Galectin-1 in rezidivierenden Tumoren höher im Vergleich zu primären Glioblastomtumoren ist. Wir fanden auch eine direkte Korrelation zwischen den *LGALS1*-Transkriptmengen und der onkolytischen Aktivität von H-1PV in 59 Krebszelllinien unterschiedlicher Tumorherkunft. Zusammengefasst legen diese Ergebnisse nahe, dass Tumore mit einem höheren Gehalt an Galectin-1 ein geeigneteres Ziel für H-1PV sein könnten. Bemerkenswerterweise sensibilisiert die Zugabe von gereinigtem Galectin-1 schlecht-anfällige Gliomzelllinien für die abtötende Wirkung von H-1PV, indem der

Eintritt des Virus in den Zellen wiederhergestellt wird. *(iii)* AP2 $\mu$ 1, codiert von *AP2M1*, ist eine Untereinheit aus dem Adapter 2, einem zentralen Regulator der clathrinabhängigen Endozytose. In der Tat verringerte der siRNA Knockdown von *AP2M1* oder die chemische Hemmung der clathrinabhängigen Endozytose den Eintritt von H-1PV in die Zellen stark. Anhand von Elektronenmikroskopie und konfokaler Mikroskopie wurden H-1PV-Partikel in Clathrin-beschichteten Membranvertiefungen und Vesikeln nachgewiesen, wodurch weiter bestätigt wurde, dass H-1PV die clathrinabhängige Endozytose für den Zelleintritt verwendet. Im Gegensatz dazu beobachtete ich keine Hinweise auf einen Viruseintritt durch Caveolae-vermittelte Endozytose. Außerdem zeige ich, dass die Internalisierung von H-1PV von der Aktivität von Dynamin abhängt und dass der Virustransport von den frühen bis zu den späten Endosomen stattfindet, wobei für eine erfolgreiche Infektion ein niedriger endosomaler pH-Wert erforderlich ist. Basierend auf den hier gesammelten Beweisen schlage ich ein Modell vor, bei dem H-1PV an die Sialinsäure der  $\gamma$ 1-Ketten von Lamininen bindet und Galectin-1 die effiziente Internalisierung von Viruspartikeln durch clathrinabhängige Endozytose fördert. Zum ersten Mal beschreibt diese Dissertation die Zelleintrittswege von onkolytischem H-1PV.

# Table of contents

<b>Acknowledgements</b> .....	<b>vi</b>
<b>Abstract</b> .....	<b>ix</b>
<b>Zusammenfassung</b> .....	<b>xi</b>
<b>Table of contents</b> .....	<b>xiii</b>
<b>List of Figures</b> .....	<b>xvi</b>
<b>List of Abbreviations</b> .....	<b>xix</b>
<b>1 Chapter 1: General Introduction</b> .....	<b>1</b>
1.1 Oncolytic Virus, a Warrior Against Cancer .....	1
1.1.1 Emergence of oncolytic virotherapy .....	1
1.1.2 Mechanisms behind viral oncotropism .....	4
1.1.3 Features required for an ideal oncolytic virus.....	9
1.2 <i>Parvoviridae</i> , a Family Filled with Diversity .....	12
1.2.1 Taxonomy .....	12
1.2.2 Parvoviral proteins .....	14
1.2.3 Early steps of infection .....	16
1.2.4 Replication and egress.....	19
1.3 H-1PV, Bench to Bedside and Back Again.....	22
1.3.1 Determinants of parvovirus infection.....	22
1.3.2 Parvovirus-induced cell death.....	25
1.3.3 Clinical evaluation of H-1PV treatment .....	29
1.3.4 Strategies to improve H-1PV anticancer activity .....	31
1.3.5 Combination therapy .....	32
1.3.6 Development of second-generation parvovirus vectors .....	33
1.3.7 Characterisation of H-1PV life cycle.....	34
1.4 Research objectives.....	38
<b>2 Chapter 2: Materials and Methods</b> .....	<b>39</b>
2.1 Cells .....	39
2.1.1 Cell culture .....	39
2.1.2 Generation of <i>LGALS1</i> knockout cell line.....	40
2.2 Viruses .....	40
2.2.1 Wild-type H-1PV .....	40
2.2.2 Recombinant H-1PV expressing EGFP .....	41
2.3 High-throughput siRNA library screening.....	41
2.4 Cell viability and proliferation assays.....	42
2.4.1 MTT viability assay .....	42
2.4.2 xCELLigence .....	43
2.5 Microscopy.....	44

2.5.1	Fluorescent Microscopy .....	44
2.5.2	Confocal microscopy .....	44
2.5.3	Electron microscopy.....	45
2.6	Enzyme-linked Immunosorbent Assay (ELISA) .....	45
2.7	siRNA-mediated knockdown .....	46
2.8	Western Blotting .....	47
2.9	Plasmid transfection.....	47
2.10	Binding/entry assays.....	48
2.11	Polymerase chain reaction (PCR) .....	48
2.11.1	Quantitative PCR (qPCR).....	48
2.11.2	Reverse transcriptase quantitative PCR (RT-qPCR) .....	49
2.12	Flow cytometry (FACS).....	50
2.13	Tissue Microarray .....	50
2.14	Determination of the H-1PV EC50 for the NCI-60 cell lines .....	50
2.15	Measurement of transcript levels .....	51
2.16	Treatment with inhibitors of endocytosis pathways .....	52
2.17	Transferrin uptake analysis.....	52
2.18	Statistical analysis.....	52

### **3 Chapter 3: Laminin- $\gamma$ 1 and Galectin-1 have a crucial role in H-1PV infection..... 53**

3.1	Previous results from the laboratory.....	53
3.1.1	Identification of putative modulators of the H-1PV life cycle by siRNA library screening.....	53
3.1.2	H-1PV uses laminin $\gamma$ 1 for its attachment at the cell surface.....	57
3.2	Galectin-1, but not galectin-3, knockdown hampers H-1PV infection	60
3.3	Galectin-1 knockout impairs H-1PV infection in NCH125 cells.....	62
3.4	Galectin-1 knockout decreases H-1PV oncolytic activity in NCH125 cells	64
3.5	H-1PV uptake, but not cell surface attachment, is reduced in NCH125 LGALS1 KO cells.....	65
3.6	Both laminin $\gamma$ 1 and galectin-1 participate in virus binding/entry....	67
3.7	H-1PV binds directly to galectin-1 .....	68
3.8	Galectin-1 is a marker of bad prognosis in various tumour types including glioblastoma .....	69
3.9	<i>LGALS1</i> expression profile of NCI-60 cells positively correlates with H-1PV oncotoxicity.....	73

3.10	<i>LGALS1</i> expression positively correlates with H-1PV oncolysis in glioma cell lines.....	76
<b>4</b>	<b>Chapter 4: H-1PV enters cancer cells through clathrin-mediated endocytosis.....</b>	<b>79</b>
4.1	Electron microscopy shows H-1PV associated with clathrin-coated pits	79
4.2	H-1PV co-localises with clathrin upon entry.....	80
4.3	H-1PV enters cells preferentially <i>via</i> clathrin-mediated endocytosis	81
4.4	H-1PV does not enter cells <i>via</i> caveolae-dependent endocytosis....	86
4.5	H-1PV internalisation is dependent on dynamin.....	88
4.6	H-1PV hijacks endosomes during intracellular trafficking.....	89
4.7	Low endosomal pH is required for a productive H-1PV infection ...	91
<b>5</b>	<b>Chapter 5: General discussion.....</b>	<b>93</b>
5.1	H-1PV in the race against cancer.....	93
5.2	Laminin- $\gamma$ 1 and Galectin-1 proteins have a crucial role in H-1PV infection .....	96
5.3	H-1PV enters cancer cells through clathrin-mediated endocytosis	100
5.4	Model of H-1PV entry and infection .....	103
<b>6</b>	<b>Chapter 6: Future Perspectives and Concluding Remarks.....</b>	<b>105</b>
6.1	Early steps of H-1PV infection .....	105
6.1.1	What is the H-1PV receptor(s)? .....	105
6.1.2	Is Gal-1 and H-1PV endocytosis linked?.....	106
6.1.3	Can Gal-1 (and laminin $\gamma$ 1) role be validated <i>in vivo</i> ? .....	106
6.1.4	Are there other galectins involved in H-1PV infection? .....	108
6.1.5	Is caveolin-1 a negative modulator of H-1PV infection? .....	108
6.2	General aspects to be considered in the virotherapy field.....	109
6.3	Concluding remarks.....	111
	<b>Bibliography.....</b>	<b>112</b>
	<b>Appendix.....</b>	<b>140</b>

# List of Figures

## Chapter 1

Figure 1.1. Overview of oncolytic virotherapy in the clinical setting. ....	3
Figure 1.2. Oncolytic viruses target receptors aberrantly expressed in cancer cells.....	5
Figure 1.3. Oncolytic viruses target aberrant cellular signalling pathways. ....	6
Figure 1.4. Oncolytic viruses take advantage of cancer immune evasion pathways. ....	8
Figure 1.5. <i>Parvoviridae</i> family.....	13
Figure 1.6. Protoparvovirus genome.....	16
Figure 1.7. Different endocytic pathways taken by parvoviruses. ....	18
Figure 1.8. Protoparvovirus life cycle, from cellular binding to reaching the nucleus.....	21
Figure 1.9. Cell disturbances induced upon parvovirus infection.....	24
Figure 1.10. Current status of protoparvovirus-based studies in various models.....	26
Figure 1.11. Oncolytic parvovirus-induced (immunogenic) cell death. ....	28
Figure 1.12. Strategies to improve H-1PV anticancer efficacy.....	32
Figure 1.13. Galectin-1, Galectin-3 and Galectin-9 effect on viral infections..	37

## Chapter 3

Figure 3.1. siRNA library screening reveals factors putatively involved in H-1PV life cycle.....	55
Figure 3.2. Distribution of activators of H-1PV life cycle.....	57
Figure 3.3. H-1PV binds directly to laminins <i>via</i> sialic acid likely within the heparin-binding site(s). ....	59



Figure 3.4. H-1PV transduction is reduced in <i>LGALS1</i> , but not <i>LGALS3</i> , knockdown cell lines. ....	61
Figure 3.5. Cell proliferation of NCH125 Control <i>versus</i> NCH125 <i>LGALS1</i> KO. ....	62
Figure 3.6. H-1PV infectivity is reduced in NCH125 <i>LGALS1</i> KO cells. ....	63
Figure 3.7. H-1PV has a reduced oncolytic activity in NCH125 <i>LGALS1</i> KO cells which is rescued by supplementing recombinant Gal-1 protein. ....	64
Figure 3.8. H-1PV cellular uptake, but not cell surface binding, is reduced in NCH125 <i>LGALS1</i> KO cells. ....	66
Figure 3.9. Effect of <i>LAMC1</i> knockdown in NCH125 <i>LGALS1</i> KO cells on H-1PV entry. ....	67
Figure 3.10. H-1PV binds directly to galectin-1. ....	68
Figure 3.11. <i>LGALS1</i> is overexpression in high-grade glioma. ....	69
Figure 3.12. Higher levels of <i>LGALS1</i> are associated with poor prognosis in glioma. ....	70
Figure 3.13. Differential expression of galectin-1 in normal tissues, primary and recurrent GBM biopsies. ....	72
Figure 3.14. NCI-60 cancer cell lines susceptibility to H-1PV oncolytic activity. ....	74
Figure 3.15. Correlation between H-1PV oncolytic activity and <i>LGALS1</i> gene expression of cancer cell lines. ....	75
Figure 3.16. Galectin-1 levels in glioma cell lines determine the success of H-1PV infection. ....	77

## Chapter 4

Figure 4.1. H-1PV is internalised <i>via</i> clathrin-mediated endocytosis. ....	80
Figure 4.2. Co-localisation of H-1PV and clathrin upon virus entry. ....	81
Figure 4.3. Pharmacological inhibitors do not hinder cellular proliferation. .	82

Figure 4.4. Blocking clathrin-mediated endocytosis using chemical inhibitors results in significant reduction of H-1PV transduction.....	84
Figure 4.5. Hypertonic sucrose has no effect on H-1PV transduction if added 3 hours post-infection. ....	84
Figure 4.6. Knockdown of <i>AP2M1</i> results in significant reduction of H-1PV transduction. ....	85
Figure 4.7. Inhibition of caveolae-mediated endocytosis does not decrease H-1PV transduction.....	86
Figure 4.8. Knockdown of <i>CAV1</i> increases H-1PV transduction. ....	87
Figure 4.9. Treatment with higher concentrations of M $\beta$ CD do not result in increased H-1PV transduction. ....	88
Figure 4.10. Dynamin is involved in H-1PV cell entry .....	89
Figure 4.11. H-1PV intracellular trafficking takes place through the endosomal system. ....	90
Figure 4.12. Low endosomal pH is essential for a productive H-1PV infection. ....	91

## Chapter 5

Figure 5.1. Schematic model of the interaction of laminins with H-1PV.....	96
Figure 5.2. Schematic model of H-1PV entry and infection.....	104

## List of Abbreviations

AAV	Adeno-associated virus
Ad	Adeno
AP-2	Adaptor protein 2
BafA1	Bafilomycin A1
BPV	Bovine parvovirus
BSA	Bovine serum albumin
CaCl <sub>2</sub>	Calcium chloride
CCL	Broad Institute Cancer Cell Line Encyclopedia
CD	Cluster of differentiation
cDNA	Complementary deoxyribonucleic acid
CHC	Clathrin heavy chain
CME	Clathrin-mediated endocytosis
CPV	Canine parvovirus
CPZ	Chlorpromazine
CRISPR	Clustered Regularly Interspaced Short Palindromic Repeats
DAPI	4',6-diamidino-2-phenylindole
DMEM	Dulbecco's modified Eagle medium
DMSO	Dimethyl sulfoxide
DNA	Deoxyribonucleic acid
ds	Double-stranded
EC50	Half maximal effective concentration
EDTA	Ethylenediamine tetraacetic acid
EEA1	Early Endosome Antigen 1
EGFP	Enhanced green fluorescent protein
ELISA	Enzyme-linked immunosorbent assay
FACS	Fluorescence-activated cell sorting
FBS	Fetal bovine serum
FISH	Fluorescence in situ hybridization
Gal	Galectin
GAPDH	Glyceraldehyde 3-phosphate dehydrogenase
GBM	Glioblastoma
GMP	Good manufacturing practice
H-1PV	H-1 parvovirus
H <sub>2</sub> O	Water
HCl	Hydrochloric acid
HIV	Human immunodeficiency virus
KD	Knockdown
KO	Knockout
LAMP-1	Lysosome-associated membrane glycoprotein 1
M $\beta$ CD	Methyl- $\beta$ -cyclodextrin
MEM	Minimum Essential Medium

MgCl <sub>2</sub>	Magnesium chloride
MOI	Multiplicity of infection
mRNA	Messenger ribonucleic acid
MTT	3-(4,5-dimethylthiazol-2-yl)-2,5-diphenyl tetrazolium bromide
MVMp	Minute virus of mice prototype strain
NA	Neuraminidase
NaCl	Sodium chloride
NCI-60	National Cancer Institute 60 human tumour cell lines
ND	Not determined
NH <sub>4</sub> Cl	Ammonium chloride
NOS	Nitric oxide species
ns	Not significant
NS	Non-structural protein
O.D.	Optical Density
PBS	Phosphate-buffered saline
pfu	Plaque-forming unit
pH	Potential hydrogen
PK	Protein kinase
PLA <sub>2</sub>	Phospholipase A <sub>2</sub>
PLK1	Polo-like kinase 1
PPV	Porcine parvovirus
PtPV	Protoparvovirus
qPCR	Quantitative polymerase chain reaction
Rab	Ras-related protein
RIPA	Radioimmunoprecipitation assay
RNA	Ribonucleic acid
RNase	Ribonuclease
ROS	Reactive oxygen species
RPMI	Roswell Park Memorial Institute Medium
RT-qPCR	Reverse transcription quantitative polymerase chain reaction
SA	Sialic acid
SD	Standard deviation
SDS	Sodium dodecyl sulfate
siRNA	Small-interference RNA
ss	Single-stranded
STAT	Signal transducer and activator of transcription
TE	Tris-EDTA buffer
TMB	3,3',5,5'-Tetramethylbenzidine
VP	Viral structural protein

## *Units*

°C	Degree Celsius
bp	Base pairs
Da	Dalton
g	Gram
h	Hour
kDa	Kilodalton
L	Litre
µg	Microgram
µL	Microlitre
µM	Micromolar
M	Molar
mg	Milligram
mL	Millilitre
mM	Millilitre
min	Minutes
ng	Nanogram
nm	Nanometre
pg	Picogram
rpm	Revolutions per minute
sec	Seconds
TU	Transduction units
Vg	Viral genome



## Chapter 1: General Introduction

**H**-1 parvovirus (H-1PV) shows an excellent safety profile and is endowed with natural oncolytic and oncosuppressive properties. Thanks to these features, H-1PV is considered a promising anticancer agent. More than 50 years of research at the pre-clinical level elucidated many aspects of the H-1PV life cycle, making it one of the most extensively studied autonomously replicating parvoviruses. However, the early steps of H-1PV infection are still poorly understood. The main objective of this dissertation is to help to fill in this knowledge gap and provide new knowledge that could be used to improve H-1PV-based anticancer therapies.

In the section 1.1, I first give a general overview on the oncolytic virus field. Thereafter, in the section 1.2, I introduce the *Parvoviridae* family (which H-1PV belongs to), from taxonomy to virus life cycle. In the section 1.3, I cover the mechanisms involved in H-1PV anticancer properties leading to its clinical assessment, and how to further improve them.

### 1.1 Oncolytic Virus, a Warrior Against Cancer

#### 1.1.1 Emergence of oncolytic virotherapy

Oncolytic viruses are viruses that preferentially infect and kill cancer cells, while sparing normal cells/tissues. The concept of using viruses as therapeutic agents for the treatment of cancer dates back to the beginning of the 20<sup>th</sup> century. Italian physician DePace realised a brief tumour regression in patients with cervical cancer after being administered with rabies vaccine (De Pace, 1912). Shortly after, Levaditi and Nicolau proposed that the virus replicated in the tumour and was able to destroy it (Levaditi and Nicolau, 1922). Over time, case-study reports of cancer regression in cervical cancer, Burkitt lymphoma, and Hodgkin lymphoma after virus infection, provided further evidence that viruses may also have oncosuppressive properties in certain conditions (Kuruppu and Tanabe, 2005). However, the absence of neither complete nor durable anti-tumour activity of viruses in some human trials, along with some safety issues, led to the almost abandonment of virotherapy.

In recent decades, the emergence of genetic engineering made the modification of viruses possible in order to improve their safety, specific oncotropism and potency, thereby advancing biological therapy for cancer. Even though conventional therapies (chemo- and radio- therapies) constitute the preferable treatment options, these often present limitations by not offering a definitive cure. As a result, the oncolytic virotherapy field has received renewed attention ([Russell et al., 2012](#)). Currently, more than forty oncolytic viruses belonging to ten different families are currently evaluated in clinical trials against different cancers (Figure 1.1A, B) ([Kaufman et al., 2015](#)) [please refer to the following systemic review for a thorough overview of all oncolytic viruses in phase I, II, and III clinical trials published to date ([Cook and Chauhan, 2020](#))]. Oncolytic viruses include viruses that are naturally oncotropic and viruses that have been genetically engineered to preferentially infect cancer cells. Naturally oncolytic viruses include reovirus ([Maitra et al., 2012](#)), Newcastle-disease virus (NDV) ([Phuangsab et al., 2001](#)) and H-1PV – the subject of this study ([Geletneky et al., 2012](#)). In contrast, adenovirus (Ad) ([Sato-Dahlman and Yamamoto, 2018](#)), measles (MeV) ([Bajzer et al., 2008](#)), vesicular stomatitis virus (VSV) ([Ammayappan et al., 2013](#)), vaccinia virus (VV) ([Guo et al., 2019](#)) or herpes simplex virus (HSV) ([Miyagawa et al., 2015](#)) are examples of genetically modified viruses. These genetic alterations may include limiting the virus binding to surface antigens typically present in cancer cells, to improve immunogenicity or simply to attenuate virus-induced pathogenicity ([de Matos et al., 2020](#)).

Despite clinical trials using oncolytic viruses having reported no deaths or clinically serious side-effects, and pre-clinical evidence of their potential as anticancer agents being increasingly growing, implementation of virotherapy has been slow (Figure 1.1C). Even so, three oncolytic viruses have already been approved for the treatment of advanced cancers. In 2004, ECHO-7 picornavirus (Rigvir) constituted the first approved virus to treat melanoma in Latvia ([Alberts et al., 2018](#)). However, in March 2019, Rigvir distribution was stopped after the amount of virus was in smaller quantities than those declared. In 2005, a genetically-modified Ad (H101) was approved in China to treat nasopharyngeal carcinoma in combination with chemotherapy ([Liang, 2018](#)). The first U.S. Food and Drug Administration (FDA)-approved virus occurred in 2015, and it was named Talimogene laherparepvec (T-VEC) ([Johnson et al., 2015](#)). T-VEC comprises an attenuated herpes simplex virus 1



(HSV-1) encoding granulocyte-macrophage colony-stimulating factor (GM-CSF) and was authorised for the local treatment of unresectable cutaneous, subcutaneous, and nodal lesions in patients with melanoma recurrent after initial surgery (Andtbacka et al., 2015). Subsequently, T-VEC has been also approved in Israel, Australia and Europe.

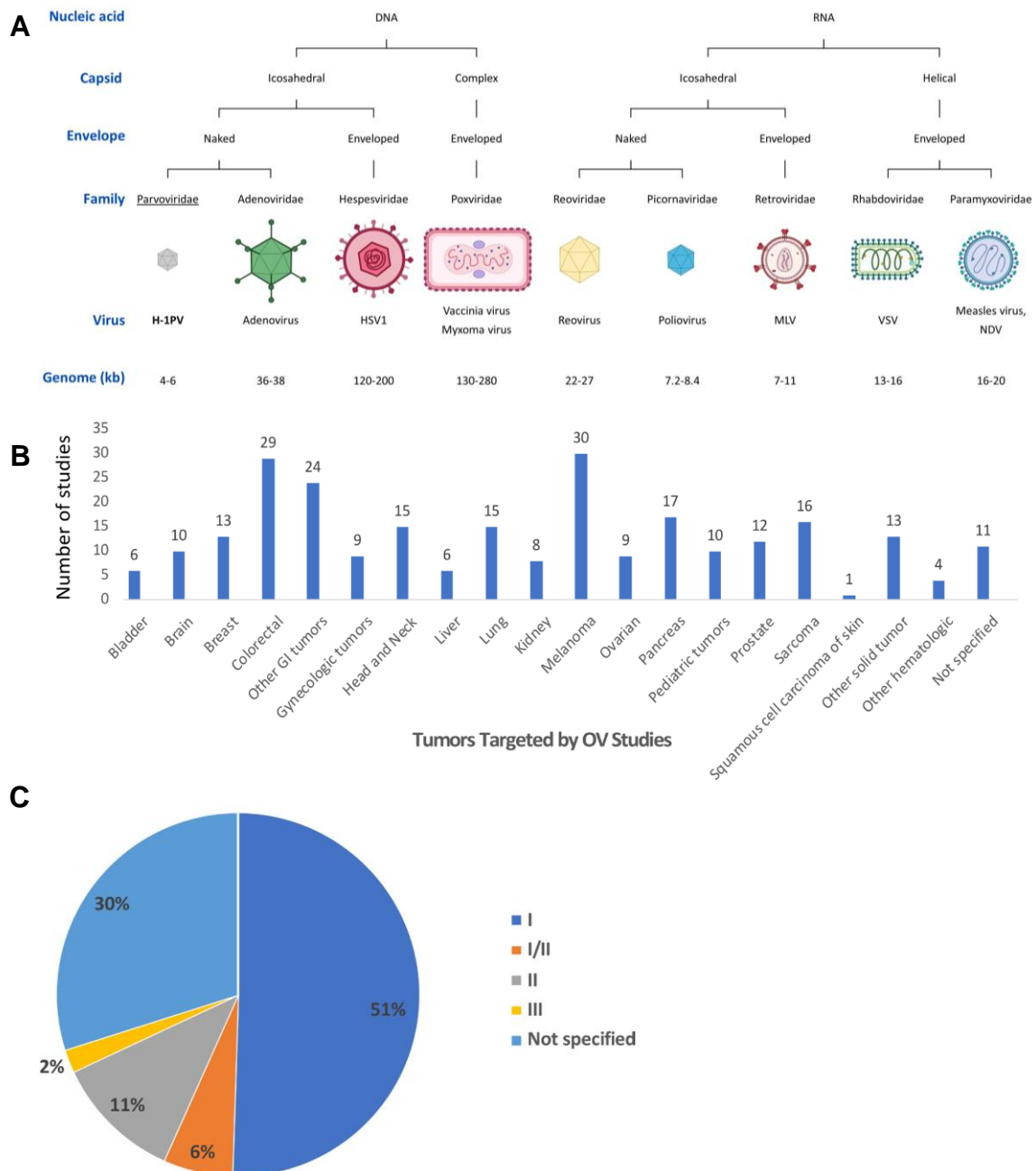


**Figure 1.1. Overview of oncolytic virotherapy in the clinical setting.**

(A) Summary of the basic characteristics of oncolytic viruses currently being tested in clinical trials. Abbreviations: H-1PV: H-1 parvovirus; HSV1: herpes simplex virus 1; MLV: murine leukaemia virus; VSV: vesicular stomatitis virus; NDV: Newcastle disease virus. Adapted from (Cattaneo et al., 2008) and (Miest and Cattaneo, 2014)

using the BioRender.com software. **(B)** Cancer types tested in clinical trials using oncolytic viruses, and respective number of clinical studies. Abbreviations: GI, gastrointestinal. Figure retrieved from (Macedo et al., 2020). **(C)** Distribution of oncolytic viruses by clinical stage. Out of a total of 97 clinical trials reported from 2000 to 2020: phase I ( $n=49$ ), phase I/II ( $n=6$ ), phase II ( $n=11$ ), phase III ( $n=2$ ) and not specified ( $n=29$ ). Pie chart retrieved from (Macedo et al., 2020).

### 1.1.2 Mechanisms behind viral oncotropism

The concept of oncolytic virotherapy comprises viral replication and consequent lysis restricted to tumour cells. This selective replication may result from inherent or engineered features and need to be carefully taken into consideration. There are three main parameters playing a role in viral oncotropism: (i) abnormal cell receptors, (ii) aberrant signalling pathways, and (iii) tumour microenvironment (Kaufman et al., 2015).

#### (i) Abnormal cell receptors

The earliest steps of the virus-host cell interaction comprise the binding of the virus to the cell surface and its subsequent entry. Several oncolytic viruses possess a natural tropism towards cell surface proteins which are aberrantly expressed in cancer cells (Figure 1.2). This is the case of Poliovirus co-receptor CD155 overexpressed in glioma cells (Merrill et al., 2004); Sindbis virus binds to the high-affinity laminin receptor, which promotes cancer cell invasion and is overexpressed in several cancers (Van den Brule et al., 1996); or echovirus 1 affinity for integrin  $\alpha 2\beta 1$ , present at high levels in ovarian cancer (Shafren et al., 2005).

On the other hand, oncolytic viruses can be modified in order to bind cell surface receptors expressed by cancer cells (Figure 1.2). For instance, the modification of Ad to incorporate an RGD sequence in the viral fibre increases infectivity by promoting the binding to  $\alpha \nu \beta 3$  and  $\alpha \nu \beta 5$  integrins, which are overexpressed at the surface of numerous tumours or tumour angiogenic vasculature (Wickham et al., 1994, Wickham et al., 1993, Martínez-Vélez et al., 2019). Another example is the attenuation of VSV by virus pseudotyping in order to contain the non-neurotropic envelope glycoprotein of lymphocytic choriomeningitis virus (LCMV) instead of the VSV G protein. This modification increases tropism towards brain cancer cells and reduce neurotoxicity (Muik et al., 2011).

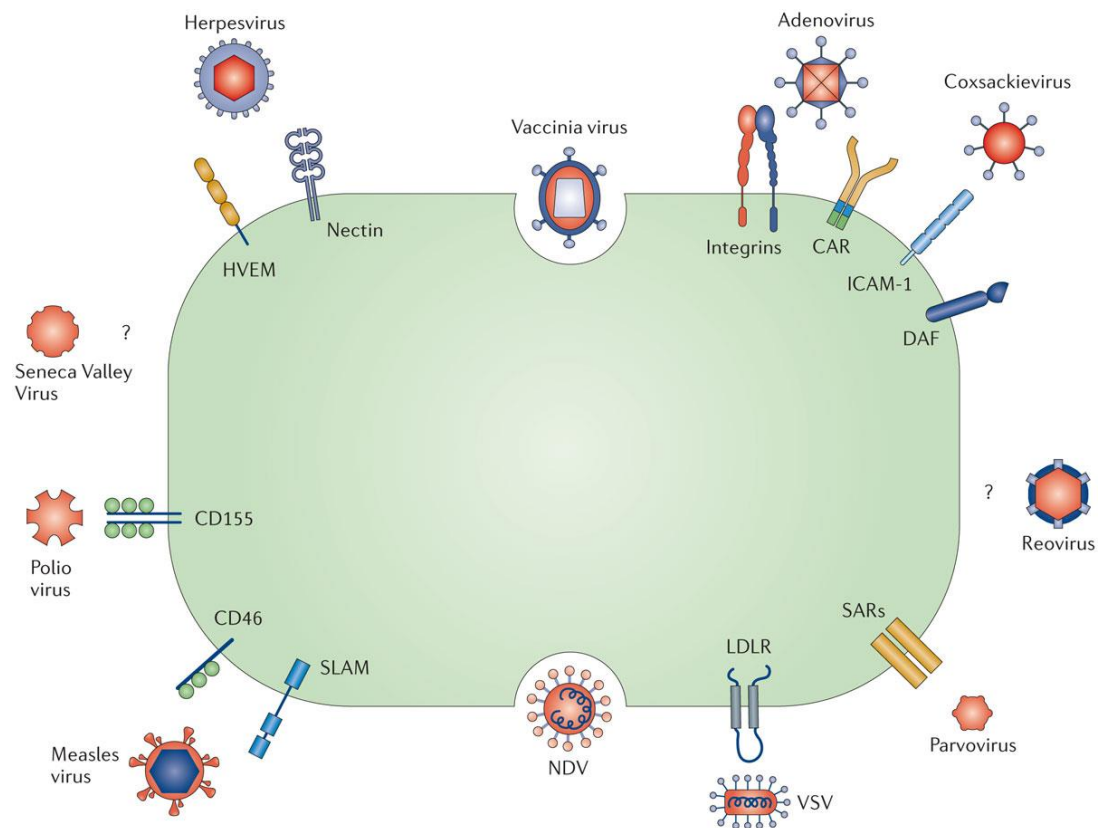


**Figure 1.2. Oncolytic viruses target receptors aberrantly expressed in cancer cells.**

Cell surface receptors which are often upregulated in carcinogenesis are targeted by oncolytic viruses to enter into cancer cells. Certain viruses can enter cells through more than a one receptor, and in turn, certain receptors can be involved in the entry of more than one virus. Alternatively, certain viruses can enter cells *via* membrane fusion and syncytia formation. Question marks correspond to viruses for which a receptor has not yet been identified. Abbreviations: CAR: coxsackievirus-adenovirus receptor; DAF: decay accelerating factor; HVEM1: herpesvirus entry mediator 1; ICAM-1: intercellular adhesion molecule 1; LDLR: low-density lipoprotein receptor; NDV: Newcastle disease virus; SARs: sialic acid-containing receptors; SLAM: signalling lymphocytic activation molecule; VSV: vesicular stomatitis virus. Figure retrieved from (Kaufman et al., 2015).

## (ii) Aberrant signalling pathways

The second main mechanism concerns viruses which exploit aberrant signalling pathways responsible for maintaining continuous cancer growth (Figure 1.3). The Ras signalling pathways are crucial regulators of cell proliferation and carcinogenesis (Gimple and Wang, 2019). In fact, Ras-transformed cells are significantly more susceptible to reovirus and VV infection. When reovirus infects normal cells, the protein kinase R (PKR) pathway is activated, which in turn halts protein synthesis and

stops viral spread (Bischoff and Samuel, 1989). However, Ras-transformed cancer cells do not activate the PKR pathway, and therefore, provide more favourable conditions for viral infection and virus-induced cell lysis (Gong and Mita, 2014). As well, an attenuated HSV-1 oncolytic virus having the ICP34.5 and unique short 11 glycoprotein (US11) viral genes deleted leads to preferential lysis of cancer cells (Liu et al., 2003, Hu et al., 2006). These deletions incapacitate the virus from blocking PKR phosphorylation, and thus, only allow the virus to replicate in PKR-defective cancer cells (Poppers et al., 2000). Another example concerns the frequent dysregulation of B cell lymphoma (BCL)-2 family of proteins in cancer cells to evade cell death (Adams and Cory, 2007), while NDV oncotropism depends on tumour resistance to apoptosis. In this manner, BCL-xL-overexpressing cells provide the incubation time needed for the virus to replicate and form syncytia essential for virus spread (Mansour et al., 2011).

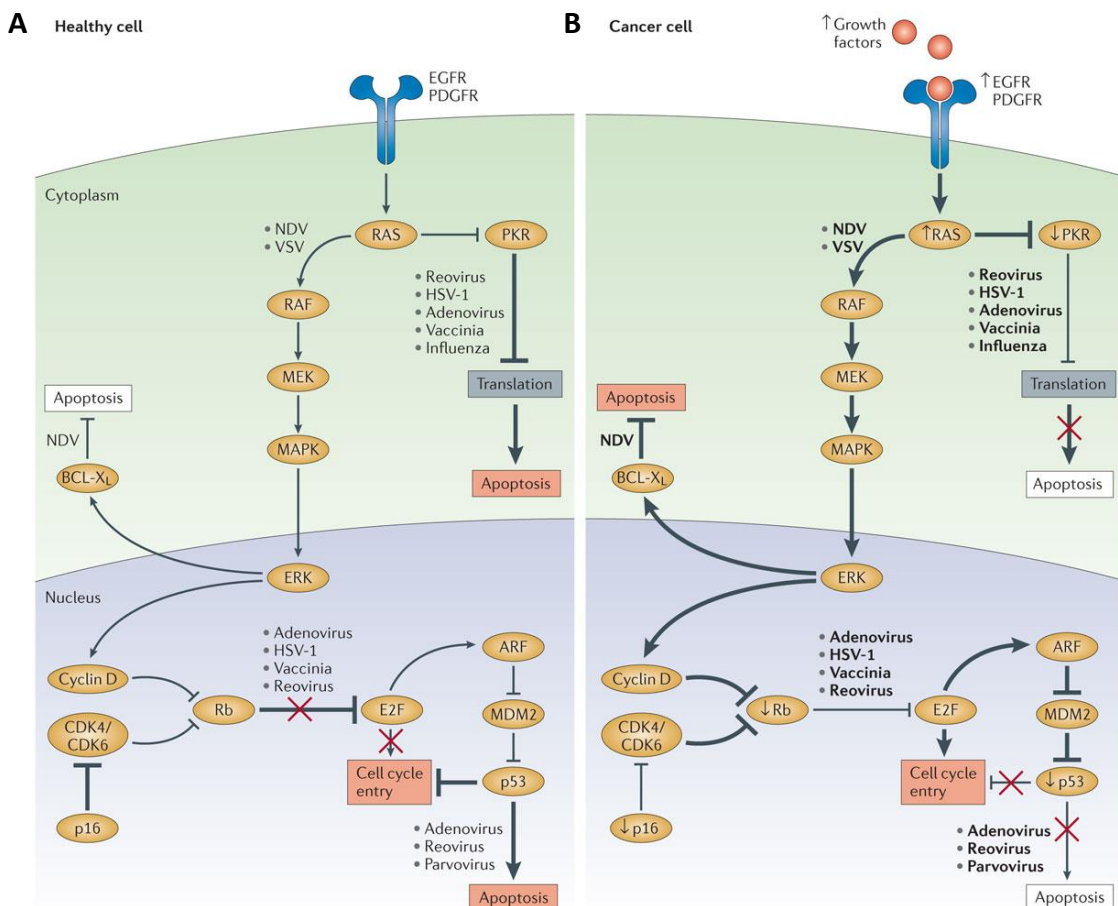


**Figure 1.3. Oncolytic viruses target aberrant cellular signalling pathways.**

The expression of aberrant host cell proteins, responsible for maintaining continuous cancer growth, can be targeted by oncolytic viruses. (A) In normal cells, the cell cycle and growth are regulated by numerous elements, including the p53 tumour suppressor,

p16, protein kinase R (PKR) and retinoblastoma (Rb). When the cell cycle is dysregulated, these factors trigger an abortive apoptosis. PKR can also halt protein synthesis upon a virus infection. **(B)** In cancer cells, there is an uncontrolled cell division in which cell cycle arrest and/or programmed cell death are usually inhibited. For instance, mutations in RAS lead to exacerbated cellular proliferation can be exploited by reovirus, Newcastle disease virus (NDV) and vesicular stomatitis virus (VSV). Moreover, upregulation of RAS inhibits PKR, a feature that promotes the selective replication of reovirus, herpes simplex virus type 1 (HSV-1), adenovirus (Ad), vaccinia virus (VV) and influenza virus. Likewise, mutations in p53 tumour suppressor unable the activation of abortive apoptosis, and therefore, p53-defective cells are preferential targets of Ad, reovirus and parvoviruses. Additionally, abnormal expression of Rb and p16 increase susceptibility of cancer cells to oncolytic virus, namely Ad, HSV-1, VV and Reovirus. Upregulation of anti-apoptotic B cell lymphoma (BCL)-xL, commonly observed in cancer cells, facilitates NDV replication by providing the incubation time needed. Abbreviations: CDK, cyclin-dependent kinase; EGFR, epidermal growth factor receptor; ERK, extracellular signal-regulated kinase; MAPK, mitogen-activated protein kinase; MEK, MAPK/ERK kinase; PDGFR, platelet-derived growth factor receptor. Figure retrieved from ([Kaufman et al., 2015](#)).

Besides having a dysfunctional cell growth rate, cancer cells frequently present defective antiviral response pathways (Figure 1.4). In healthy cells, type I interferons are important mediators of cellular antiviral and antitumour responses since they trigger immune responses to clear the viral infection as well as decrease cellular proliferation by triggering p53 pro-apoptotic signalling ([Muñoz-Fontela et al., 2008](#)). In cancer cells, replication of VV ([Parato et al., 2012](#)), NDV ([Wilden et al., 2009](#)), reovirus ([Bischoff and Samuel, 1989](#)), VSV ([Stojdl et al., 2000](#)), among others, can occur due to a flawed interferon antiviral response.

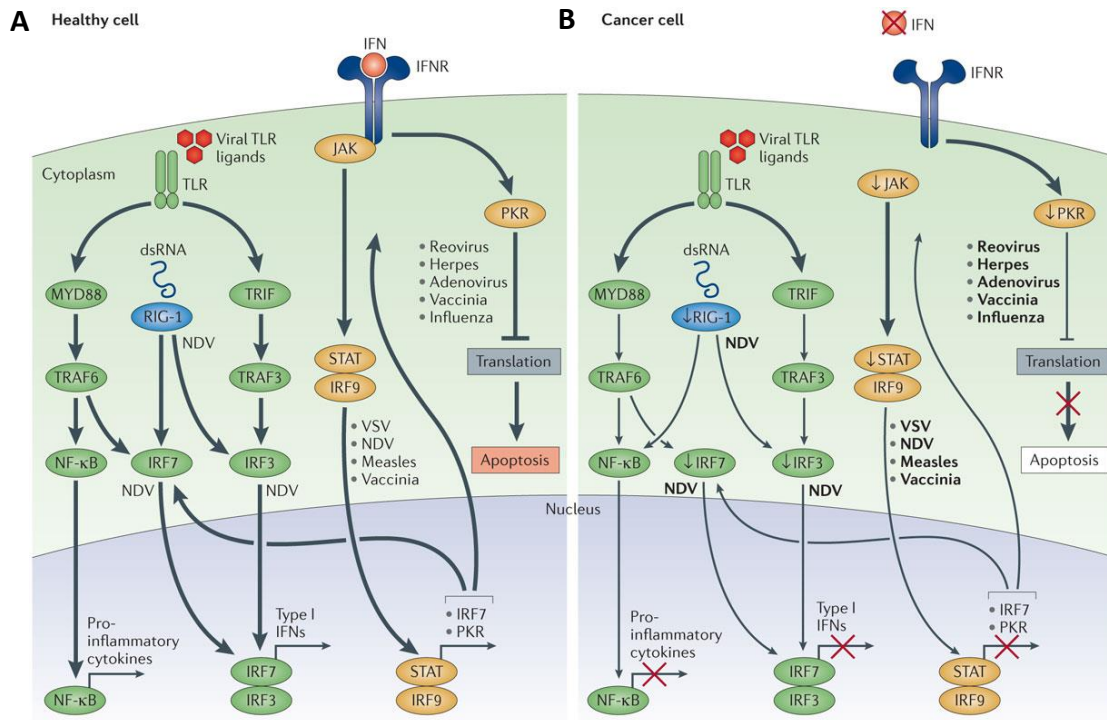


**Figure 1.4. Oncolytic viruses take advantage of cancer immune evasion pathways.**

(A) A virus infection normally triggers an antiviral response in healthy cells to restrict the viral infection. Toll-like receptors (TLRs) are triggered by viral pathogen-associated molecular patterns (PAMPs) while retinoic acid-inducible gene 1 (RIG-1) detects viral nucleic acid. After detection, there is activation of a signalling cascade including the myeloid differentiation primary response protein MYD88, TIR-domain-containing adapter-inducing IFN $\beta$  (TRIF), IRF7, IRF3 and nuclear factor- $\kappa$ B (NF  $\kappa$ B), leading to the production of type I interferon and pro-inflammatory cytokines. Local interferon production signal through the Janus kinase-signal transducer and activator of transcription (JAK-STAT) pathway, leading to upregulation of cell cycle regulators, including protein kinase R (PKR) and interferon-regulatory factor (IRF7), which restrict virus spread and further induces type I interferon transcriptional pathways. (B) The interferon-related antiviral response is often disrupted in cancer cells, where most of these factors (RIG-1, IRF3, IRF7) are downregulated. By downregulating molecules involved in virus detection, cancer cells are inevitably more susceptible to virus infection, as well as those factors involved in type I interferon signalling. The figure indicates viruses which have been described to have their replication facilitated by factors specifically deficient in cancer cells. Abbreviations: dsRNA: double-stranded RNA; NDV: Newcastle disease virus; TRAF: TNF-associated factor; VSV: vesicular stomatitis virus. Figure retrieved from (Kaufman et al., 2015).

### (iii) Tumour microenvironment

The third major regulator of viral oncotropism is the tumour microenvironment. As the tumour grows, the blood supply quickly reaches a point where it is not sufficient, and some regions are left with an oxygen concentration lower than that observed in healthy tissues. The resulting hypoxic microenvironment with reduced perfusion confers resistance to conventional therapeutics like radio- and chemotherapy (Guo, 2011). While lower oxygen levels have also been demonstrated to inhibit virus replication and oncolysis, replication of oncolytic HSV-1 is potentiated partly due to an increased expression of Growth Arrest and DNA Damage-Inducible Protein (GADD34) in cells in hypoxic conditions (Aghi et al., 2009). Likewise, VSV has been shown to have the inherent capacity to replicate under hypoxic tumour cells (Zhou et al., 2016).

Cancer cells also secrete higher levels of matrix metalloproteinases than normal cells, which in turn degrade the extracellular matrix faster to promote tumour dissemination (Egeblad and Werb, 2002). Given this fact, MeV was genetically engineered to include metalloproteinase cleavage sites in its fusion protein. This modification makes the virus dependant on the host protease furin secreted by cancer cells, to process and activate its envelope fusion protein, ultimately enhancing virus safety (Springfeld et al., 2006). Another example is the preferential infection of tumour vasculature by some OV's (Hartley et al., 2020). For instance, VSV was shown to infect and kill tumour-associated endothelial cells, thus destroying tumour vasculature. This was associated with a lower supply of nutrients and oxygen into the tumour microenvironment, and consequently, tumour shrinkage (Breitbach et al., 2011)

### 1.1.3 Features required for an ideal oncolytic virus

Oncolytic virotherapy emerged as a strategy to alleviate or even cure malignant tumours. However, not every virus is considered to be a good candidate. In truth, there are some features expected of oncolytic viruses in order to be used effectively in patients (Parato et al., 2005): not harmful/pathogenic to humans, have specificity for tumour over normal cells, have a fast replication cycle, do not recombine with host

genome, possibility of being systematically administered, induce a strong anti-cancer immunity, and allow genetic engineering.

The first clear requirement is the lack of pathogenicity for humans. Oncolytic viruses should ideally not be human pathogens to reduce the chances of a pre-existing immunity which compromise the therapeutic success. As well, oncolytic viruses should present an excellent safety profile by specifically infecting cancer cells in order to avoid damage on normal tissues.

Another important aspect of oncolytic virotherapy is the viral life cycle. The virus should replicate rapidly, not involve recombination with the host cell DNA, induce cytolysis and spread before the establishment of an antiviral immune response. A virus capable of cell-to-cell transmission is believed to have an additional advantage since it is not as exposed, and therefore, the immune involvement would be delayed.

Systemic administration of the virus is also very desirable to treat patients with advanced/metastatic disease, given that this administration route allows the targeting of the metastases apart from the primary tumour. Moreover, this delivery route may enhance the generation of antitumour immune responses compared to intratumorally administration (Kuhn et al., 2008). As well, systemic administration is less invasive and more standardisable, and therefore, preferable for the treatment of patients with inaccessible cancers, including brain cancer (when the virus has the ability to cross the blood brain barrier).

The potential of oncolytic viruses to induce a strong anti-tumour immunity is also an important aspect. Ideally, the oncolytic virus is able to turn an immunosuppressive tumour into an inflammatory environment. Due to the resulting recruitment of macrophages and T cells, as well as other immune cells attracted by the cytokines released, the oncolytic viruses are able to destroy the tumour and generate immunological memory to restrict later tumour relapses.

Last but not least, an ideal oncolytic virus candidate should be receptive to genetic modifications, including insertion of immunostimulatory genes to further increase the anti-cancer immune response (e.g. a gene encoding for an immune modulator), or genes that increase the oncolytic potential of the virus (e.g. a pro-drug convertase or a pro-apoptotic gene).



Taken together, it becomes unlikely that a virus presents all the above-mentioned characteristics. Uncertainties about the advantages of one virus over another, or even about the possibility of a certain oncolytic virus being more appropriate for a particular cancer type than another, demands further research on the field.

## 1.2 *Parvoviridae*, a Family Filled with Diversity

Among the oncolytic viruses, the protoparvovirus H-1PV, belonging to the *Parvoviridae* family, is the subject of this study. H-1PV constitutes the most extensively studied oncolytic parvovirus and has shown remarkable oncolytic potential. In this section, I firstly cover the taxonomy as well as the basic biology of parvoviruses. At last, I describe the several steps of the H-1PV life cycle.

### 1.2.1 Taxonomy

The family consists of two subfamilies, *Parvovirinae*, which includes viruses of vertebrates, and *Densovirinae*, which includes viruses of insects and other invertebrates (Cotmore et al., 2014) (Figure 1.5). Currently, there are eight genera classified as members of the *Parvovirinae* subfamily, considering their molecular properties: (i) *Amdoparvovirus*, with mustelids, skunk, and raccoons as natural hosts; (ii) *Bocaparvovirus*, comprising a variety of parvoviruses from dogs, marine mammals, primates, and ungulates; (iii) *Dependoparvovirus*, including the adeno-associated viruses (AAV), which is composed, with a few exceptions, of viruses which rely on a helper virus for their own replication (Naso et al., 2017); (iv) *Erythroparvovirus*, viruses with specific tropism for erythroid cells; (v) *Copiparvovirus*, having pigs and cows as natural hosts; (vi) *Aveparvovirus*, which infect birds; (vii) *Tetraparvovirus*, includes at least two ungulate parvoviruses (James, 2017); and the (viii) *Protoparvovirus* (PtPV), which comprises rodent parvoviruses e.g. H-1PV (see below) (Ros et al., 2017).

Within the *Parvovirinae* subfamily, there are viruses from five genera known to infect humans: the *Bocaparvovirus* human bocavirus (HBoV), whose infection cause respiratory diseases in children and rare fetal infections (Manteufel and Truyen, 2008); the *Dependoparvovirus* AAV types 1 to 5, whose infection alone is not known to cause any disease (Rajapaksha et al., 2018); the *Erythroparvovirus* B19, that causes the fifth disease that usually affects children, but can also affect adults (Lunardi et al., 2008); the *Tetraparvovirus* human parvovirus (PARV) 4, which is asymptomatic (Matthews et al., 2014); and the PtPV bufavirus thought to cause gastroenteritis in both children

and adults (Qiu et al., 2017). Up to now, no human viruses were known to exist in the other three genera (*Amdoparvovirus*, *Aveparvovirus* and *Copiparvovirus*).

The genus PtPV of the *Parvoviridae* contains the following species (Cotmore et al., 2014, Ros et al., 2017): *Rodent protoparvovirus 1* (H-1PV, minute virus of mice (MVM), Kilham rat virus, LuIII virus, mouse parvovirus, tumor virus X, rat minute virus); *Rodent protoparvovirus 2* (rat parvovirus 1); *Carnivore protoparvovirus 1* (canine parvovirus (CPV) and feline panleukopenia parvovirus (FPV)); *Primate protoparvovirus 1* (bufavirus) and *Ungulate parvovirus 1* (porcine parvovirus (PPV)). The oncotropic and oncolytic properties of rodent PtPVs, with particular emphasis to H-1PV, have been extensively studied at the pre-clinical level. Thanks to their remarkable ability to preferentially infect and kill human cancer cell lines of different origins, there has been a growing interest to use these viruses as anti-cancer agents (Rommelaere et al., 2010).

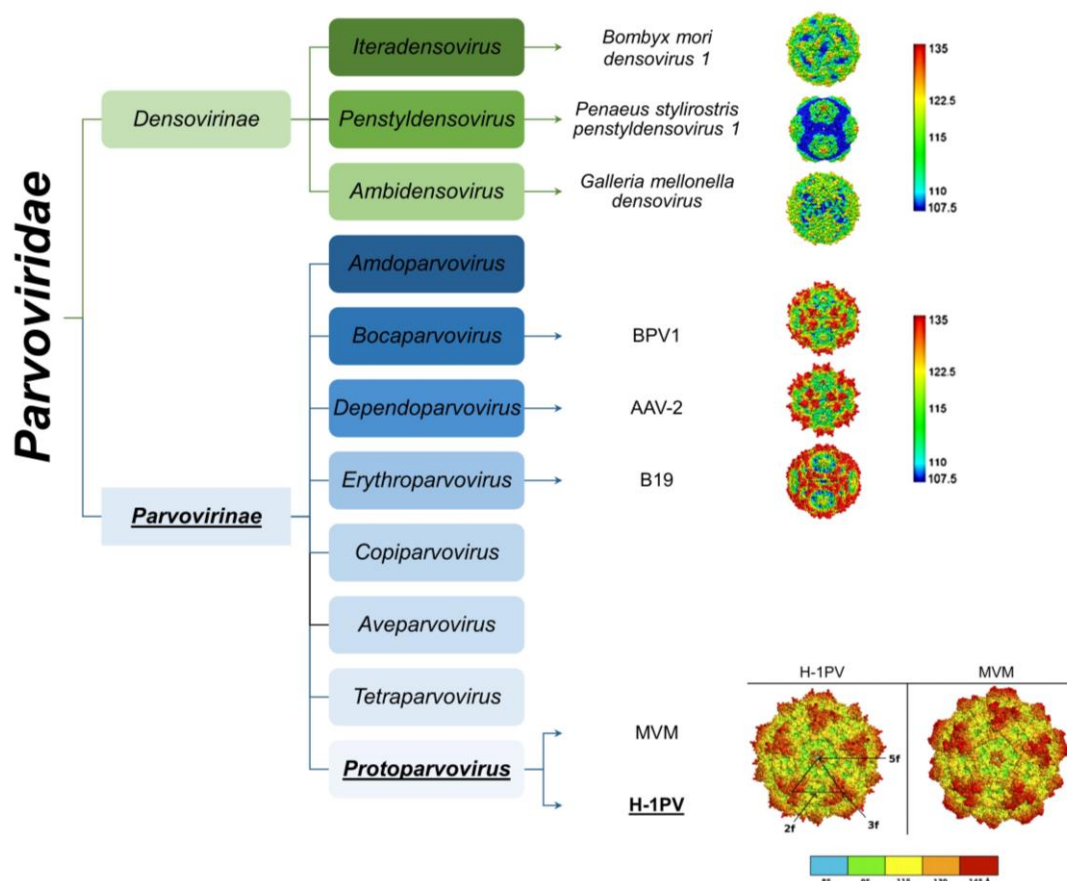


**Figure 1.5. *Parvoviridae* family.**

Overview of a simplified phylogenetic tree of the genera in subfamilies *Densovirinae* (boxes in green) and *Parvovirinae* (boxes in blue). Selected examples of viruses with respective atomic structures are shown. Viral atomic structures were retrieved as

follows: *Bombyx mori densovirus* 1, *Penaeus stylirostris penstyldensovirus* 1, *Galleria mellonella densovirus*, bovine parvovirus 1 (BPV1), adeno-associated virus 2 (AAV-2), human parvovirus B19 (B19) were all obtained from (Cotmore et al., 2019); while comparison of minute virus of mice (MVM) to H-1 parvovirus (H-1PV) was obtained from (Allaume et al., 2012). Radial distances (Å) from the particle centre are coloured according to scales bars ranging from blue to red. An asymmetric unit diagram is labelled to indicate icosahedral 2-, 3- and 5- fold axes in the H-1PV structure.

In general terms, the PtPV genome is a linear, single-stranded DNA molecule of approximately 5 kb enclosed within an icosahedral capsid of 25 nm in diameter (Bretscher and Marchini, 2019). The capsid structure is characterised by three main elements: (i) a spike-like protrusion at the 3-fold axis of symmetry; (ii) a depression, called dimple, at the 2-fold axis; (iii) a pore located at 5-fold axis, connecting the inside of the virion to the exterior (Cotmore and Tattersall, 2007). The PtPV genome encompasses two gene units: the non-structural (*NS*) and the viral particle (*VP*) gene units (Figure 1.6). The early P4 promoter controls the expression of *NS* encoding for NS1 and NS2 proteins, whereas the late P38 promoter (transactivated by NS1) controls the expression of *VP* gene unit encoding the VP1, VP2 capsid proteins and the small alternatively translated protein (SAT) (Cotmore and Tattersall, 2007). VP3, another structural protein, is created through proteolytic cleavage of the VP2 N-terminal region (Cotmore and Tattersall, 2007). At both extremities, the viral genome contains palindromic sequences that form hairpin structures, which serve as self-priming origins during viral DNA replication (Li et al., 2013b).

### 1.2.2 Parvoviral proteins

NS1 is a multifunctional protein which regulates many PtPVs processes (Nüesch and Rommelaere, 2014). In H-1PV, the protein consists of 672 amino acids with a molecular weight of approximately 83 kDa. It is expressed early after infection and it is mainly located in the nucleus due to a nuclear localisation signal (NLS) in its sequence (Legendre and Rommelaere, 1994). Still, a fraction of the protein can also be found in the cytoplasm (Nüesch and Tattersall, 1993). Given its ATPase and helicase activities, NS1 initiates viral DNA amplification and regulates virus gene expression by modulating the activity of its own P4 promoter and transactivating the late P38 promoter (Noesch et al., 1992, Wilson et al., 1991, Rhode, 1985, Li and

Rhode, 1990). NS1 activities are tightly regulated in time and space through post-translational modifications (Nüesch, 2006). A pertinent example is the phosphorylation pattern of NS1 changing throughout the MVM infection cycle. These changes are carried out by members of the phosphoinositide-dependent kinase 1 (PDK1) / protein kinase C (PKC) / protein kinase B (PKB) signalling cascade (Nüesch et al., 2003, Dettwiler et al., 1999, Lachmann et al., 2003, Nüesch et al., 2001). During H-1PV infection, in addition to be phosphorylated, acetylation of NS1 was found to modulate NS1-mediated transcription and cytotoxicity (Li et al., 2013a, Hristov et al., 2010) (see also sub-section 1.3.2).

NS2 is a protein of about 25 kDa and is generated through the alternative splicing of NS1. NS2 exists as three isoforms: NS2P, NS2Y and NS2L (in order of abundance) (Ruiz et al., 2006). The functions of this protein in H-1PV infection are not entirely known, yet studies in MVM show that NS2 indirectly promotes virus replication and is required for full cytopathic potential (Legrand et al., 1993, Brandenburger et al., 1990).

The recently identified SAT protein is expressed at later stages of infection. It is encoded within the *VP* gene unit a few nucleotides downstream of the VP2 initiation codon. SAT of PPV accumulates in the endoplasmic reticulum and plays a role in virus release and spreading (Zádori et al., 2005). Indeed, PPV SAT knockout spreads slower as a consequence of prolonged cell integrity. Additionally, SAT increases endoplasmic reticulum stress and accelerates the cell death during infection (Mészáros et al., 2017).

The capsid VP proteins present an overlapping amino acid sequence, with VP1 (81 kDa) and VP2 (65 kDa) generated by alternative splicing from the same mRNA, and are expressed at a ratio 1:5 (Tattersall et al., 1976). Apart from VP1 and VP2 sharing a common C-terminal sequence (593 amino acids), VP1 presents a unique N-terminal region of 142 amino acids. This region contains a phospholipase A<sub>2</sub> (PLA<sub>2</sub>) enzymatic domain as well as basic NLS, both essential for targeting the capsid to the cellular nucleus (Vihinen-Ranta et al., 1997) (see also sub-section 1.2.3). VP3, a truncated version of VP2, is generated by proteolytic cleavage of 25 amino acids at the VP2 N-terminus. The viral capsid is, in its whole, composed of 60 protein subunits: ~10 copies of VP1 and ~50 copies of VP2 in empty capsids or a combination of VP2 and VP3 in full virions (Halder et al., 2013a).

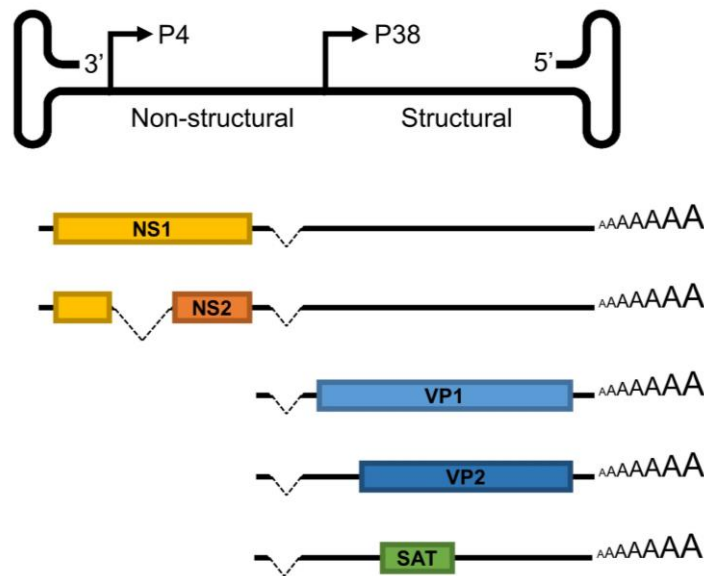


**Figure 1.6. Protoparvovirus genome.**

Parvovirus genome is flanked by hairpin structures on either end. Arrows indicate early P4 and late P38 promoters, responsible for transcription of non-structural (*NS*) and capsid (*VP*) gene units, respectively. From top to bottom, segments represent transcripts of *NS1*, *NS2*, *VP1*, *VP2* and small alternatively translated (*SAT*) genes; along with AAAAAA polyadenylation sites. This figure was adapted from The ViralZone database (<http://viralzone.expasy.org>) using the BioRender.com software.

### 1.2.3 Early steps of infection

Recognition of cell surface factors is the first step in the viral infection, and consequently, represents a key parameter of tropism and pathogenesis. Up to now, different receptor molecules, including proteins or carbohydrates, have been discovered to be involved in parvovirus-binding interactions. For instance, CPV and FPV interact with the transferrin receptor to bind and infect cells (Parker et al., 2001). Considered to be one of the most commonly receptors used in nature, sialic acid (SA; N-acetylneuraminic acid) glycan was first shown to play a role in MVM cellular binding and entry (López-Bueno et al., 2006, Olofsson and Bergström, 2005, Cotmore and Tattersall, 1987). Later, it was also demonstrated that SA is required for the infection of PPV (Boisvert et al., 2010) and H-1PV (Allaume et al., 2012). Neuraminidase treatment, resulting in cleavage of SA from the cellular surface, indeed impairs the cell attachment of these viruses (Allaume et al., 2012). While Chinese hamster ovary (CHO) Pro-5 cells, which present SA on the cell surface, are permissive to H-1PV infection, the two isogenic CHO Lec 1 and Lec 2 mutants lacking SA, are resistant.

Additionally, the capsid 2-fold axis of symmetry was described to be quite important to dictate H-1PV infectivity. In particular, I367 and H373 residues in H-1PV capsid (I362 and K368, respectively, in MVM) were identified to participate in the interaction with SA exposed on the cellular membrane (Allaume et al., 2012, López-Bueno et al., 2008).

After virus attachment to the cellular membrane, PtPVs can be internalised by the host cell through different pinocytic pathways (Harbison et al., 2008) (Figure 1.7). Clathrin- and caveolae-mediated endocytosis are two pathways dependent on dynamin, while macropinocytosis, lipid raft-mediated and clathrin/caveolae-independent endocytosis do not rely on dynamin activity (Doherty and McMahon, 2009, Mercer et al., 2010). Clathrin-mediated endocytosis (CME) is the route commonly employed by small viruses to enter into cells. The same holds true for most PtPVs (Boisvert et al., 2010, Dudleenamjil et al., 2010, Parker and Parrish, 2000, Vendeville et al., 2009, Quattrocchi et al., 2012), yet the route used by H-1PV in particular remains to be described. Initially, adaptor protein 2 (AP2) complexes are recruited to the plasma membrane, which is followed by the formation of a three-dimensional clathrin coat. As the event progresses, invagination of the membrane occurs, leading to a clathrin-coated pit. Thereafter, dynamin self-assembles around the vesicle neck to cleave a mature pit from the plasma membrane.

Apart from the typical CME, PtPVs are known to use alternative endocytic pathways. For instance, both FPV and CPV are uptaken by cells *via* binding to the transferrin receptor, which is typically endocytosed by CME. However, even though deletions or mutations on the internalisation motif of the transferrin receptor decreased virus uptake from the cell surface, viral infection still took place (Hueffer et al., 2004), suggesting the possibility of alternative internalisation mechanisms. In what concerns MVM entry, the virus has been shown to take at least three different endocytic routes. In murine A9 fibroblasts, MVM endocytosis occurs through clathrin- and caveolae-mediated endocytosis dependent on dynamin activity. However, in transformed cells, clathrin-independent carriers (CLIC)-mediated internalisation was shown to take place independently of dynamin (Garcin and Panté, 2015). PPV can also enter cells through macropinocytosis (Boisvert et al., 2010). These findings show that even though internalisation by clathrin represents the main entry route of PtPVs, alternative routes are sometimes involved in the viral uptake, in parallel or in certain cells.

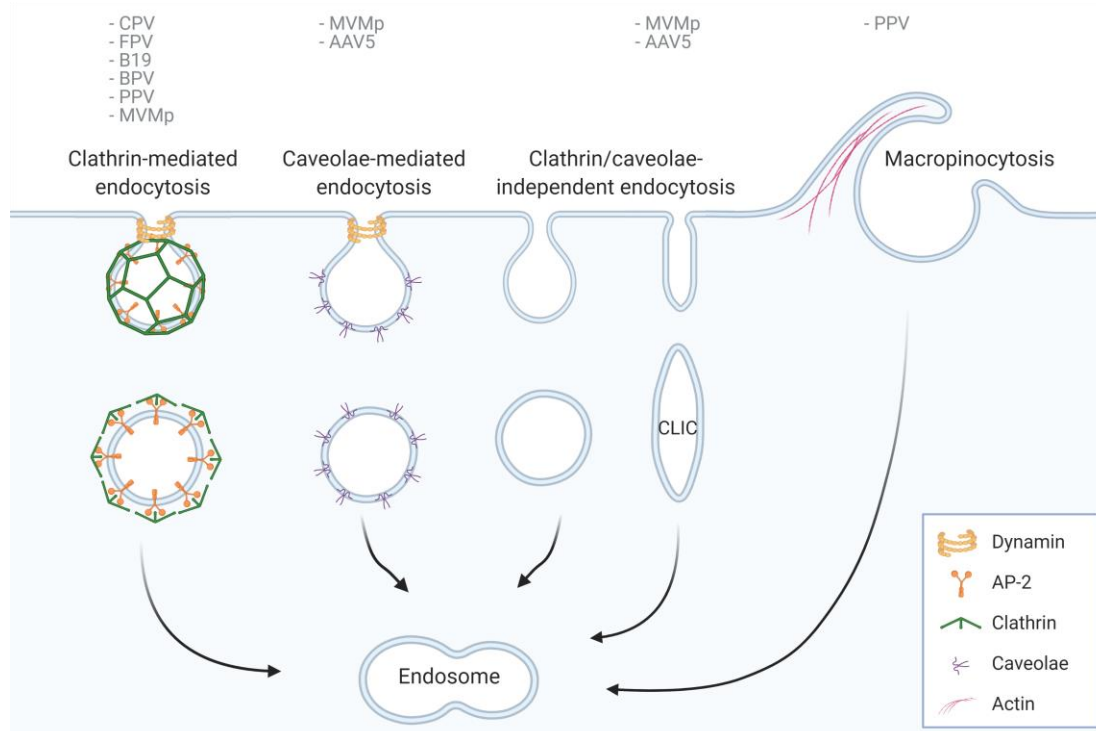


**Figure 1.7. Different endocytic pathways taken by parvoviruses.**

Clathrin-mediated endocytosis (CME) and caveolae-mediated endocytosis are the most common endocytic pathways. In addition, viruses can take other endocytic routes, such as clathrin/caveolae-independent, clathrin-independent carriers (CLIC) or macropinocytosis. At last, vesicles fuse with sorting endosomes. At the top, parvoviruses reported to enter cells through each pathway are listed. AAV: adeno-associated virus; AP-2: adaptor protein 2; B19: parvovirus B19; BPV: bovine parvovirus; CPV: canine parvovirus; CLIC: Clathrin-independent carriers; FPV: feline parvovirus; MVMp: minute virus of mice prototype; PPV: porcine parvovirus. Refer to text for further details. This figure was created with BioRender.com.

Subsequently, the vesicle is released into the interior of the cell, uncoats and typically fuses with an endosome (McMahon and Boucrot, 2011) (Figure 1.8). However, endosomal trafficking of PtPV virions was suggested to be a slow process, with endosomal escape being the limiting factor of MVM nuclear translocation. The viral capsid slowly undergoes conformational changes in the VP1 protein driven by the lysosomal acidic pH. As a result, the PLA<sub>2</sub> enzymatic domain of VP1 is exposed and leads to the digestion of the endosomal membrane, facilitating the release of virus particles from the late endosome to the cytoplasm (Cotmore and Tattersall, 2007, Suikkanen et al., 2003, Cnaan et al., 2004, Zádori et al., 2001, Dorsch et al., 2002). Studies using lysosomotropic drugs have demonstrated that several PtPVs rely on the endosomal acidification for a productive infection, such as CPV (Parker and Parrish,



2000, Vihinen-Ranta et al., 1998, Basak and Turner, 1992), MVM (Mani et al., 2006, Ros et al., 2002), among other parvoviruses.

Incoming PtPV particles are then transported to the nucleus, in the case of MVM assisted by the cytoskeleton and motor proteins like dynein (Suikkanen et al., 2003). In the case of H-1PV, entry into the nucleus starts with the virus interacting with nuclear pore complex proteins, subsequently leading to the exposure of the unique sequence of VP1 containing NLS. VP1 triggers the permeabilisation of the nuclear membrane, ultimately causing the amplified calcium efflux in the nuclear periphery and the activation of PKC- $\alpha$  and cyclin-dependent kinase 2 (cdk2), a central factor governing the structure of the nuclear envelope. These kinases induce hyperphosphorylation of lamins, the components of the nuclear matrix, causing depolymerization and transient nuclear disruption (Porwal et al., 2013).

The mechanism and exact time where PtPVs undergo uncoating (prior, during or after entry into the nucleus) is not well defined. There is evidence that viral capsids stay assembled in the cytoplasm and enter the nucleus intact. Indeed, CPV infection is prevented by neutralising antibodies that recognise intact capsids in the cytoplasm and nucleus (Vihinen-Ranta et al., 2000). Research indicates that PtPV DNA is most likely pushed out from intact capsids, as different treatments were able to expose viral DNA without causing complete capsid disassembly (Cotmore et al., 1999). In this manner, the 3' terminal hairpin is left accessible to prime DNA synthesis, while the 5' end is unreachable and remains attached to the capsid (Cotmore et al., 2010).

#### **1.2.4 Replication and egress**

Similarly to most DNA viruses, PtPVs replicate in the nucleus making extensive use of the cellular replication machinery. The virus remains silent waiting for the host cell to enter S-phase in order to begin viral DNA replication (Cotmore and Tattersall, 2005). The replication process involves the conversion of viral ssDNA into double-stranded DNA (dsDNA) intermediate which permits subsequent transcription of viral messenger RNA (mRNA). Thereafter, replication of the viral genome occurs through a complex “rolling hairpin” mechanism (Berns, 1990). This process integrates several cellular proteins (including the replicator protein A (RPA) and cyclin A (Christensen

and Tattersall, 2002, Bashir et al., 2000)) along with a large group of transcription factors which activates the P4 promoter and lead to the expression of NS proteins (Deleu et al., 1999) (see also sub-section 1.3.1). After translation of NS1 in the cytoplasm, it travels into the nucleus to drive viral DNA replication and *VP* gene unit transcription (Cotmore and Tattersall, 2007). Once the structural proteins are produced in the cytoplasm and imported to the nucleus, the progeny virions are assembled (Lombardo et al., 2000, Lombardo et al., 2002) and actively released to the cytoplasm (Eichwald et al., 2002, Maroto et al., 2004, Miller and Pintel, 2002). At last, progeny virions are trafficked *via* the endoplasmic reticulum, passing through the Golgi to the plasma membrane, while undergoing post-assembly modifications essential for infectivity (Bär et al., 2008, Bär et al., 2013).

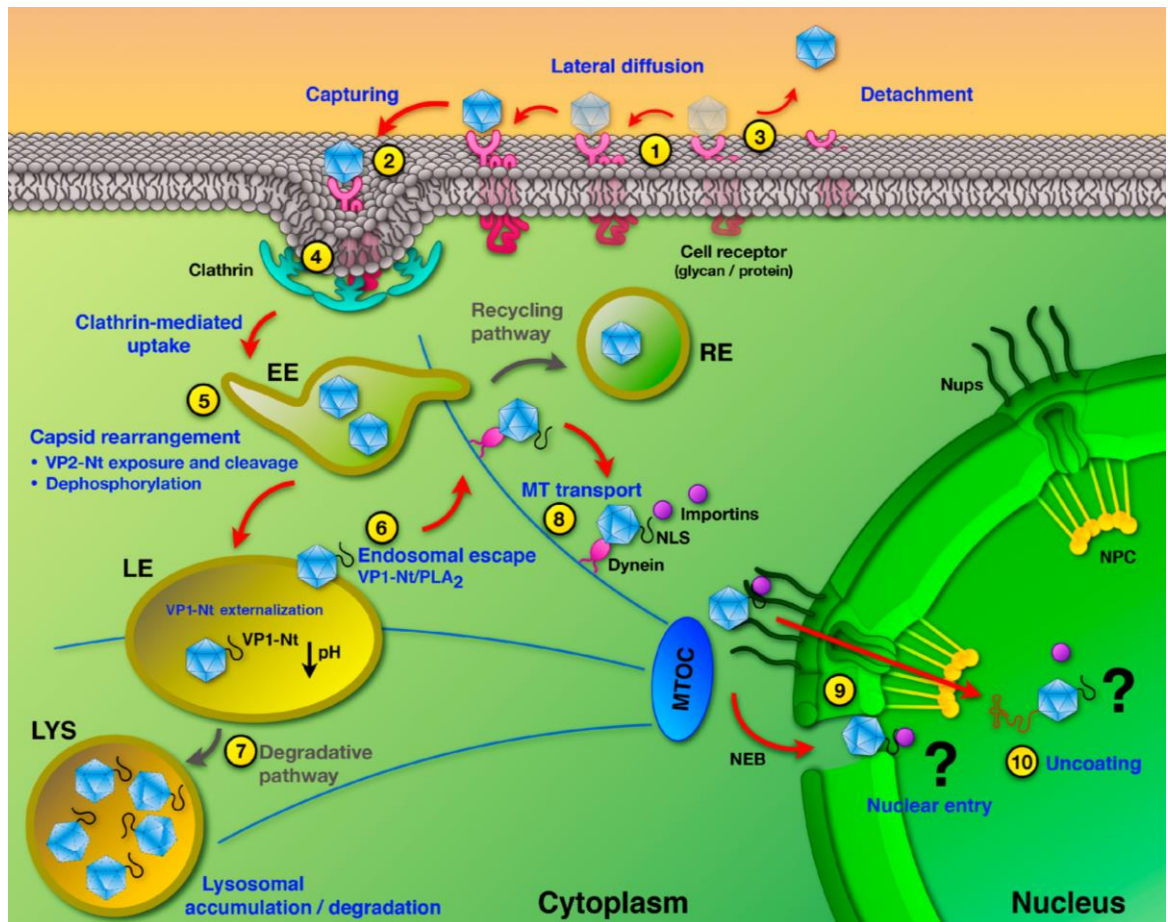


**Figure 1.8. Protoparvovirus life cycle, from cellular binding to reaching the nucleus.**

(1) Initially, PtPV capsids bind to receptor(s) on the cell surface. (2) After lateral diffusion, viral capsids are taken into pre-formed/forming clathrin pits. (3) Alternatively, viral capsids may detach from their receptors. (4) Viral capsids are internalised through CME and subsequently, (5) follow the endocytic route in which the acidic pH and enzymes trigger structural changes in the virus capsid. (6) These structural rearrangements lead to the exposure of VP2-Nt, and subsequently to VP1-Nt. Usually, only a small percentage of virus particles manage to escape the endosomal membrane *via* VP1-encoded phospholipase A2 activity. (7) On the other hand, many incoming virus particles fail to escape from endosomes and end up accumulating in the degradative lysosomes. (8) In the cytoplasm, PtPV particles take advantage of the cellular cytoskeleton and motor proteins to make their way to the nucleus. (9) Entry *via* nuclear pore or permeabilization of the nuclear envelope have both been suggested to be the mechanisms through which the virus and/or the genome enters the nucleus. (10) The timing and site of capsid uncoating are also not known. However, it has been proposed that viral capsids enter the nucleus intact, and the uncoating would occur upon interaction with the nuclear pore complex (NPC) proteins and/or after nuclear entry. Retrieved from (Ros et al., 2017).

## 1.3 H-1PV, Bench to Bedside and Back Again

In this section, the major discoveries regarding the main cellular factors involved in the H-1PV life cycle and the mechanisms underlying virus-induced cancer cell death are reported. Importantly, these studies set the foundation for the recent clinical trials in glioblastoma and pancreatic carcinoma.

### 1.3.1 Determinants of parvovirus infection

Even though parvoviruses were isolated from transplanted human tumours ([Toolan et al., 1960](#)), following studies quickly disregarded the virus to be oncogenic. Instead, they were found to present a natural tropism towards cancer cells and to spare healthy cells ([Toolan, 1961](#), [Rommelaere and Cornelis, 1991](#)). The oncoselectivity observed is a complex phenomenon mostly due to various factors at different steps of the virus life cycle which are underrepresented in non-tumour cells ([Angelova et al., 2015](#)) (Figure 1.9). Part of these factors are not solely present in tumours, but instead characteristic of actively proliferating cells. A pertinent example is related to the S-phase dependence: the cyclin A/CDK2 complex is required for viral genome replication, as well as the E2F family of transcription factors for activation of the early P4 viral promoter ([Bashir et al., 2001](#), [Deleu et al., 1999](#)). PtPVs possess a limited coding capacity and are unable to make quiescent cells undergo S-phase ([Weitzman, 2006](#), [Bashir et al., 2000](#)). Therefore, since transformed cells often skip growth control and are constantly in proliferation, oncolytic PtPVs replicate in these cells more efficiently. Cell migration, which is a common feature of aggressive tumours, was recently demonstrated to promote MVM uptake in cancer cells ([Garcin and Panté, 2014](#)).

Other factors are inherently more specific for cancer cells, resulting from aberrant overexpression or atypical activation due to (epi)genetic changes. It is known that H-1PV life cycle is dependent on the activity of PKC $\alpha$  and CDK1, responsible for nuclear envelope breakdown to promote virus translocation into the nucleus ([Porwal et al., 2013](#)). At the level of viral gene expression, the Ets and ATF transcription factors were described to activate the early P4 MVM promoter ([Perros et al., 1995](#), [Fuks et al., 1996](#)). Additionally, while PKC $\eta$ /Rdx complex formation and simultaneous PDK1

phosphorylation represent a hallmark of highly aggressive brain tumours, these also favour H-1PV amplification and NS1-induced cell death (Bär et al., 2015). As well, high-mobility group box protein 1 (HMBG-1) was shown to initiate MVM DNA amplification from the right-hand viral origin (Cotmore and Tattersall, 1998, Cotmore and Tattersall, 2005). Still at the viral replication level, ATM kinase-mediated DNA damage response was demonstrated to promote MVM replication and virus-induced cell cycle arrest (Adeyemi et al., 2010). Another example concerns the Raf kinase isoforms, which are often overexpressed, activated, or mutated in cancer cells (Leicht et al., 2007). At the level of progeny virion assembly, Raf-1 kinase was found to phosphorylate VP proteins of MVM, an important step to further import these intermediates into the nucleus for capsid assembly (Riolobos et al., 2010). Proteins like XPO1, PKB, PKC and Radixin are implicated at various steps concerning MVM viral maturation and egress (Bär et al., 2008, Nüesch et al., 2009, Eichwald et al., 2002)

Some factors are shown to act as direct binding partners of PtPV proteins, such as cellular transcription factors [TATA binding protein (TBP), general transcription factor 2A (TFIIA), and SP1/3] or replication factors (RPA) (Lorson et al., 1998, Krady and Ward, 1995, Christensen and Tattersall, 2002). Some other factors are not found in complexes with PtPV proteins, but instead, come together in certain areas of infected cells. Particularly, factors of the cell DNA replication machinery (e.g. RPA, POLA1/POLa, PCNA, and RF-C) and DNA damage response (e.g. RPAP32,  $\gamma$ H2AX, NBS1-P, and ATM) are recruited to subnuclear viral replication centres called APAR bodies (Bashir et al., 2001, Adeyemi et al., 2010, Ruiz et al., 2011). As a result, this redistribution is thought to support PtPV multiplication and promote host DNA synthesis shutoff.

Interferon is another cellular feature that is considered to have a role in oncotropism. Regarding MVM, the virus showed to be able to counteract the production of type I interferon in transformed cells, whereas it failed to do so in normal cells (Grekova et al., 2010). However, the sensitivity of PtPVs to interferons remains controversial. PtPV infection (including of H-1PV) failed to induce type I interferon production in several human cancer cells, as well as in normal human cells (Paglino et al., 2014, Angelova and Rommelaere, 2019).

Altogether, the aforementioned highlights only explain in part the PtPV oncrotropism, and additional studies are needed to fully understand why these viruses are oncrotropic.

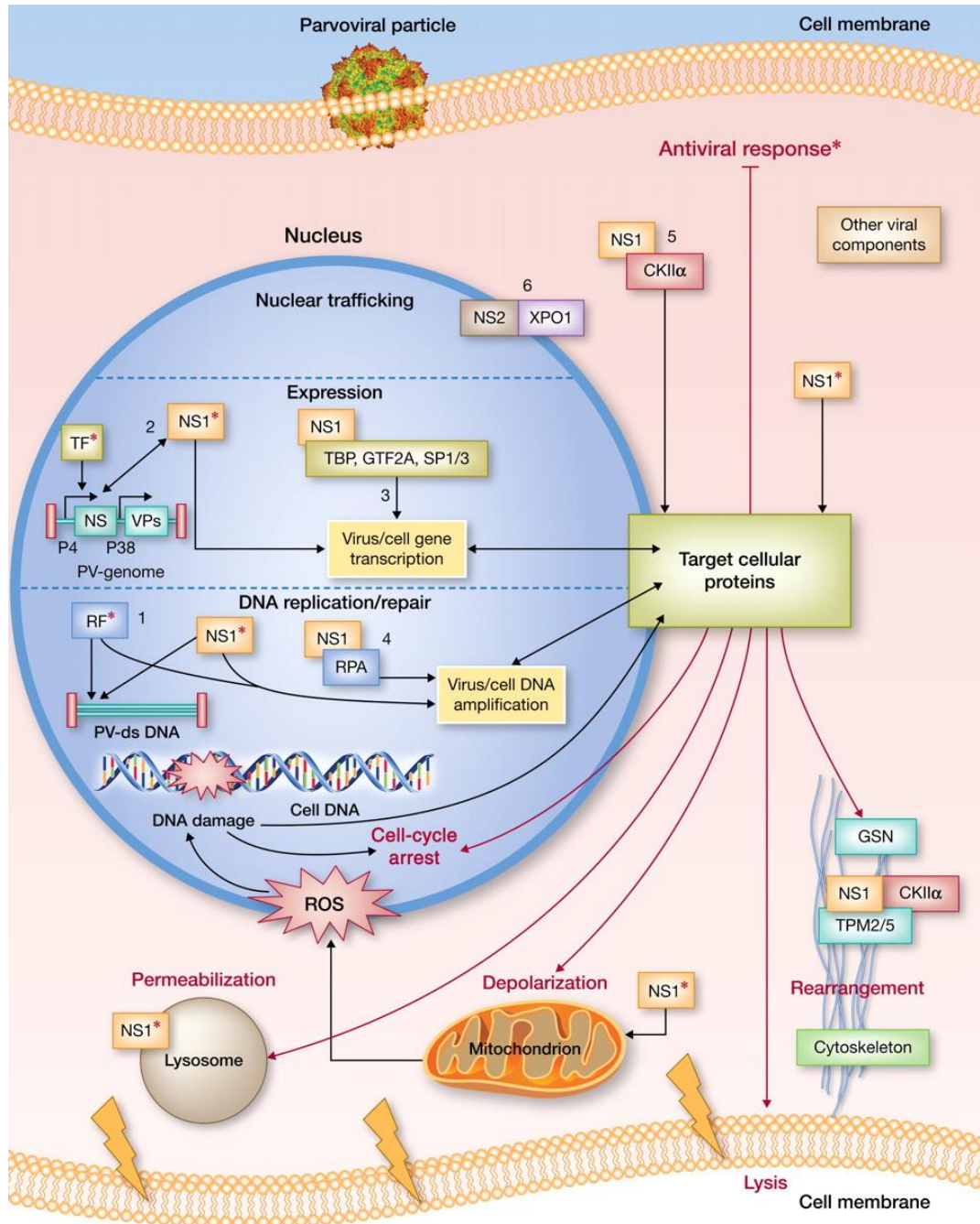


**Figure 1.9. Cell disturbances induced upon parvovirus infection.**

Parvovirus replication occurs in the nucleus and strictly depends on factors present during the cellular S-phase. Conversion of viral single-stranded into double-stranded DNA is carried out by RFs under the control of cyclin A. Thereafter, E2F and transcription factors (ATF/CREB, ETS, and NF-Y) turn on the parvoviral early P4 promoter, responsible for the expression of NS1 and NS1 non-structural proteins. In

turn, NS1 transactivates the late p38 promoter which leads to expression of structural genes. Besides, NS1 interacts directly with factors of the DNA replication (RPA 1-3) and transcription (TBP, TFIIA, and SP1) machineries to promote parvoviral DNA replication/transcription and to disturb DNA/RNA metabolic processes. Interactions with NS1-CKII and NS2-XPO1 mostly interfere with cell signalling and nuclear export, respectively. As a result, these events cause oxidative stress, DNA damage, cell-cycle arrest, cytoskeleton structure rearrangements, mitochondrial membrane depolarization, and/or lysosome permeabilisation, ultimately leading to cell death. Of note, expression of NS1 alone is sufficient to cause cell death. The oncoselectivity of parvoviruses is mainly attributed to two features: the presence of permissive factors and the flawed antiviral response observed in cancer cells (indicated with \*). Abbreviations: ds, double-stranded; GSN, gelsolin; GTF2A/TFIIA, general transcription factor 2A; RF, replication factor; SP1/3, Sp1/3 transcription factor; TBP, TATA binding protein; TF, transcription factor; TPM2/5: tropomyosin 2/5; VP, PV capsid proteins; XPO1, exportin 1 (CRM1 yeast homolog). Retrieved from (Nüesch et al., 2012).

### 1.3.2 Parvovirus-induced cell death

PtPVs usurp cellular mechanisms and interfere with cellular signalling cascades in order to induce cell growth arrest and cytotoxicity (Figure 1.9). Assessment of PtPV oncolytic activity *in vitro* and *in vivo* has been primarily performed with H-1PV and MVM. These viruses have been showing oncolytic and oncosuppressive potential in a broad range of cancer types, including glioblastoma (GBM) (Herrero y Calle et al., 2004), pancreatic ductal adenocarcinoma (Li et al., 2013a), cervical carcinoma (Li et al., 2013a), lung cancer (Marchini, Bonifati & Rommelaere, unpublished results), melanoma (Moehler et al., 2011), gastric cancer (Liu et al., 2005), neuroblastoma (Lacroix et al., 2010), breast cancer (Muharram et al., 2010), hepatoma (Moehler et al., 2001), sarcoma (Lacroix et al., 2018, Geiss et al., 2017), Burkitt lymphoma (Angelova et al., 2009a), colon cancer (Malerba et al., 2003), and medulloblastoma (Lacroix et al., 2014) (Figure 1.10).

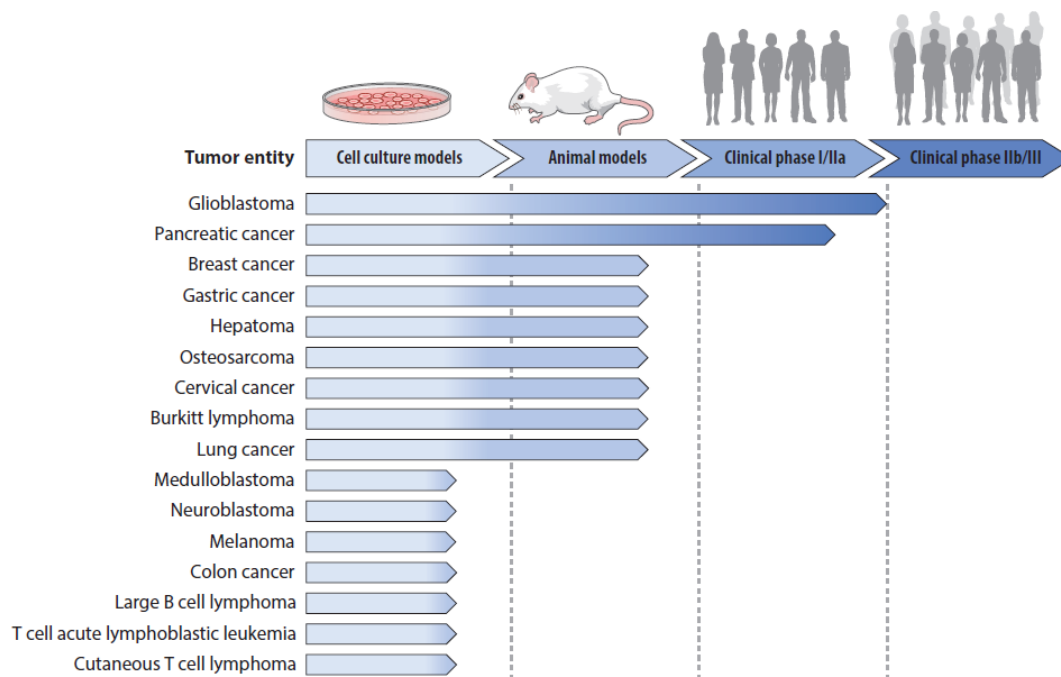


**Figure 1.10. Current status of protoparvovirus-based studies in various models.**

Tumour entities already tested for susceptibility to PtPV treatment are listed. These studies collectively show that PtPVs have a broad tropism. Retrieved from (Hartley et al., 2020).

Cell death resulting from an oncolytic virus infection can take place through various mechanisms and pathways simultaneously. With respect to PtPV, viral infection has been demonstrated to lead to great disturbances in different organelles of the host cell. While CPV was shown to depolarise the mitochondria during infection (Nyky et al., 2014), PPV induces irreversible endoplasmic reticulum stress through SAT viral protein (Mészáros et al., 2017). Moreover, H-1PV is able to induce nuclear envelope disintegration (Porwal et al., 2013), and disturb the lysosomal membrane leading to the release of cathepsin B into the cytosol (Krämer, Hristov & Marchini, unpublished results). MVM was described to disrupt the host cell cytoskeleton actin and tropomyosin filaments through casein kinase IIa (CKIIa)-mediated phosphorylation of NS1 (Nüesch et al., 2005, Bär et al., 2008, Nüesch and Rommelaere, 2007, Daeffler et al., 2003). This is thought to have a greater impact on tumour cells, which lack the most rigid actin or the abundant levels of tropomyosin 1 (Bhattacharya et al., 1990). In the long run, the abovementioned processes lead to the activation of a stress response and cell death. The specific cell death mechanism triggered depends on the parvovirus and the cellular physiological status. For example, NS1 of H-1PV can



induce cell cycle arrest in G2 phase (Hristov et al., 2010) and trigger apoptosis (Ohshima et al., 1998, Hristov et al., 2010, Li et al., 2013a), necrosis (Chen and Qiu, 2010, Ran et al., 1999), or cathepsin-mediated lysosomal cell death (Di Piazza et al., 2007). This way, H-1PV manages to overcome a possible resistance of cancer cells to a particular cell death pathway. Furthermore, H-1PV triggers oxidative stress *via* accumulation of reactive oxygen species (ROS) and reactive nitrogen species (RNS), culminating in cell death (Hristov et al., 2010, Li et al., 2013a). However, the magnitude of the oxidative stress is largely dependent on the antioxidative capacity of the host cell, which can also account for the discrepancies in the virus-induced cell death pathways. While cells that manage to neutralise ROS/RNS usually die through controlled cytochrome c-mediated apoptosis, those cells which tolerate more damage likely undergo necrosis (Scherz-Shouval and Elazar, 2007).

PtPVs have the potential to trigger an immunogenic cell death associated with the release of pathogen- and danger-associated molecular patterns (PAMPs, DAMPs) and tumour-associated antigens (TAAs), leading to potent and long-lasting anti-cancer immunity (Figure 1.11). In pancreatic cancer cells, H-1PV alone induced the release of HMGB-1, a hallmark of immunogenic cell death (Angelova et al., 2014). In melanoma cells, H-1PV infection provoked a high and long-lasting release of heat-shock protein 72, thereby enhancing tumour immunogenicity (Moehler et al., 2003). Consequently, an immunogenic cell death leads to the activation of the dendritic cells (Moehler et al., 2005), a feature also observed in glioma cells upon H-1PV and MVM infection (Grekova et al., 2012, Angelova and Rommelaere, 2019). Thereafter, the cascade involves the release of pro-inflammatory cytokines such as type I interferons, tumour necrosis factor alpha (TNF- $\alpha$ ), and interleukin (IL)-6, triggering natural killer (NK) and T cell activation. The latter are responsible for killing cancer cells by secreting perforin and granzyme B (Geletneky et al., 2017, Bhat and Rommelaere, 2013, Bhat et al., 2011). Indeed, the immune system is crucial for full therapeutic potential (Angelova and Rommelaere, 2019, Geletneky et al., 2015, Marchini et al., 2019). Cytotoxic T cells are key to fight metastases of Morris hepatoma cells in rats administered with a therapeutic vaccine consisting of H-1PV-infected autologous tumour cells (Raykov et al., 2007). Likewise, antibody depletion of cytotoxic T cells in an immunocompetent rat GBM model markedly reduced H-1PV oncosuppressive properties (Geletneky et al., 2010b). NOD SCID mice with xenografted human

pancreatic adenocarcinoma, later reconstituted with autologous dendritic cells and T cells primed with H-1PV-infected cell lysates caused a strong inhibition of tumour development (Grekova et al., 2014).

Overall, the reasons behind the growing interest in H-1PV as an anti-cancer agent lie within several aspects. Firstly, H-1PV offers a remarkable safety profile. The virus is not a human pathogen and was never associated with any human disease. Secondly, since the rat is the natural host of H-1PV, humans have generally not been exposed to it, which prevents the quick elimination of the virus inoculum by a pre-existing antiviral immunity (Allaume et al., 2012). H-1PV presents an oncolytic oncosuppressive potential extensively shown in numerous pre-clinical models, including tumours resistant to standard therapies (Hartley et al., 2020). H-1PV-induced cell death is immunogenic with ability to elicit strong anticancer immune responses (Marchini et al., 2019). Last but not least, the fact that H-1PV lacks an envelope and is currently the smallest oncolytic virus under development, facilitates the crossing of physiological barriers such as the brain-blood barrier and the virus distribution within the tumour bed. Together, these constituted the grounds to proceed to clinical evaluation (Bretscher and Marchini, 2019).

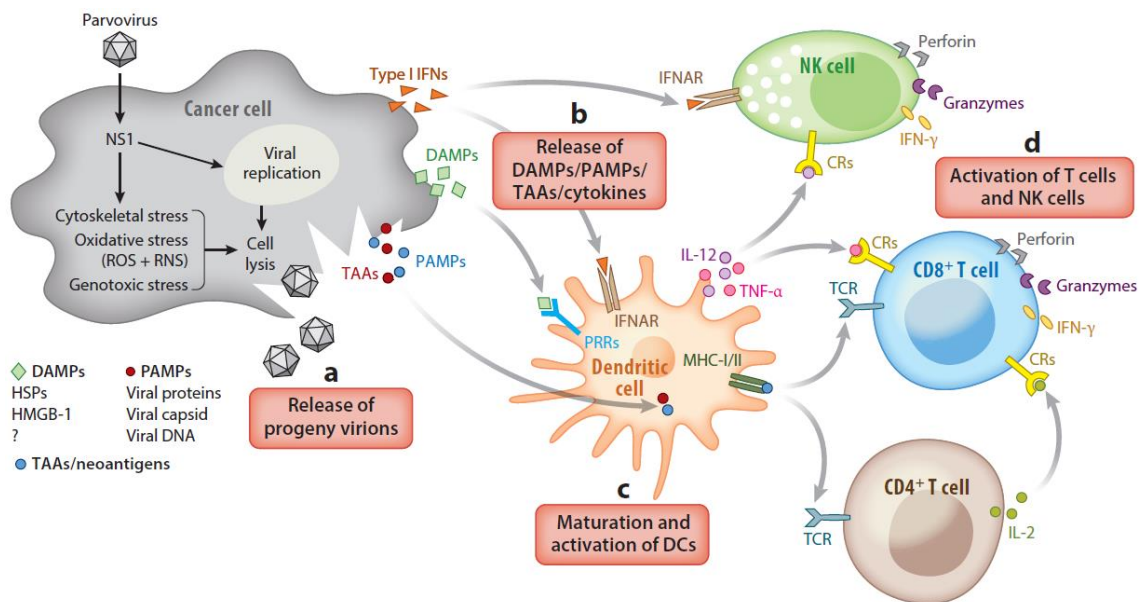


**Figure 1.11. Oncolytic parvovirus-induced (immunogenic) cell death.**

(A) Parvovirus infection triggers cytoskeletal stress, production of reactive oxygen/nitrogen species (ROS/RNS) and the DNA damage response. These events lead to cell lysis and release of progeny virions. (B) Cell lysis leads to release of

damage-associated molecular patterns (DAMPs), including heat shock proteins (HSPs) and high-mobility group box protein 1 (HMGB-1); pathogen-associated molecular patterns (PAMPs) including viral nucleic acid, proteins, and capsids; tumour-associated antigens (TAAs); and pro-inflammatory cytokines such as type I interferons. (C) The listed factors promote the maturation and activation of dendritic cells (DC) and natural killer cells (NK). PAMPs are recognised by pattern recognition receptors (PRRs) and type I interferons by interferon- $\alpha$  receptors (IFAR) both expressed by DCs. Consequently, DCs generate pro-inflammatory cytokines (including interleukin (IL)-12 and tumour necrosis factor (TNF)- $\alpha$ ), which are recognised by cytokine receptors (CR) on T and NK cells. (D) Mature DCs proceed to antigen cross-presentation *via* the major histocompatibility complex (MHC) to T cells to promote their activation and expansion. Ultimately, the release of perforins, granzymes and cytokines by T cells and NK cells mediates the lysis of cancer cells.

### 1.3.3 Clinical evaluation of H-1PV treatment

The first clinical use of H-1PV in humans dates back to 1965. Under compassionate use, two young patients with advanced disseminated osteosarcoma were treated intramuscularly with H-1PV (Toolan et al., 1965). Virus treatment was well tolerated, and patients developed an extensive viremia and subsequent virus neutralising antibodies. Later on, a phase I clinical study was carried out in France in 1993 (Le Cesne et al., 1993). A group of 12 patients with skin metastases resulting from various types of solid tumours were submitted to an intralesional dose-escalation H-1PV treatment. The virus treatment took place every 10 days, and seroconversion was observed 10-15 days after the first injection. Apart from a low-grade fever in 3/12 patients, no other significant H-1PV-induced side-effects were observed, providing evidence that H-1PV treatment is safe. Remarkably, two patients stabilised the disease throughout the observation period, and patients who had been injected at a location far from the metastasis showed traces of viral genomes/proteins.

Thanks to the encouraging progress it had been made so far, the first phase I/IIa clinical trial was launched in 2015 to treat 18 patients with recurrent GBM (ParvOryx01) (Geletneky et al., 2017, Geletneky et al., 2014a, Geletneky et al., 2014b). The primary goals of this study concerned safety, tolerability, pharmacokinetics, and maximum tolerated dose. Additionally, tissue samples were harvested during tumour resection for later analysis of viral components and tumour microenvironment assessment. Firstly, half of the total viral dose was administered either intravenously or intratumourally prior to tumour resection. Ten days after virus

treatment, the second half of the viral dose was administered into the wall of the resection cavity. As a result, the ParvOryx01 trial successfully proved that H-1PV is safe and well tolerated, with risk assessment excluding a maximum tolerated dose reached or virus spread from person to person. As anticipated from studies in rats (Geletneky et al., 2010b), analysis of post-treatment tumour tissues revealed that H-1PV was able to cross the blood-brain barrier and spread widely through the tumour after intravenous administration. Patients submitted to H-1PV treatment also presented markers of virus replication, microglia/macrophage activation and cytotoxic T cell infiltration within the tumour, with scarce T regulatory cells, suggesting a H-1PV-induced immunogenic stimulus. Consequently, the treatment led to an improved progression-free survival and median overall survival in comparison with historical recurrent GBM cases (noncontemporary controls, a meta-analysis of the survival trends of GBM patients treated with all different modalities). Given that the rat is the natural host for H-1PV, humans have no pre-existing immunity against the virus and therefore, the therapeutic window of H-1PV is supposed to be larger in comparison to that of other oncolytic viruses based on human pathogens. Nevertheless, seroconversion was later detected in patients in a dose-dependent manner after 10 days from administration (Geletneky et al., 2017). Taken as a whole, the outcome remains highly favourable and provides a new stimulus towards further clinical development.

In a later attempt to enhance H-1PV efficacy, patients suffering from GBM were treated in a compassionate use program with a combination of H-1PV followed by angiogenesis inhibitor (bevacizumab), and some co-treated with PD-1 checkpoint blockade (nivolumab) and a histone deacetylase inhibitor (valproic acid) (Geletneky et al., 2018, Geletneky et al., 2016). At last, seven out of nine patients presented an objective tumour response, with two of these showing a complete (albeit temporary) remission and five a partial tumour reduction.

More recently, another clinical trial was launched, this time to treat inoperable metastatic pancreatic cancer with a co-treatment of H-1PV and gemcitabine (Hajda et al., 2017). Seven patients with at least one hepatic metastasis were first treated intravenously with 40% of the total viral dose, while the remaining dose was later administered intra-metastatic followed by gemcitabine treatment. ParvOryx02 presented additional endpoints regarding the immunogenic potential of H-1PV, comprising the assessment of tumour-infiltrating cells as well as cytokines released

upon virus treatment. The ParvOryx02 trial was completed in the first trimester of 2019 and the entire assessment has not been disclosed yet. As of now, the excellent safety and tolerability of the treatment was confirmed. Additionally, two out of seven patients responded to the treatment by showing clear changes in the tumour microenvironment, induction of specific immune responses, as well as extended overall survival (Hajda et al., 2017).

#### **1.3.4 Strategies to improve H-1PV anticancer activity**

H-1PV has successfully demonstrated *in vitro* and *in vivo* its broad tumour-suppressive potential. In early phase clinical trials, H-1PV treatment showed to be safe and well-tolerated in glioma and pancreatic carcinoma patients. Virus treatment was also associated with first evidence of efficacy, including ability to cross the blood-brain barrier after intravenous delivery; effective distribution and expression in the tumour bed; immuno-conversion of tumour microenvironment; and improved patient overall survival in comparison to historical controls (Ungerechts et al., 2017, Geletneky et al., 2017). However, similar to other oncolytic viruses, H-1PV treatment was unable to eradicate the tumour in patients at the regimes used (Hartley et al., 2020). Therefore, there is an urgent need to improve the clinical outcome of H-1PV oncolytic therapy. The main approaches being currently followed are summarised in Figure 1.12: combination therapy, development of second-generation viral vectors, and characterisation of the H-1PV life cycle. In the following sub-sections, I report some examples of success within each strategy.

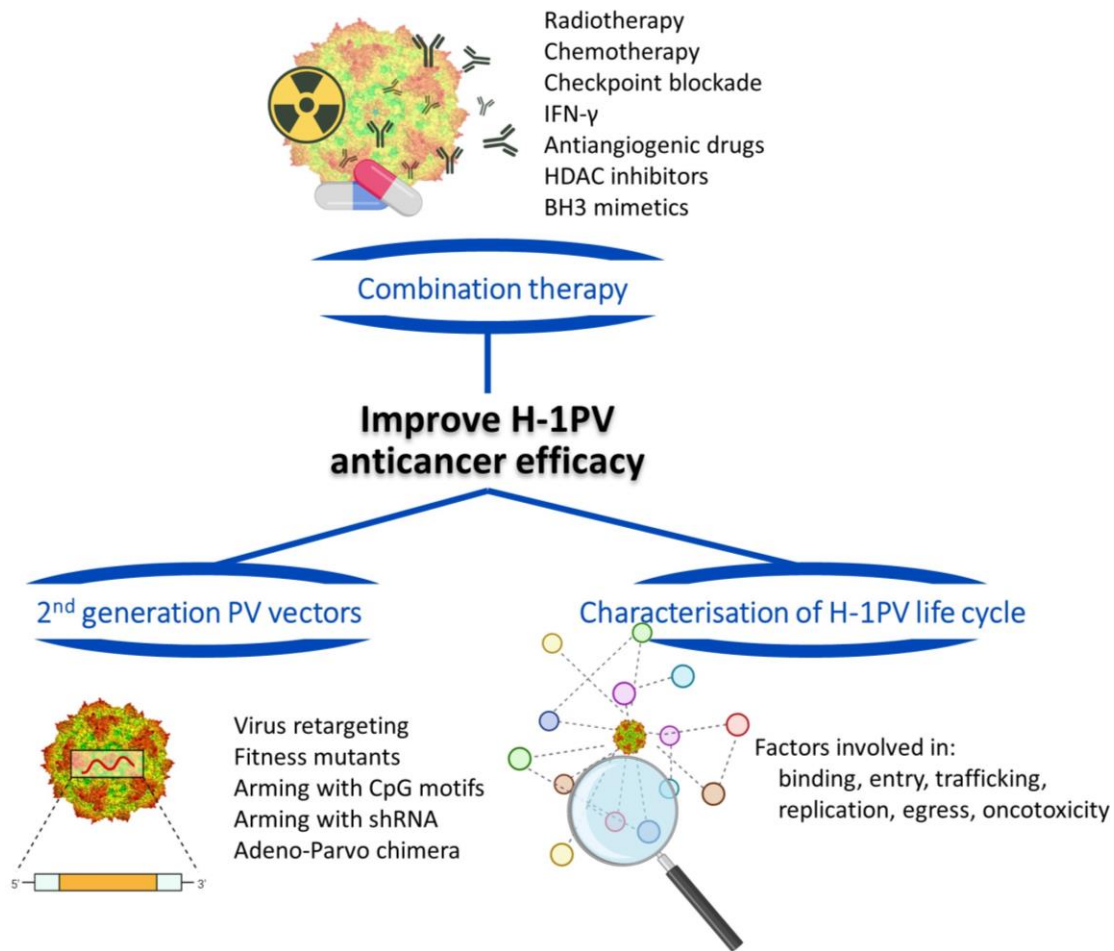


**Figure 1.12. Strategies to improve H-1PV anticancer efficacy.**

There are three main strategies being adopted to improve H-1PV anticancer efficacy: combination therapy with other treatment modalities, development of second-generation parvovirus vectors, and characterisation of H-1PV life cycle (of particular relevance to this study). The latter may contribute to identify permissive factors (positive or negative modulators) for a successful virus infection. This knowledge can reveal biomarkers to help find patients who may respond better to H-1PV-based therapies. This figure was adapted from (Hartley et al., 2020). Abbreviations: Ad, adenovirus; H-1PV, H-1 parvovirus; HDAC, histone deacetylase; IFN, interferon; PV, parvovirus; shRNA, short hairpin RNA.

### 1.3.5 Combination therapy

A human tumour is described as a (epi)genetically and phenotypically heterogeneous population of (cancer) cells (Lawrence et al., 2013). It is, therefore, unlikely that an oncolytic virus could infect and destroy a widespread disseminated disease entirely in every patient. An encouraging approach to improve virus anticancer efficacy relies on combining different therapeutics (thoroughly reviewed in (Angelova et al., 2021)).

Parvo-virotherapy has been combined with radiotherapy (Geletneky et al., 2010a), chemotherapy (Moehler et al., 2011, Li et al., 2013a, Angelova et al., 2009b), immunotherapy (Goepfert et al., 2019, Geletneky et al., 2018), histone deacetylase inhibitors (Marchini et al., 2013, Marchini et al., 2016), BH3 mimetics (Marchini et al., 2015b), and interferon-gamma (Grekova et al., 2011).

Gemcitabine (cytostatic) (Angelova et al., 2009b, Angelova et al., 2014, Hajda et al., 2017) and valproic acid (anti-epileptic) (Li et al., 2013a) are two drugs already available on the pharmaceutical market which have demonstrated to synergise with H-1PV in the fight against pancreatic cancer. In GBM, the first clinical indications of improved anticancer efficacy were observed with a co-treatment of H-1PV + bevacizumab + nivolumab, in addition to valproic acid (mentioned in sub-section 1.3.3) (Geletneky et al., 2018, Geletneky et al., 2016).

### **1.3.6 Development of second-generation parvovirus vectors**

Another strategy which has been implemented to improve H-1PV anticancer efficacy relies on developing improved versions of wild-type H-1PV, by selecting fitness virus mutants, modifying the virus capsid, arming the virus with immune stimulators / RNA interference cassettes, or even generating chimeric viruses.

Naturally occurring parvovirus variants sporadically occur due to spontaneous genetic modifications. A H-1PV variant with a 114 nucleotide in-frame deletion was isolated from a newborn human kidney cell line during a routine viral plaque purification (Faisst et al., 1995). Yet, the deletion turned out to enhance viral fitness by improving nuclear export and spreading in comparison to wild-type H-1PV (Weiss et al., 2012).

H-1PV can also be subjected to genetic engineering. Given that H-1PV enters in most normal cells (even though these infections are not productive (Angelova et al., 2015)), there was an attempt to get the virus to target cancer cells more specifically. For this purpose, residues in the viral capsid were altered, rendering H-1PV unable to recognise the SA present at the cell surface. Thereafter, a RGD-4C peptide was inserted in the dimple region of the H-1PV capsid to force the virus to bind to  $\alpha\beta3$  and  $\alpha\beta5$  integrins (Allaume et al., 2012), which are frequently overexpressed in cancer cells and tumour vasculature. Another example concerns the insertion of CpG

motifs, which are well described to have immunostimulatory activity, into the untranslated region of the H-1PV *VP* gene unit (Raykov et al., 2008). Indeed, modified viruses presented enhanced immunogenicity in *in vitro* and *in vivo* studies (Grekova et al., 2014).

The creation of chimeric viruses was also adopted to overcome some of limitations encountered when using wild-type H-1PV, namely its limited packaging capacity. To this end, a novel adenovirus-parvovirus (Ad-PV) chimeric virus was generated through insertion of an engineered H-1PV genome into the Ad5 genome. The Ad acts as a carrier to efficiently bring the H-1PV genome into cancer cells, from which progeny virions are produced and propagate independently within the tumour bed (El-Andaloussi et al., 2012a). The chimera has several advantages, namely bringing H-1PV specifically to cancer cells (by taking advantage of the experience accumulated about the retargeting of the Ad to cancer cells), bringing the H-1PV genome inside cells which are refractory to H-1PV at the level of binding and/or entry, as well as the possibility of insertion of large transgenes into the Ad backbone to potentiate the ability of H-1PV to kill cancer cells and trigger more robust anticancer immune responses.

### **1.3.7 Characterisation of H-1PV life cycle**

The strategy followed in this thesis primarily relates to the identification of host cell factors modulating H-1PV life cycle. A deeper understanding of H-1PV life cycle can help identifying biomarkers to predict which patients would most likely benefit from virus treatment. In addition, this knowledge can provide hints on which drugs could be combined with the virus in order to enhance its oncotoxicity (Hartley et al., 2020).

The earliest and arguably the most important stage of the virus infection occurs when a virus particle encounters a host cell and interacts with surface receptors as a means to enter into the cell. In the case of H-1PV, SA has been shown to be an essential component for cell attachment, a property shared with other PtPVs (Halder et al., 2013b, Allaupe et al., 2012). In order to identify host proteins that could be involved in the binding and/or entry of H-1PV, our laboratory recently performed a druggable genome-wide siRNA library screening to identify putative modulators of H-1PV



infection. As a result, laminin- $\gamma$ 1 and galectin-1 were highlighted as potential players in H-1PV life cycle (these results laid the foundation for this study and are described in sub-section 3.1.1).

### ***Laminins***

Laminins are a family of heterotrimeric glycoproteins containing an  $\alpha$ , a  $\beta$  and a  $\gamma$  chain. In humans, there have been described 15 isoforms named after the corresponding combination out of the five  $\alpha$ , four  $\beta$  and three  $\gamma$  chains (Aumailley et al., 2005). The chains are connected *via* disulphide bonds at their C-terminal regions and together make up a triple coiled-coil structure resulting in a “crucifix”-shaped macro-molecule of at least 400 kDa. Laminins are part of the extracellular matrix and are important constituents of the basal lamina, shaping cell differentiation, migration and adhesion (Durbeej, 2010). Laminins are ubiquitously expressed, yet isoforms are typically cell- and tissue-specific (Qin et al., 2017). As well, laminins are heavily glycosylated, and importantly, contain terminal SA residues (Bouchara et al., 1997).

Even though laminins are a component of the extracellular matrix, which acts as a physical barrier to protect tissues from invading pathogens, several microorganisms (including viruses) have been described to hijack laminins as attachment factors (Singh et al., 2012). For instance, human papilloma virus (HPV) type 11 has been demonstrated to bind to laminin-5 (Laminin  $\alpha$ 3 $\beta$ 3 $\gamma$ 2) (Culp et al., 2006). Likewise, laminins were found to participate in VV cell attachment (Chiu et al., 2007). Retroviruses have also been reported to interact with elements from the extracellular matrix. In particular, human immunodeficiency virus type 1 (HIV-1) proteins gp120/160 were shown to bind to the C-terminal heparin-binding domain of laminins, as well as of fibronectin and vitronectin. Yet surprisingly, this interaction was reported to reduce HIV-1 infectivity of CD4<sup>+</sup> T cells (Bozzini et al., 1998). Altogether, these findings indicate that laminin-pathogen interactions play an important role during infection, and while in some cases these are beneficial for the pathogen, some others are detrimental.

## *Galectins*

Besides laminins, the siRNA library screening also revealed the possible involvement of galectins in H-1PV life cycle. In truth, in the past few years, there has been a growing interest in the role of lectin-glycan interactions related to the field of host-microbe interactions. Up to now, 15 galectins have been identified in mammals encoded by the *LGALS* genes, but only 12 have been found in humans (Vasta et al., 2012a). Yet, they are also conserved through evolution across many phyla, namely birds, fish, amphibians, drosophila, nematodes, fungi and sponges (Leffler et al., 2002). All galectins share a highly conserved ~130 amino acid carbohydrate recognition domain (CRD) that interacts with  $\beta$ -galactosides (Di Lella et al., 2011), generally found in N-linked or O-linked glycans. They can also be labelled as S-type lectins given that their stability and carbohydrate binding is dependent on disulphide bonds (Kuroi et al., 2020). However, despite the presence of a highly conserved CRD, galectins present noticeable differences in their binding properties. In fact, galectins can be sub-divided into three groups: prototype, tandem repeat and chimera. In the prototype galectins belong Gal-1, 2, 5, 7, 10, 13, 14 and 15 as monomers, with Gal-1, 2, 11, 13, 14 and 15 able to form homodimers. Tandem repeat-type galectins, namely Gal-4, 6, 8, 9 and 12 have two different CRDs connected by a flexible peptide linker. Gal-3 is the only chimera-type galectin which presents one CRD and one non-lectin domain. Galectins are synthesised in the cytoplasm and accumulate there until they are secreted *via* a poorly characterised pathway. Transport across the plasma membrane may occur through vesicles or direct protein translocation through a poorly characterised pathway, termed as non-classical (Wilson et al., 1989, Elola et al., 2007).

Galectins are multivalent and are able to bind to multiple glycans on the same cell, with the extracellular matrix or even on neighbouring cells (Garner and Baum, 2008, Vasta et al., 2012b, Chen et al., 2014). They are involved in a variety of physiological functions including cell migration, mediation of cell–cell interactions, cell–matrix adhesion, transmembrane signalling, inflammation, and immune response (Johannes et al., 2018). In addition, galectins have been reported to have a broad activity in the modulation of host-microbe interactions. Of particular interest for this thesis, galectins and their role in regulating viral infections have been the subject of numerous reviews recently (Machala et al., 2019b, Wang et al., 2019) as well as of a book chapter (Li et al., 2020). Galectins play a significant role, from initiation of infection and virus

recognition, to modulating the innate and adaptive immune response, which can be attributed to their remarkable ability to crosslink glycosylated receptors and/or viral glycoproteins. To date, Gal-1 (prototype), Gal-3 (chimeric) and Gal-9 (tandem-repeat) have been considered the major regulators of viral infection within the galectin family. While Gal-1 and Gal-3 can promote or inhibit virus infections, Gal-9 usually antagonises the infection (Li et al., 2020) (Figure 1.13). Even so, the specific outcome of these galectin-virus interactions heavily depends on the particular galectin, cell type, pathogen, and the surrounding microenvironment. For instance, Gal-1 was reported to stabilise the binding of HIV to the host CD4 receptor on the surface of T cells by crosslinking CD4 and viral gp120 (Ouellet et al., 2005). On the other hand, Gal-1 inhibits Influenza A virus infection by directly interacting with the viral envelope glycoproteins (Yang et al., 2011). Gal-3 is the only galectin identified up to date to modulate the infection of a PtPV. Indeed, MVM uptake into LA9 mouse cells is facilitated by Gal-3 (Garcin et al., 2015). In contrast, Gal-9 was found to block human cytomegalovirus entry into multiple permissive cell types (Machala et al., 2019a).

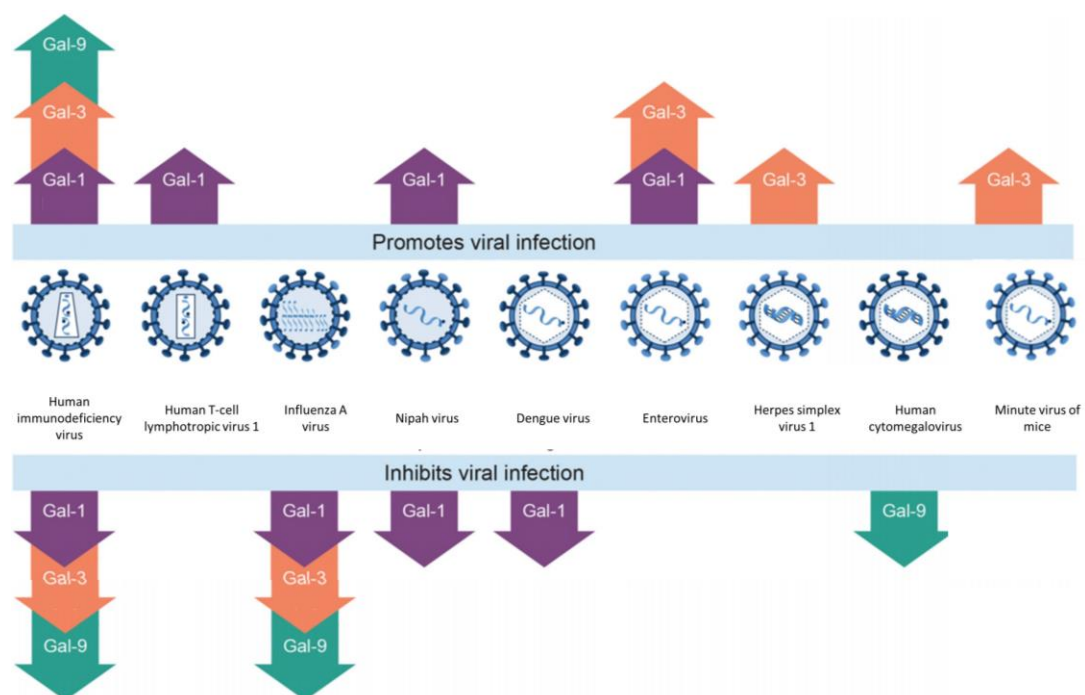


**Figure 1.13. Galectin-1, Galectin-3 and Galectin-9 effect on viral infections.**

Galectins can promote and/or inhibit viral infections. Galectin-1 (purple), galectin-3 (orange) and galectin-9 (green). Arrows pointing up (↑) refer to a promoting role, while arrows pointing downwards (↓) indicate inhibition. Schematic summary adapted from (Machala et al., 2019b).

## 1.4 Research objectives

The ultimate aim of this thesis was to characterise the early steps of H-1PV infection, particularly how the virus binds to the cell membrane and enters into cancer cells. This study builds upon previous results of the laboratory, including the discovery that SA plays a key role in H-1PV infection (Allaume et al., 2012), and the identification of possible modulators of H-1PV life cycle by a siRNA library screening previously performed (described in sub-section 3.1.1.). I particularly focused on those factors which have been described to play a role in mediating cell attachment and entry of a number of microorganisms, including several viruses. The factors identified in the siRNA library screening as putative top-activators of H-1PV infection (i.e. siRNA-mediated silencing of genes which strongly decreased H-1PV transduction) were:

- Laminin  $\gamma$ 1 chain, encoded by the *LAMC1* gene.
- Galectin-1, encoded by the *LGALS1* gene.
- Adaptor protein 2 subunit  $\mu$ 1, encoded by the *AP2M1* gene.

Initially, I participated in the study that demonstrated that laminins, in particular those containing the  $\gamma$ 1 chain, play a pivotal role in H-1PV attachment at the cell surface, and entry into the cells (Kulkarni et al., in press). Nevertheless, most of my work focused on the characterisation of the role of Gal-1 and AP2 $\mu$ 1 in H-1PV infection. More specifically, the main goals of my thesis were:

- i. The confirmation that Gal-1 is a positive modulator of H-1PV life cycle.
- ii. The elucidation of the role of Gal-1 in H-1PV infection.
- iii. The confirmation that AP2 $\mu$ 1 participates in the H-1PV life cycle.
- iv. The characterisation of the endocytic pathways used by H-1PV to enter cancer cells.

## **Chapter 2: Materials and Methods**

### **2.1 Cells**

#### **2.1.1 Cell culture**

The cervical carcinoma-derived HeLa cell line was a gift from Angel Alonso (German Cancer Research Center, Heidelberg, Germany). The pancreatic ductal adenocarcinoma-derived BxPC3 cell line was procured from Tumorbank (German Cancer Research Center). The low-passage-number glioblastoma-derived NCH125 and NCH37 cell lines were given by Karsten Geletneky (Heidelberg University Hospital, Heidelberg, Germany). The glioblastoma-derived U251 cell line was obtained from the National Cancer Institute (NCI; Rockville, MD, USA). Glioblastoma-derived LN308, T98G, and A172-MG were obtained from Iris Augustin's laboratory (German Cancer Research Center). The NCH125 LGALS1 KO and NCH125 CRISPR Control cell lines have been established in this study (see below). All cells were cultured in Dulbecco's modified Eagle's medium (DMEM), supplemented with 10% FBS, 100 units/mL penicillin, 100 µg/mL streptomycin, and 2 mM L-glutamine (all from Gibco, Thermo Fischer Scientific, Darmstadt, Germany) in a humidified incubator at 37 °C.

NB324K cells were obtained from ATCC (LGS Standards GmbH, Wesel, Germany) and cultured in Minimum Essential Medium (MEM) supplemented with 5% FBS, 100 units/mL penicillin, 100 µg/mL streptomycin, and 2 mM L-glutamine.

The 53 cancer lines belonging to the NCI-60 panel were cultured in Roswell Park Memorial Institute medium (RPMI) supplemented with 10% FBS and 2 mM L-glutamine.

All cancer cell lines were regularly tested for mycoplasma contamination using a VenorGEM OneStep Mycoplasma contamination kit (Minerva Biolabs, Berlin, Germany) and tested by a human cell authentication test (Multiplexion GmbH, Mannheim, Germany).

### **2.1.2 Generation of *LGALS1* knockout cell line**

CRISPR/Cas9-mediated knockout of *LGALS1* in NCH125 was accomplished using galectin-1 Double Nickase Plasmid ([h]sc-400941-NIC), whereas the CRISPR/Cas9 negative control was obtained using the Control CRISPR/Cas9 Plasmid (sc-418922; both from Santa Cruz). NCH125 cells were seeded in a 6-well plate at about 70% confluency. Twenty-four hours later, 2 µg of DNA were transfected using Lipofectamine LTX (ThermoFisher Scientific) according to the vendor's protocol. Selection of transfected cells was carried out in normal growth medium containing 1 µg/mL puromycin (ThermoFisher Scientific) for 72 hours. Individual clones were obtained by limiting dilution. Knockout was confirmed by Western Blotting (see below).

## **2.2 Viruses**

### **2.2.1 Wild-type H-1PV**

Wild-type H-1PV was produced as previously described ([Allaume et al., 2012](#)). In brief, virus stocks were amplified by infecting NB324K cells at a multiplicity of infection (MOI) of 100 viral genomes/cell. When cell lysis became apparent (generally 5-7 days post-infection), cells were harvested and subjected to three freeze and thaw cycles. Crude cell extracts were digested using 50 U/mL Benzonase nuclease ultrapure (E8263; Sigma Aldrich, Taufkirchen, Germany) for 30 min at 37 °C. Afterwards, viral particles were purified through an iodixanol discontinuous gradient as described by Zolotukhin and colleagues ([Pace et al., 1999](#)).

Viral titres were quantified by plaque assay as previously described ([El-Andaloussi et al., 2011](#)). In short, NBK324K cells were infected with serial dilutions of purified H-1PV for 1 hour, followed by replacement of virus suspension with an overlay of 0.68% Bacto Agar (BD 214010; Becton, Dickinson and Company, Heidelberg, Germany) in MEM supplemented with 5% FBS. At five days post-infection, plaque formation was detected by incubating cells with 0.18% neutral red containing 0.85% Bacto Agar diluted in PBS. Plaques were counted from duplicates and titres were expressed as plaque forming units (pfu) per mL.

### 2.2.2 Recombinant H-1PV expressing EGFP

The recombinant H-1PV containing the green fluorescent protein-encoding gene (recH-1PV-EGFP) was produced as previously described (El-Andaloussi et al., 2012b). This parvovirus is non-replicative and has the same capsid of the wild-type. Furthermore, recH-1PV-EGFP contains the *EGFP* gene under the control of the natural P38 late promoter (in turn regulated by NS1).

In brief, virus stocks were amplified by infecting NB324K cells with recH-1PV-EGFP and Ad-VP-helper (El-Andaloussi et al., 2011). When cytotoxicity became apparent (generally starting 36-48 hours post-infection), cells were harvested and subjected to three freeze and thaw cycles. Crude cell extracts were digested using 50 U/mL Benzonase nuclease ultrapure for 30 min at 37 °C. Afterwards, viral particles were purified through an iodixanol discontinuous gradient as described by Zolotukhin and colleagues (Pace et al., 1999).

In order to titrate the recH-1PV-EGFP,  $4.0 \times 10^4$  HeLa cells were seeded in 96-well plates and infected on the next day with 100  $\mu$ L of different dilutions of purified recH-1PV-EGFP. At 24 hours post-infection, EGFP-positive cells were counted by fluorescence microscopy (see below). Virus titers were calculated as number of green cells  $\times$  dilution factor  $\times$  10; and expressed as transduction units (TU) per mL.

### 2.3 High-throughput siRNA library screening

The screening was performed by Dr. Laurent Brino and first described here (Kulkarni et al., in press). In short, the human druggable genome siRNA set 4.0 library consists of siRNA pools (each gene was targeted by a pool of four siRNAs) targeting a total of 6961 cellular genes (Qiagen, Hilden, Germany). The transfection protocol was optimised to achieve 90-95% efficiency with minimal toxicity, and it was performed in triplicates. Firstly, the siRNA pools were reverse transfected using the INTERFERin transfection reagent (Polyplus-transfection SA, Illkirch, France) into HeLa cells growing in  $\mu$ Clear 96-well microplates (Greiner, Frickenhausen, Germany). After 48 hours, two sets of cells were infected with recH-1PV-EGFP used

at 0.3-0.4 TU/cell. A third set of cells was left untreated to control cytotoxicity associated with each siRNA pool. Three additional siRNAs were used as internal controls in every microplate:

(i) NS1 siRNA\_5 (5'GAATGGTTACCAATCTACC3') targets the NS1 coding region, used as a positive control given that NS1 viral protein is indispensable for H-1PV transduction.

(ii) scramble siRNA (5'AATTCTCCGAACGTGTCACGT3' – Qiagen) is a negative control given that it is a non-targeting siRNA.

(iii) polo-like kinase-1 (PLK1) siRNA (5'CAACCAAAGTCGAATATGA3') was used to control transfection efficiency given that its silencing leads to cell death.

Twenty-four hours post-infection, plates were processed as described for Fluorescent microscopy (see below) and EGFP-positive cells were counted. For this purpose, high-throughput cell imaging was carried out with the INCELL1000 HCS epifluorescent microscope (GE Healthcare Life Sciences, Freiburg, Germany). The Multi Target Analysis module (IN Cell Investigator software, GE Healthcare Life Sciences, Chicago, IL, USA) was used to detect DAPI-stained cell nuclei (total number of cells) and EGFP in order to calculate the percentage of EGFP-positive cells. Analysis of single-cell data and statistical significance were carried out with the RReportGenerator software ([Raffelsberger et al., 2008](#)). The percentage of EGFP-positive cells obtained from transfecting cells with the scramble siRNA was used as a baseline to normalise the percentage obtained from transfecting cells with all the other siRNA pools.

## **2.4 Cell viability and proliferation assays**

### **2.4.1 MTT viability assay**

To determine cell viability after virus infection, the conversion of 3-(4,5-dimethylthiazol-2-yl)-2,5-diphenyl-2H-tetrazolium bromide (MTT) (Sigma-Aldrich Chemie GmbH, Steinheim, Germany) was measured. For this purpose, cells were seeded on a 96-well plate at a density of 2,000 cells/well in 50 µL of culture medium supplemented with 10% FCS. The day after, 50 µL of serum-free medium containing wild-type H-1PV were added on top of the cells. In rescue experiments, cells were



treated with H-1PV at an MOI of 5 pfu/cell, or 5 µg/mL of recombinant galectin-1 (ab50237, Abcam, Cambridge, UK), or both simultaneously. Every 24 hours post-treatment, over a total of 4 time-points, 10 µL of 5 mg/mL MTT were added and subsequently incubated for 2 hours at 37 °C. Thereafter, the supernatant was aspirated, and the plates were air-dried at 37 °C overnight. To solubilise the formazan product, cells were then incubated with 100 µL of isopropanol for 20 min with moderate shaking and the absorbance was read with an ELISA reader at 570 nm. Viability of treated cells was expressed as a ratio of the measured absorbance (average of 3 replicates per condition) to the corresponding absorbance of untreated cells (arbitrarily defined as 100%).

### **2.4.2 xCELLigence**

Cell proliferation was monitored using the xCelligence system (ACEA Biosciences Inc., San Diego, CA, USA) in real time according to the manufacturer's instructions. In short,  $8 \times 10^4$  cells were seeded per well in a 96-well E-plate (Roche, Mannheim, Germany) in a total volume of 100 µL of complete DMEM medium.

Concerning the Gal-1 experiments, cells were treated during the cellular growth phase with H-1PV at an MOI of 5 pfu/cell, or 5 µg/mL of recombinant galectin-1 (ab50237, Abcam), or both simultaneously. Cell proliferation was monitored in real time every 30 min. Data is expressed as "Cell index" ( $n=3$ ) calculated by the RTCA software as a measure of cell adhesion, and therefore, cell viability.

Concerning the endocytic pathways experiments, cells were treated during the cellular growth phase with different inhibitors (see below) for 45 min, and subsequently washed with PBS. Cellular proliferation was monitored in real time every 30 min. Data is expressed as "Normalised cell index" ( $n=3$ ) calculated by the RTCA software based on the average values of each experimental condition.

## 2.5 Microscopy

### 2.5.1 Fluorescent Microscopy

Cells were first washed one time with PBS, fixed on ice for 15 min with 3.7 % paraformaldehyde, permeabilised for 10 min with 1% Triton X-100, and stained with 4',6-diamidin-2-phenylindol (DAPI) to visualise the cell nuclei. Fluorescence images of EGFP-positive cells were acquired using a BZ-9000 fluorescence microscope (Keyence Corporation, Osaka, Japan) with a 10X objective (Ferreira et al., 2020).

### 2.5.2 Confocal microscopy

For the galectins study, cells were seeded at a density of  $3.5 \times 10^3$  cells per spot on spot-slides and cultured in 50  $\mu$ L of complete medium. On the next day, cells were infected with wild-type H-1PV at a MOI of 500 pfu/cell (total volume of 70  $\mu$ L) in DMEM medium containing 5% FCS. At 2 hours post-infection, cells were processed as described for *Fluorescence microscopy*. Antibody staining was performed for 1 hour using the following antibodies (dilution 1:500): mouse monoclonal anti-H-1PV capsid (a conformational antibody kindly provided by Barbara Leuchs; DKFZ Virus Production and Development Unit, Heidelberg, Germany (Leuchs et al., 2016)), and rabbit polyclonal anti-galectin-1 (HPA000646; Sigma-Aldrich).

For the endocytic pathways study, cells were first put on ice for 15 min and then infected with wild-type H-1PV at a MOI of 500 pfu/cell (total volume of 70  $\mu$ L) in DMEM medium containing 5% FCS. At 1 hour post-infection, the temperature was shifted to 37 °C for different times, and then processed as described for *Fluorescence microscopy*. Antibody staining was performed for 1 hour using the following antibodies (dilution 1:500): mouse monoclonal anti- H-1PV capsid, rabbit monoclonal anti-clathrin heavy chain (D3C6; Cell Signalling), rabbit monoclonal anti-EEA1 (3288; Cell Signalling), rabbit monoclonal anti-Rab7 (9367T; Cell Signalling) and rabbit polyclonal anti-LAMP-1 (CD107a) (AB2971; Merck).

Afterwards, the following antibodies were used as secondary antibodies: anti-mouse Alexa Fluor 594 IgG (A11005; Thermo Fisher Scientific), and anti-rabbit Alexa Fluor 488 IgG (A11008; Thermo Fisher Scientific). Nuclei were stained with DAPI. Images

in the red channel (H-1PV), green channel (varied cellular proteins), or blue channel (DAPI) were acquired with a confocal microscope (Leica TCS SP5 II). Picture analysis was performed recurring to the Leica LAS X Software (Ferreira et al., 2020).

### **2.5.3 Electron microscopy**

The electron microscopy experiments were performed in collaboration with the Electron Core Facility of DKFZ, in particular with Dr. Karsten Richter (Ferreira et al., 2020). Firstly, HeLa cells were seeded at a density of  $8 \times 10^4$  cells/well on punched sheets of ACLAR-Fluoropolymer films (Electron Microscopy Sciences) placed in 24-well plates. On the next day, cells were infected with H-1PV at a MOI of 2000 pfu/cell for 1 hour at 4 °C in DMEM medium containing 5% FCS– this step refers to the viral attachment at the cell surface. Temperature was shifted to 37 °C for 0, 5, 10, 20 or 30 min in order to catch the different steps involved in the internalisation event. Afterwards, ACLAR-Fluoropolymer films were embedded in epoxy resin for ultrathin sectioning according to a routine protocol. In short, chemical fixation was performed in buffered aldehyde (1 mM CaCl<sub>2</sub>, 2% glutaraldehyde, 4% formaldehyde, 1 mM MgCl<sub>2</sub> in 100 mM Ca-cacodylate, pH 7.2). Post-fixation was carried out in buffered 1% osmium tetroxide, while en bloc staining was carried out in 1% uranylacetate. After adherent cells were dehydrated using graded steps of ethanol, they were flat-embedded in epoxy resin (mixture of methyl nadic anhydride, glycid ether and dodecenyl-succinic-anhydride; Serva). Contrast-staining was achieved with lead-citrate and uranylacetate. Analysis of ultrathin sections (thickness of 60 nm) was performed with a Zeiss EM 910 (Carl Zeiss) at 120 kV and electron micrographs taken with a slow-scan charge-coupled device camera (TRS, Olympus).

## **2.6 Enzyme-linked Immunosorbent Assay (ELISA)**

Microtiter 96-well plates (Nunc-Immuno MaxiSorp surface plate; Thermo Fisher Scientific) were pre-coated overnight at 4° C with 1 µg/well of purified laminin LN411 (BioLamina, Sundbyberg, Sweden), 1 µg/well of recombinant galectin-1 (ab50237, Abcam), 2.56 µg/well of collagen type IV (Sigma), 2.56 µg/well of human plasma fibronectin (Merck Millipore), or 2.5% albumin bovine fraction V (BSA; SERVA)

diluted in 50 mM sodium carbonate (pH 9.6). Washing was performed five times between every step with 0.1% Tween 20/PBS. Blocking was performed using 2% BSA/PBS for 2 hours at room temperature. Afterwards,  $7 \times 10^8$  pfu H-1PV diluted in 2% BSA/PBS were added or not to the wells and incubated overnight at 4 °C. Detection of bound viral particles was carried out using a mouse anti-H-1PV capsid antibody (dilution 1:500)(Leuchs et al., 2016) for 2 hours at room temperature, followed by peroxidase-conjugated goat anti-mouse antibody (1:500) for another 2 hours. Finally, we incubated each well with 3,3',5,5'-tetramethylbenzidine (TMB) substrate solution (Pierce™, Thermo Fisher Scientific) for approximately 7 min, by which time the reaction was stopped using Stop solution (N600; Thermo Fisher Scientific). Optical density was read at 450 nm using the Thermo Multiskan EX Microplate photometer (Thermo Fisher Scientific).

## 2.7 siRNA-mediated knockdown

Cells were seeded at a density of  $4 \times 10^4$  cells/well in 24-well plates and cultured in 500  $\mu$ L of regular growth medium. After 24 hours, cells were transfected with 10 nM siRNA using Lipofectamine RNAiMAX (Thermo Fisher Scientific, Carlsbad, California, USA) according to the vendor's recommended protocol. The following siRNAs were used for the galectins study (all purchased from Life Technologies, Paisley, Scotland): Silencer Select *LGALS1* siRNA (Cat. N. 4390824), Silencer *LGALS3* siRNA (Cat. N. 11332) and Silencer Select Negative Control #2 siRNA (Cat. N. 4390846). The following siRNAs were used to target laminin  $\gamma$ 1 (all purchased from Qiagen): LAMC1#1 (Cat. N. SI00035742), LAMC1#2 (Cat. N. SI02757475), and AllStars Negative siRNA (Cat. N. SI03650318) used as negative control. For the endocytic pathway study, the following siRNAs were used: *AP2M1* ON-TARGET plus Human siRNA SMARTpool (L-008170-00-0005) and, as a negative control, the plus Non-targeting pool (D-001810-10-05) (Dharmacon, Thermo Fisher Scientific); two *CAVI* Silencer Select Validated siRNAs (s2446 and s2448; Life Technologies) and Silencer Select Negative Control #2 siRNA (Life Technologies) as a control.

After 24 hours, the medium was replaced, and cells were grown for an additional 24 hours to allow efficient gene silencing. The cells were then infected for 24 hours with recH-1PV-EGFP at 0.3-0.4 TU/cell. Cells were then washed once with PBS and

processed for fluorescence microscopy as described below. At least three independent experiments, each performed in duplicate, were performed for every condition.

## 2.8 Western Blotting

Firstly, cells were harvested, washed one time with PBS, and lysed for 30 min on ice using RIPA buffer (1% NP-40; 150 mM NaCl; 10 mM Tris-HCl pH 7.5; 1 mM EDTA pH 8; 0.5% Na-deoxycholate; 0.5% SDS) containing EDTA-free protease inhibitor (11697498001; Roche). After removing cellular debris by centrifugation, the protein content was measured using the bicinchoninic acid (BCA) assay (Thermo Fisher Scientific), following the manufacturer's instructions. Protein separation was carried out by SDS-PAGE using 30 to 50 µg of protein. Afterwards, separated proteins were transferred onto Hybond-P membrane (GE Healthcare). Target proteins were identified using the following antibodies: rabbit anti-NS1 SP8 anti-serum (Bodendorf et al., 1999) and rabbit anti-VP1/2 anti-serum (Kestler et al., 1999) at 1:5000 dilution; rabbit polyclonal anti-galectin-1 (HPA000646; Sigma Aldrich, Hamburg, Germany), rabbit monoclonal anti-caveolin-1 (D46G3; Cell Signalling), mouse monoclonal anti-β-tubulin (T8328; Sigma Aldrich), mouse monoclonal anti-GAPDH (sc-365062; Santa Cruz Biotechnology), mouse monoclonal anti-vinculin (sc-25336; Santa Cruz Biotechnology) at 1:1000 dilution, and rabbit polyclonal AP2M1 (ab96679; Abcam) at 1:500 dilution. Thereafter, membranes were incubated with horseradish peroxidase-conjugated secondary antibodies (Santa Cruz, Heidelberg, Germany) at dilution 1:1000. Detection of proteins was carried out using the Western Blot Chemiluminescence Reagent *Plus* (Perkin Elmer Life Sciences) and exposed to films (Hyperfilm™ ECL; GE Healthcare).

## 2.9 Plasmid transfection

To rescue the *LGALS1* expression, the plasmid encoding for *LGALS1* gene was used (SC118705, OriGene Technologies, Inc., Rockville, MD, USA). NCH125 Control and *LGALS1* KO cells were seeded at a density of  $3 \times 10^5$  cells/well in a 6-well plate. On the next day, NCH125 Control and *LGALS1* KO cells were transfected with 2.5 µg of

DNA using Lipofectamine LTX (ThermoFisher Scientific) or mock-transfected for 48 hours.

## **2.10 Binding/entry assays**

Firstly, the culture medium was replaced with 200  $\mu$ L serum-free medium containing H-1PV at MOI 5 pfu/cell. In Gal-1 rescue experiments, cells were treated with H-1PV at an MOI of 5 pfu/cell, or 5  $\mu$ g/mL of recombinant galectin-1 (ab50237, Abcam), or both simultaneously. Infection was performed for 1 hour at 4  $^{\circ}$ C to only allow cell surface virus binding or for 4 hours at 37  $^{\circ}$ C to also allow virus cell internalisation. Cells were extensively washed with PBS, and trypsinised for 5 min and collected in 200  $\mu$ L of serum-containing medium. Cells were then subjected to three snap freeze-thaw cycles. Viral DNA was purified from cell lysates using the QiAamp MinElute Virus Spin kit (Qiagen, Hilden, Germany) according to the manufacturer's instructions. Afterwards, cell-associated H-1PV genomes were assessed by quantitative PCR (see below).

## **2.11 Polymerase chain reaction (PCR)**

### **2.11.1 Quantitative PCR (qPCR)**

Viral genomes were quantified by following a parvovirus-specific TaqMan qPCR protocol as previously described (Allaume et al., 2012). Briefly, the TaqMan probe costume-designed targets the viral DNA region encoding for NS1 (forward primer: 5'-GCGCGGCAGAATTCAAAC-3'; reverse primer: 5'-CCACCTGGTTGAGCCATCAT-3', purchased from Applied biosystem). As well, the probe contains a fluorophore at the 5' end and a quencher molecule at the 3' end (5'-6-FAM-ATGCA GCCAGACAGTTA-MGB-3', Applied biosystem). The primers recognising the NS1 region are the following: forward primer: 5'-GCGCGGCAGAAT TCAAAC-3'; reverse primer: 5'-CCACCTGGTTGAGCC ATCAT-3' (Applied biosystem). The DNA concentration of the samples was calculated based on a standard curve. The curve was generated by performing a regression line on eight dilutions of the plasmid pMVM+ $\Delta$ 800 (containing the H-1PV NS1 target sequence) with known copy numbers

( $10^1$ - $10^8$ ). The master mix (40  $\mu$ L/samples) was prepared as follows: 1.3  $\mu$ L forward primer (10 pmol/ $\mu$ L), 1.3  $\mu$ L reverse primer (10 pmol/ $\mu$ L), 1.3  $\mu$ L TaqMan probe (10 pmol/ $\mu$ L), 23.4  $\mu$ L reaction mix (TaqMan Universal PCR Master Mix 2X, Applied Biosystem), 13  $\mu$ L sterile H<sub>2</sub>O. Afterwards, 6.7  $\mu$ L of sample DNA, standard or H<sub>2</sub>O (negative control) were mixed with 40  $\mu$ L of master mix. At last, 20  $\mu$ L of the mixture were applied on a 96-well PCR plate in duplicate, and the plate was subsequently sealed with adhesive transparent cover and centrifuged at 3000 rpm for 5 min. Thermal cycling conditions included 2 min at 50 °C, 10 min at 95 °C, proceeding with 40 cycles of 95 °C for 15 sec and 60 °C for 1 min.

### 2.11.2 Reverse transcriptase quantitative PCR (RT-qPCR)

Total RNA was extracted using the RNeasy Mini kit (Qiagen) according to the manufacturer's protocol. Thereafter, cDNA was synthesised using the QuantiTect Reverse Transcription Kit (Qiagen) according to the manufacturer's protocol. The Applied Biosystems 7300 Real-Time PCR System (Applied Biosystems GmbH, Darmstadt, Germany) was used for qPCR analysis. Amplification reaction mixture was added to 96-well optical reaction plate containing 3  $\mu$ L of template cDNA pre-diluted 1:10, 12.5  $\mu$ L 2 $\times$ QuantiFast SYBR Green PCR Master Mix, 2.5  $\mu$ L 10 $\times$  QuantiTect Primer Assay and RNase-free water.

QuantiTect Primer Assay used:

*AP2M1*      Hs\_AP2M1\_1\_SG QuantiTect Primer Assay      (QT00089334)

*GAPDH*      Hs\_GAPDH\_1\_SG QuantiTect Primer Assay      (QT00079247)

A non-template reaction was also included. RT-PCR was performed to assess the expression levels of *AP2M1* and of the endogenous control *GAPDH*, which was found to have the most consistent expression level in this study. Each reaction was performed with two biological replicates with three technical replicates each. Cycling conditions recommended by the manufacturer for fast two-step RT-PCR were followed. The  $2^{-\Delta\Delta C_t}$  method was applied in order to determine the fold-change for *AP2M1* gene expression between control siRNA- and *AP2M1* siRNA-treated cells.

## 2.12 Flow cytometry (FACS)

Cells were seeded at a density of  $5 \times 10^5$  cells/well in a 6-well plate. On the following day, cells were infected with H-1PV at a MOI of 25 pfu/cell for 1 hour at 4 °C. The following steps were all performed on ice. Cells were washed with ice-cold PBS and then gently scrapped off with a cell lifter. Next, cells were fixed with 2% PFA for 15 min and blocked with 2.5% BSA/PBS for 20 min. Cells were then incubated with H-1PV anti-capsid antibody (dilution 1:500) for 30 min, and subsequently with Alexa Fluor 488 goat  $\alpha$ -mouse (1:500) for 30 min. Three washes with 2.5% BSA/PBS were performed between each staining step. FACS analysis was carried out using a FACS Calibur (BD Biosciences, San Jose, CA).

## 2.13 Tissue Microarray

The tissue microarray was performed by Dr. Jubayer Hossain. GBM biopsies obtained from the Haukeland University Hospital, Bergen, Norway (project approved by the regional ethical committee) were used to carry out GBM tissue microarrays. The microarray includes 122 biopsies from GBM patients: 61 primary GBM and 49 recurrent GBM, plus 12 biopsies from normal tissues (brain, tonsil and liver, 4 from each organ). Immunohistochemical staining was carried out as described previously (Hossain et al., 2019b) using galectin-1 antibody (sc-166618, Santa Cruz) at a dilution of 1:200 followed by a biotinylated anti-mouse antibody (Vector Laboratories) at a dilution of 1:1100. Galectin-1 positive cells were counted *via* automated counting as described previously (Hossain et al., 2019a).

## 2.14 Determination of the H-1PV EC50 for the NCI-60 cell lines

This screening was performed Dr. Serena Bonifati, a previous member of the laboratory, and was first described here (Kulkarni et al., in press). Briefly, cell proliferation was monitored in real time using the xCELLigence system (see above). Cells were seeded on a 96-well E-Plate at a density of 4,000–16,000 cells/well (according to cell doubling rate). After 24–72 hours, cells were infected with increasing amounts of wild-type H-1PV (MOI



= 0, 0.05, 0.25, 1, 5, 10 and 50 pfu/cell). Cell proliferation was monitored for 5–7 days, every 30 min, and expressed as “Normalised cell index” ( $n=3$ ). Only 53 cancer cell lines were included given that sic leukaemia cancer cell lines, which grow in suspension, were not compatible with the xCELLigence system.

The subsequent analysis was performed by Dr. Francisco Azuaje and described here (Kulkarni et al., in press). In short, a two-step data analysis method (Kinsner-Ovaskainen et al., 2013) was used to derive EC50 values (H-1PV concentration able to kill 50% of cells) for each cell line at 24, 48, 72 and 96 hours post-infection using the “Normalised cell index” values obtained from the xCELLigence system as an input.

Correlations between gene expression and EC50 analyses were calculated in R (Hmisc and ggplot2 libraries, Pearson correlation and corresponding  $P$  values). Two independent gene expression datasets were used: the NCI-60 (53 cell lines) and the CCLE (The Cancer Cell Line Encyclopaedia – with 38 cell lines in common with the NCI-60 panel found in the database) (Barretina et al., 2012).

## 2.15 Measurement of transcript levels

Gene expression levels of *LGALS1*, as well as of *ACTB*, *GAPDH* and *PGK1* reference genes, were quantified recurring to NanoString Technologies (Seattle, WA, USA) as described here (Kulkarni et al., in press). The analysis was performed at the NCounter Core Facility of the University of Heidelberg by Ralph Roth and Beate Niessler. Accession numbers and target sequences of genes analysed by nCounter expression profiling can be found below:

*LGALS1* gene (accession number NM\_002305.4):

GGTGCGCCTGCCCGGGAACATCCTCCTGGACTCAATCATGGCTTGTGGTCTG  
GTCGCCAGCAACCTGAATCTCAAACCTGGAGAGTGCCTTCGAGTGCGA

*ACTB* gene (accession number NM\_001101.2):

TGCAGAAGGAGATCACTGCCCTGGCACCCAGCACAATGAAGATCAAGATCA  
TTGCTCCTCCTGAGCGCAAGTACTCCGTGTGGATCGGCGGCTCCATCCT

*GAPDH* gene (NM\_001256799.1):

GAACGGGAAGCTTGTCATCAATGGAAATCCCATCACCATCTTCCAGGAGCG  
AGATCCCTCCAAAATCAAGTGGGGCGATGCTGGCGCTGAGTACGTCGTG

*PGK1* gene (NM\_000291.2):

GCAAGAAGTATGCTGAGGCTGTCACTCGGGCTAAGCAGATTGTGTGGAATG  
GTCCTGTGGGGGTATTTGAATGGGAAGCTTTTGCCCGGGGAACCAAAGC

## 2.16 Treatment with inhibitors of endocytosis pathways

The following inhibitors were used at sublethal concentrations: hypertonic sucrose (Carl Roth), 0.40 M; chlorpromazine (Sigma-Aldrich), 2.5 µg/mL for HeLa or 5 µg/mL for NCH125; pitstop 2 (Sigma-Aldrich), 30 µM; nystatin (Sigma-Aldrich), 10 µg/mL; methyl-β-cyclodextrin (MβCD; Sigma-Aldrich), 10 mM; Dynole™ Series Kit containing Dynole 31-2 and 34-2 (Abcam), 5 µM; bafilomycin A1 (BafA1; Cell Signalling), 10 nM; and ammonium chloride (NH<sub>4</sub>CL; 1145, Merck), 25 mM.

In short, cells were seeded at a density of  $8 \times 10^4$  cells/well in 24-well plates. On the next day, cells were pre-treated for 45 min with the different pharmacological inhibitors, and subsequently infected with recH-1PV-EGFP at an MOI of 0.2–0.3 TU/cell for 4 hours. Next, cells were washed two times with PBS and cultured for additional 20 hours. At 24 hours post-infection, cells were processed as described for *Fluorescent microscopy*.

## 2.17 Transferrin uptake analysis

Transferrin uptake control assays were performed using human transferrin Texas-Red conjugated (T2875, Invitrogen, Thermo Fisher Scientific). For this purpose, cells were incubated for 10 min with 25 µg/mL transferrin in serum-free media and processed as described for *Fluorescent microscopy*.

## 2.18 Statistical analysis

Results are shown as the average of three replicated experiments ± standard deviation (SD). Statistical significance was determined by one-way ANOVA using GraphPad Prism. Only values above  $p < 0.05$  were considered significant:  $p \leq 0.05$  (\*),  $p \leq 0.01$  (\*\*) and  $p \leq 0.001$  (\*\*\*)

## Chapter 3: Laminin- $\gamma$ 1 and Galectin-1 have a crucial role in H-1PV infection

In this chapter, I start by summarising the results obtained from a siRNA library screening previously performed in the laboratory which led to the identification of laminin- $\gamma$ 1, Gal-1 and AP2 $\mu$ 1 as putative cellular factors involved in H-1PV cell infection. These findings constitute the starting point of this dissertation, and therefore, are described in the section 3.1. They are part of a paper accepted for publication in *Nature Communications* in which I contributed for and listed as second author (Kulkarni et al., in press). Thus, this chapter contains figures and text taken from or based on this manuscript.

The results concerning Gal-1 are described from section 3.2. onwards and have also formed a manuscript which is ready to be submitted to a peer-reviewed journal. The findings referring to AP2 $\mu$ 1 are later described in Chapter 4 and have also been published recently (Ferreira et al., 2020).

### 3.1 Previous results from the laboratory

#### 3.1.1 Identification of putative modulators of the H-1PV life cycle by siRNA library screening

RNA interference is an effective approach to study gene function by silencing gene transcription. At a large scale, high throughput siRNA screenings can provide the insights on which genes are important in a particular biological context (Silva et al., 2008). In our particular case, we were interested in identifying host cell factors which could modulate the H-1PV infection. For this purpose, previous members of the laboratory have carried out a high-throughput siRNA library screening in cervical carcinoma-derived HeLa cells using a siRNA library targeting the human druggable-genome (6961 genes, each targeted by a pool of four siRNAs) (Figure 3.1A). Briefly, cells were reverse transfected with siRNA and subsequently infected with recH-1PV-EGFP (El-Andaloussi et al., 2011). Twenty-four hours post-infection, cells were fixed, and EGFP-positive cells were counted. This parvovirus is non-replicative and has the same capsid of the wild-type. Furthermore, recH-1PV-EGFP contains the *EGFP* gene

under the control of the natural P38 late promoter (in turn regulated by NS1). Therefore, the EGFP signal directly correlates with the ability of the virus to reach the nucleus and initiate its own gene transcription.

Upon analysis of the EGFP transduction levels, the genes were categorised into activators (gene silencing leads to lower EGFP signal), repressors (gene silencing leads to higher EGFP signal), or unrelated (silencing did not significantly affect EGFP signal) (Figure 3.1B). In parallel, uninfected siRNA-transfected cells were submitted to a cell viability assay in order to assess knockdown-induced cytotoxicity. All those genes whose silencing led to viability levels lower than 70% were excluded from subsequent analysis.

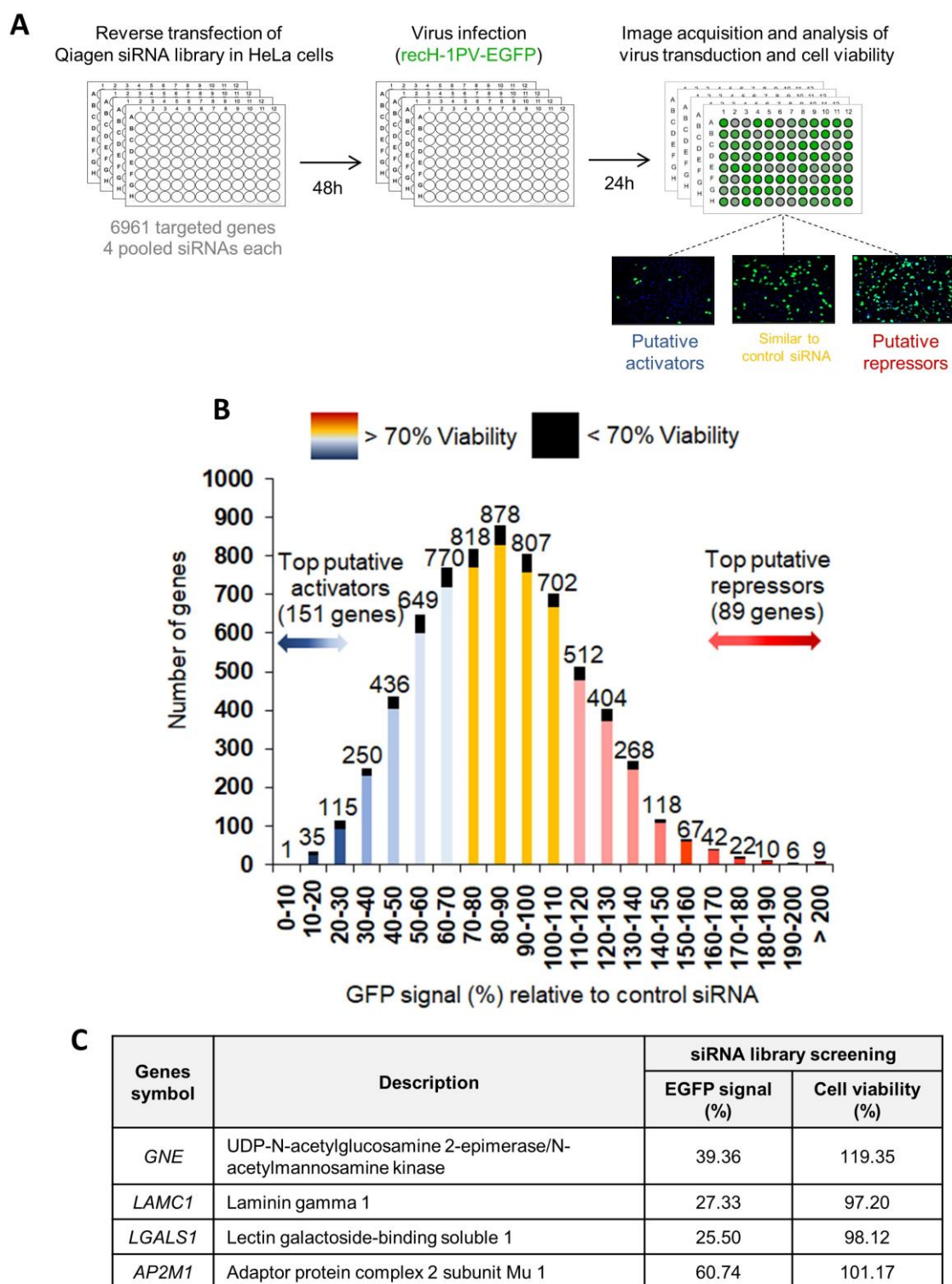


**Figure 3.1. siRNA library screening reveals factors putatively involved in H-1PV life cycle.**

(A) The whole human druggable genome siRNA library, composed of 6961 siRNA pools (four siRNAs per pool for each gene) was reverse transfected into HeLa cells. The reactions were performed in 96-well plates in triplicate. After 48 hours, cells were infected with recH-1PV-EGFP. After 24 hours, the percentage of EGFP-positive cells were quantified as a measure of H-1PV transduction efficiency. Representative images

of putative activators and putative repressors are shown. In addition, cell viability was also measured (the whole process is described in Chapter 2: Materials and Methods). **(B)** The bar graph depicts the distribution of the results. The x-axis indicates the percentage of EGFP-positive cells, whereas the y-axis indicates the number of genes in which that percentage was observed. EGFP levels observed upon control scrambled siRNA transfection was used as a baseline. In this manner, bars coloured in blue indicate those genes where knockdown led to a decrease in virus transduction (putative activators); bars coloured in red indicate those genes where knockdown led to an increase in virus transduction (putative repressors); and bars coloured in yellow indicate those genes where knockdown did not significantly alter the virus transduction (unrelated). The portion of the bars coloured in black refer to those genes in which gene knockdown in non-infected cells decreased viability by more than 70%, and therefore, excluded from further analysis. Numbers on top of each column designate the number of genes in each group. **(C)** The table lists the results obtained for *GNE*, *LAMC1*, *LGALS1* and *AP2M1*.

Firstly, we focused on host cell factors which positively modulate the H-1PV infection. Therefore, we proceeded for subsequent analysis with those genes which presented H-1PV transduction levels lower than 70% (top activators) and viability levels greater than 70%. As a result, we obtained 151 genes. Within the top activators, we focused on candidates possibly involved in the first steps of H-1PV infection, that is binding and entry. It is known that H-1PV entry occurs through SA, a property shared with other PtPVs (Halder et al., 2013b, Alloume et al., 2012). Correspondingly, among the top activators, there is bifunctional UDP-N-acetylglucosamine 2-epimerase/N-acetylmannosamine kinase (*GNE*) which initiates and regulates the biosynthesis of N-acetylneuraminic acid (NeuAc), a precursor of SA (Hinderlich et al., 2013). Indeed, siRNA-mediated knockdown of *GNE* led to a decrease of H-1PV transduction of 70% (Figure 3.1C). Afterwards, we entered the activators into the PANTHER classification system in order to group them into protein classes (Figure 3.2). As a result, we found that the top protein classes were protein modifying enzymes (25.30%), metabolite interconversion enzyme (22.20%), translational protein (7.10%), transmembrane signal receptor (7.10%), and gene-specific transcriptional regulator (6.10%). Of particular interest to virus cell attachment and entry, we found *LAMC1* and *LGALS1* genes within the extracellular matrix proteins (2%), and *CCKAR*, *TGFBR2*, *ACVRL1*, *DRD4*, *MC4R*, *IFNAR2*, and *GPR92* as transmembrane signal receptors (7.1%).

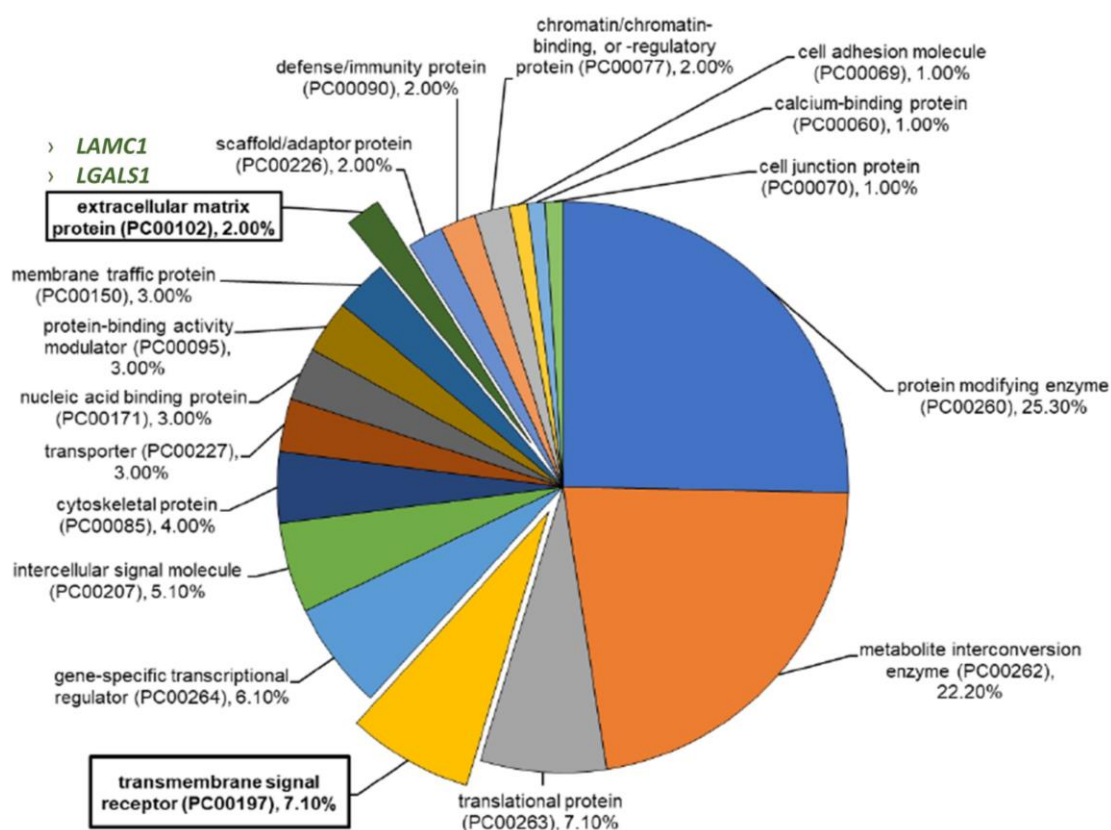


**Figure 3.2. Distribution of activators of H-1PV life cycle.**

The top 151 activators of H-1PV life cycle were classified based on their cellular function through a PANTHER analysis (<http://www.pantherdb.org/>). This tool was used to annotate the genes/proteins according to their cellular functions.

### 3.1.2 H-1PV uses laminin $\gamma$ 1 for its attachment at the cell surface

*LAMC1* gene, encoding for laminin  $\gamma$ 1 chain, caught our attention since its knockdown reduced H-1PV transduction by more than 70%. As well, laminins are known to be heavily glycosylated proteins with terminal SA residues. Bearing in mind that H-1PV infection is strictly dependent on SA, Kulkarni et al., investigated the role of laminins in H-1PV cell attachment (Kulkarni et al., in press). Characterisation of H-1PV/laminin interaction revealed that laminins, and in particular those containing the  $\gamma$ 1 chain, play a key role in mediating H-1PV attachment at the cell surface, and subsequent entry into cancer cells. While siRNA-mediated knockdown of *LAMC1* strongly reduces binding and entry into permissive cells, overexpression of *LAMC1* cDNA enhances H-1PV binding and entry in the same cells. Additionally, heparin, a known ligand of laminins, inhibits cellular binding of H-1PV in a concentration-dependent manner.

Given the involvement of laminins in H-1PV life cycle, my contribution to this study was to verify whether there was a direct binding of H-1PV to laminins. To this end, I performed an ELISA in which plates were pre-coated with different laminins containing the  $\gamma$ 1 chain (LN211, LN221, LN411, LN421), a laminin not containing the  $\gamma$ 1 chain (LN332), collagen IV and fibronectin, as well as BSA (negative control). I found that H-1PV binds strongly to those laminins containing  $\gamma$ 1 chain, whereas binding to laminin 332, collagen IV and fibronectin occurred at a much lower extent (Figure 3.3A). Thereafter, I assessed whether the binding of H-1PV to laminin occurred through SA. For this purpose, I repeated the ELISA experiment with an additional step of neuraminidase treatment, in order to remove the SA residues from the laminins, prior to virus incubation. As a result, I found that the binding of H-1PV to laminins was completely abolished, suggesting that H-1PV binds to laminins through SA moieties (Figure 3.3B).

At last, given that Kulkarni et al., had shown that treatment with heparin binding domain of laminins reduced H-1PV transduction in HeLa cells in a dose-dependent manner, I attempted to recapitulate this finding in an ELISA setting. For this purpose, I started by pre-coating wells with laminin 421 which showed high level of binding to H-1PV in the previous assay. Then, I treated wells with heparin before the addition of H-1PV. As a result, heparin significantly decreased H-1PV-laminin interactions (Figure 3.3C). Given that binding of H-1PV to BSA-conjugated heparin was comparable to that of wells pre-coated with BSA alone, this ruled out direct binding of the virus to heparin. Collectively, these findings provided further evidence towards demonstrating that H-1PV binds to laminins *via* SA moieties likely present within the heparin-binding site(s).



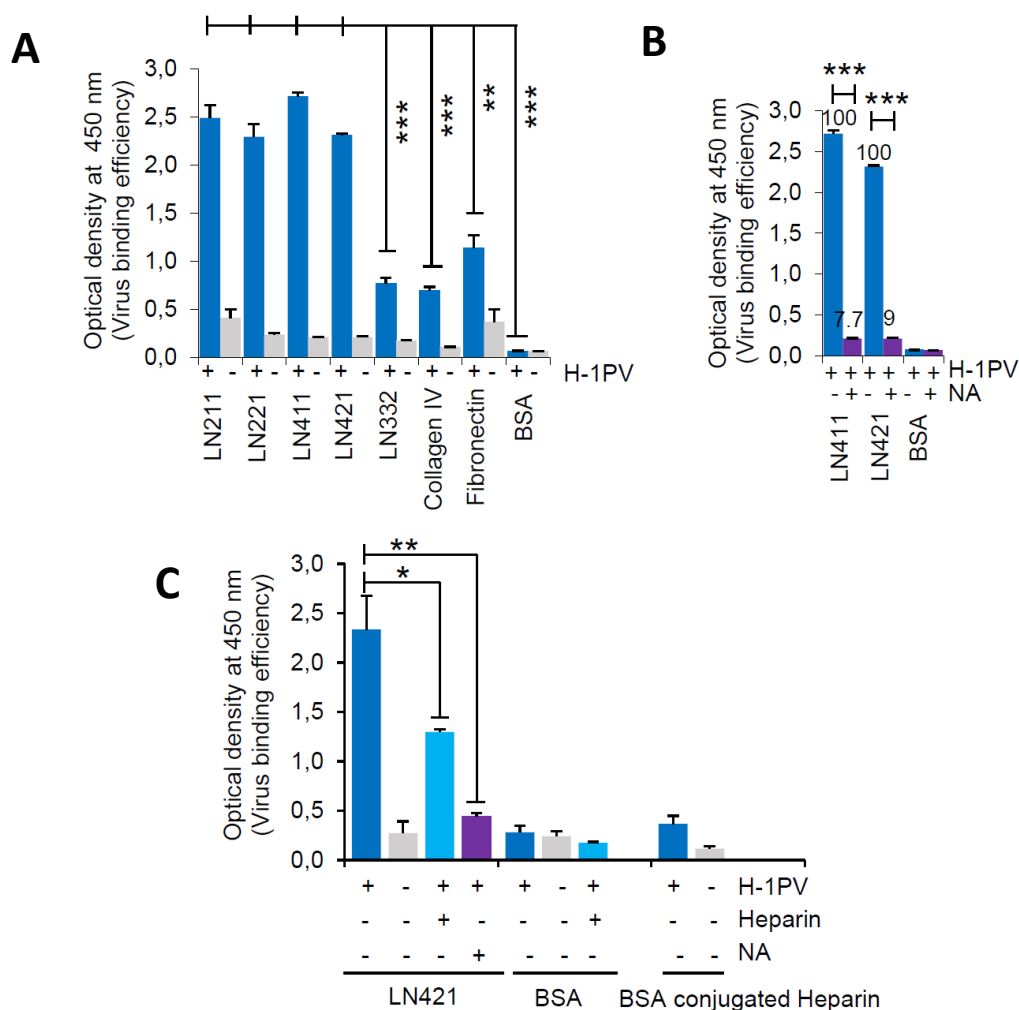


**Figure 3.3. H-1PV binds directly to laminins *via* sialic acid likely within the heparin-binding site(s).**

(A) Wells were pre-coated with purified laminins (LN211, LN221, LN411, LN421, LN332), collagen type IV, fibronectin or BSA. After blocking of non-specific binding, wells were incubated with H-1PV or left untreated. Subsequently, wells were subjected to repeated washing steps to remove unbound/loosely bound viral particles. Those viral particles which remained bound were detected using a virus capsid conformational antibody by ELISA. (B) Wells were pre-coated with purified laminins (LN411, LN421) or BSA, and subsequently incubated or not with neuraminidase (NA). Bound particles were detected by ELISA as per (A). (C) Wells were pre-coated with purified LN421, BSA-conjugated heparin or BSA. The wells containing LN421 or BSA were pre-treated with heparin, NA or left untreated. ELISA was performed as per (A). Each column indicates the mean value  $\pm$  the standard deviation bars ( $n=2$ ; \*\* $p<0.01$ ; \*\*\* $p\leq 0.001$ ). Retrieved from (Kulkarni et al., in press).

### 3.2 Galectin-1, but not galectin-3, knockdown hampers H-1PV infection

Besides laminins, the *LGALS1* gene, encoding for Gal-1, emerged in the same screening as another top-activator of H-1PV transduction, as its silencing decreased H-1PV transduction by approximately 70%. It is also known that galectins interact with laminins (Cousin and Cloninger, 2016). These reasons prompted us to hypothesise that Gal-1 could be involved in H-1PV infection at the level of virus entry. This hypothesis was also supported by the recent discovery that MVM (a PtPV closely related to H-1PV) requires Gal-3 to efficiently infect mouse cells (Garcin et al., 2013, Garcin et al., 2015).

I started by confirming the results of the siRNA library screening by performing a knockdown of *LGALS1* by using an independent siRNA. Additionally, given the role of Gal-3 in MVM cell entry, the effect of siRNA-mediated silencing of *LGALS3* was also investigated. The recH-1PV-EGFP was used for the experiments since the EGFP signal directly correlates with the ability of the virus to reach the nucleus and initiate its own gene transcription (El-Andaloussi et al., 2011).

Cervical cancer-derived HeLa, glioma-derived NCH125 and pancreatic carcinoma-derived BxPC3 cell lines were transfected with siRNAs targeting *LGALS1* or *LGALS3* genes, or a scrambled siRNA. After 48 hours, cells were infected with recH-1PV-EGFP and grown for further 24 hours. Efficient gene silencing was achieved for both genes in cells transfected with respective siRNAs (Figure 3.4 lower panel). However, only the siRNA targeting *LGALS1* significantly decreased H-1PV transduction by more than 55%. As opposed to what was observed during MVM infection, silencing of *LGALS3* did not significantly alter H-1PV transduction when compared with scrambled-transfected cells (Figure 3.4 upper panel). These results confirm original data from siRNA library screening which indicate that Gal-1, but not Gal-3, plays a key role in H-1PV infection in the cell lines tested.

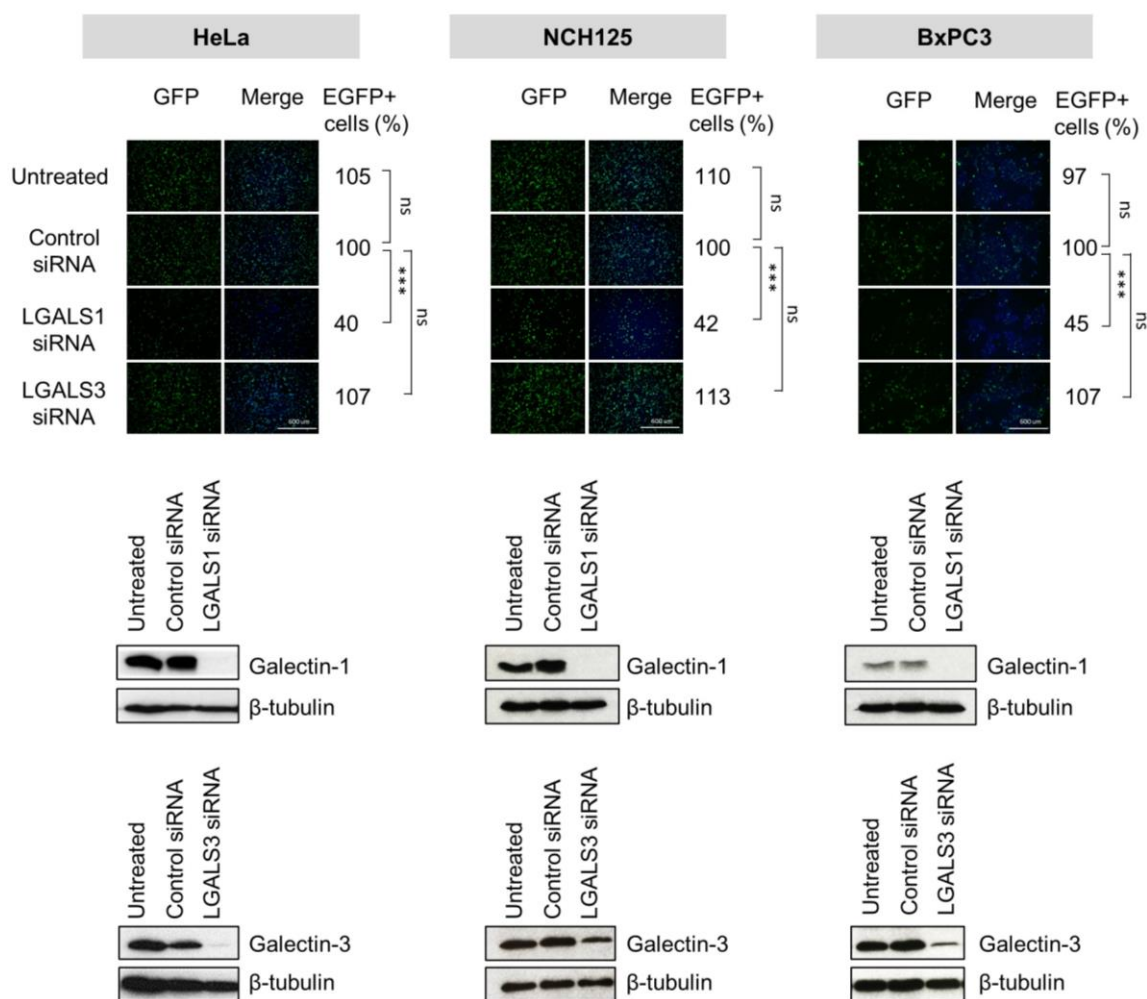


**Figure 3.4. H-1PV transduction is reduced in *LGALS1*, but not *LGALS3*, knockdown cell lines.**

HeLa, NCH125 and BxPC3 cells were transfected with siRNAs targeting *LGALS1*, *LGALS3* or with a scrambled siRNA. At 48 hours post-transfection, cells were infected with recH-1PV-EGFP for 4 hours and grown for additional 20 hours. Cells were then processed as described in Chapter 2: Materials and Methods. Numbers represent the average percentage of EGFP-positive cells relative to the number of EGFP-positive cells observed in untreated cells, which was arbitrarily set as 100% ( $ns=p>0.05$ ;  $***p\leq 0.001$ ). The protein levels of Gal-1 and Gal-3 on lysates derived from HeLa, NCH125 and BxPC3 siRNA-transfected cells were analysed by Western blotting. Beta-tubulin was used as a loading control.

### 3.3 Galectin-1 knockout impairs H-1PV infection in NCH125 cells

To further investigate the biological role of Gal-1 in H-1PV infection, I took advantage of the CRISPR-Cas9 technology and established the NCH125 LGALS1 KO cell line (LGALS1 KO) in which the *LGALS1* was knocked out. Alongside, I established the NCH125 Control cell line (Control) for which a non-targeting guide RNA control sequence was used. Given that H-1PV requires S-phase factors expressed in proliferating cells for a productive infection (Nuesch et al., 2012), I evaluated the proliferation of LGALS1 KO *versus* Control cells. Both cell lines proliferate at a similar rate as shown by real time monitoring of cell proliferation *via* xCELLigence (Figure 3.5).

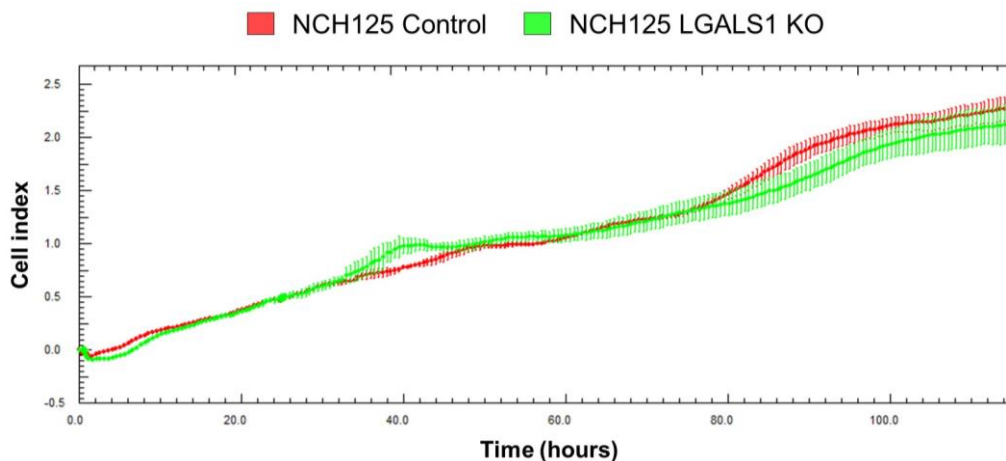


**Figure 3.5. Cell proliferation of NCH125 Control *versus* NCH125 LGALS1 KO.**

NCH125 Control and LGALS1 KO cells were seeded in a 96-well E-plate and grown for five days. Cell proliferation was monitored with the xCELLigence System. Curves represent the mean Cell Index value  $\pm$  standard deviation ( $n=3$ ).

I analysed H-1PV transduction efficiency by infecting both cell lines with recH-1PV-EGFP. As a result, a significant decrease in transduction activity was found in LGALS1 KO cells (47%) in comparison with Control cells (Figure 3.6A). Strikingly, transfection of LGALS1 KO cells with a plasmid encoding the *LGALS1* gene 48 hours prior to infection rescued the reduction in H-1PV transduction and re-established Gal-1 levels to those observed in NCH125 Control cells (Figure 3.6A). Additionally, I evaluated the levels of the viral proteins after 48 hours post-infection with the wild-type H-1PV. In agreement with previous results, Western blotting analysis revealed that NS1 and VP1

viral protein levels were lower in NCH125 LGALS1 KO in comparison to Control cells (Figure 3.6B).

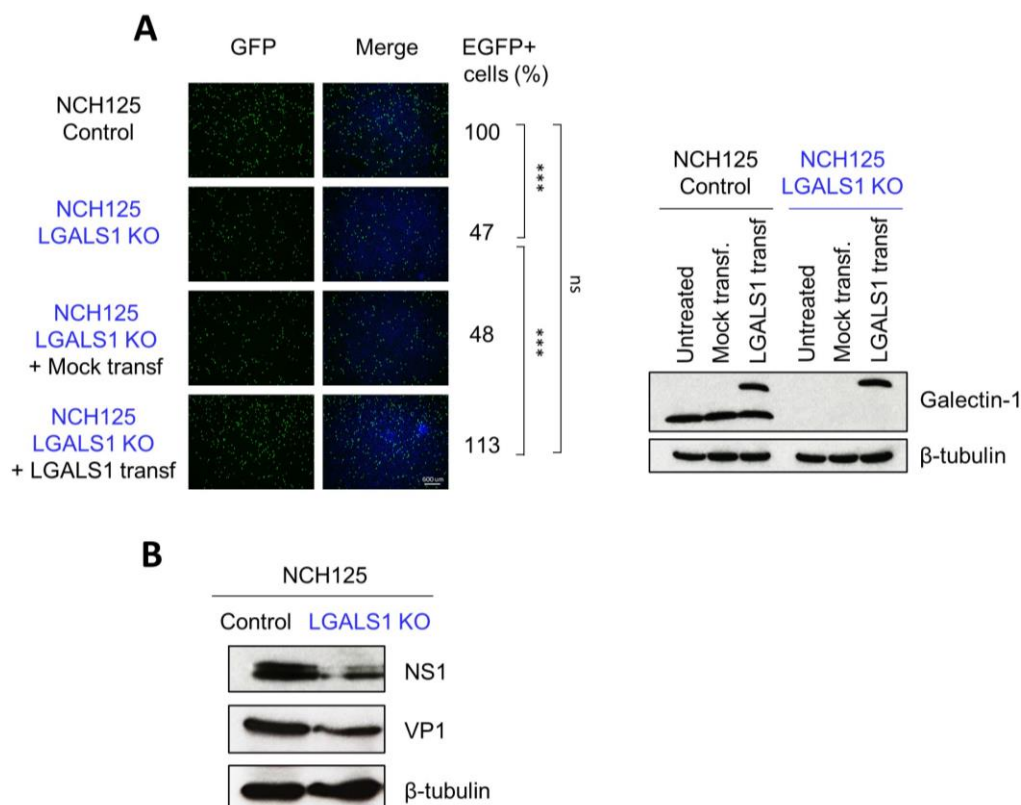


**Figure 3.6. H-1PV infectivity is reduced in NCH125 LGALS1 KO cells.**

(A) H-1PV transduction is decreased in NCH125 LGALS1 KO cells and re-established by transfecting the cells with a plasmid carrying the *LGALS1* gene. LGALS1 KO cells were transfected with a plasmid encoding the *LGALS1* gene, treated only with lipofectamine (Mock transf) or left untreated. Forty-eight hours post-transfection, cells were infected with recH-1PV-EGFP for 24 hours. NCH125 Control cells were also included, and the level of virus transduction set arbitrarily at 100% ( $ns=p>0.05$ ;  $***p\leq 0.001$ ). On the right side, Western blotting analysis shows the levels of galectin-1 at the time of infection. B-tubulin was used as a loading control. (B) NCH125 Control and NCH125 LGALS1 KO cells were infected with H-1PV used at an MOI of 2 pfu/cell for 48 hours, and NS1 and VP1 viral protein levels were assessed by Western blotting. Beta-tubulin was used as a loading control.

### 3.4 Galectin-1 knockout decreases H-1PV oncolytic activity in NCH125 cells

As the *LGALS1* knockdown/out decreases the overall amount of H-1PV inside the cells, I further assessed whether this would ultimately result in a reduced oncolytic activity. For this purpose, I assessed the susceptibility of LGALS1 KO and Control cell lines to H-1PV infection in a time course experiment in which cell viability of infected cells was assessed every 24 hours for a total of 96 hours. As shown in Figure 3.7A, while viability of Control cells decreased progressively over time, LGALS1 KO cells were less sensitive to H-1PV infection and their viability remained high throughout the experiment (above 75%). Remarkably, the susceptibility of LGALS1 KO cells to H-1PV oncototoxicity was re-established by infecting cells together with human recombinant Gal-1. Indeed, cell viability of LGALS1 KO cells infected with H-1PV dropped from 74 to 18% in the presence of Gal-1, while control experiment showed that the protein itself at the concentrations used was not toxic to the cells (Figure 3.7B). Altogether, these results highlight the critical role of Gal-1 in H-1PV infection in NCH125 glioma cells.

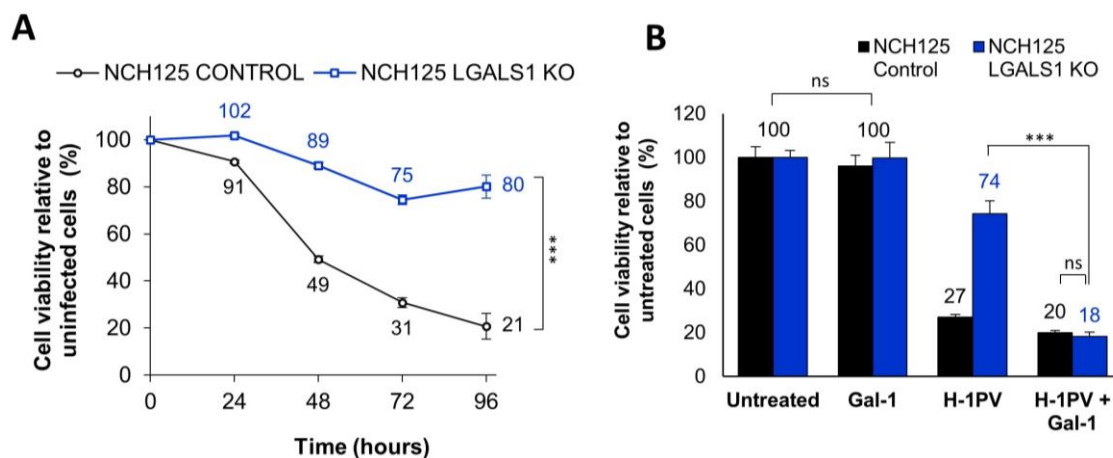


**Figure 3.7. H-1PV has a reduced oncolytic activity in NCH125 LGALS1 KO cells which is rescued by supplementing recombinant Gal-1 protein.**

(A) H-1PV oncolytic activity is reduced in NCH125 LGALS1 KO cells. Control and LGALS1 KO cells were infected with H-1PV at an MOI of 1 pfu/cell. Cell viability was assessed every 24 hours for a total of 96 hours by MTT. The curve plot depicts the mean  $\pm$  standard deviation ( $n=3$ ;  $***p \leq 0.001$ ) for each time-point expressed as a percentage of cell viability compared to corresponding uninfected cells. (B) Purified Gal-1 rescues H-1PV oncolytic activity in NCH125 LGALS1 KO cells. Control and LGALS1 KO cells were infected (or not) with H-1PV at an MOI of 1 pfu/cell, in the presence or

absence of 5 µg/mL of human recombinant Gal-1. Cell viability was assessed at 72 hours post-infection by MTT. Columns depict the percentage (mean value) of cell viability compared to uninfected cells ± standard deviation bars ( $n=3$ ;  $ns=p>0.05$ ;  $***p\leq 0.001$ ).

### **3.5 H-1PV uptake, but not cell surface attachment, is reduced in NCH125 LGALS1 KO cells**

The results shown above demonstrate that Gal-1 is involved in the H-1PV infection mechanism. However, whether Gal-1 is required for H-1PV attachment at the cell surface, internalisation or both events, remains to be defined. To elucidate the role of Gal-1 in H-1PV infection, I first performed virus binding/entry assays. LGALS1 KO and Control cell lines were infected with wild-type H-1PV at 37 °C for different amounts of time (0.5, 1, 2 and 4 hours) and subsequently, cell-associated viral DNA was assessed by qPCR. In agreement with previous results, I observed a decrease in the amount of cell-associated H-1PV DNA in LGALS1 KO cells compared to the Control cell line (Figure 3.8A). Addition of recombinant Gal-1 increased the amount of cell-associated H-1PV genome to values that were similar to those found in H-1PV-infected Control cells (Figure 3.8B).

Concerning the possible involvement of Gal-1 in H-1PV cell surface attachment, LGALS1 KO and Control cell lines were infected with H-1PV at 4 °C for 1 hour. Under these conditions, only virus attachment at the cell surface occurs, while cell entry is prevented. After removing cell unbound H-1PV particles, those that remained attached to the cell surface were stained with an anti-capsid antibody and analysis was performed by FACS. No significant differences were observed in the fluorescence signal (H-1PV binding) between the LGALS1 KO and Control cells (Figure 3.8C). The same findings were obtained by qPCR analysis (Figure 3.8D). Together, these results support that Gal-1 is involved in H-1PV cell entry rather than H-1PV cell attachment.

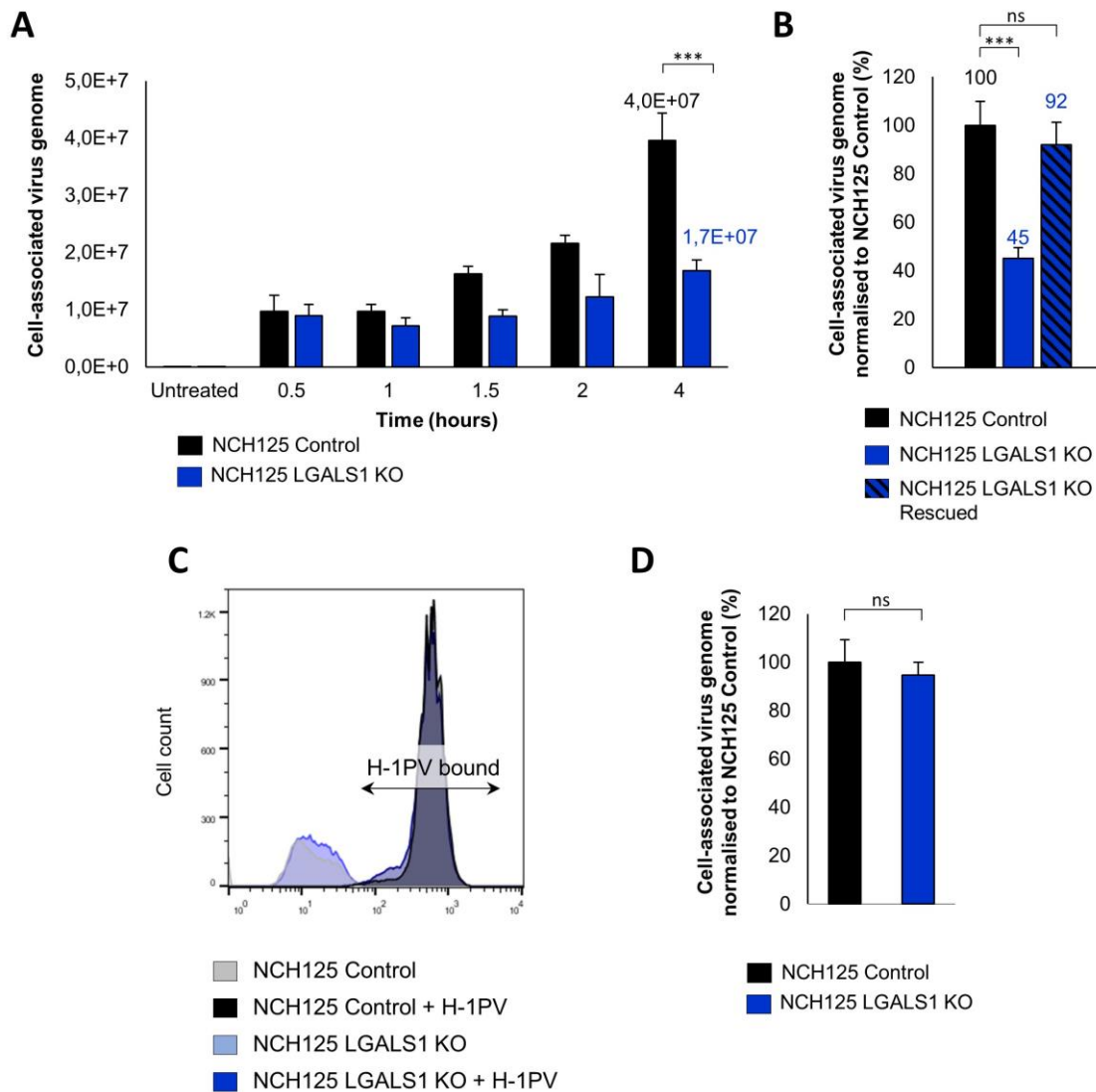


**Figure 3.8. H-1PV cellular uptake, but not cell surface binding, is reduced in NCH125 LGALS1 KO cells.**

(A) H-1PV binding/entry assays by qPCR. NCH125 Control and LGALS1 KO cells were infected with H-1PV for 0.5, 1, 1.5, 2 and 4 hours at 37 °C. Cells were then extensively washed, harvested, and encapsidated viral DNA was extracted and subjected to a qPCR. Columns in the graph show the number of copies of cell-associated H-1PV genome with relative standard deviations ( $***p \leq 0.001$ ). (B) Binding/entry is rescued by the addition of purified recombinant Gal-1. At the time of H-1PV infection, Gal-1 was added (or not) to the culture medium. Infection was carried out for 4 hours. Numbers indicate the percentage of cell-associated genome relative to NCH125 Control cells infected with H-1PV arbitrarily set as 100% ( $ns = p > 0.05$ ;  $***p \leq 0.001$ ). (C) H-1PV cell surface binding-assessed by FACS. A representative flow cytometry histogram with overlay of NCH125 Control (black) and NCH125 LGALS1 KO cells (blue) showing no difference in H-1PV-associated cells is shown. Cells were either mock- or H-1PV-infected for 1 hour at 4 °C. Cells were not permeabilised for the FACS analysis and cell surface bound H-1PV particles were detected with a specific anti-capsid antibody. (D) H-1PV binding-only assessed by qPCR. NCH125 Control and LGALS1 KO cells were infected with H-1PV for 1 hour at 4 °C. Cells were then washed, harvested, and extracted encapsidated viral DNA was then quantified by qPCR.



### 3.6 Both laminin $\gamma$ 1 and galectin-1 participate in virus binding/entry

Given that laminin  $\gamma$ 1 was described to have a determinant role in H-1PV cellular attachment and subsequent internalisation, I assessed whether the absence of both laminin  $\gamma$ 1 and Gal-1 would lead to a further decrease of internalised H-1PV compared to either one alone. For this purpose, siRNA-mediated knockdown of *LAMC1* was performed in NCH125 Control or LGALS1 KO cells. Cells were subsequently infected with H-1PV for 4 hours at 37 °C and viral genomes were analysed by qPCR. Quantification of cell-associated viral genomes revealed that knockdown of *LAMC1* led to 23% or 66% of viral genomes (upon *LAMC1* siRNA 1 or 2, respectively) in comparison to NCH125 Control cells treated solely with control siRNA (Figure 3.9). NCH125 LGALS1 KO cells treated with control siRNA presented a 50% decrease of internalised H-1PV as previously observed. Yet, this amount was further reduced to 13% or 35% (upon *LAMC1* siRNA 1 or 2, respectively) (Figure 3.9). These results demonstrate that these two factors cooperate in bringing H-1PV into cancer cells, and are therefore, determinant for a successful infection.

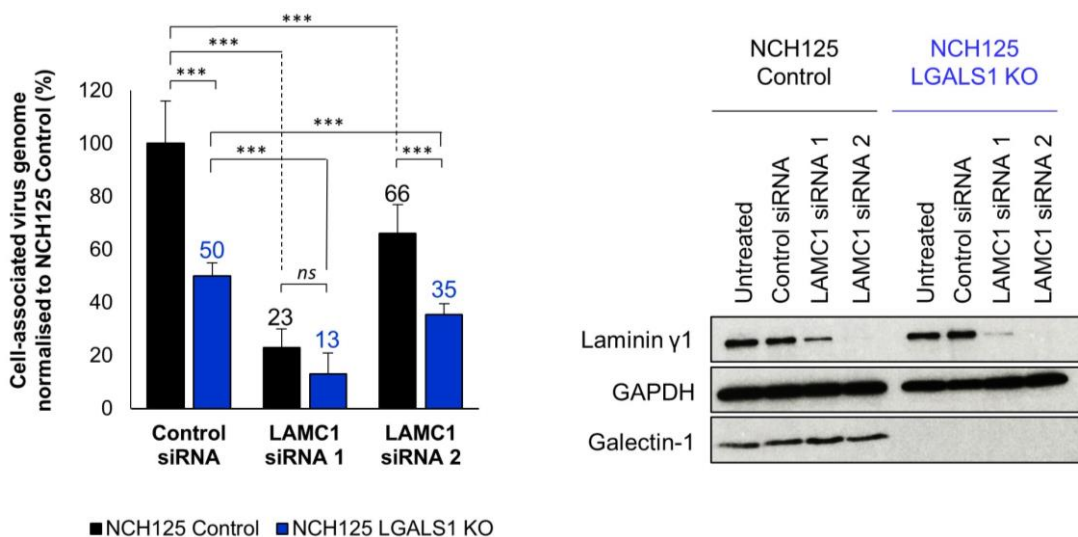


**Figure 3.9. Effect of *LAMC1* knockdown in NCH125 LGALS1 KO cells on H-1PV entry.**

NCH125 Control and NCH125 LGALS1 KO cells were transfected with two different siRNAs targeting *LAMC1* or a negative control siRNA. At 48 hours post-transfection, cells were infected with wild-type H-1PV for 4 hours at 37 °C. Cells were then extensively washed, harvested, and encapsidated viral DNA was extracted and subjected to a qPCR. Numbers indicate the percentage of cell-associated genome relative to NCH125 Control cells transfected with the control siRNA arbitrary set as 100%

( $ns=p>0.05$ ;  $***p\leq 0.001$ ). The protein levels of laminin  $\gamma 1$  and Gal-1 on cell lysates were analysed by Western blotting. GAPDH was used as a loading control.

### 3.7 H-1PV binds directly to galectin-1

Results above support that Gal-1 is involved in the entry of H-1PV into cancer cells. To further characterise H-1PV/Gal-1 interaction at the molecular level, I investigated whether the virus has the ability to directly bind to purified Gal-1. To this end, I performed ELISA assays in which wells were pre-coated either with Gal-1 or BSA as a negative control, and subsequently incubated with an increasing number of H-1PV particles. As plotted in Figure 3.10A, I found that H-1PV binds to Gal-1 in a dose-dependent manner, whereas BSA failed to capture the virus. Next, I performed ELISA experiments in which the binding affinity of H-1PV to Gal-1 was compared with that of laminin  $\gamma 1$  chain, previously shown to strongly interact with H-1PV (Kulkarni et al., in press) (sub-section 3.1.2.). As controls, wells were also pre-coated with Gal-3, collagen, fibronectin or BSA. A strong binding activity of H-1PV was observed only in wells pre-coated with Gal-1 and laminin  $\gamma 1$ , whereas binding to Gal-3, collagen or fibronectin occurred at a much lower extent (Figure 3.10B).

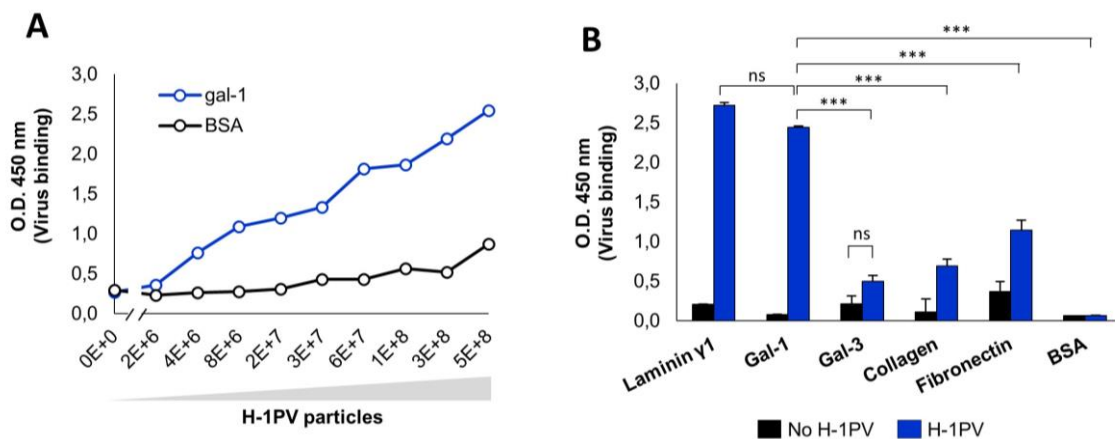


**Figure 3.10. H-1PV binds directly to galectin-1.**

(A) H-1PV binds to Gal-1 in a dose dependent manner. A 96-well plate was coated with either human recombinant galectin-1 or BSA. Increasing amounts of H-1PV were allowed to bind overnight to the immobilised protein. After washing, captured virus particles were detected by ELISA using specific anti-capsid antibody as described in the Materials and Methods section. (B) H-1PV binds to Gal-1 and laminin  $\gamma 1$  chain with similar efficiency. A 96-well plate was coated with the indicated proteins, including laminin  $\gamma 1$  chain and Gal-3. On the following day, half of the wells were treated with  $7 \times 10^8$  H-1PV particles. ELISA was performed as described in panel A. Columns show

binding affinity values (O.D. 450nm) expressed as a mean  $\pm$  standard deviation bars ( $n=2$ ;  $ns=p>0.05$ ;  $***p\leq 0.001$ ).

### 3.8 Galectin-1 is a marker of bad prognosis in various tumour types including glioblastoma

Growing evidence indicate that overexpression of Gal-1 is associated with metastasis formation, tumour recurrence and poor tumour prognosis (Wu et al., 2018). Analysis of brain tumour expression datasets using the GlioVis web application (<http://gliovis.bioinfo.cnio.es/>) confirmed that *LGALS1* overexpression is associated with worse overall survival in brain tumours. Focusing particularly on GBM, we also observed that these tissues have significantly higher expression of *LGALS1* in comparison to those from healthy individuals (Figure 3.11A). Furthermore, the analysis revealed a steady increase in *LGALS1* expression from the WHO grade II to IV gliomas (Figure 3.11B). As well, high *LGALS1* expression is associated with poor prognosis in glioma (Figure 3.12).

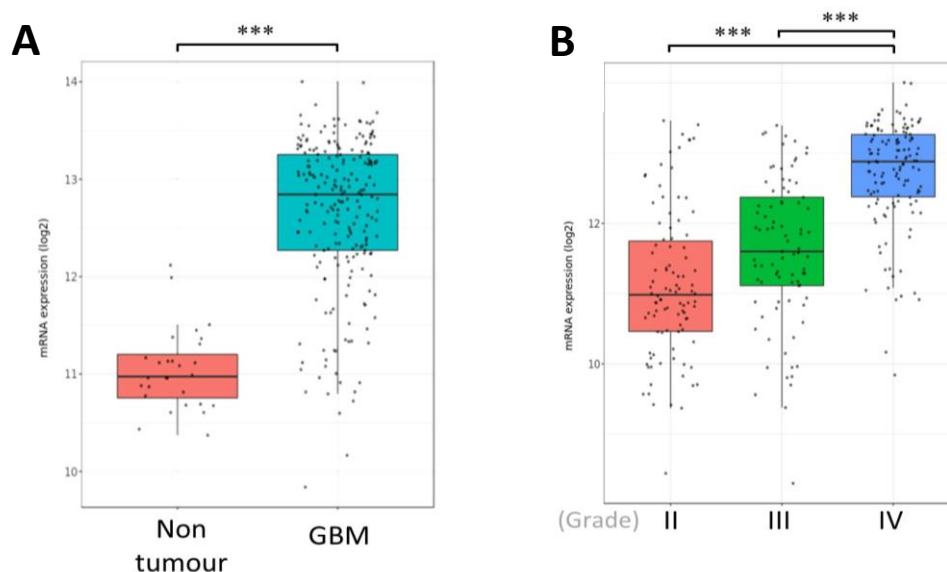


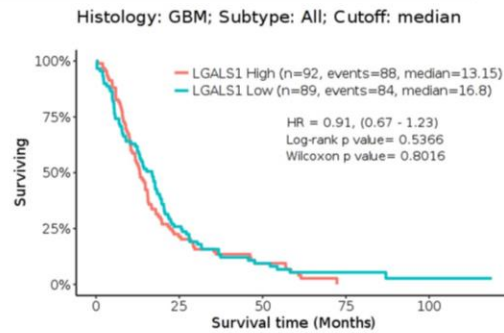
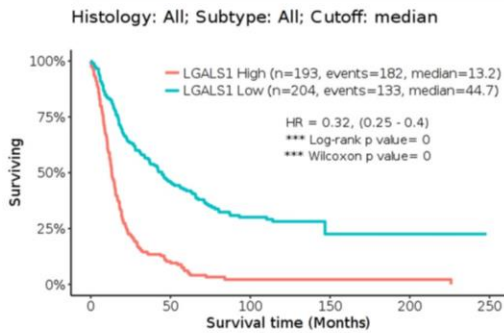
**Figure 3.11. *LGALS1* is overexpression in high-grade glioma.**

Analysis of *LGALS1* expression retrieved from the REMBRANDT dataset using the GlioVis portal. (A) Comparison based on histology, namely non-tumour *versus* glioblastoma multiforme (GMB). (B) Comparison based on WHO grade II, III and IV gliomas. Statistical significance was assessed by Tukey's honestly significant difference test ( $***p<0.001$ ).

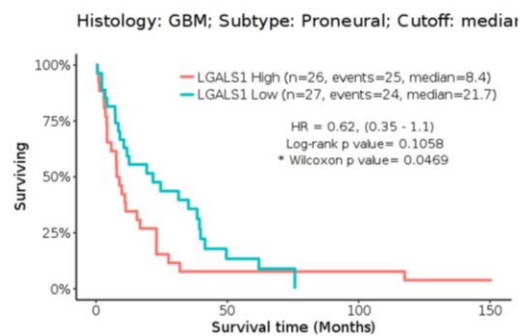
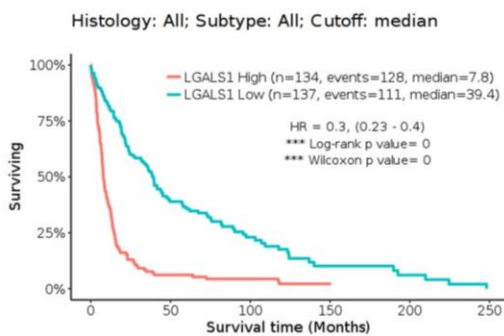
Kaplan-Meier estimator  
survival analysis in **glioma**

Kaplan-Meier estimator  
survival analysis in **GBM**

Rembrandt dataset



Gravendeel dataset



TCGA\_GBMLGG dataset

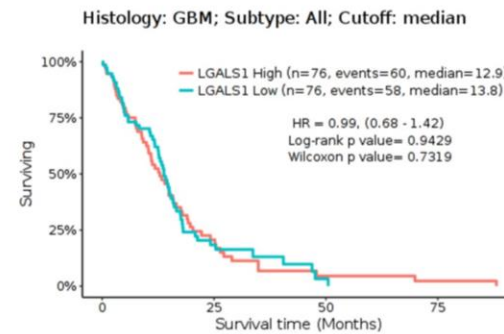
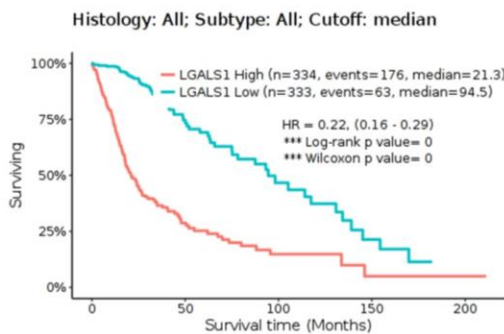


**Figure 3.12. Higher levels of LGALS1 are associated with poor prognosis in glioma.**

Kaplan-Meier survival curves for patients with glioma and glioblastoma (GBM) are divided in two groups based on the *LGALS1* expression. Analysis was retrieved from the Rembrandt, Gravendeel and TCGA\_GBMLGG datasets using the GlioVis portal. The number of patients in each group and the log-rank *p* value are indicated. HR: hazard ration.

Next, we investigated whether Gal-1 varied between normal brain tissue, primary and recurrent GBM. For this purpose, I collaborated with Dr. Miletic and Dr. Hossain in the University of Bergen performed a home-made protein tissue microarray in a cohort of 122 GBM patient biopsies, comprised by 12 biopsies from normal tissues (brain, liver and tonsil – 4 from each organ), 61 primary and 49 recurrent tumour biopsies (Figure 3.13A). Expression pattern of Gal-1 in these biopsies was analysed by immunohistochemistry using an anti-galectin-1 antibody. Overall, low levels of Gal-1 in normal tissues were observed when compared to GBM biopsies (1.9 vs 10.0) (Figure 3.13B). Among GBM samples, a diversified Gal-1 expression profile was found, with recurrent GBM expressing significantly higher levels of Gal-1 in comparison with primary GBM (13.7 vs 7.0) (Figure 3.13C). As well, (45% of recurrent GBM expressed Gal-1 at medium or high levels were observed against 20% in primary GBM) (Figure 3.13A).

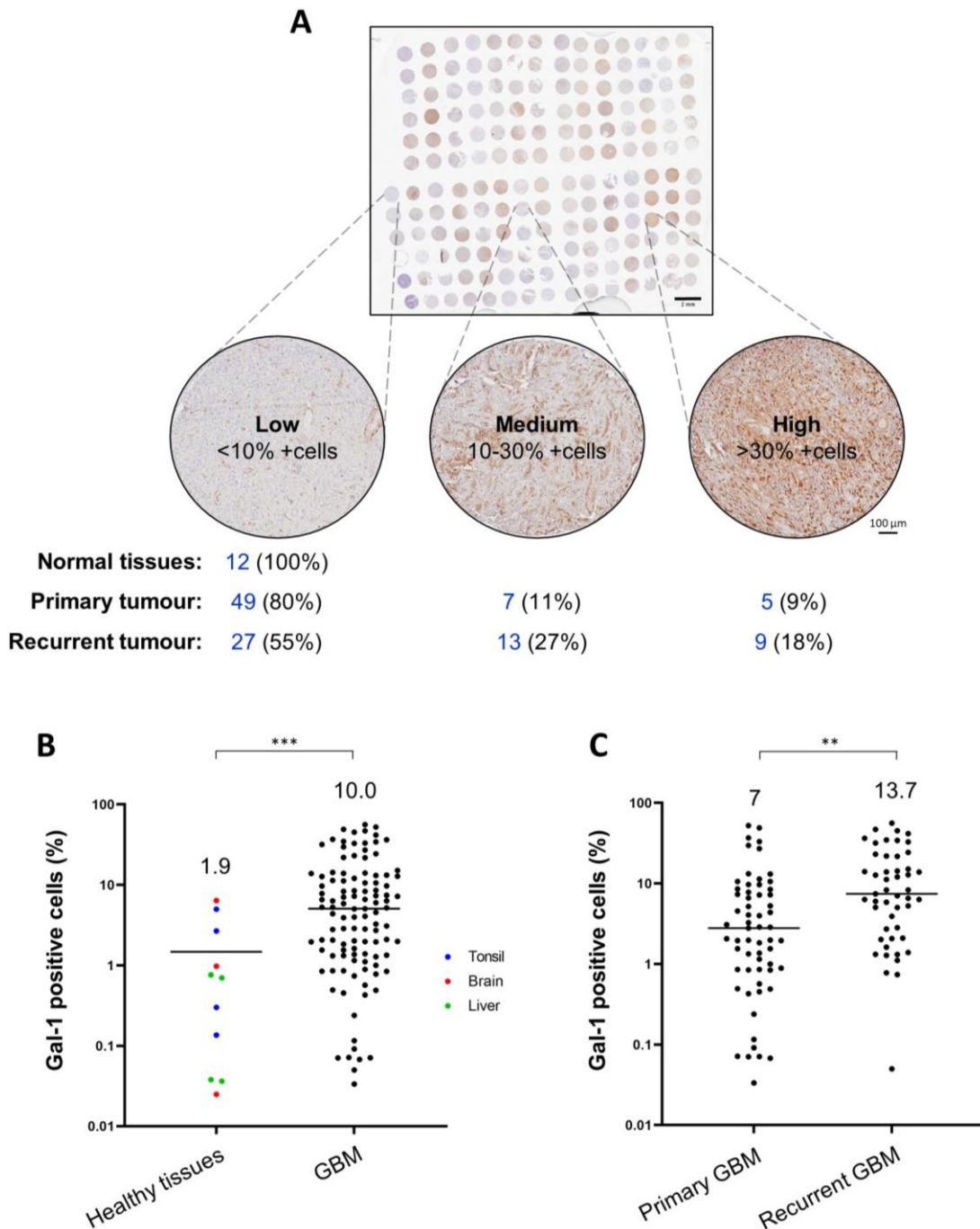


**Figure 3.13. Differential expression of galectin-1 in normal tissues, primary and recurrent GBM biopsies.**

(A) Overview of the tissue microarray. This study included biopsies from normal tissue ( $n=12$ ), primary GBM ( $n=61$ ) and recurrent GBM ( $n=49$ ). Biopsies were categorised based on galectin-1 expression after immunostaining with anti-galectin-1 antibody: low (<10% positive cells), medium (10-30% positive cells) or high expression (>30% positive cells). Number of biopsies which fell into each category are indicated under each representative image. Quantification of galectin-1 positive cells (%) was performed as described in the M&M section using in-house software. (B) Comparative analysis of galectin-1 expression between healthy tissues and GBM (primary and recurrent); or (C) between primary and recurrent GBM. The average number of galectin-1-positive cells is indicated with a horizontal line and with the value on top. (\*\* $p \leq 0.01$ ; \*\*\* $p \leq 0.001$ ).

### 3.9 *LGALS1* expression profile of NCI-60 cells positively correlates with H-1PV oncotoxicity.

At this point of my study, I looked for a putative correlation between the *LGALS1* gene expression levels and H-1PV oncotoxicity. To this end, Serena Bonifati, and *Coll.* (during her PhD studies in Dr. Marchini's laboratory) have screened cancer cell lines belonging to the National Cancer Institute (NCI)-60 panel for their susceptibility to H-1PV. This panel includes 60 cell lines derived from different tissue origins, namely lung, central nervous system, melanoma, breast, renal, ovarian, colon, prostate, and leukaemia (Shoemaker, 2006). Analysis of virus-mediated oncotoxicity was performed by xCELLigence in 53 cell lines for 5-7 days in response to increasing amounts of wild-type H-1PV. The seven leukemic cell lines had to be excluded from the panel since they were suspension-growing cells, and therefore, not compatible with the xCELLigence system. The viral MOI responsible for killing 50% of the cell population at 72 hours post-infection (EC50) was calculated (Figure 3.14). As a result, 36 cell lines were found to be highly susceptible to H-1PV oncolytic activity (cytotoxic and cytostatic effects observed at MOI  $\leq 10$ ); 11 cell lines to have low sensitivity (effects observed between MOI 10–50); and 6 cell lines to be refractory to the highest H-1PV dose tested (MOI 50).

The NCI-60 cancer cell lines have had their gene expression profile fully characterised and made publicly available (Shoemaker, 2006). In this manner, the EC50 values were merged with the *LGALS1* gene expression levels to investigate a possible correlation between the two. Indeed, the *LGALS1* mRNA levels moderately anti-correlated with the EC50 values (Figure 3.15). To corroborate this finding, an independent gene expression dataset was also assessed – the Cancer Cell Line Encyclopaedia (CCLE) – using the 38 NCI-60 cell lines that were found in the database. A consistent anti-correlation was found both using the NCI-60 and the CCLE, suggesting that cells expressing higher levels of *LGALS1* may be more susceptible to virus killing activity (Figure 3.15).

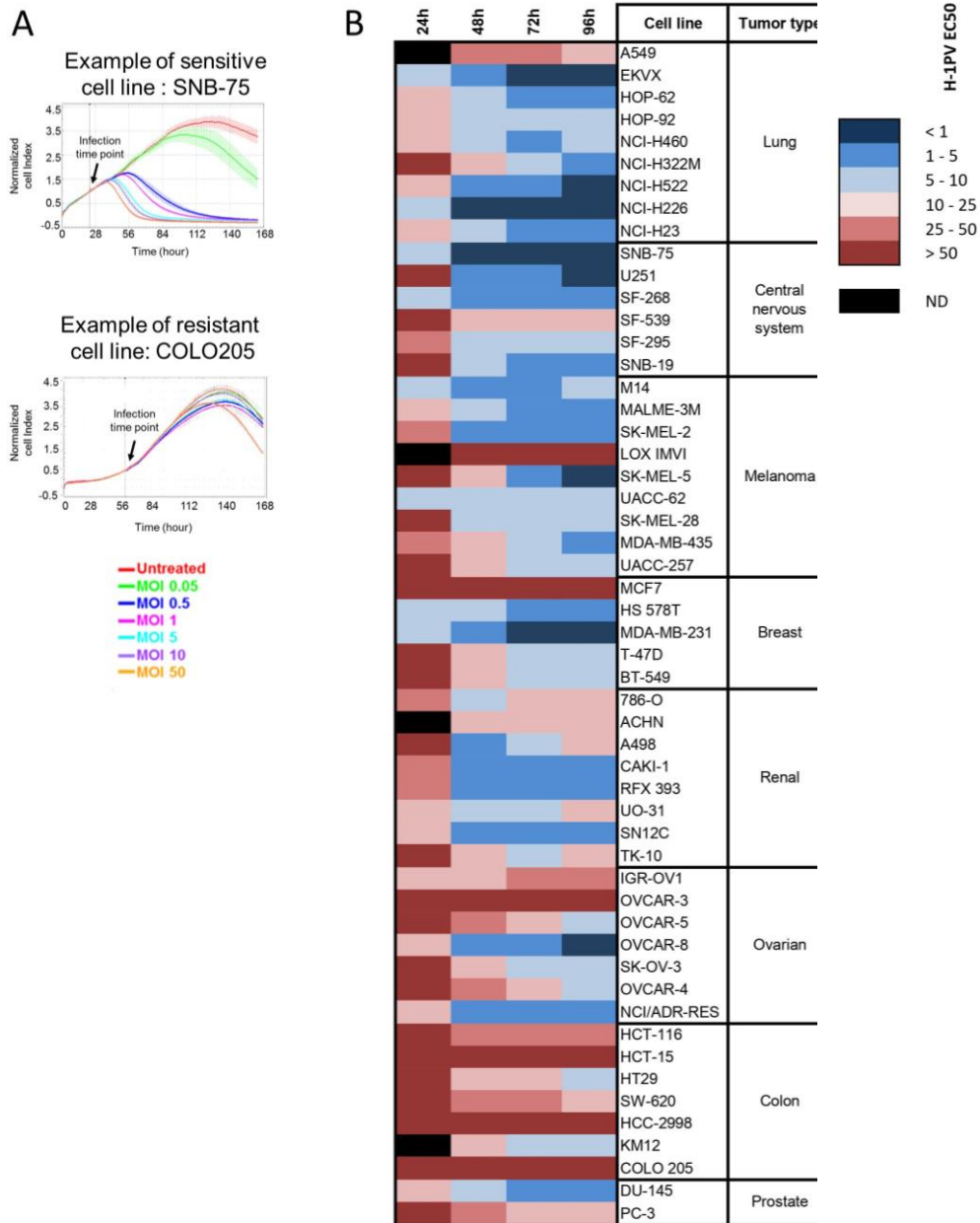


**Figure 3.14. NCI-60 cancer cell lines susceptibility to H-1PV oncolytic activity.**

Susceptibility of cancer cell lines from the NCI-60 panel to H-1PV infection was assessed by the xCELLigence system. A total of 53 cancer cells were incubated with different amounts of wild-type H-1PV or left untreated. (A) The cell viability profile of SNB-75 (H-1PV-sensitive) and COLO205 (H-1PV-resistant) cell lines are shown as representative examples. (B) The heatmap depicts the susceptibility of each cell line based on the H-1PV MOI causing 50% of cell death (EC50) at 24, 48, 72 and 96 hours post-infection measured by xCELLigence. EC50 values range from dark blue (lowest) to dark red (highest). Black indicates those cases where EC50 values were not determined (ND).



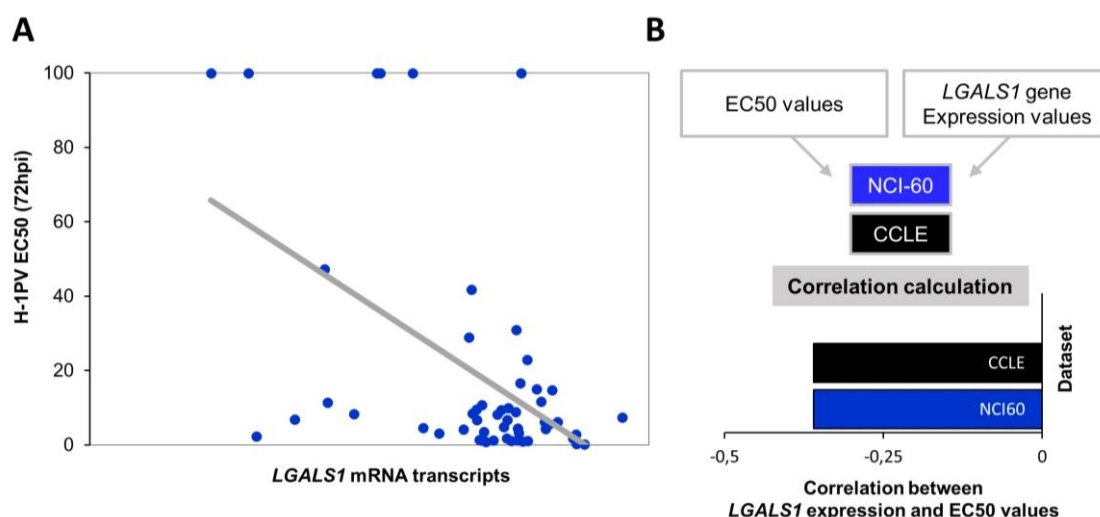


**Figure 3.15. Correlation between H-1PV oncolytic activity and *LGALS1* gene expression of cancer cell lines.**

Fifty-three cancer cell lines from the National Cancer Institute (NCI)-60 panel were tested for their susceptibility in response to H-1PV infection by xCELLigence. H-1PV EC50 values were calculated as the viral MOI that kills 50% of the cell population at 72 hours post-infection measured by xCELLigence (see Figure 3.14). **(A)** *LGALS1* expression versus H-1PV EC50. *LGALS1* gene expression was retrieved from the NCI-60 database. Scatter plot depicts the *LGALS1* expression levels of the 53 cancer cell lines on the x-axis, and the corresponding EC50 (at 72 hours post-infection) on the y-axis. Each blue dot corresponds to a cell line and the black line corresponds to a linear regression. **(B)** *LGALS1* levels are moderately anti-correlated with H-1PV EC50. *LGALS1* gene expression was retrieved from the NCI-60 (53 cell lines) and Cancer Cell Line Encyclopedia (CCLE) (38 cell lines). Bar plot depicts the correlation between the gene expression of each independent dataset and the EC50 values (Pearson's correlation). Significant anti-correlation with  $r = -0.36$  and  $p < 0.001$  (null hypothesis:  $r = 0$ )

### **3.10 *LGALS1* expression positively correlates with H-1PV oncolysis in glioma cell lines.**

Glioma cancer cell lines are generally susceptible to H-1PV oncolysis (Herrero y Calle et al., 2004). However, not all cancer cell lines respond similarly, ranging from highly to lowly permissive, or even resistant to H-1PV. Kulkarni et al., has recently described four semi-permissive glioma cell lines to H-1PV infection, namely U251, LN308, T98G and A172-MG which express low levels of *LAMC1* (Kulkarni et al., in press). Yet, it is possible that other cell components may account for the poor susceptibility of these cell lines to H-1PV infection. Using the NanoString technology, assessment of *LGALS1* levels revealed that the levels were much lower in the four semi-permissive glioma cell lines than those found in the two H-1PV-sensitive glioma cell lines (NCH125 and NCH37) (Figure 3.16A). Monitoring of cell viability in real time by xCELLigence confirmed previous results showing that NCH125 and NCH37 cell lines are efficiently killed by H-1PV at an MOI of 5 (pfu/cell); while U251, LN308, T98G and A172-MG cell lines are not. Remarkably, susceptibility of these cell lines to H-1PV oncotoxicity was substantially enhanced by addition of human recombinant Gal-1 (Figure 3.16B). Consistent with previous results, addition of exogenous Gal-1 promoted H-1PV entry in the four glioma cell lines, by increasing the cell-associated viral genomes by 1.5- to 2.8-fold, while not interfering with the viral binding to the cell surface (Figure 3.16C). Together, these results confirmed that Gal-1 plays a critical role in H-1PV infection at the level of virus entry and provide important evidence that Gal-1 levels can determine the outcome of H-1PV infection. As well, these results further support the assessment of *LGALS1*/Gal-1 levels and pave the way for its usage to predict the success of H-1PV infection.

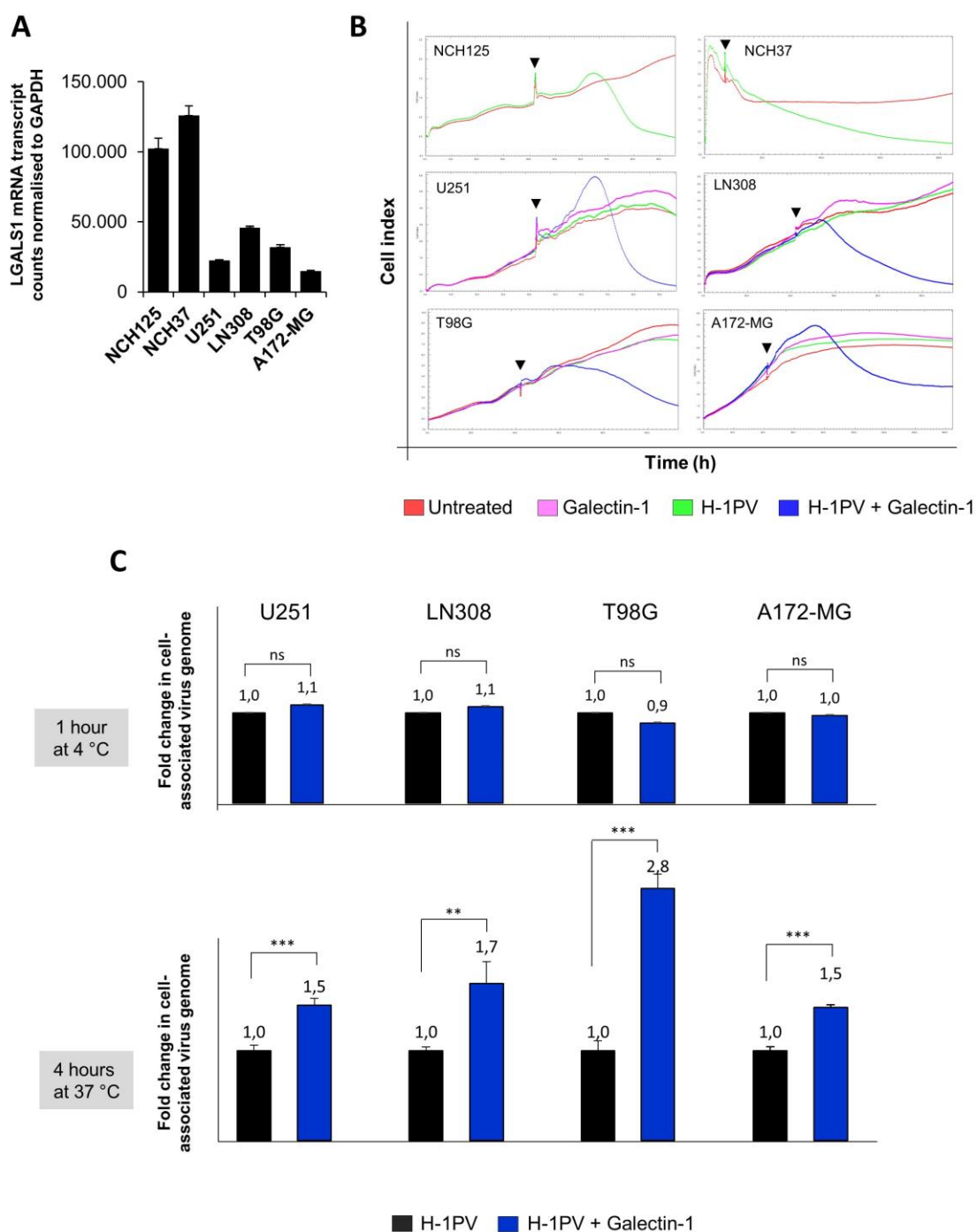


**Figure 3.16. Galectin-1 levels in glioma cell lines determine the success of H-1PV infection.**

(A) Total mRNA was isolated from glioma cell lines susceptible (NCH125; NCH37) or semi-permissive (U251; LN308; T98G; A172-MG) to H-1PV infection and *LGALS1* mRNA transcripts were measured using NanoString analysis. Bar graph depicts the *LGALS1* transcript counts and numbers on the top of the columns indicate gene expression fold-changes between susceptible (NCH125 or NCH37) and semi-permissive (U251, LN308, T98G, and A172-MG) cancer cell lines. (B) NCH125 and NCH37 cell lines were either infected with H-1PV at an MOI of 5 pfu/cell (green) or left untreated (red). Poorly susceptible cell lines were infected with H-1PV at an MOI

of 5 pfu/cell (green), incubated with 5 µg/mL of human recombinant Gal-1 (pink), H-1PV and Gal-1 simultaneously (blue), or left untreated (red). Cell viability was assessed by xCELLigence every 30 min in real time. The curve shows the “Cell index” mean ( $n=3$ ) at any given time proportional to the viability of the cell population. Black arrows indicate the time of treatment. (C) H-1PV entry is rescued upon Gal-1 administration. U251; LN308; T98G and A172-MG cells were incubated with H-1PV alone or H-1PV and Gal-1. Incubations were carried out either for 1 hour at 4 °C (binding-only), or for 4 hours at 37 °C (binding/entry). Cells were then washed, harvested, and encapsidated viral DNA was extracted and subsequently quantified by qPCR. Columns in the graph show the fold change of number of copies of cell-associated H-1PV genome relative to the virus-infected cells arbitrarily set as 1, with respective standard deviations ( $ns=p>0.05$ ;  $**p\leq 0.01$ ;  $***p\leq 0.001$ ).

## Chapter 4: H-1PV enters cancer cells through clathrin-mediated endocytosis

Contrarily to other parvoviruses, the H-1PV entry pathways remain to be elucidated. In this chapter, I report the study on the route that H-1PV uses to enter in cervical carcinoma HeLa and glioma NCH125 cells. For this purpose, in collaboration with the DKFZ Electron Microscopy Core Facility and with Dr. Clemens Bretscher, post-doc in the laboratory, I performed electron microscopy and immunofluorescence analyses. Afterwards, I carried out siRNA-mediated knockdown and chemical inhibition of key factors involved in the endocytic pathways. These are part of a paper recently published in *Viruses* (Ferreira et al., 2020) (see Appendix).

### 4.1 Electron microscopy shows H-1PV associated with clathrin-coated pits

In collaboration with Dr. Karsten Richter from the DKFZ Electron Microscopy facility, we performed an electron microscopy analysis to gain insights into the H-1PV entry pathways. For this purpose, a high MOI (2000 pfu/cell) was used given that ultrathin sections of cells need a considerable number of viruses for a successful detection. Infection of HeLa cells with H-1PV was carried out at 4 °C for 1 hour to only allow the virus to bind to the cell surface. H-1PV was detected at the plasma membrane bound to darker regions resembling clathrin-enriched areas (Figure 4.1A) (Locker and Schmid, 2013). Afterwards, cells were shifted to 37 °C to allow virus internalisation. After 5 min, the regions rich in clathrin and associated with H-1PV particles started to bend (Figure 4.1B). Between 10 to 30 min, H-1PV particles were found in clathrin-coated pits (Figure 4.1C) or already in the cytoplasm inside a clathrin-coated vesicle (Figure 4.1D).

Of note, H-1PV was never found inside small flask-shaped vesicles which are typically associated to caveolae-mediated endocytosis (Short, 2018). Therefore, these findings suggest that H-1PV is internalised mostly (if not exclusively) through CME.

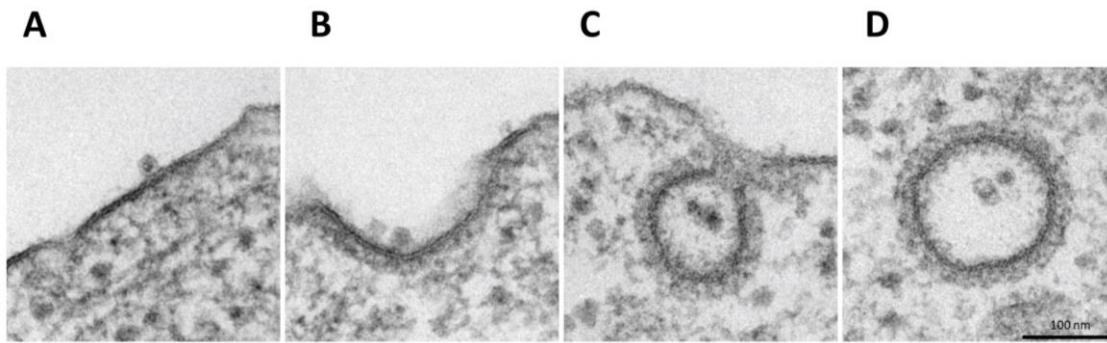


**Figure 4.1. H-1PV is internalised *via* clathrin-mediated endocytosis.**

HeLa cells were infected with H-1PV at an MOI of 2000 pfu/cell for various amounts of time. **(A)** Infection for 1 hour at 4 °C showed the virus associated to thickened (clathrin-rich) regions on the plasma membrane. **(B)** Infection at 37 °C revealed that in the first 5 min, H-1PV particles are observed in zones of membrane curvature. **(C)** Roughly 10 min after infection at 37 °C, viral particles are detected in clathrin-coated pits which are still joined to the plasma membrane. The pit is progressively invaginated into the cell and the neck constricted. **(D)** Between 10–30 min at 37 °C, viral particles are detected in the cytoplasm inside a clathrin-coated vesicle.

## 4.2 H-1PV co-localises with clathrin upon entry

The electron microscopy analysis provided initial evidence that H-1PV enters cells *via* a clathrin-dependent pathway. In order to investigate this mechanism through an independent approach, together with CB, we looked for a potential co-localisation of H-1PV particles and clathrin heavy chain (CHC). For this purpose, I infected HeLa cells with H-1PV for 1 hour at 4 °C and shifted the temperature to 37 °C for 30 min to achieve a synchronised infection. Analysis by confocal microscopy revealed patches of H-1PV overlaid with CHC (Figure 4.2). This result corroborates the evidence supporting that H-1PV is internalised *via* CME.

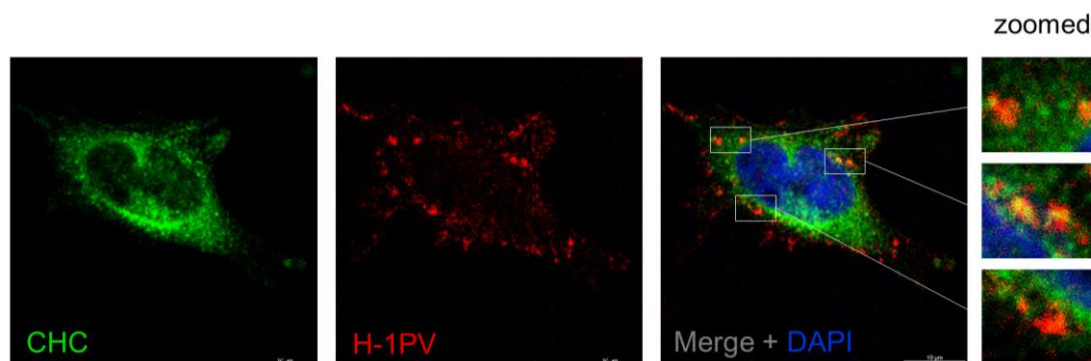


**Figure 4.2. Co-localisation of H-1PV and clathrin upon virus entry.**

HeLa cells were infected with H-1PV for 1 hour at 4 °C and followed by an incubation for 30 min at 37 °C. Subsequently, cells were processed for confocal microscopy, including the staining using anti-H-1PV capsid and anti-clathrin-heavy chain (CHC) antibodies. Cell nuclei were visualised by DAPI staining. Confocal microscopy analysis showed that H-1PV particles (Alexa Fluor 594, red) co-localised with CHC (Alexa Fluor 488, green) during infection. On the right, three examples of regions where co-localisation was observed are shown zoomed in.

### **4.3 H-1PV enters cells preferentially *via* clathrin-mediated endocytosis**

Given the previous results, I assessed whether H-1PV infection would be affected if certain endocytic pathways were targeted using pharmacological inhibitors. I chose HeLa and NCH125 cancer cell lines, which are highly permissive to H-1PV infection (Hristov et al., 2010, Li et al., 2013a), and evaluated the impact of the inhibition using the recH-1PV-EGFP.

To inhibit CME, I used hypertonic sucrose, chlorpromazine (CPZ) and pitstop 2. Hypertonic sucrose is one of the most popular inhibitors of CME and is responsible for trapping clathrin in microcages (Heuser and Anderson, 1989). CPZ is a cationic amphiphatic chemical inhibitor that causes the misassembly of clathrin lattices at the cell surface (Wang et al., 1993). Pitstop 2 mechanism consists of binding to and blocking the amino terminus domain of clathrin (von Kleist et al., 2011). Taking into consideration that H-1PV is strictly dependent on the host cell to enter S-phase to start viral DNA replication, I first checked if the inhibitors altered normal cellular proliferation. At the concentrations used, the different inhibitors did not alter the proliferation rate of HeLa or NCH125 cells (Figure 4.3).

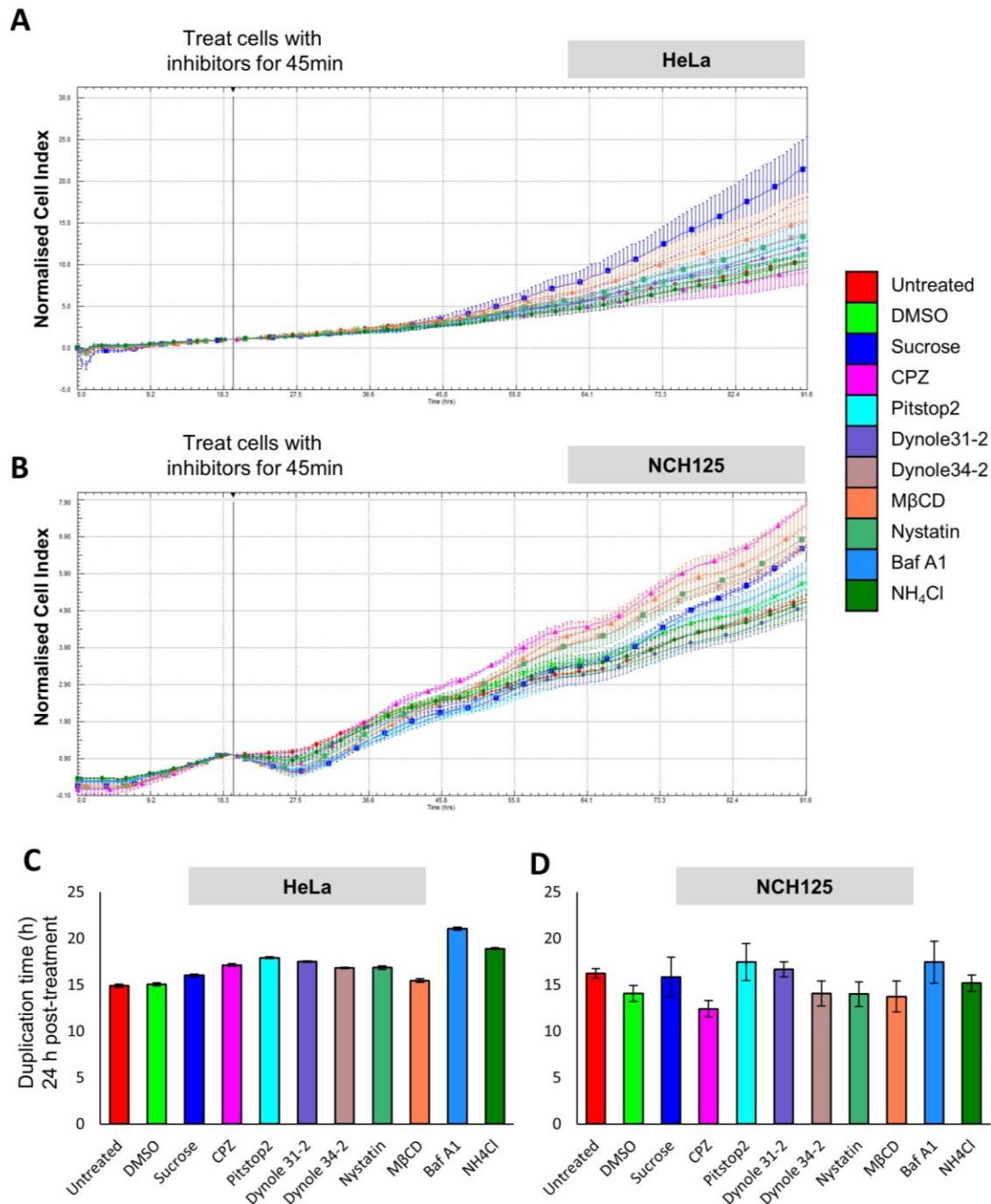


**Figure 4.3. Pharmacological inhibitors do not hinder cellular proliferation.**

(A) HeLa and (B) NCH125 cells were seeded in a 96-well E-plate and left untreated or treated with DMSO, hypertonic sucrose, chlorpromazine (CPZ), pitstop 2, Dynole 31-2, Dynole 34-2, M $\beta$ CD, nystatin, bafilomycin A1 (BafA1) or ammonium chloride (NH<sub>4</sub>Cl) for 45 min and then grown for an additional 72 hours. Inhibitors were applied at the same concentrations used for studying H-1PV entry pathways. Cell growth was monitored with the xCELLigence System. Curves represent the mean Cell Index value from 3 wells  $\pm$  SD ( $n=3$ ). (C) HeLa or (D) NCH125 cells' doubling time for the first 24 hours after treatment was generated using the xCELLigence System. Data is plotted as the "Normalised Cell Index", that is the Cell Index mean from 3 wells  $\pm$  SD, normalised to the time of treatment.



Then, I tested if the drugs were efficient at inhibiting the CME at the concentrations which did not affect cell proliferation. To this end, I monitored the internalisation of TexasRed-labelled transferrin, a protein proven to enter cells exclusively *via* CME (Mayle et al., 2012). Having proven that, the three inhibitors were used at the minimum concentration at which an efficient block of transferrin uptake was observed (Fig. 4.4 lower panel).

Pre-treatment with sucrose drastically reduced H-1PV transduction by over 90% in HeLa and 80% in NCH125 cell lines compared to cells left untreated (Figure 4.4 upper panel). In contrast, when cells were treated with sucrose 3 hours post-infection (by the time H-1PV particles had already been internalised), the H-1PV transduction was not substantially affected, showing that sucrose restricts H-1PV transduction at the level of virus entry (Figure 4.5). In agreement with these results, I observed a solid decrease of H-1PV transduction upon pre-treatment of cells with CPZ (roughly 90% reduction in both cell lines) or with pitstop 2 (60% reduction in HeLa and more than 70% in NCH125 cells) compared to cells left untreated (Figure 4.4).

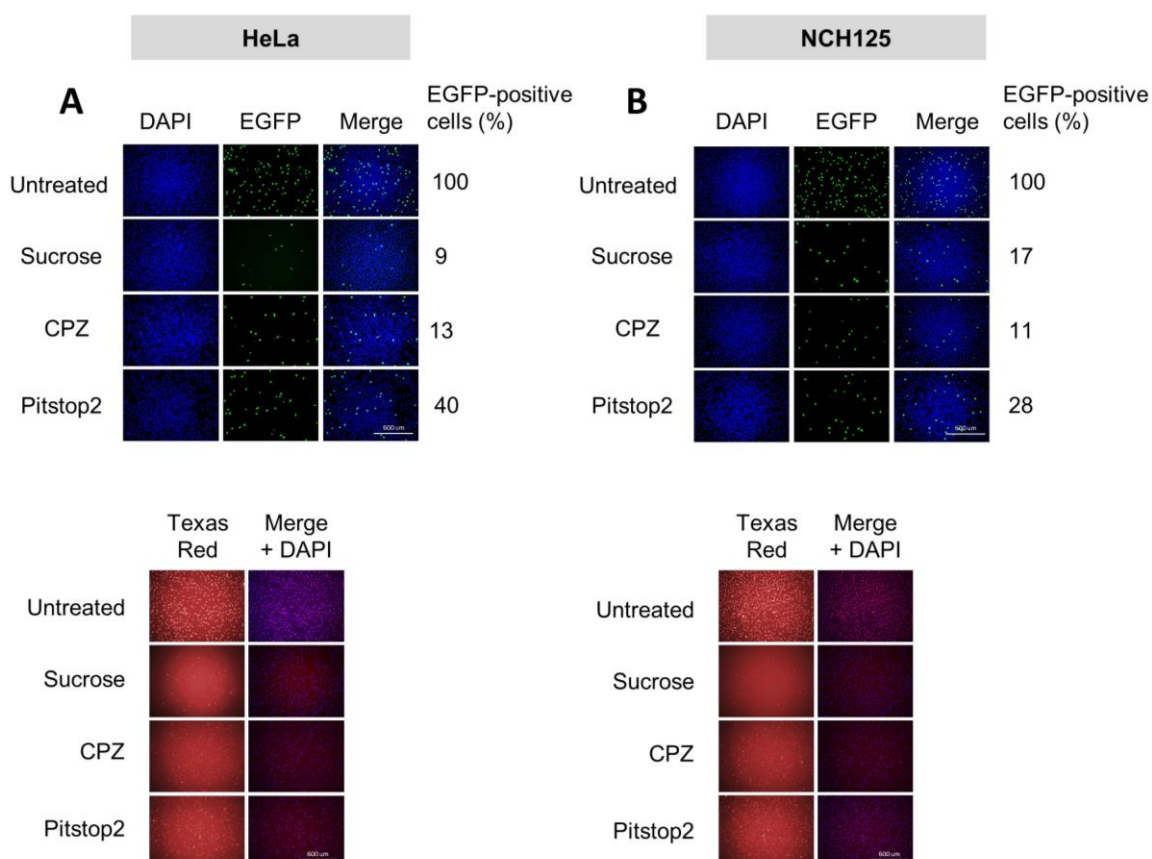


**Figure 4.4. Blocking clathrin-mediated endocytosis using chemical inhibitors results in significant reduction of H-1PV transduction.**

(A) HeLa and (B) NCH125 cells were pre-treated for 45 min with different inhibitors of CME (hypertonic sucrose, chlorpromazine (CPZ) or pitstop 2) or left untreated. Subsequently, cells were infected with recH-1PV-EGFP for 4 hours in the presence of the inhibitor. At 20 hours post-infection, cells were processed as described in Chapter 2: Materials and Methods. Numbers indicate the average percentage of EGFP-positive cells observed after each treatment relative to the number of EGFP-positive cells observed in untreated cells, which was arbitrarily set as 100%. On the lower panel, the transferrin uptake control (Texas-Red) for every pharmacological inhibitor is shown.

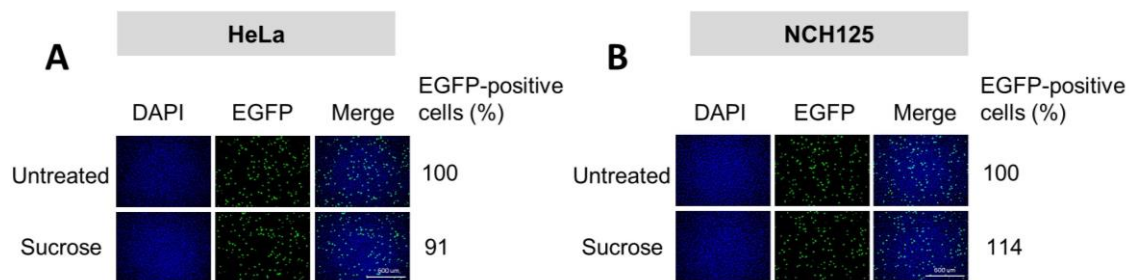


**Figure 4.5. Hypertonic sucrose has no effect on H-1PV transduction if added 3 hours post-infection.**

(A) HeLa and (B) NCH125 cells were infected with recH-1PV-EGFP for 3 hours, and then treated or not with sucrose for 45 min. At 20 hours post-infection, cells were processed as described in Chapter 2: Materials and Methods. Numbers indicate the average percentage of EGFP-positive cells observed after treatment relative to the number of EGFP-positive cells observed in untreated cells, which was arbitrarily set as 100%.

AP-2 complexes are heterotetramers which play an essential role in CME. These adaptors are responsible for initiating the CME and the assembly of clathrin-coated pits (McMahon and Boucrot, 2011). To further confirm the involvement of CME in H-1PV uptake, I performed siRNA-mediated silencing of *AP2M1*, the gene encoding for the subunit  $\mu 1$  of AP2 (Kadlecova et al., 2017). In order to do so, I transfected HeLa and NCH125 cells with pool of siRNAs targeting *AP2M1* or a pool of non-targeting siRNAs (scrambled), and subsequently infected cells with recH-1PV-EGFP. As a result, I observed a robust reduction in H-1PV transduction in both cell lines (more than 60% when compared with the scrambled siRNA-treated cells) (Figure 4.6 upper panel). Under these conditions, transferrin uptake was efficiently blocked (Figure 4.6 middle panel). Additionally, even though AP2 $\mu 1$  protein was under our detection limit with the antibodies used in both cell lines, I validated the knockdown efficiency by quantitative

reverse transcription PCR (RT-qPCR) (Figure 4.6 lower panel). These results demonstrate that H-1PV enters HeLa and NCH125 cells through CME, and confirm AP2 $\mu$ 1 involvement in H-1PV life cycle as previously suggested by the siRNA library screening (Figure 3.1).

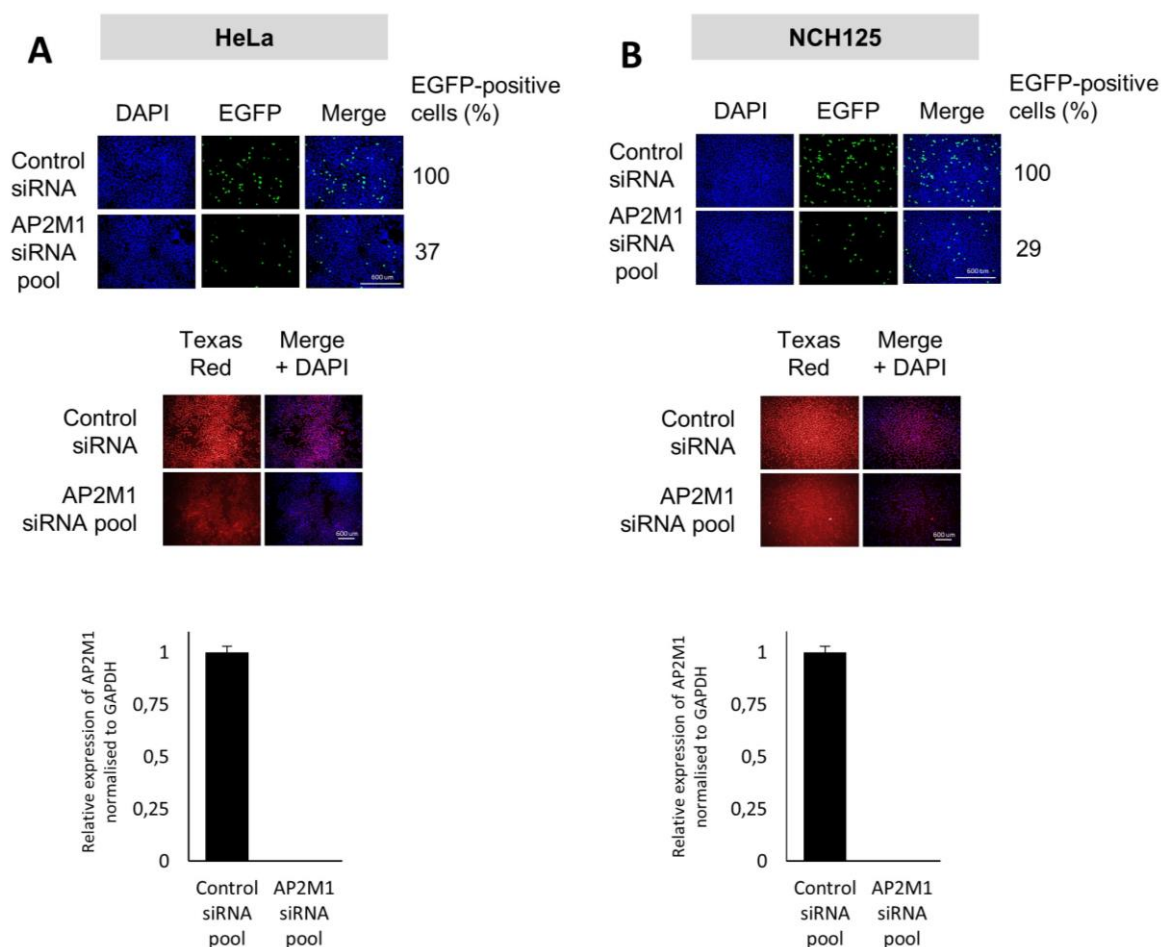


**Figure 4.6. Knockdown of *AP2M1* results in significant reduction of H-1PV transduction.**

(A) HeLa and (B) NCH125 cells were transfected with a siRNA pool targeting either *AP2M1* or control siRNA (scrambled). At 48 hours post-transfection, cells were infected with recH-1PV-EGFP for 4 hours and grown for an additional 20 hours. Cells were processed as described in Chapter 2: Materials and Methods. Numbers indicate the average percentage of EGFP-positive cells relative to the number of EGFP-positive cells observed in control siRNA-transfected cells, which was arbitrarily set as 100%. On the middle panel, the transferrin uptake (Texas-Red) for after siRNA knockdown is shown. On the lower panel, the assessment of *AP2M1* gene relative expression by RT-qPCR is shown. Presented values were calculated using the  $2^{-\Delta\Delta C_t}$  method in order to determine the fold-change for *AP2M1* gene expression between control siRNA- and *AP2M1* siRNA-treated cells using GAPDH as the endogenous control. The values represent the mean  $\pm$  SD ( $n=3$ ).

## 4.4 H-1PV does not enter cells *via* caveolae-dependent endocytosis

To explore if H-1PV uses other endocytic pathways apart from the CME to enter HeLa and NCH125 cells, I used nystatin and methyl- $\beta$ -cyclodextrin (M $\beta$ CD) to inhibit the caveolae-mediated endocytosis. Both inhibitors act by disrupting lipid rafts, in particular by depleting cells from cholesterol required for caveolae-mediated viral uptake (Anderson et al., 1996, Kilsdonk et al., 1995). Pre-treatment of cells with nystatin or M $\beta$ CD at the concentrations used did not significantly increase or decrease H-1PV transduction, providing evidence that H-1PV does not take this endocytic route to enter in HeLa or NCH125 cells (Figure 4.7).

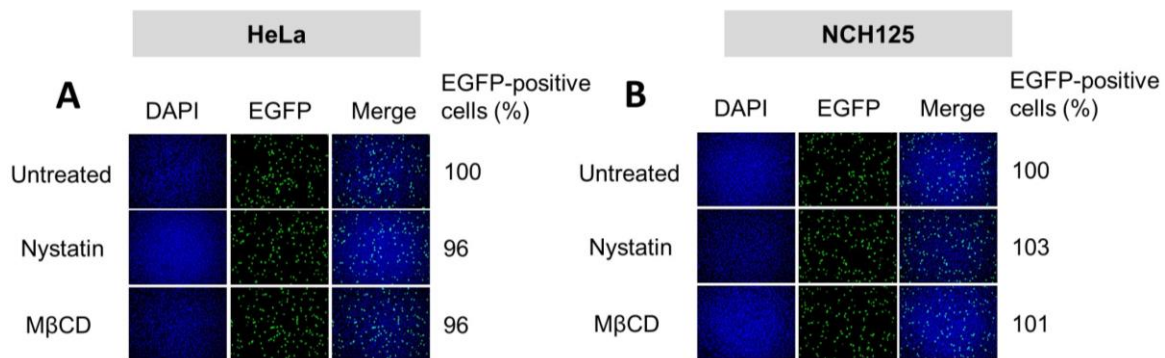


**Figure 4.7. Inhibition of caveolae-mediated endocytosis does not decrease H-1PV transduction.**

(A) HeLa and (B) NCH125 cells were pre-treated for 45 min with 10  $\mu$ g/mL nystatin, 10mM methyl- $\beta$  cyclodextrin (M $\beta$ CD) or left untreated. Cells were then infected with recH-1PV-EGFP for 4 hours in the presence of the inhibitors. At 20 hours post-infection, cells were processed as described in Chapter 2: Materials and Methods. Numbers indicate the average percentage of EGFP-positive cells observed after each treatment relative to the number of EGFP-positive cells observed in untreated cells, which was arbitrarily set as 100%.

To confirm these results, I performed a siRNA-mediated knockdown of *CAVI*. This gene encodes for caveolin-1, which represents the key factor in caveolae-mediated endocytosis. Knockdown of *CAVI* using two different siRNAs did not reduce H-1PV transduction when compared to control siRNA-transfected cells. On the contrary and surprisingly, I observed an increase of H-1PV transduction upon *CAVI* downregulation

(Figure 4.8), suggesting that caveolin-1 may represent a negative modulator of virus life cycle.

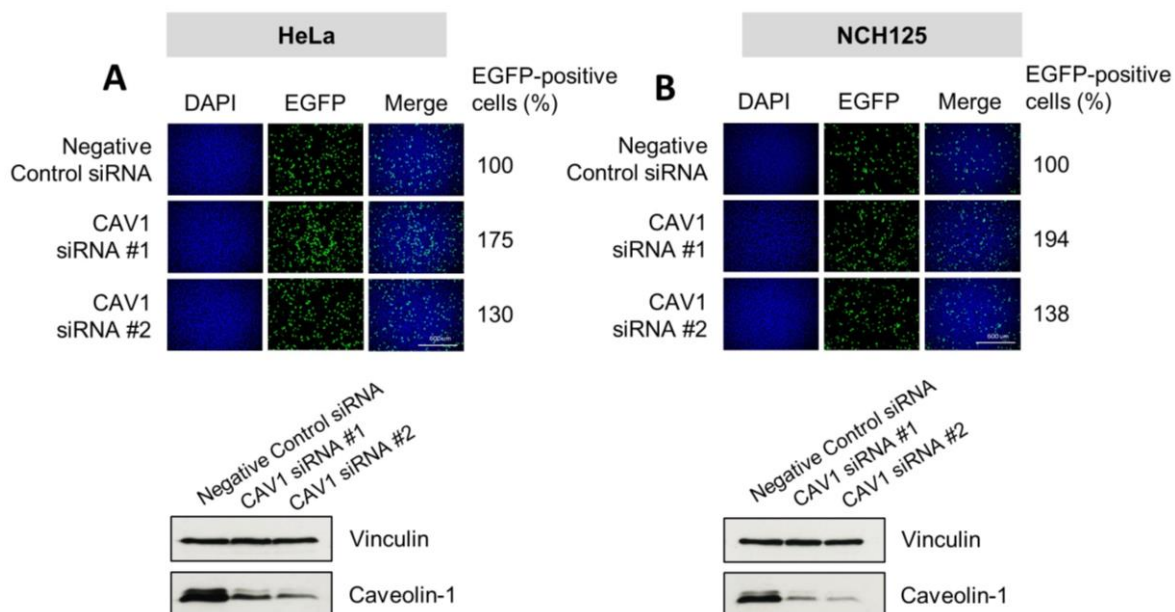


**Figure 4.8. Knockdown of *CAV1* increases H-1PV transduction.**

(A) HeLa and (B) NCH125 cells were transfected with two different siRNAs (#1 or #2) targeting *CAV1* or a control siRNA. At 48 hours post-transfection, cells were infected with rech-1PV-EGFP for 4 hours and grown for an additional 20 hours. Cells were then processed as described in Chapter 2: Materials and Methods. Numbers indicate the average percentage of EGFP-positive cells relative to the number of EGFP-positive cells observed in control siRNA-transfected cells, which was arbitrarily set as 100%. On the lower panel, analysis by Western blotting show caveolin-1 protein levels present on lysates derived from HeLa or NCH125 siRNA-transfected cells. Vinculin was used as a loading control.

Given the phenotype observed in *CAV1* siRNA-transfected cells, I reconsidered the possibility that similarly to the siRNA, targeting caveolae-mediated endocytosis with M $\beta$ CD (at different concentrations to those described in Fig. 4.7) could enhance H-1PV transduction. Cells were pre-treated with different concentration of M $\beta$ CD ranging from 10 to 320  $\mu$ M (Figure 4.9). Consistent with previous results, no significant differences in H-1PV transduction levels were observed in all conditions tested. These results suggest that although caveolin-1 may act as a negative modulator of H-1PV infection, its role in virus life cycle is most likely not at the level of virus entry. Altogether, the results described here do not support a role of caveolae-mediated endocytosis in H-1PV entry into HeLa and NCH125 cells.

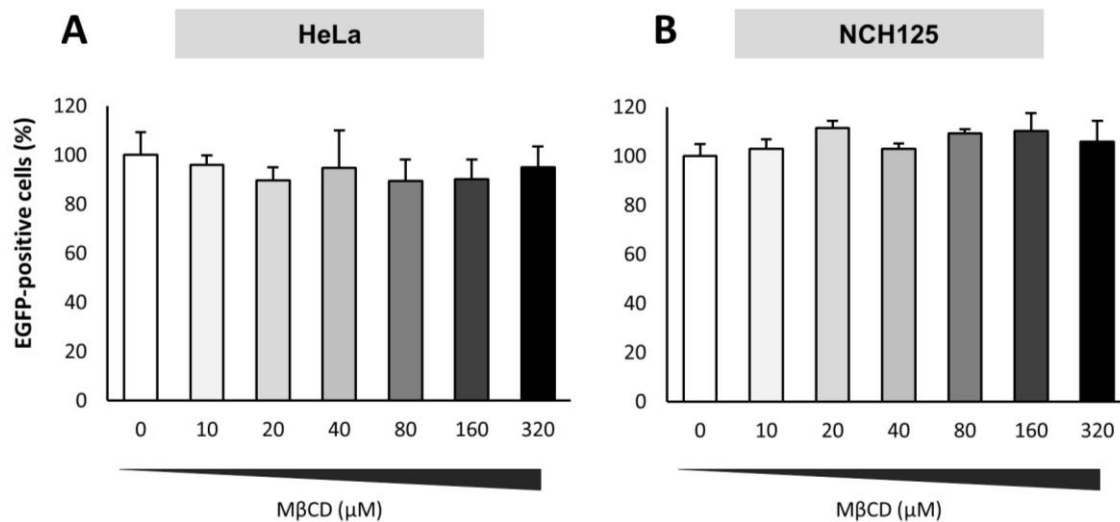


**Figure 4.9. Treatment with higher concentrations of MβCD do not result in increased H-1PV transduction.**

(A) HeLa and (B) NCH125 cells were pre-treated with increasing concentrations of MβCD ranging from 0 to 320 μM. Cells were subsequently infected with recH-1PV-EGFP for 4 hours in presence of the inhibitor. At 20 hours post-infection, cells were processed as described in Chapter 2: Materials and Methods. Graph represents the average percentage of EGFP-positive cells ± SD (n=3) observed after treatment relative to the number of EGFP-positive cells observed in untreated cells, which was arbitrarily set as 100%.

## 4.5 H-1PV internalisation is dependent on dynamin

Dynamin is a GTPase responsible for mediating the fission of the plasma membrane during endocytosis. Upon invagination of the newly formed clathrin-coated pit, dynamin reaches the vesicle neck and excises the endocytic vesicle (Kumari et al., 2010). Dynamin is reported to be involved in clathrin- and caveolae-mediated endocytosis, yet generally not in macropinocytosis (Singh et al., 2017). In order to assess the importance of dynamin activity in H-1PV entry, I used a highly selective inhibitor, Dynole 34-2 (Hill et al., 2009, Robertson et al., 2014), as well as Dynole 31-2, its inactive counterpart. Firstly, I optimised the concentration of the drugs to achieve an efficient block of transferrin uptake (Fig. 4.10 lower panel). Then, I found that Dynole 34-2, at the concentration used to block transferrin uptake, markedly decreased H-1PV transduction to only 8% in HeLa and 13% in NCH125 cells when compared to untreated cells (Figure 4.10 upper panel). In contrast, Dynole 31-2 negative control did not significantly alter H-1PV transduction. These findings show that dynamin plays an important role in H-1PV infection.

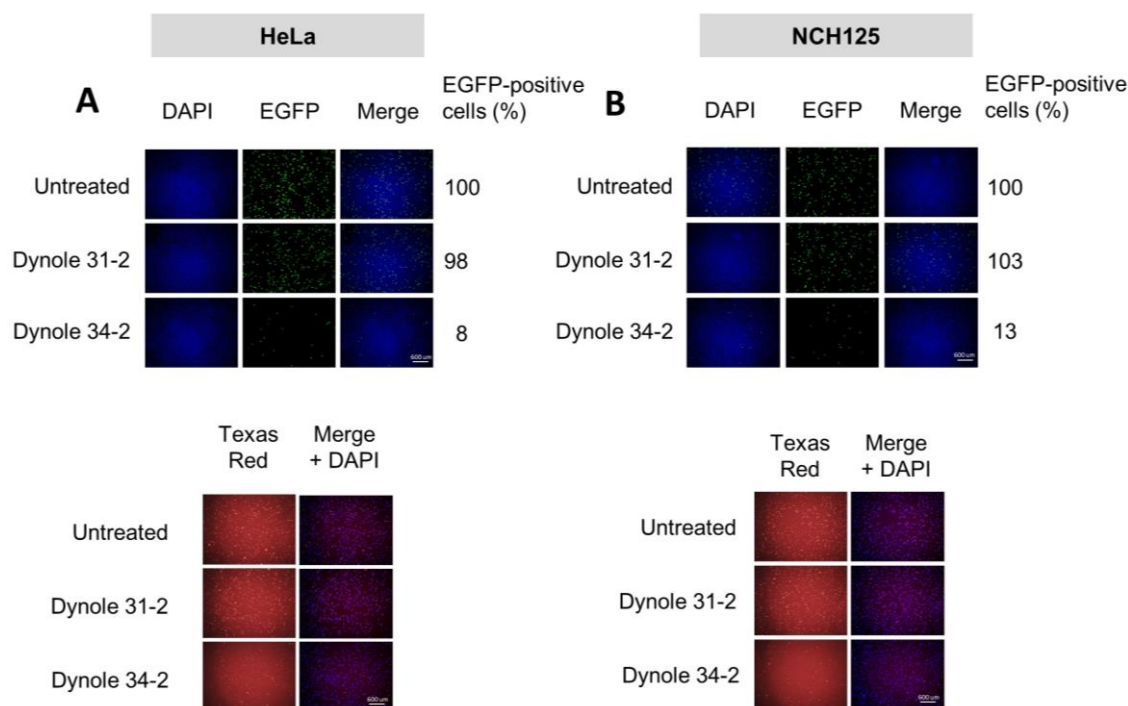


**Figure 4.10. Dynamin is involved in H-1PV cell entry**

(A) HeLa and (B) NCH125 cells were pre-treated with the active Dynole 34-2 or its inactive counterpart, Dynole 31-2, as a negative control. Cells were subsequently infected with recH-1PV-EGFP for 4 hours in the presence of the inhibitor. At 20 hours post-infection, cells were processed as described in Chapter 2: Materials and Methods. Numbers indicate the average percentage of EGFP-positive cells observed after each treatment relative to the number of EGFP-positive cells observed in untreated cells, which was arbitrarily set as 100%. On the lower panel, the transferrin uptake control (Texas-Red) for each treatment is shown.

## 4.6 H-1PV hijacks endosomes during intracellular trafficking

The Rab GTPases are a large family of proteins playing a key role in endosomal formation, maintenance and trafficking (Jordens et al., 2005). Early endosome antigen 1 (EEA1) is a Rab-5A effector protein involved in sorting early endocytic vesicles (Wilson et al., 2000). Rab-7 is considered to be the key regulator of trafficking from early to late endosome (Vanlandingham and Ceresa, 2009). Lysosomal-associated membrane protein 1 (LAMP-1) is abundant in both late endosomes and lysosomes, where is responsible for maintaining lysosomal integrity and pH (Eskelinen et al., 2003, Eskelinen, 2006). In order to track the endocytic trafficking of H-1PV, I infected HeLa cells for 1 hour at 37 °C, and subsequently analysed whether H-1PV colocalised with

EEA1, Rab-7 and LAMP-1 endosomal markers by antibody staining. Analysis by confocal microscopy revealed that H-1PV co-localised with EEA1, Rab-7 and LAMP-1 proteins during viral entry (Figure 4.11), providing further important evidence that H-1PV hijacks the endocytic machinery to reach the nucleus.

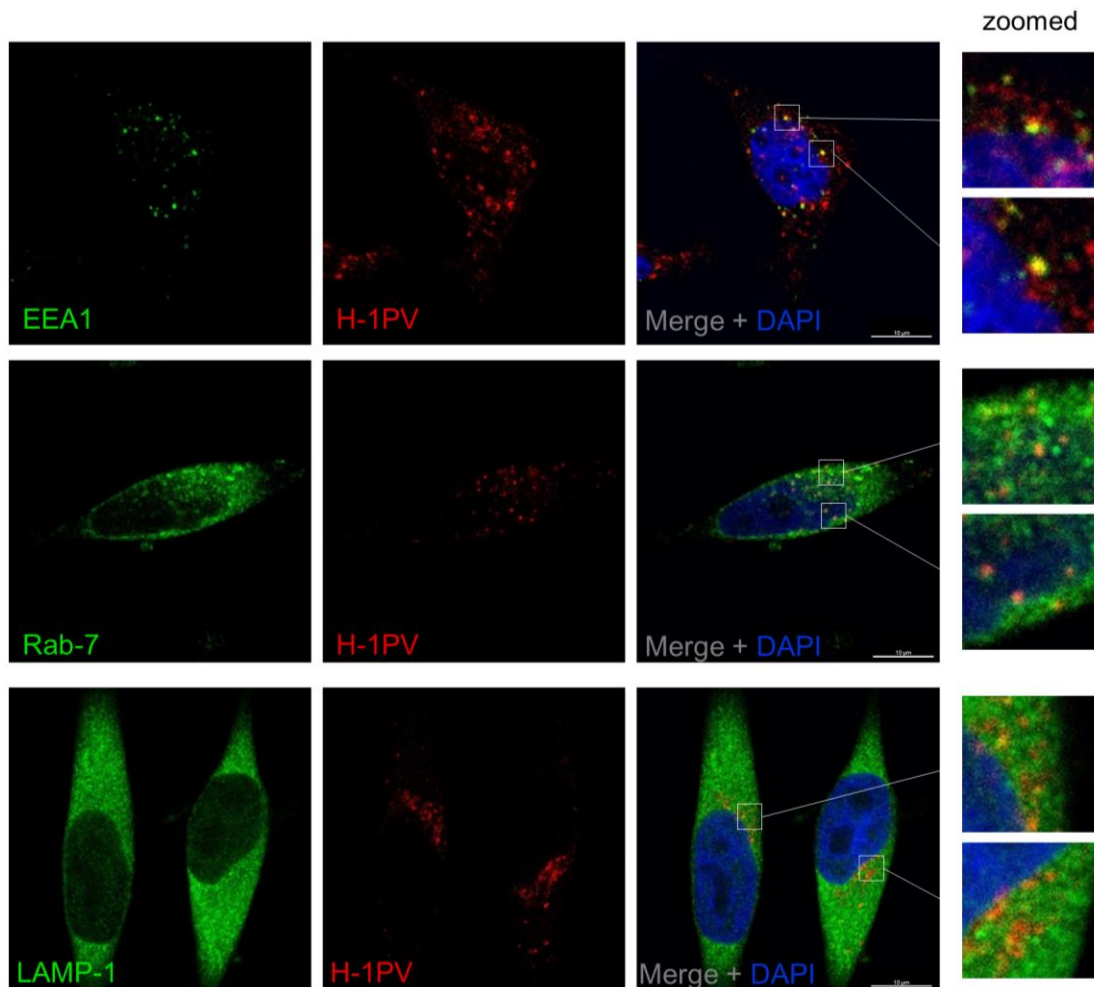


**Figure 4.11. H-1PV intracellular trafficking takes place through the endosomal system.**

HeLa cells were infected with H-1PV at a MOI of 500 (pfu/cell) for 1 hour at 37 °C. Then, H-1PV capsid (Alexa Fluor 594) and individual endosomal markers (EEA1, Rab-7 or LAMP-1 – Alexa Fluor 488) were detected using antibodies as described in Chapter 2: Materials and Methods. Cell nuclei were visualised by DAPI staining. Two examples of co-localisation are shown enlarged on the right side.



## 4.7 Low endosomal pH is required for a productive H-1PV infection

At last, I investigated whether the low pH present in the endosomes could provide the conditions necessary for a successful H-1PV infection. According to what has been described for other PtPVs, the acidic pH triggers conformational changes leading to virus uncoating and nuclear translocation (Mani et al., 2006). To test the importance of acidic pH during H-1PV infection, two drugs were used. Ammonium chloride (NH<sub>4</sub>Cl) is a lysosomotropic weak base capable of increasing the pH (Misinzo et al., 2008). Bafilomycin A1 (BafA1) is an inhibitor of vacuolar H<sup>+</sup>-ATPases which prevents the acidification of endosomes (Yoshimori et al., 1991).

Pre-treatment with NH<sub>4</sub>Cl led to a marked reduction of H-1PV transduction in HeLa and NCH125 cells (39% and 30%, respectively) compared to untreated cells (Figure 4.12 A, B). An even stronger reduction was observed upon treatment with BafA1, which almost abolished H-1PV transduction (Figure 4.12 C, D). Taken together, these findings indicate that H-1PV, similarly to other PtPVs (Ros et al., 2017), requires low endosomal pH to achieve a productive infection.

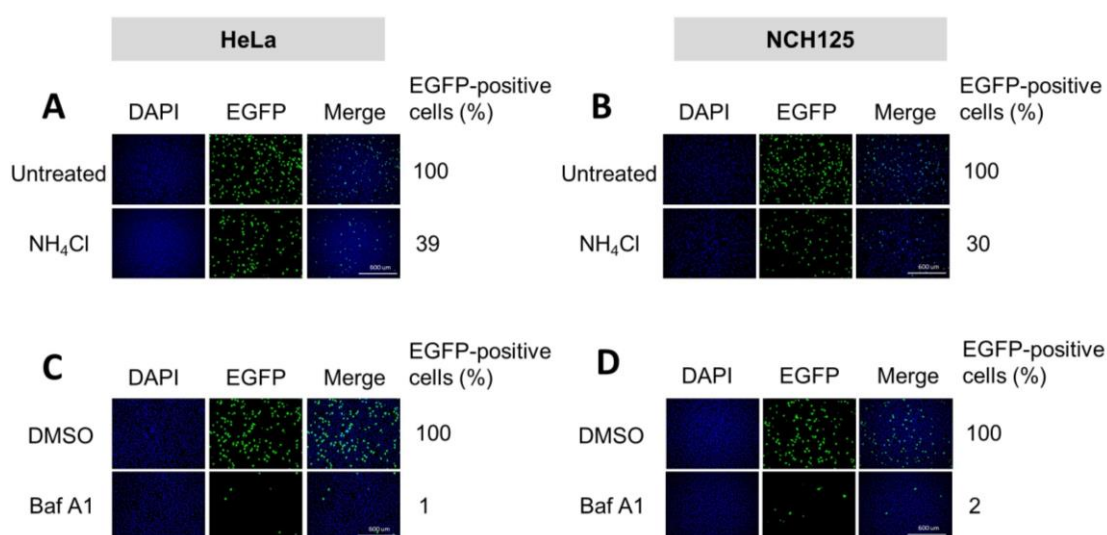


**Figure 4.12. Low endosomal pH is essential for a productive H-1PV infection.**

(A, C) HeLa and (B, D) NCH125 cells were pre-treated for 45 min with either ammonium chloride (NH<sub>4</sub>CL) or bafilomycin A1 (BafA1), respectively, or left untreated. Cells were subsequently infected with recH-1PV-EGFP for 4 hours in the presence of each inhibitor. At 20 hours post-infection, cells were processed as described in Chapter 2: Materials and Methods. Numbers indicate the average percentage of

EGFP-positive cells observed after each treatment relative to the number of EGFP-positive cells observed in untreated cells, which was arbitrarily set as 100%.

## Chapter 5: General discussion

### 5.1 H-1PV in the race against cancer

Oncolytic viruses are a thriving new addition to current cancer therapies. An assessment of the clinical trials reveals that the most common oncolytic viruses under clinical evaluation are Ad, HSV-1, reovirus and poxvirus (Macedo et al., 2020). In general, most studies did confirm the safe and highly tolerable profile of virotherapy across different viruses, combination options and delivery routes (Macedo et al., 2020). However, the majority of the studies constituted early phase trials revealing how novel this approach still is (Figure 1.1C). At the later stages of clinical testing, the outcome has not been always positive. For example, a recent phase III clinical trial of Pexa-Vec, an oncolytic vaccinia virus encoding for GM-CSF, in combination with sorafenib did not improve overall survival in patients bearing hepatocellular carcinoma (GEN, 2019). Another instance implicates the vocimagene amiretrorepvec (Toca 511). This is a replicating retrovirus encoding a cytosine deaminase, an enzyme which converts the pro-drug 5-fluorocytosine (Toca FC) into 5-fluorouracil in the tumour microenvironment. A phase II/III randomised clinical trial of Toca 511/FC ( $n=201$ ) versus standard of care treatment ( $n=202$ ) for assessment in patients with recurrent high-grade glioma has been completed by the end of 2019. The outcome revealed that the administration of Toca 511/FC did not improve overall survival compared with standard of care treatment (Cloughesy et al., 2020).

On the other hand, T-VEC, an attenuated HSV-1 encoding GM-CSF, offers a more positive view over the oncolytic virus field. T-VEC has been approved by the competent agencies of the United States of America (FDA) and Europe (EMA) to treat advanced melanoma (Andtbacka et al., 2015). Building on this success, T-VEC was further tested in combination with ipilimumab in a small phase I trial (Puzanov et al., 2016), and in a larger phase II trial with 198 patients with melanoma (Chesney et al., 2018). The outcome of the latter study revealed that the response rate went from 18% (ipilimumab alone) to 38% (combination treatment). Another pilot phase I trial involving a combination treatment with T-VEC and pembrolizumab resulted in a response rate of 62% in patients with advanced melanoma (Ribas et al., 2017). However, a large randomised clinical trial assessing T-VEC and pembrolizumab

against pembrolizumab alone was recently terminated due to futility (ClinicalTrials.gov: NCT02263508).

Among the oncolytic viruses currently being tested in the clinical setting, there is H-1PV with promising and distinguishing features. Firstly, H-1PV is not pathogenic to humans and has never been associated with any disease in humans. Secondly, H-1PV presents remarkable oncotropic and oncosuppressive potential, as demonstrated *in vitro* and in several animal models (Marchini et al., 2015a, Bretscher and Marchini, 2019). Thirdly, given that the rat is the natural host for H-1PV, the human population does not have pre-existing antiviral immunity. These features confer H-1PV an advantage over other oncolytic viruses based on human pathogens, for which neutralising antibodies could exist and clear the virus right after administration (Hartley et al., 2020).

H-1PV has been evaluated in patients with recurrent GBM and pancreatic carcinoma in early phase clinical trials (Geletneky et al., 2012, Hajda et al., 2017). Monotherapeutic treatment of H-1PV was demonstrated to be safe and well tolerated. In addition, first surrogate signs of anticancer efficacy were observed, including immunoconversion of the tumour microenvironment, improved patient tumour progression-free survival and overall survival in comparison with historical controls (Hartley et al., 2020). However, the virus was unable to eradicate the tumours at the regimen used. A few possible reasons might explain this finding, such as insufficient viral doses, restricted virus spreading, high tumour heterogeneity, exceptionally immunosuppressive microenvironment within the glioma, emergence of tumour cells resistant to virus infection and/or the development of anti-H-1PV neutralising antibodies. In fact, seroconversion was detected in patients in a dose-dependent manner (Geletneky et al., 2017). However, seroconversion also indicates that there is an activation of antiviral immunity, which ultimately enhances intratumoural infiltration of immune cells (Gujar et al., 2018). Taken as a whole, the outcome remains highly favourable and provides a new stimulus towards further clinical development in order to improve H-1PV anticancer efficacy.

To this end, several strategies have been adopted (reviewed in (Hartley et al., 2020)). In this dissertation, my main goals referred to the improvement of H-1PV-based therapies by characterising the infection mechanisms of H-1PV, particularly at the

level of binding and entry into cancer cells. For instance, this knowledge can help identify new drugs to enhance H-1PV replication in cancer cells and/or its oncolytic activity by modulating H-1PV-related cellular pathways. Furthermore, these factors may also serve as reliable biomarkers that could predict whether a tumour is susceptible or resistant to H-1PV infection. Patients could be screened for the presence of specific markers, and subsequently referred for *smart* clinical trials based on how likely they would respond to virotherapy. Groups of patients presenting parameters associated with poor response to treatment could be submitted to combination therapy and/or second-generation H-1PV vectors, or redirected to other treatments (e.g. other oncolytic viruses or immunotherapies).

Along these lines, our laboratory has previously performed a high-throughput siRNA library screening to dissect the interplay between H-1PV and the host. This approach has been widely used to identify virus cellular modulators (Hirsch, 2010). Within the oncolytic virus field, Allan and colleagues elucidated some of the mechanisms underlying Maraba rhabdovirus infection by using a genome-wide siRNA library screening (Brun et al., 2010, Mahoney et al., 2011). The screening revealed that transient inhibition of components involved in the endoplasmic reticulum stress response sensitised cancer cells to caspase-2-dependent apoptosis induced by a subsequent Maraba infection (Mahoney et al., 2011). As well, Maraba oncolytic virus combined with a small molecule inhibitor of IRE1 $\alpha$ , an endoplasmic reticulum kinase, demonstrated significantly increased oncolytic efficacy in resistant tumour models (Mahoney et al., 2011). These findings further supported the potential of the siRNA screening technology to improve H-1PV-based therapies. Our high-throughput siRNA library screening in HeLa cells using a siRNA library targeting the human druggable-genome revealed three positive modulators involved in binding and entry into cancer cells: *LAMC1*, *LGALS1* and *AP2M1* genes.

## 5.2 Laminin- $\gamma$ 1 and Galectin-1 proteins have a crucial role in H-1PV infection

The virus life cycle is a multistep process heavily dependent on the presence and abundance of viral (co-)receptors, processing enzymes and proteins required for a productive infection. Levels and activity of these determinants may vary in different cancer cells, determining their susceptibility to a particular virus.

Kulkarni et al., found that laminins, in particular those containing the laminin  $\gamma$ 1 chain, have an important role in virus cell attachment and entry, and therefore, are crucial factors for a successful H-1PV infection (Kulkarni et al., *in press*)(Fig. 5.1). Moreover, I showed that the SA moieties of laminins are essential for H-1PV/laminins interaction by ELISA, thus indicating that laminin-SA provides a docking place for the virus to anchor at the cell surface. Nevertheless, other sialylated proteins are also likely implicated in H-1PV early steps of infection. This hypothesis is supported by the fact that NA treatment fully prevented H-1PV binding and entry, whereas a residual activity was still seen upon knockdown of laminins (Kulkarni et al., *in press*).

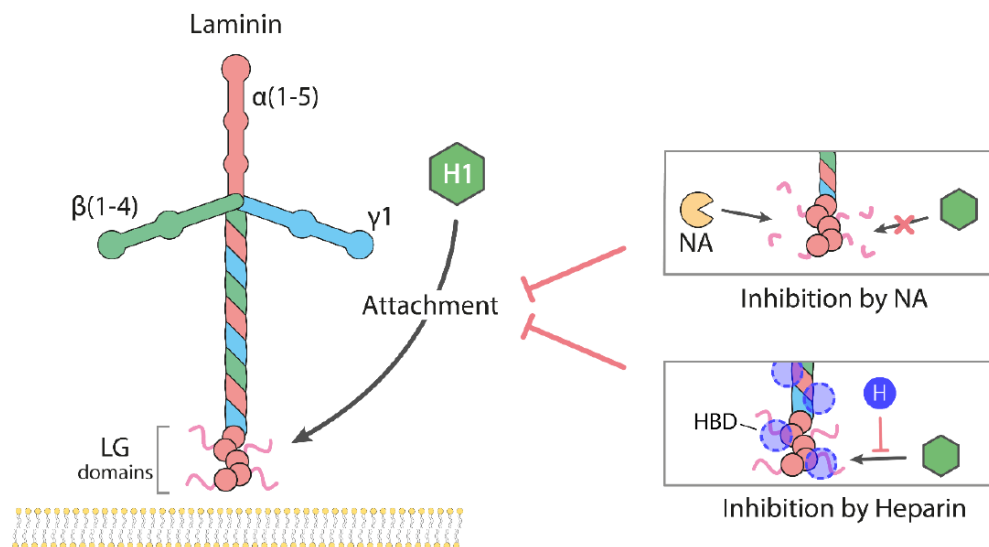


**Figure 5.1. Schematic model of the interaction of laminins with H-1PV.**

Laminins containing the  $\gamma$ 1 chain may form different heterodimer complexes with  $\alpha$  chains (1-5) and  $\beta$  chains (1-4). Binding of H-1PV to laminins occurs through SA moieties, and therefore, neuraminidase (NA) inhibits this interaction by cleaving the SA. Heparin (H) can also interfere with the laminin/H-1PV interaction likely by competing with H-1PV for the heparin-binding domains present on laminins. Figure retrieved from (Kulkarni et al., *in press*).

The siRNA library screening also revealed that silencing of *LGALS1* strongly impaired H-1PV virus transduction by approximately 70% in HeLa cells. In this manner, these results prompted us to explore whether Gal-1 is involved in H-1PV early steps of infection.

In Chapter 3, I demonstrate that Gal-1 plays a central role in H-1PV infection at the level of H-1PV cell entry, rather than cell attachment, indicating a distinct role from laminins in virus cell cycle. Furthermore, I provide evidence that H-1PV physically interacts with Gal-1 as confirmed by ELISA (Figure 3.10A). On the other hand, H-1PV did not bind to immobilised Gal-3 (Figure 3.10B) and knockdown of *LGALS3* did not impair H-1PV infection (Figure 3.4), further supporting the specificity of the H-1PV/Gal-1 interaction.

Up to now, Gal-3 was the only galectin implicated in a PtPV infection. Indeed, knockdown of *LGALS3* rendered LA9 mouse fibroblasts less susceptible to MVM infection. This phenotype was not due to a reduced binding to the cell surface; instead, Gal-3 was responsible for promoting an efficient virus uptake (Garcin et al., 2013). My findings indicate that Gal-1 is essential for a productive H-1PV infection at the level of entry, with no evidence of its requirement in viral binding to the plasma membrane of NCH125 cells. Therefore, these results suggest that the mechanisms through which Gal-1 mediate H-1PV entry are similar to that of Gal-3 in MVM infection (Garcin et al., 2015). However, the fact that H-1PV and MVM engage different galectins for their entry process may contribute to their different tropism.

Based on these results, we propose a model in which H-1PV interacts with different classes of molecules, rather than with a single cell surface receptor, in order to enter into cancer cells. Laminins containing  $\gamma 1$  chains would accumulate virus in the vicinity of the cell surface *via* SA, while Gal-1 would promote the efficient internalisation of virus particles. The exact mechanisms through which Gal-1 participates in H-1PV cell entry still remain to be elucidated. One possibility is that H-1PV hijacks extracellular Gal-1 to enter into the cells. Our results show that addition of exogenous purified Gal-1 boosts H-1PV infection at the level of virus entry, thereby sensitising semi-permissive cancer cells to H-1PV-mediated oncolysis. The exact mechanism through which galectin(s) translocate across the cell membrane remains poorly understood (Bänfer and Jacob, 2020). Even so, previous research has shown that inhibition of the

lipid raft-dependent pathway does not impede Gal-1 internalisation; instead, a total block of Gal-1 internalisation was only observed when both CME and lipid rafts were disrupted, demonstrating that Gal-1 enters cells through various mechanisms, including CME (Fajka-Boja et al., 2008, Lepur et al., 2012). Therefore, it may be possible that H-1PV uses Gal-1 to enter cancer cells through CME (the pathway taken by H-1PV, as further discussed below).

Alternatively, Gal-1 could bridge the virus to other cellular factors involved in H-1PV entry e.g. a transmembrane receptor or a co-receptor (further discussed below in Chapter 6). A number of studies have shown that the multivalent binding activity of Gal-1 and other galectins are able to cross-link carbohydrates and glycoconjugates (Brewer, 2002, Garner and Baum, 2008). For instance, Gal-1 cross-linking has the ability to massively redistribute a diverse population of glycoproteins on the cell surface of T cells and segregate them into membrane microdomains (Pace et al., 1999). Gal-1 has also been associated with the assembly and remodelling of the extracellular matrix, and to bind to various components there present, especially those containing polylectosamine chains, such as laminins (Moiseeva et al., 2003, Moiseeva et al., 2000). In this respect, *LAMC1* knockdown on NCH125 *LGALS1* KO cells further decreased H-1PV cell uptake (Figure 3.9), providing evidence that laminins and Gal-1 may cooperate in the early steps of H-1PV infection with not entirely overlapping roles. Yet, as there is still a residual internalisation of H-1PV in *LGALS1* knockout / *LAMC1* knockdown cells, it is possible that H-1PV may use alternative pathways to enter the cells and that other still unidentified cell factors are involved in the process. On the other hand, remaining laminins containing or not the laminin- $\gamma$ 1 chain may contribute for residual H-1PV entry, independently from Gal-1. Future studies need to be carried out to shed light on the different cellular factors involved in the early stages of H-1PV infection.

Gal-1, and galectins in general, have been described to be involved in various viral infections at different levels, leading to their promotion or inhibition. For instance, Gal-1 was shown to stabilise the binding of HIV-1 to CD4<sup>+</sup> T cells by cross-linking the viral gp120 and the host CD4 receptor, thereby assisting the infection of such cells (Ouellet et al., 2005). Furthermore, soluble Gal-1 enhanced the uptake of HIV-1 by monocyte-derived macrophages, while Gal-3 had no effect on infection (Mercier et al., 2008). Enterovirus 71 is another example where Gal-1 has a supporting role. Gal-



1 was shown to facilitate the infection by interacting with the carbohydrate residues in VP1 and VP3 domains, leading to a more efficient release and dissemination to other cells (Lee et al., 2015). During Nipah virus infection, Gal-1 enhances virus cell attachment to primary human endothelial cells (Garner et al., 2015). In contrast, the same group showed that later in the replication cycle, Gal-1 exerts inhibitory effects. Indeed, Gal-1 specifically binds to NiV-F and NiV-G viral glycoproteins which are responsible for cell-cell fusion and syncytia formation. This block by Gal-1 in such a crucial step ultimately results in Nipah virus infection inhibition (Levroney et al., 2005, Garner et al., 2010). The inhibitory effect by Gal-1 is also observed in influenza A infection both *in vitro* and *in vivo*. Gal-1 binds directly to the envelope glycoproteins stopping influenza from inducing hemagglutination, thereby impairing infectivity. Accordingly, *LGALS1* KO mice presented poorer survival rates in comparison to wild-type mice after influenza infection (Yang et al., 2011).

Apart from the role of galectins in virus infections, they are also linked to apoptosis, angiogenesis, cell migration and tumour-immune escape (Chou et al., 2018a). In particular, high levels of Gal-1 have been reported to be associated with cancer progression, poor prognosis and recurrence (reviewed in (Wu et al., 2018)). Several cancer types have been implicated, including gastric cancer (Chen et al., 2013), ovarian cancer (Schulz et al., 2017), pancreatic cancer (Martinez-Bosch et al., 2018) and GBM (Chou et al., 2018b), to only name a few. In accordance with previous studies, our *in-silico* analysis revealed that GBM presents significantly higher levels of *LGALS1* than normal tissues, and that *LGALS1* expression increases from grade II to IV gliomas (Figure 3.11). In terms of survival, high *LGALS1* expression is associated with a poor prognosis in glioma (Figure 3.12). To complement the bioinformatic analysis, I collaborated with Dr. Miletic and Dr. Hossain (University of Bergen, Norway) to assess a cohort of 122 patient biopsies by immunohistochemistry, where we found higher levels of Gal-1 in biopsies from patients with recurrent versus primary GBM, while in normal tissues the levels were relatively low (Figure 3.13). These findings corroborate previous studies showing that elevated levels of Gal-1 are associated with GBM (Jung et al., 2008, Verschuere et al., 2013, Astorgues-Xerri et al., 2014), and further support the usage of H-1PV to treat GBM, especially those with high Gal-1 protein content, given the key role that this protein has in virus entry and oncolysis.

We also found a correlation between the *LGALS1* expression levels and the ability of H-1PV to induce oncolysis in 59 cancer cell lines (Figures 3.14, 3.15, 3.16). These results suggest that tumours with elevated *LGALS1* expression levels are likely to be more susceptible to H-1PV oncolytic activity. Furthermore, I show that while virus attachment is unaffected, virus entry is enhanced in U251, LN308, U87 and A172-MG semi-permissive cell lines when H-1PV is administrated together with recombinant Gal-1 (Figure 3.16). Consequently, susceptibility of these glioma cells to H-1PV oncolytic activity increases, suggesting that certain levels of Gal-1 are required for an efficient productive H-1PV infection. Altogether, these findings support the idea that Gal-1 represents a limiting factor for H-1PV oncolysis, and therefore, that tumours with high Gal-1 expression are more likely to respond to H-1PV treatment. As well, these findings open up new scenarios of treatment in which exogenous administration of recombinant Gal-1 could constitute a promising adjunctive in H-1PV-based therapies. However, given the role of Gal-1 in carcinogenesis ([Blanchard et al., 2016](#)), a possible use of Gal-1 together with H-1PV has to be carefully evaluated.

### **5.3 H-1PV enters cancer cells through clathrin-mediated endocytosis**

We demonstrated that H-1PV uses CME to infect HeLa and NCH125 cancer cells through independent methods. (i) Electron microscopy analysis of HeLa cells infected with H-1PV revealed viral particles in regions resembling clathrin-enriched plasma membrane, as well as inside clathrin-coated vesicles minutes later in the infection (Figure 4.1). Of note, there was no evidence of H-1PV entering cells through a pathway that was not CME during this analysis. (ii) Confocal microscopy analysis confirmed association of H-1PV to CHC (Figure 4.2). (iii) Usage of pharmacological inhibitors (hypertonic sucrose, CPZ and pitstop 2) provided further evidence for the dependence of H-1PV on CME (Figure 4.4). (iv) siRNA-mediated knockdown of *AP2M1*, a gene encoding for the  $\mu 1$  subunit of the AP2, further validated the role of CME as a key endocytic pathway (Figure 4.6).

Previous studies have shown that PtPVs use CME for cell entry (reviewed in ([Ros et al., 2017](#))). Therefore, our findings are in accordance with the generalised idea that

PtPVs use CME as the default endocytic pathway. Nonetheless, some PtPVs have also proven to make use of alternative endocytic routes. For example, MVM hijacks at least three pathways, namely caveolae- and clathrin-independent carrier-mediated endocytosis, besides CME (Garcin and Panté, 2015). Furthermore, PPV enters cells through CME as well as macropinocytosis (Boisvert et al., 2010). Both CPV and FPV bind to the transferrin receptor, normally taken up *via* CME. Nevertheless, FPV is believed to enter cells through alternative routes. This idea stems from the fact that mutations or deletions in the internalisation motif of the transferrin receptor do not arrest viral infection completely; instead, they only decrease virus uptake (Hueffer et al., 2004). Even though it is not possible to entirely exclude the possibility of H-1PV, similar to other PtPVs, taking other endocytic pathways, the findings in HeLa and NCH125 cancer cells seem to rule out caveolae-mediated endocytosis as a crucial entry route. In fact, cells pre-treated with inhibitors of caveolae-mediated endocytosis, namely nystatin or M $\beta$ CD, did not affect H-1PV transduction in HeLa or NCH125 cells, indicating that these inhibitors do not alter H-1PV uptake (Figure 4.7). These findings are consistent with earlier studies showing that PPV (Boisvert et al., 2010) and BPV (Dudleenamjil et al., 2010) are not internalised *via* caveolae-mediated endocytosis. On the other hand, siRNA silencing of *CAVI* boosted H-1PV transduction levels (Figure 4.8), suggesting that caveolin-1 could potentially interfere with H-1PV infection. During HIV infection, caveolin-1 restricts infection in different ways. For instance, caveolin-1 suppresses NF- $\kappa$ B p65 acetylation in macrophages which leads to viral gene expression repression. As well, caveolin-1 was shown to interact with HIV viral proteins in order to hinder virus infection (Simmons Jr et al., 2012, Lin et al., 2012). Another example is seen during influenza A virus infection when abundant levels of caveolin-1 prevents infection in mouse embryo fibroblasts, while depletion of caveolin-1 reverses the phenotype (Bohm et al., 2014). In any case, further research has to be done to effectively demonstrate if caveolin-1 acts as a negative modulator of H-1PV infection. In case caveolin-1 role is validated, antagonists or specific inhibitors could represent a successful approach to enhance H-1PV clinical outcome in those cancers presenting high levels of caveolin-1.

I also provide valuable findings showing that dynamin is implicated in H-1PV cell entry (Figure 4.10). Likewise, dynamin is also involved in MVM entry in murine A9 fibroblasts, a mechanism which follows clathrin- and caveolae-mediated endocytosis

(Garcin and Panté, 2015). On the other hand, dynamin was also shown to not be required in MVM entry in mouse mammary cells transformed with polyomavirus middle T antigen, which occurs through clathrin-independent carrier-mediated endocytosis (Garcin and Panté, 2015).

Macropinocytosis is another entry pathway utilised by viruses, and is usually defined as a dynamin-independent mechanism (Swanson and Watts, 1995, Preta et al., 2015). Within the group of PtPVs, PPV has been identified to use macropinocytosis to enter cells (Boisvert et al., 2010). Regarding H-1PV, the fact that inhibition of dynamin practically abolished the infection, makes it highly improbable that H-1PV enters HeLa and NCH125 cancer cells through macropinocytosis.

Many viruses have been reported to hijack Rab-dependent entry routes to get inside the cells. Among the most commonly used, Rab-5 and -7 GTPases are the major trafficking regulators of early and late endosomes, respectively. LAMP-1, on the other hand, is present in both late endosomes and lysosomes (Jordens et al., 2005, Zhang et al., 2018). Here, I found that H-1PV co-localises with EEA1, a marker of early endosomes, as well as with Rab-7 and LAMP-1, markers of late endosomes (Figure 4.11). These findings show that H-1PV particles take advantage of the endocytic machinery during their cytosolic trafficking, similarly to other PtPVs (Ros et al., 2017). However, it is possible that H-1PV also ends up in LAMP-1-positive lysosomes. In truth, the fact that the virus follows a non-infectious route is a finding replicated with other PtPVs. A considerable fraction of MVM incoming virions is often sequestered in LAMP1-positive lysosomes, which restricts the efficiency at which the virus translocates to the nucleus (Mani et al., 2006). Moreover, CPV particles also accumulate in perinuclear LAMP2-positive lysosomes (Suikkanen et al., 2002). Although highly probable, it remains to be demonstrated whether H-1PV gets also trapped in the lysosomes. Purification of lysosomes from H-1PV infected cells could clarify this point (Aguado et al., 2016).

Earlier work has demonstrated that the low pH inside the endocytic compartments, alterations in redox conditions, and acid proteases and phosphatases cause conformational rearrangements in the catalytic PLA<sub>2</sub> domain of the VP1 capsid protein (Zádori et al., 2001, Mani et al., 2006, Farr et al., 2005). These changes are particularly important for PtPV particles release from late endosomes to the cytoplasm, and to their

subsequent nuclear translocation (Suikkanen et al., 2003, Canaan et al., 2004, Zádori et al., 2001, Vihinen-Ranta et al., 2002). Among PVs, the acidic environment in endosomes has been demonstrated to be crucial for a successful infection of B19V (Quattrocchi et al., 2012), CPV (Parker and Parrish, 2000, Vihinen-Ranta et al., 1998, Basak and Turner, 1992) and MVM (Mani et al., 2006, Ros et al., 2002). Likewise, I showed that pre-treatment with NH<sub>4</sub>Cl or BafA1 heavily restricted H-1PV infection (Figure 4.12). The precise mechanisms through which H-1PV escapes from the endosome and subsequently enters the nucleus, and ultimately the site where the viral genome becomes available for replication remain to be elucidated.

For the first time, this study reveals that H-1PV is internalised through CME dependent on dynamin activity. As well, the entry mechanism occurs *via* EEA1 and Rab-7 and relies on the acidification of endosomes. Nevertheless, we should not exclude entirely the possibility of H-1PV using different endocytic routes in other cell types.

## 5.4 Model of H-1PV entry and infection

Based on the body of evidence gathered during this thesis, we propose a model where laminins containing  $\gamma$ 1 chains would initially accumulate virus in the vicinity of the cell surface *via* SA. Gal-1 would then promote the efficient internalisation of viral particles into a pre-formed or forming clathrin-coated pit. The CME mechanism is dependent on AP-2 adaptors, and after the clathrin-coated pit is formed, dynamin GTPase activity would constrict the vesicle neck and release it into the interior of the cell. Afterwards, H-1PV would hijack the cellular endosomal system and travel from early to late endosomes where acidic pH is essential. Those viral particles which successfully escaped the late endosome would move towards the nucleus, whereas those which did not would naturally be directed to lysosomes through a non-infectious route (Figure 5.2).

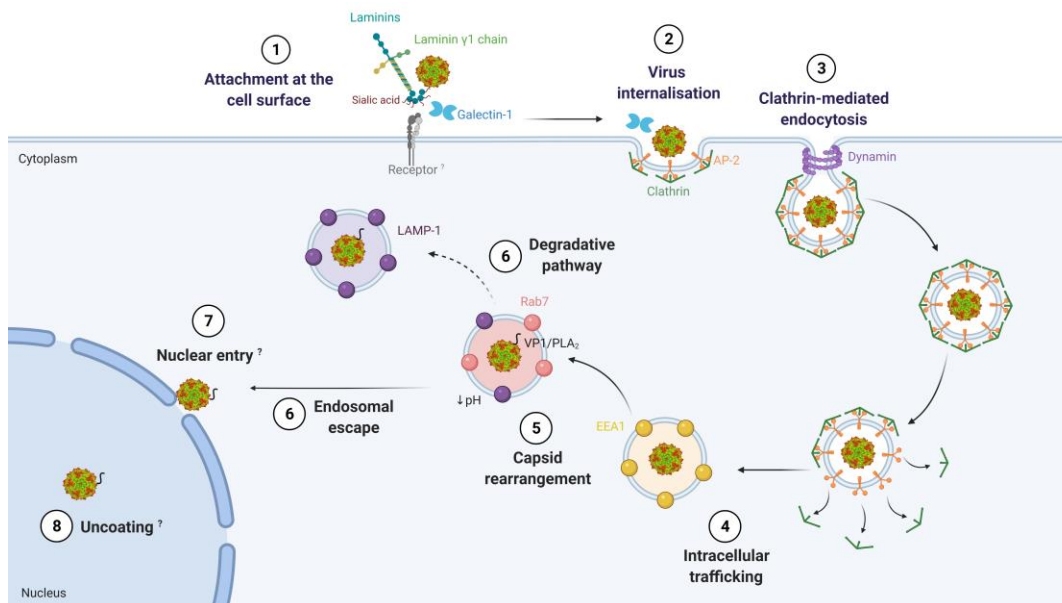


**Figure 5.2. Schematic model of H-1PV entry and infection.**

(1) Laminins, in particular those containing the  $\gamma 1$  chains, promote virus attachment at the cell surface. H-1PV binding to laminins occurs *via* the SA moieties. (2) Galectin-1 promotes efficient H-1PV internalisation. (3) H-1PV internalisation occurs through CME dependent on AP2 $\mu$ 1 and dynamin activity. (4) H-1PV particles are trafficked within the cell from early (early endosome A1 – EEA1) to late endosomes (Ras-related protein 7 – Rab-7). (5) The progressive lower pH present in late endosomes induces conformational rearrangements in the VP1 capsid leading to the exposure of the PLA<sub>2</sub> enzymatic domain. (6) H-1PV escapes from the endosome to the cytoplasm and travels to the nucleus. Alternatively, viral particles are not able to escape from the endosomes and eventually end up in lysosomes (lysosomal-associated membrane protein 1 – LAMP-1) following a non-infectious route. (7) Entry *via* nuclear pore or permeabilisation of the nuclear envelope have both been suggested to be the mechanisms through which the virus and/or the genome enters the nucleus. (8) The timing and site of capsid uncoating are also not known. However, it has been proposed that viral capsids enter the nucleus intact, and the uncoating would occur upon interaction with the nuclear pore complex proteins and/or after nuclear entry (Ros *et al.*, 2017). Created with BioRender.com

## Chapter 6: Future Perspectives and Concluding Remarks

In this chapter, I will first focus on some of the open questions regarding the H-1PV entry pathways and suggest possible approaches to address them. In the second part, I will discuss the challenges faced in the oncolytic virus field and where, in my opinion, joint efforts need to be put into to improve H-1PV clinical outcome and of onco-virotherapy in general. At the end, I will provide my concluding remarks.

### 6.1 Early steps of H-1PV infection

The work reported in this thesis provides a first characterisation of the cell entry mechanisms of H-1PV. By doing so, new questions arise warranting further work on this topic.

#### 6.1.1 What is the H-1PV receptor(s)?

We show that sialylated laminins are key mediators of virus cell attachment and entry through SA, whereas Gal-1 mediates virus entry. However, it is possible that other cellular factors yet to be identified are also involved in H-1PV binding/entry. Laminins, for instance, have many different partners at the cell surface, including a variety of integrins (e.g.  $\alpha1\beta1$ ,  $\alpha2\beta1$ ,  $\alpha3\beta1$ ,  $\alpha6\beta1$ ,  $\alpha6\beta4$ ,  $\alpha7\beta1$ ,  $\alpha9\beta1$ ,  $\alpha v\beta3$ ), 67 kDa laminin receptor, heparan sulfate proteoglycans (perlecan and agrin), dystroglycan, syndecans, carbohydrate adduct of proteins-1 (HNK-1), Lutheran, and sulphated glycolipids. Also, we found in the library screening genes encoding for transmembrane signal receptors as putative positive modulators of H-1PV infection, including *CCKAR*, *TGFBR2*, *ACVRL1*, *DRD4*, *MC4R*, *IFNAR2*, and *GPR92* (Kulkarni et al., in press), suggesting that some of these factors may play a role in virus cell entry. Yet, to my knowledge there are no reports in the literature that the products of these genes interact with members of the laminin/galectin families. Future studies should be directed in order to verify whether these genes truly represent H-1PV modulators or are simply false positive arising from siRNA off-target effects.

In addition to siRNA screenings, there are several methods to identify viral cell receptors (reviewed in (Barrass and Butcher, 2020)). For instance, a method that was successfully used to identify receptors for vaccinia virus was the “cross-linking mass spectrometry” (Frei et al., 2012). It is known that the interaction virus-receptor is transient, and therefore, the usage of cross-linkers can help detection by introducing covalent linkages between H-1PV and the host protein(s). Thereafter, the protein complexes formed are pulled down with a specific conformational antibody recognising the virus capsid and subsequently analysed through mass spectrometry. Potential candidates could be validated by performing siRNA-mediated knockdown / CRISPR knockout, co-localisation experiments, competition assays and mutagenesis, to only name a few approaches.

### **6.1.2 Is Gal-1 and H-1PV endocytosis linked?**

Results presented in this thesis described that Gal-1 is required for an efficient uptake of H-1PV and internalisation occurs *via* CME. Yet, it remains to be demonstrated whether or not Gal-1 and H-1PV are endocytosed together. To this end, an electron microscopy analysis of H-1PV entering the cells through CME could be coupled with immunolabeling of Gal-1 using a specific antibody. This would allow visualisation of Gal-1 presence (or absence) in clathrin-coated pits and/or vesicles. Previous research has shown that Gal-1 enters cells through various mechanisms, including CME (Fajka-Boja et al., 2008). In this line of thought, it would be also interesting to investigate whether Gal-1 has a role in promoting CME as the preferred route for H-1PV entry. Knowing that that H-1PV uses CME to enter NCH125 glioma cells, it would be interesting to evaluate whether the virus penetrates NCH125 LGALS1 KO through the same pathway.

### **6.1.3 Can Gal-1 (and laminin $\gamma$ 1) role be validated *in vivo*?**

We found a direct correlation between the *LGALS1* expression profile and the susceptibility of cancer cells to H-1PV oncolytic activity. Interestingly, this correlation was also found with *LAMC1* (Kulkarni et al., *in press*). These studies support the idea of using these two genes as biomarkers to predict the success of H-1PV infection.



However, their use as prediction markers needs further validation. A promising approach involves analysing spheroids derived from fresh tumour tissues. By cutting the tissues into small pieces and letting them round up in culture, these structures maintain the primary features of the primary tumour, and therefore, constitute a clinically relevant platform to study virus binding/entry, infection and oncolysis, and correlate these with Gal-1/laminin levels (Kemp et al., 2020).

Further validation could involve engrafting animal models with tumours expressing Gal-1, laminin  $\gamma$ 1 or both, at very high or low levels. After tumours grow, animals could be injected intratumourally (or intravenously) with infectious H-1PV. Monitoring of tumour growth and survival curves would validate if Gal-1/laminin high levels would render tumours more susceptible to H-1PV oncolytic activity. Concerning oncotropism, H-1PV preferential accumulation in the grafted tumours could also be tracked by immunofluorescence analysis and viral nucleic acids could be detected by fluorescence in situ hybridization (FISH) and combined with simultaneous immunofluorescent staining for Gal-1 and/or laminin  $\gamma$ 1 (Kiprianova et al., 2020).

Given that clinical trials have been carried out with H-1PV, it would be worth assessing the protein levels of Gal-1 and/or laminin  $\gamma$ 1 in tumour specimens from patients treated with H-1PV and correlate them with H-1PV presence.

In case a correlation between Gal-1/laminins expression and H-1PV oncolytic activity holds true *in vivo*, there are several subsequent approaches that can be adopted. As mentioned before, exogenous administration of Gal-1, for instance, should be considered to boost virus oncolytic activity. Alternatively, second-generation H-1PV vectors could also be designed. For example, one promising approach would be to make use of the Ad-PV chimera (El-Andaloussi et al., 2012a). In short, Ad simply acts as a carrier by bringing the H-1PV genome into cancer cells, as well as the *LGALS1* gene under a CMV promoter. Given that Gal-1 is secreted and can exert its functions in neighbouring cells, Ad-PV chimera-infected cells would release Gal-1 protein which could be later used by progeny H-1PV particles to infect neighbouring cancer cells, thereby improving overall H-1PV infection and oncolytic potential. Alternatively, it would also be possible to test a co-infection of H-1PV and replication deficient Ad encoding for Gal-1.

#### **6.1.4 Are there other galectins involved in H-1PV infection?**

Apart from investigating a possible correlation between *LGALS1* expression profile of the NCI-60 cancer cell line panel and H-1PV oncolytic activity, the analysis was also performed in a similar fashion for other galectins (data not shown). Indeed, other galectins may be involved in regulating H-1PV infection. In particular, *LGALS9* stood out as a putative negative modulator. It would be interesting to characterise Gal-9 role in infection similarly to what was done in the Gal-1 study.

Additionally, it would be worth assessing whether galectin expression levels increase or decrease over the course of H-1PV infection. A pertinent example regarding Gal-1 is the fact that human T-cell leukaemia virus type 1 (HTLV-I)-infected T cells were reported to present higher Gal-1 levels ([Gauthier et al., 2008](#)).

#### **6.1.5 Is caveolin-1 a negative modulator of H-1PV infection?**

Even though evidence of H-1PV entry through caveolae-mediated endocytosis was never found, knockdown of *CAVI*, encoding caveolin-1, increased H-1PV transduction very significantly. Hence, caveolin-1 could act as a negative modulator of H-1PV infection. To further support this hypothesis, caveolin-1 has been reported to interfere with other viral infections, such as of HIV-1 ([Simmons Jr et al., 2012](#), [Lin et al., 2012](#)) or influenza A virus ([Bohm et al., 2014](#)). Indeed, studying the negative modulators of H-1PV infection comprises an interesting line of research, very much unexplored up to now.

## 6.2 General aspects to be considered in the virotherapy field

Clinical implementation of oncolytic virotherapy has been rather slow, partly due to the many questions which remain to be elucidated for most oncolytic viruses. There are uncertainties about the advantages of one virus over another, concerning the cancer type and the stage of the patients, the delivery route, and the schedule of administration. Additionally, there are also several aspects concerning genetic modifications, transgene expression, different combination strategies and predictive biomarkers, to optimally match viral species with permissive tumour and patient features. These and other questions demand further research on the oncolytic virus field.

Another challenge in the process of successfully translating viral-based therapeutics to the clinic concerns the large-scale virus production in compliance with Good Manufacturing Practice (GMP) guidelines. Production of H-1PV-related vectors in quantity and quality to match the clinical demand requires efforts in the search for more productive packaging cell lines and optimal growth conditions (preferably by adopting scalable bioreactor platforms using suspension cell lines). As well, an improved purification protocol with higher purification yield and lower costs is needed.

Another obstacle across the oncolytic virus field is that numerous studies are carried out in monolayer cultures of cancer cell lines. These studies hardly mimic the complex and three-dimensional tumour structures actually observed in patients. Spheroids come as an alternative approach to try to replicate the tumour cells more accurately, and therefore, with more clinical relevance. Using patient-derived GBM neurospheres, H-1PV was shown to induce oncolysis and to have a preferential tropism towards stem-like cells ([Josupeit et al., 2016](#)).

Last but not least, there is an urgent need for better disease models for *in vivo* testing. Pre-clinical validation of findings obtained *in vitro*, including of combination treatments or new viral vectors, are commonly performed in one of two types of models: xenograft or immunocompetent syngeneic models. In spite of offering important hints of tolerability and efficacy, they come with serious limitations.

Xenograft models are generated by implanting cultured human cancer cells into immunocompromised rodents (Kelland, 2004). This approach usually involves growing the tumour in a non-natural site (subcutaneous) and does not take into account the crucial contribution of the immune system for the success of the treatment. As well, tumours established from cell lines rarely reflect the complexity or heterogeneity of those tumours seen in patients. On the other hand, immunocompetent syngeneic models have tumours originated from the same species (Barnes, 2015). However, these models can often be misleading given that the tumour cells are rodent, and therefore, express the rodent homologues of key factors and do not always recapitulate human diseases, human (epi)-genetic complexity, or the human immune system. In order to obtain more relevant hints on the clinical outcome of H-1PV-based therapies and move different therapeutic strategies faster to the clinics, humanised animal models are preferred since they retain a high level of similarity to human tumours. In the parvovirus field, researchers used a humanised patient-derived pancreatic cancer xenograft model, using *ex vivo* primed dendritic and T cells to reconstitute the immune system of the immunodeficient mice (Grekova et al., 2014).

In a nutshell, there is an urgent need for new and better therapies, most likely involving a combination of chemo-/radio-/immune-therapies and (likely genetically engineered) oncolytic viruses (Figure 1.12). Likewise, there is an equivalent eagerness to develop model systems which can better translate the conditions observed in a cancer patient in order to predict with accuracy the antitumour potential of a given oncolytic virus or combination treatment.

### 6.3 Concluding remarks

For the first time, this study characterises the early steps of H-1PV infection. We show that H-1PV attachment and entry are regulated by various cellular factors, including laminins and Gal-1, present in the extracellular matrix. Additionally, we also show that H-1PV enters cells through CME, and hijacks the endosomal machinery to reach the nucleus.

We show that H-1PV depends on Gal-1 expression to efficiently enter and infect glioma cells, and that *LGALS1* expression levels in 59 cancer cells lines from different tumour entities correlate with their susceptibility to H-1PV oncolytic activity. Remarkably, administration of purified Gal-1 to poorly-susceptible glioma cells rendered them more permissive to H-1PV oncolytic activity opening up new scenarios of treatment in which H-1PV could be combined with recombinant Gal-1 protein.

In conclusion, this study brings us closer to deciphering the H-1PV oncotropism and its inherent oncolytic properties. As detailed before, this new knowledge could be exploited for improving H-1PV-based therapies and increase its clinical potential in cancer virotherapy.

## Bibliography

- ADAMS, J. M. & CORY, S. 2007. The Bcl-2 apoptotic switch in cancer development and therapy. *Oncogene*, 26, 1324-1337.
- ADEYEMI, R. O., LANDRY, S., DAVIS, M. E., WEITZMAN, M. D. & PINTEL, D. J. 2010. Parvovirus minute virus of mice induces a DNA damage response that facilitates viral replication. *PLoS pathogens*, 6.
- AGHI, M. K., LIU, T.-C., RABKIN, S. & MARTUZA, R. L. 2009. Hypoxia enhances the replication of oncolytic herpes simplex virus. *Molecular Therapy*, 17, 51-56.
- AGUADO, C., PÉREZ-JIMÉNEZ, E., LAHUERTA, M. & KNECHT, E. 2016. Isolation of lysosomes from mammalian tissues and cultured cells. *Proteostasis*. Springer.
- ALBERTS, P., TILGASE, A., RASA, A., BANDERE, K. & VENSKUS, D. 2018. The advent of oncolytic virotherapy in oncology: The Rigvir® story. *European journal of pharmacology*, 837, 117-126.
- ALLAUME, X., EL-ANDALOUSSI, N., LEUCHS, B., BONIFATI, S., KULKARNI, A., MARTTILA, T., KAUFMANN, J. K., NETTELBECK, D. M., KLEINSCHMIDT, J. & ROMMELAERE, J. 2012. Retargeting of rat parvovirus H-1PV to cancer cells through genetic engineering of the viral capsid. *Journal of virology*, 86, 3452-3465.
- AMMAYAPPAN, A., PENG, K.-W. & RUSSELL, S. J. 2013. Characteristics of oncolytic vesicular stomatitis virus displaying tumor-targeting ligands. *Journal of virology*, 87, 13543-13555.
- ANDERSON, H., CHEN, Y. & NORKIN, L. 1996. Bound simian virus 40 translocates to caveolin-enriched membrane domains, and its entry is inhibited by drugs that selectively disrupt caveolae. *Molecular biology of the cell*, 7, 1825-1834.
- ANDTBACKA, R., KAUFMAN, H. L., COLLICHIO, F., AMATRUDA, T., SENZER, N., CHESNEY, J., DELMAN, K. A., SPITLER, L. E., PUZANOV, I. & AGARWALA, S. S. 2015. Talimogene laherparepvec improves durable response rate in patients with advanced melanoma. *J clin Oncol*, 33, 2780-2788.
- ANGELOVA, A., FERREIRA, T., BRETSCHER, C., ROMMELAERE, J. & MARCHINI, A. 2021. Parvovirus-Based Combinatorial Immunotherapy: A Reinforced Therapeutic Strategy against Poor-Prognosis Solid Cancers. *Cancers*, 13, 342.
- ANGELOVA, A. & ROMMELAERE, J. 2019. Immune System Stimulation by Oncolytic Rodent Protoparvoviruses. *Viruses*, 11, 415.

- ANGELOVA, A. L., APRAHAMIAN, M., BALBONI, G., DELECLUSE, H.-J., FEEDERLE, R., KIPRIANOVA, I., GREKOVA, S. P., GALABOV, A. S., WITZENS-HARIG, M. & HO, A. D. 2009a. Oncolytic rat parvovirus H-1PV, a candidate for the treatment of human lymphoma: In vitro and in vivo studies. *Molecular therapy*, 17, 1164-1172.
- ANGELOVA, A. L., APRAHAMIAN, M., GREKOVA, S. P., HAJRI, A., LEUCHS, B., GIESE, N. A., DINSART, C., HERRMANN, A., BALBONI, G. & ROMMELAERE, J. 2009b. Improvement of gemcitabine-based therapy of pancreatic carcinoma by means of oncolytic parvovirus H-1PV. *Clinical Cancer Research*, 15, 511-519.
- ANGELOVA, A. L., GELETNEKY, K., NÜESCH, J. P. & ROMMELAERE, J. 2015. Tumor selectivity of oncolytic parvoviruses: From in vitro and animal models to cancer patients. *Frontiers in bioengineering and biotechnology*, 3, 55.
- ANGELOVA, A. L., GREKOVA, S. P., HELLER, A., KUHLMANN, O., SOYKA, E., GIESE, T., APRAHAMIAN, M., BOUR, G., RÜFFER, S. & CZIEPLUCH, C. 2014. Complementary induction of immunogenic cell death by oncolytic parvovirus H-1PV and gemcitabine in pancreatic cancer. *Journal of virology*, 88, 5263-5276.
- ASTORGUES-XERRI, L., RIVEIRO, M. E., TIJERAS-RABALLAND, A., SEROVA, M., NEUZILLET, C., ALBERT, S., RAYMOND, E. & FAIVRE, S. 2014. Unraveling galectin-1 as a novel therapeutic target for cancer. *Cancer treatment reviews*, 40, 307-319.
- AUMAILLEY, M., BRUCKNER-TUDERMAN, L., CARTER, W. G., DEUTZMANN, R., EDGAR, D., EKBLÖM, P., ENGEL, J., ENGVALL, E., HOHENESTER, E. & JONES, J. C. 2005. A simplified laminin nomenclature. *Matrix biology*, 24, 326-332.
- BAJZER, Ž., CARR, T., JOSIĆ, K., RUSSELL, S. J. & DINGLI, D. 2008. Modeling of cancer virotherapy with recombinant measles viruses. *Journal of theoretical Biology*, 252, 109-122.
- BÄNFER, S. & JACOB, R. 2020. Galectins in Intra- and Extracellular Vesicles. *Biomolecules*, 10, 1232.
- BÄR, S., DAEFFLER, L., ROMMELAERE, J. & NÜESCH, J. P. 2008. Vesicular egress of non-enveloped lytic parvoviruses depends on gelsolin functioning. *PLoS pathogens*, 4.
- BÄR, S., ROMMELAERE, J. & NÜESCH, J. P. 2013. Vesicular transport of progeny parvovirus particles through ER and Golgi regulates maturation and cytolysis. *PLoS pathogens*, 9.
- BÄR, S., ROMMELAERE, J. & NÜESCH, J. P. 2015. PKC $\eta$ /Rdx-driven phosphorylation of PDK1: a novel mechanism promoting cancer cell survival and permissiveness for parvovirus-induced lysis. *PLoS pathogens*, 11.

- BARNES, S. 2015. The Rise of Syngeneic Models in Cancer Immunotherapy. *Drug Discovery & Development*.
- BARRASS, S. V. & BUTCHER, S. J. 2020. Advances in high-throughput methods for the identification of virus receptors. *Medical microbiology and immunology*, 209, 309-323.
- BARRETINA, J., CAPONIGRO, G., STRANSKY, N., VENKATESAN, K., MARGOLIN, A. A., KIM, S., WILSON, C. J., LEHÁR, J., KRYUKOV, G. V. & SONKIN, D. 2012. The Cancer Cell Line Encyclopedia enables predictive modelling of anticancer drug sensitivity. *Nature*, 483, 603-607.
- BASAK, S. & TURNER, H. 1992. Infectious entry pathway for canine parvovirus. *Virology*, 186, 368-376.
- BASHIR, T., HÖRLEIN, R., ROMMELAERE, J. & WILLWAND, K. 2000. Cyclin A activates the DNA polymerase  $\delta$ -dependent elongation machinery in vitro: a parvovirus DNA replication model. *Proceedings of the National Academy of Sciences*, 97, 5522-5527.
- BASHIR, T., ROMMELAERE, J. & CZIEPLUCH, C. 2001. In vivo accumulation of cyclin A and cellular replication factors in autonomous parvovirus minute virus of mice-associated replication bodies. *Journal of virology*, 75, 4394-4398.
- BERNS, K. I. 1990. Parvovirus replication. *Microbiology and Molecular Biology Reviews*, 54, 316-329.
- BHAT, R., DEMPE, S., DINSART, C. & ROMMELAERE, J. 2011. Enhancement of NK cell antitumor responses using an oncolytic parvovirus. *International journal of cancer*, 128, 908-919.
- BHAT, R. & ROMMELAERE, J. 2013. NK-cell-dependent killing of colon carcinoma cells is mediated by natural cytotoxicity receptors (NCRs) and stimulated by parvovirus infection of target cells. *BMC cancer*, 13, 1-9.
- BHATTACHARYA, B., PRASAD, G. L., VALVERIUS, E. M., SALOMON, D. S. & COOPER, H. L. 1990. Tropomyosins of human mammary epithelial cells: consistent defects of expression in mammary carcinoma cell lines. *Cancer research*, 50, 2105-2112.
- BISCHOFF, J. R. & SAMUEL, C. E. 1989. Mechanism of interferon action activation of the human P1/eIF-2 $\alpha$  protein kinase by individual reovirus s-class mRNAs: s1 mRNA is a potent activator relative to s4 mRNA. *Virology*, 172, 106-115.
- BLANCHARD, H., BUM-ERDENE, K., BOHARI, M. H. & YU, X. 2016. Galectin-1 inhibitors and their potential therapeutic applications: a patent review. *Expert opinion on therapeutic patents*, 26, 537-554.
- BODENDORF, U., CZIEPLUCH, C., JAUNIAUX, J.-C., ROMMELAERE, J. & SALOMÉ, N. 1999. Nuclear export factor CRM1 interacts with nonstructural



- proteins NS2 from parvovirus minute virus of mice. *Journal of Virology*, 73, 7769-7779.
- BOHM, K., SUN, L., THAKOR, D. & WIRTH, M. 2014. Caveolin-1 limits human influenza A virus (H1N1) propagation in mouse embryo-derived fibroblasts. *Virology*, 462, 241-253.
- BOISVERT, M., FERNANDES, S. & TIJSSEN, P. 2010. Multiple pathways involved in porcine parvovirus cellular entry and trafficking toward the nucleus. *Journal of virology*, 84, 7782-7792.
- BOUCHARA, J.-P., SANCHEZ, M., CHEVAILLER, A., MAROT-LEBLOND, A., LISSITZKY, J.-C., TRONCHIN, G. & CHABASSE, D. 1997. Sialic acid-dependent recognition of laminin and fibrinogen by *Aspergillus fumigatus* conidia. *Infection and immunity*, 65, 2717-2724.
- BOZZINI, S., FALCONE, V., CONALDI, P. G., VISAI, L., BIANCONE, L., DOLEI, A., TONIOLO, A. & SPEZIALE, P. 1998. Heparin-binding domain of human fibronectin binds HIV-1 gp120/160 and reduces virus infectivity. *Journal of medical virology*, 54, 44-53.
- BRANDENBURGER, A., LEGENDRE, D., AVALOSSE, B. & ROMMELAERE, J. 1990. NS-1 and NS-2 proteins may act synergistically in the cytopathogenicity of parvovirus MVMp. *Virology*, 174, 576-584.
- BREITBACH, C. J., DE SILVA, N. S., FALLS, T. J., ALADL, U., EVGIN, L., PATERSON, J., SUN, Y. Y., ROY, D. G., RINTOUL, J. L. & DANESHMAND, M. 2011. Targeting tumor vasculature with an oncolytic virus. *Molecular Therapy*, 19, 886-894.
- BRETSCHER, C. & MARCHINI, A. 2019. H-1 parvovirus as a cancer-killing agent: past, present, and future. *Viruses*, 11, 562.
- BREWER, C. F. 2002. Binding and cross-linking properties of galectins. *Biochimica et Biophysica Acta (BBA)-General Subjects*, 1572, 255-262.
- BRUN, J., MCMANUS, D., LEFEBVRE, C., HU, K., FALLS, T., ATKINS, H., BELL, J. C., MCCART, J. A., MAHONEY, D. & STOJDL, D. F. 2010. Identification of genetically modified Maraba virus as an oncolytic rhabdovirus. *Molecular Therapy*, 18, 1440-1449.
- CANAAN, S., ZÁDORI, Z., GHOMASHCHI, F., BOLLINGER, J., SADILEK, M., MOREAU, M. E., TIJSSEN, P. & GELB, M. H. 2004. Interfacial enzymology of parvovirus phospholipases A2. *Journal of Biological Chemistry*, 279, 14502-14508.
- CATTANEO, R., MIEST, T., SHASHKOVA, E. V. & BARRY, M. A. 2008. Reprogrammed viruses as cancer therapeutics: targeted, armed and shielded. *Nature Reviews Microbiology*, 6, 529-540.
- CHEN, A. Y. & QIU, J. 2010. Parvovirus infection-induced cell death and cell cycle arrest. *Future virology*, 5, 731-743.

- CHEN, H.-Y., WENG, I.-C., HONG, M.-H. & LIU, F.-T. 2014. Galectins as bacterial sensors in the host innate response. *Current opinion in microbiology*, 17, 75-81.
- CHEN, J., ZHOU, S.-J., ZHANG, Y., ZHANG, G.-Q., ZHA, T.-Z., FENG, Y.-Z. & ZHANG, K. 2013. Clinicopathological and prognostic significance of galectin-1 and vascular endothelial growth factor expression in gastric cancer. *World Journal of Gastroenterology: WJG*, 19, 2073.
- CHESNEY, J., PUZANOV, I., COLLICHIO, F., SINGH, P., MILHEM, M. M., GLASPY, J., HAMID, O., ROSS, M., FRIEDLANDER, P. & GARBE, C. 2018. Randomized, open-label phase II study evaluating the efficacy and safety of talimogene laherparepvec in combination with ipilimumab versus ipilimumab alone in patients with advanced, unresectable melanoma. *Journal of Clinical Oncology*, 36, 1658.
- CHIU, W.-L., LIN, C.-L., YANG, M.-H., TZOU, D.-L. M. & CHANG, W. 2007. Vaccinia virus 4c (A26L) protein on intracellular mature virus binds to the extracellular cellular matrix laminin. *Journal of virology*, 81, 2149-2157.
- CHOU, F.-C., CHEN, H.-Y., KUO, C.-C. & SYTWU, H.-K. J. 2018a. Role of galectins in tumors and in clinical immunotherapy. *International journal of molecular sciences*, 19, 430.
- CHOU, S.-Y., YEN, S.-L., HUANG, C.-C. & HUANG, E.-Y. 2018b. Galectin-1 is a poor prognostic factor in patients with glioblastoma multiforme after radiotherapy. *BMC cancer*, 18, 105.
- CHRISTENSEN, J. & TATTERSALL, P. 2002. Parvovirus initiator protein NS1 and RPA coordinate replication fork progression in a reconstituted DNA replication system. *Journal of virology*, 76, 6518-6531.
- CLOUGHESY, T. F., PETRECCA, K., WALBERT, T., BUTOWSKI, N., SALACZ, M., PERRY, J., DAMEK, D., BOTA, D., BETTEGOWDA, C., ZHU, J. J., IWAMOTO, F., PLACANTONAKIS, D., KIM, L., ELDER, B., KAPTAIN, G., CACHIA, D., MOSHEL, Y., BREM, S., PICCIONI, D., LANDOLFI, J., CHEN, C. C., GRUBER, H., RAO, A. R., HOGAN, D., ACCOMANDO, W., OSTERTAG, D., MONTELLANO, T. T., KHEOH, T., KABBINAVAR, F. & VOGELBAUM, M. A. 2020. Effect of Vocimagene Amiretrorepvec in Combination With Flucytosine vs Standard of Care on Survival Following Tumor Resection in Patients With Recurrent High-Grade Glioma: A Randomized Clinical Trial. *JAMA Oncol*, 6, 1939-1946.
- COOK, M. & CHAUHAN, A. 2020. Clinical Application of Oncolytic Viruses: A Systematic Review. *International journal of molecular sciences*, 21, 7505.
- COTMORE, S. F., AGBANDJE-MCKENNA, M., CANUTI, M., CHIORINI, J. A., EIS-HUBINGER, A.-M., HUGHES, J., MIETZSCH, M., MODHA, S., OGLIASTRO, M. & PÉNZES, J. J. 2019. ICTV virus taxonomy profile: Parvoviridae. *The Journal of general virology*, 100, 367.

- COTMORE, S. F., AGBANDJE-MCKENNA, M., CHIORINI, J. A., MUKHA, D. V., PINTEL, D. J., QIU, J., SODERLUND-VENERMO, M., TATTERSALL, P., TIJSSEN, P. & GATHERER, D. 2014. The family parvoviridae. *Archives of virology*, 159, 1239-1247.
- COTMORE, S. F., D'ABRAMO JR, A. M., TICKNOR, C. M. & TATTERSALL, P. 1999. Controlled conformational transitions in the MVM virion expose the VP1 N-terminus and viral genome without particle disassembly. *Virology*, 254, 169-181.
- COTMORE, S. F., HAFENSTEIN, S. & TATTERSALL, P. 2010. Depletion of virion-associated divalent cations induces parvovirus minute virus of mice to eject its genome in a 3'-to-5' direction from an otherwise intact viral particle. *Journal of virology*, 84, 1945-1956.
- COTMORE, S. F. & TATTERSALL, P. 1987. The autonomously replicating parvoviruses of vertebrates. *Adv. Virus Res*, 33, 1-174.
- COTMORE, S. F. & TATTERSALL, P. 1998. High-mobility group 1/2 proteins are essential for initiating rolling-circle-type DNA replication at a parvovirus hairpin origin. *Journal of virology*, 72, 8477-8484.
- COTMORE, S. F. & TATTERSALL, P. 2005. A rolling-hairpin strategy: basic mechanisms of DNA replication in the parvoviruses. *Parvoviruses. London: Hodder Arond*, 171-181.
- COTMORE, S. F. & TATTERSALL, P. 2007. Parvoviral host range and cell entry mechanisms. *Advances in virus research*, 70, 183-232.
- COUSIN, J. M. & CLONINGER, M. J. 2016. The role of galectin-1 in cancer progression, and synthetic multivalent systems for the study of galectin-1. *International journal of molecular sciences*, 17, 1566.
- CULP, T. D., BUDGEON, L. R., MARINKOVICH, M. P., MENEGUZZI, G. & CHRISTENSEN, N. D. 2006. Keratinocyte-secreted laminin 5 can function as a transient receptor for human papillomaviruses by binding virions and transferring them to adjacent cells. *Journal of virology*, 80, 8940-8950.
- DAEFFLER, L., HÖRLEIN, R., ROMMELAERE, J. & NÜESCH, J. P. 2003. Modulation of minute virus of mice cytotoxic activities through site-directed mutagenesis within the NS coding region. *Journal of virology*, 77, 12466-12478.
- DE MATOS, A. L., FRANCO, L. S. & MCFADDEN, G. 2020. Oncolytic viruses and the immune system: the dynamic duo. *Molecular Therapy-Methods & Clinical Development*, 17, 349-358.
- DE PACE, N. 1912. Sulla scomparsa di un enorme cancro vegetante del collo dell'utero senza cura chirurgica. *GINECOLOGIA*, 9, 82-88.

- DELEU, L., PUJOL, A., FAISST, S. & ROMMELAERE, J. 1999. Activation of promoter P4 of the autonomous parvovirus minute virus of mice at early S phase is required for productive infection. *Journal of virology*, 73, 3877-3885.
- DETTWILER, S., ROMMELAERE, J. & NÜESCH, J. P. 1999. DNA unwinding functions of minute virus of mice NS1 protein are modulated specifically by the lambda isoform of protein kinase C. *Journal of virology*, 73, 7410-7420.
- DI LELLA, S., SUNDBLAD, V., CERLIANI, J. P., GUARDIA, C. M., ESTRIN, D. A., VASTA, G. R. & RABINOVICH, G. A. 2011. When galectins recognize glycans: from biochemistry to physiology and back again. *Biochemistry*, 50, 7842-7857.
- DI PIAZZA, M., MADER, C., GELETNEKY, K., Y CALLE, M. H., WEBER, E., SCHLEHOFER, J., DELEU, L. & ROMMELAERE, J. 2007. Cytosolic activation of cathepsins mediates parvovirus H-1-induced killing of cisplatin and TRAIL-resistant glioma cells. *Journal of virology*, 81, 4186-4198.
- DOHERTY, G. J. & MCMAHON, H. T. 2009. Mechanisms of endocytosis. *Annual review of biochemistry*, 78, 857-902.
- DORSCH, S., LIEBISCH, G., KAUFMANN, B., VON LANDENBERG, P., HOFFMANN, J. H., DROBNIK, W. & MODROW, S. 2002. The VP1 unique region of parvovirus B19 and its constituent phospholipase A2-like activity. *Journal of virology*, 76, 2014-2018.
- DUDLEENAMJIL, E., LIN, C.-Y., DREDGE, D., MURRAY, B. K., ROBISON, R. A. & JOHNSON, F. B. 2010. Bovine parvovirus uses clathrin-mediated endocytosis for cell entry. *Journal of general virology*, 91, 3032-3041.
- DURBEEJ, M. 2010. Laminins. *Cell and tissue research*, 339, 259-268.
- EGEBLAD, M. & WERB, Z. 2002. New functions for the matrix metalloproteinases in cancer progression. *Nature Reviews Cancer*, 2, 161-174.
- EICHWALD, V., DAEFFLER, L., KLEIN, M., ROMMELAERE, J. & SALOMÉ, N. 2002. The NS2 proteins of parvovirus minute virus of mice are required for efficient nuclear egress of progeny virions in mouse cells. *Journal of virology*, 76, 10307-10319.
- EL-ANDALOUSSI, N., BONIFATI, S., KAUFMANN, J. K., MAILLY, L., DAEFFLER, L., DERYCKÈRE, F., NETTELBECK, D. M., ROMMELAERE, J. & MARCHINI, A. 2012a. Generation of an adenovirus-parvovirus chimera with enhanced oncolytic potential. *Journal of virology*, 86, 10418-10431.
- EL-ANDALOUSSI, N., ENDELE, M., LEUCHS, B., BONIFATI, S., KLEINSCHMIDT, J., ROMMELAERE, J. & MARCHINI, A. 2011. Novel adenovirus-based helper system to support production of recombinant parvovirus. *Cancer gene therapy*, 18, 240-249.

- EL-ANDALOUSSI, N., LEUCHS, B., BONIFATI, S., ROMMELAERE, J. & MARCHINI, A. 2012b. Efficient recombinant parvovirus production with the help of adenovirus-derived systems. *JoVE (Journal of Visualized Experiments)*, e3518.
- ELOLA, M., WOLFENSTEIN-TODEL, C., TRONCOSO, M., VASTA, G. & RABINOVICH, G. 2007. Galectins: matricellular glycan-binding proteins linking cell adhesion, migration, and survival. *Cellular and Molecular Life Sciences*, 64, 1679-1700.
- ESKELINEN, E.-L. 2006. Roles of LAMP-1 and LAMP-2 in lysosome biogenesis and autophagy. *Molecular aspects of medicine*, 27, 495-502.
- ESKELINEN, E.-L., TANAKA, Y. & SAFTIG, P. 2003. At the acidic edge: emerging functions for lysosomal membrane proteins. *Trends in cell biology*, 13, 137-145.
- FAISST, S., FAISST, S. R., DUPRESSOIR, T., PLAZA, S., PUJOL, A., JAUNIAUX, J.-C., RHODE, S. L. & ROMMELAERE, J. 1995. Isolation of a fully infectious variant of parvovirus H-1 supplanting the standard strain in human cells. *Journal of Virology*, 69, 4538-4543.
- FAJKA-BOJA, R., BLASKO, A., KOVACS-SOLYOM, F., SZEBENI, G., TOTH, G. & MONOSTORI, E. 2008. Co-localization of galectin-1 with GM1 ganglioside in the course of its clathrin- and raft-dependent endocytosis. *Cellular and Molecular Life Sciences*, 65, 2586-2593.
- FARR, G. A., ZHANG, L.-G. & TATTERSALL, P. 2005. Parvoviral virions deploy a capsid-tethered lipolytic enzyme to breach the endosomal membrane during cell entry. *Proceedings of the National Academy of Sciences*, 102, 17148-17153.
- FERREIRA, T., KULKARNI, A., BRETSCHER, C., RICHTER, K., EHRLICH, M. & MARCHINI, A. 2020. Oncolytic H-1 Parvovirus Enters Cancer Cells through Clathrin-Mediated Endocytosis. *Viruses*, 12, 1199.
- FREI, A. P., JEON, O.-Y., KILCHER, S., MOEST, H., HENNING, L. M., JOST, C., PLÜCKTHUN, A., MERCER, J., AEBERSOLD, R. & CARREIRA, E. M. 2012. Direct identification of ligand-receptor interactions on living cells and tissues. *Nature biotechnology*, 30, 997.
- FUKS, F., DELEU, L., DINSART, C., ROMMELAERE, J. & FAISST, S. 1996. ras oncogene-dependent activation of the P4 promoter of minute virus of mice through a proximal P4 element interacting with the Ets family of transcription factors. *Journal of virology*, 70, 1331-1339.
- GARCIN, P., COHEN, S., TERPSTRA, S., KELLY, I., FOSTER, L. J. & PANTÉ, N. 2013. Proteomic analysis identifies a novel function for galectin-3 in the cell entry of parvovirus. *Journal of proteomics*, 79, 123-132.
- GARCIN, P. O., NABI, I. R. & PANTE, N. 2015. Galectin-3 plays a role in minute virus of mice infection. *Virology*, 481, 63-72.

- GARCIN, P. O. & PANTÉ, N. 2014. Cell migration is another player of the minute virus of mice infection. *Virology*, 468, 150-159.
- GARCIN, P. O. & PANTÉ, N. 2015. The minute virus of mice exploits different endocytic pathways for cellular uptake. *Virology*, 482, 157-166.
- GARNER, O. B., AGUILAR, H. C., FULCHER, J. A., LEVRONEY, E. L., HARRISON, R., WRIGHT, L., ROBINSON, L. R., ASPERICUETA, V., PANICO, M. & HASLAM, S. M. 2010. Endothelial galectin-1 binds to specific glycans on nipah virus fusion protein and inhibits maturation, mobility, and function to block syncytia formation. *PLoS pathog*, 6, e1000993.
- GARNER, O. B. & BAUM, L. G. 2008. Galectin–glycan lattices regulate cell-surface glycoprotein organization and signalling. *Biochemical Society Transactions*, 36, 1472-1477.
- GARNER, O. B., YUN, T., PERNET, O., AGUILAR, H. C., PARK, A., BOWDEN, T. A., FREIBERG, A. N., LEE, B. & BAUM, L. G. 2015. Timing of galectin-1 exposure differentially modulates Nipah virus entry and syncytium formation in endothelial cells. *Journal of virology*, 89, 2520-2529.
- GAUTHIER, S., PELLETIER, I., OUELLET, M., VARGAS, A., TREMBLAY, M. J., SATO, S. & BARBEAU, B. 2008. Induction of galectin-1 expression by HTLV-I Tax and its impact on HTLV-I infectivity. *Retrovirology*, 5, 1-15.
- GEISS, C., KIS, Z., LEUCHS, B., FRANK-STÖHR, M., SCHLEHOFER, J. R., ROMMELAERE, J., DINSART, C. & LACROIX, J. 2017. Preclinical testing of an oncolytic parvovirus: standard protoparvovirus H-1PV efficiently induces osteosarcoma cell lysis in vitro. *Viruses*, 9, 301.
- GELETNEKY, K., ANGELOVA, A., LEUCHS, B., BHAT, R., JUST, A., CAPPER, D., KREBS, O., DAHM, M., HUBER, B. & UNTERBERG, A. 2014a. ET-21 COMBINATION OF INTRAVENOUS AND INTRACEREBRAL INJECTION OF ONCOLYTIC PARVOVIRUS H-1 IN A PHASE I/IIA CLINICAL TRIAL OF PATIENTS WITH RECURRENT GLIOBLASTOMA MULTIFORME: PENETRATION OF H-1 VIRUS ACROSS THE BLOOD-BRAIN BARRIER. *Neuro-oncology*, 16, v83-v84.
- GELETNEKY, K., BARTSCH, A., WEISS, C., BERNHARD, H., MARCHINI, A. & ROMMELAERE, J. 2018. ATIM-40. High rate of objective anti-tumor response in 9 patients with glioblastoma after viro-immunotherapy with oncolytic parvovirus H-1 in combination with bevacicumab and PD-1 checkpoint blockade. *Neuro-Oncology*, 20, vi10.
- GELETNEKY, K., HAJDA, J., ANGELOVA, A. L., LEUCHS, B., CAPPER, D., BARTSCH, A. J., NEUMANN, J.-O., SCHÖNING, T., HÜSING, J. & BEELTE, B. 2017. Oncolytic H-1 parvovirus shows safety and signs of immunogenic activity in a first phase I/IIa glioblastoma trial. *Molecular Therapy*, 25, 2620-2634.

- GELETNEKY, K., HARTKOPF, A. D., KREMPIEN, R., ROMMELAERE, J. & SCHLEHOFER, J. R. 2010a. Therapeutic implications of the enhanced short and long-term cytotoxicity of radiation treatment followed by oncolytic parvovirus H-1 infection in high-grade glioma cells. *Bioengineered bugs*, 1, 429-433.
- GELETNEKY, K., HUESING, J., DAHM, M., KREBS, O., HUBER, B., CAPPER, D., ROMMELAERE, J., HAJDA, J. & UNTERBERG, A. 2014b. First combined intravenous and intracerebral application of an oncolytic virus, parvovirus h-1, in a phase I/IIa clinical trial in patients with recurrent glioblastoma multiforme (ParvOryx01). American Society of Clinical Oncology.
- GELETNEKY, K., HUESING, J., ROMMELAERE, J., SCHLEHOFER, J. R., LEUCHS, B., DAHM, M., KREBS, O., VON KNEBEL DOEBERITZ, M., HUBER, B. & HAJDA, J. 2012. Phase I/IIa study of intratumoral/intracerebral or intravenous/intracerebral administration of Parvovirus H-1 (ParvOryx) in patients with progressive primary or recurrent glioblastoma multiforme: ParvOryx01 protocol. *BMC cancer*, 12, 99.
- GELETNEKY, K., KIPRIANOVA, I., AYACHE, A., KOCH, R., HERRERO Y CALLE, M., DELEU, L., SOMMER, C., THOMAS, N., ROMMELAERE, J. & SCHLEHOFER, J. R. 2010b. Regression of advanced rat and human gliomas by local or systemic treatment with oncolytic parvovirus H-1 in rat models. *Neuro-oncology*, 12, 804-814.
- GELETNEKY, K., NÜESCH, J. P., ANGELOVA, A., KIPRIANOVA, I. & ROMMELAERE, J. 2015. Double-faceted mechanism of parvoviral oncosuppression. *Current opinion in virology*, 13, 17-24.
- GELETNEKY, K., WEISS, C., BERNHARD, H., CAPPER, D., LEUCHS, B., MARCHINI, A. & ROMMELAERE, J. 2016. ATIM-29. FIRST CLINICAL OBSERVATION OF IMPROVED ANTI-TUMOR EFFECTS OF VIRO-IMMUNOTHERAPY WITH ONCOLYTIC PARVOVIRUS H-1 IN COMBINATION WITH PD-1 CHECKPOINT BLOCKADE AND BEVACICUMAB IN PATIENTS WITH RECURRENT GLIOBLASTOMA. *Neuro-Oncology*, 18, vi24-vi24.
- GEN 2019. Pexa-Vec/Nexavar Combination Fails Phase III Trial in Liver Cancer. gen tech trends in biotech.
- GIMPLE, R. C. & WANG, X. 2019. RAS: striking at the core of the oncogenic circuitry. *Frontiers in oncology*, 9, 965.
- GOEPFERT, K., DINSART, C., ROMMELAERE, J., FOERSTER, F. & MOEHLER, M. 2019. Rational combination of parvovirus H1 with CTLA-4 and PD-1 checkpoint inhibitors dampens the tumor induced immune silencing. *Frontiers in oncology*, 9, 425.

- GONG, J. & MITA, M. M. 2014. Activated ras signaling pathways and reovirus oncolysis: an update on the mechanism of preferential reovirus replication in cancer cells. *Frontiers in oncology*, 4, 167.
- GREKOVA, S., RAYKOV, Z., ZAWATZKY, R., ROMMELAERE, J. & KOCH, U. 2012. Activation of a glioma-specific immune response by oncolytic parvovirus Minute Virus of Mice infection. *Cancer gene therapy*, 19, 468-475.
- GREKOVA, S., ZAWATZKY, R., HÖRLEIN, R., CZIEPLUCH, C., MINCBERG, M., DAVIS, C., ROMMELAERE, J. & DAEFFLER, L. 2010. Activation of an antiviral response in normal but not transformed mouse cells: a new determinant of minute virus of mice oncotropism. *Journal of virology*, 84, 516-531.
- GREKOVA, S. P., APRAHAMIAN, M., DAEFFLER, L., LEUCHS, B., ANGELOVA, A., GIESE, T., GALABOV, A., HELLER, A., GIESE, N. A. & ROMMELAERE, J. 2011. Interferon  $\gamma$  improves the vaccination potential of oncolytic parvovirus H-1PV for the treatment of peritoneal carcinomatosis in pancreatic cancer. *Cancer biology & therapy*, 12, 888-895.
- GREKOVA, S. P., APRAHAMIAN, M., GIESE, N. A., BOUR, G., GIESE, T., GREWENIG, A., LEUCHS, B., HÖRLEIN, R., HELLER, A. & ANGELOVA, A. L. 2014. Genomic CpG enrichment of oncolytic parvoviruses as a potent anticancer vaccination strategy for the treatment of pancreatic adenocarcinoma. *J Vaccines Vaccin*, 5.
- GUJAR, S., POL, J. G., KIM, Y., LEE, P. W. & KROEMER, G. 2018. Antitumor benefits of antiviral immunity: an underappreciated aspect of oncolytic virotherapies. *Trends in immunology*, 39, 209-221.
- GUO, Z. S. 2011. The impact of hypoxia on oncolytic virotherapy. *Virus Adaptation and Treatment*, 3, 71-82.
- GUO, Z. S., LU, B., GUO, Z., GIEHL, E., FEIST, M., DAI, E., LIU, W., STORKUS, W. J., HE, Y. & LIU, Z. 2019. Vaccinia virus-mediated cancer immunotherapy: cancer vaccines and oncolytics. *Journal for immunotherapy of cancer*, 7, 6.
- HAJDA, J., LEHMANN, M., KREBS, O., KIESER, M., GELETNEKY, K., JÄGER, D., DAHM, M., HUBER, B., SCHÖNING, T. & SEDLACZEK, O. 2017. A non-controlled, single arm, open label, phase II study of intravenous and intratumoral administration of ParvOryx in patients with metastatic, inoperable pancreatic cancer: ParvOryx02 protocol. *BMC cancer*, 17, 1-11.
- HALDER, S., NAM, H.-J., GOVINDASAMY, L., VOGEL, M., DINSART, C., SALOMÉ, N., MCKENNA, R. & AGBANDJE-MCKENNA, M. 2013a. Structural characterization of H-1 parvovirus: comparison of infectious virions to empty capsids. *Journal of virology*, 87, 5128-5140.
- HALDER, S., NAM, H. J., GOVINDASAMY, L., VOGEL, M., DINSART, C., SALOME, N., MCKENNA, R. & AGBANDJE-MCKENNA, M. 2013b.



- Structural characterization of H-1 parvovirus: comparison of infectious virions to empty capsids. *J Virol*, 87, 5128-40.
- HARBISON, C. E., CHIORINI, J. A. & PARRISH, C. R. 2008. The parvovirus capsid odyssey: from the cell surface to the nucleus. *Trends in microbiology*, 16, 208-214.
- HARTLEY, A., KAVISHWAR, G., SALVATO, I. & MARCHINI, A. 2020. A Roadmap for the Success of Oncolytic Parvovirus-Based Anticancer Therapies. *Annual Review of Virology*, 7, 537-557.
- HERRERO Y CALLE, M., CORNELIS, J. J., HEROLD-MENDE, C., ROMMELAERE, J., SCHLEHOFER, J. R. & GELETNEKY, K. 2004. Parvovirus H-1 infection of human glioma cells leads to complete viral replication and efficient cell killing. *International journal of cancer*, 109, 76-84.
- HEUSER, J. E. & ANDERSON, R. 1989. Hypertonic media inhibit receptor-mediated endocytosis by blocking clathrin-coated pit formation. *The Journal of cell biology*, 108, 389-400.
- HILL, T. A., GORDON, C. P., MCGEACHIE, A. B., VENN-BROWN, B., ODELL, L. R., CHAU, N., QUAN, A., MARIANA, A., SAKOFF, J. A. & CHIRCOP, M. 2009. Inhibition of Dynamin Mediated Endocytosis by the Dynoles · Synthesis and Functional Activity of a Family of Indoles. *Journal of medicinal chemistry*, 52, 3762-3773.
- HINDERLICH, S., WEIDEMANN, W., YARDENI, T., HORSTKORTE, R. & HUIZING, M. 2013. UDP-GlcNAc 2-epimerase/ManNAc kinase (GNE): a master regulator of sialic acid synthesis. *SialoGlyco Chemistry and Biology I*, 97-137.
- HIRSCH, A. J. 2010. The use of RNAi-based screens to identify host proteins involved in viral replication. *Future microbiology*, 5, 303-311.
- HOSSAIN, J. A., LATIF, M. A., YSTAAS, L. A., NINZIMA, S., RIECKEN, K., MULLER, A., AZUAJE, F., JOSEPH, J. V., TALASIL, K. M. & GHIMIRE, J. 2019a. Long-term treatment with valganciclovir improves lentiviral suicide gene therapy of glioblastoma. *Neuro-oncology*, 21, 890-900.
- HOSSAIN, J. A., RIECKEN, K., MILETIC, H. & FEHSE, B. 2019b. Cancer suicide gene therapy with TK. 007. *Suicide Gene Therapy*. Springer.
- HRISTOV, G., KRÄMER, M., LI, J., EL-ANDALOUSSI, N., MORA, R., DAEFFLER, L., ZENTGRAF, H., ROMMELAERE, J. & MARCHINI, A. 2010. Through its nonstructural protein NS1, parvovirus H-1 induces apoptosis via accumulation of reactive oxygen species. *Journal of virology*, 84, 5909-5922.
- HU, J. C., COFFIN, R. S., DAVIS, C. J., GRAHAM, N. J., GROVES, N., GUEST, P. J., HARRINGTON, K. J., JAMES, N. D., LOVE, C. A. & MCNEISH, I. 2006.

- A phase I study of OncoVEXGM-CSF, a second-generation oncolytic herpes simplex virus expressing granulocyte macrophage colony-stimulating factor. *Clinical cancer research*, 12, 6737-6747.
- HUEFFER, K., PALERMO, L. M. & PARRISH, C. R. 2004. Parvovirus infection of cells by using variants of the feline transferrin receptor altering clathrin-mediated endocytosis, membrane domain localization, and capsid-binding domains. *Journal of virology*, 78, 5601-5611.
- JAMES, N. 2017. *FENNER'S VETERINARY VIROLOGY*, Elsevier Academic Press.
- JOHANNES, L., JACOB, R. & LEFFLER, H. 2018. Galectins at a glance. *Journal of cell science*, 131.
- JOHNSON, D. B., PUZANOV, I. & KELLEY, M. C. 2015. Talimogene laherparepvec (T-VEC) for the treatment of advanced melanoma. *Immunotherapy*, 7, 611-619.
- JORDENS, I., MARSMAN, M., KUIJL, C. & NEEFJES, J. 2005. Rab proteins, connecting transport and vesicle fusion. *Traffic*, 6, 1070-1077.
- JOSUPEIT, R., BENDER, S., KERN, S., LEUCHS, B., HIELSCHER, T., HEROLD-MENDE, C., SCHLEHOFER, J. R., DINSART, C., WITT, O. & ROMMELAERE, J. 2016. Pediatric and adult high-grade glioma stem cell culture models are permissive to lytic infection with parvovirus H-1. *Viruses*, 8, 138.
- JUNG, T.-Y., JUNG, S., RYU, H.-H., JEONG, Y.-I., JIN, Y.-H., JIN, S.-G., KIM, I.-Y., KANG, S.-S. & KIM, H.-S. 2008. Role of galectin-1 in migration and invasion of human glioblastoma multiforme cell lines. *Journal of neurosurgery*, 109, 273-284.
- KADLECOVA, Z., SPIELMAN, S. J., LOERKE, D., MOHANAKRISHNAN, A., REED, D. K. & SCHMID, S. L. 2017. Regulation of clathrin-mediated endocytosis by hierarchical allosteric activation of AP2. *Journal of Cell Biology*, 216, 167-179.
- KAUFMAN, H. L., KOHLHAPP, F. J. & ZLOZA, A. 2015. Oncolytic viruses: a new class of immunotherapy drugs. *Nature reviews Drug discovery*, 14, 642-662.
- KELLAND, L. 2004. "Of mice and men": values and liabilities of the athymic nude mouse model in anticancer drug development. *European journal of cancer*, 40, 827-836.
- KEMP, V., LAMFERS, M. L., VAN DER PLUIJM, G., VAN DEN HOOGEN, B. G. & HOEBEN, R. C. 2020. Developing oncolytic viruses for clinical use: A consortium approach. *Cytokine & growth factor reviews*.
- KESTLER, J., NEEB, B., STRUYF, S., DAMME, J. V., COTMORE, S. F., D'ABRAMO, A., TATTERSALL, P., ROMMELAERE, J., DINSART, C. & CORNELIS, J. J. 1999. cis requirements for the efficient production of

- recombinant DNA vectors based on autonomous parvoviruses. *Human gene therapy*, 10, 1619-1632.
- KILSDONK, E. P., YANCEY, P. G., STOUDET, G. W., BANGERTER, F. W., JOHNSON, W. J., PHILLIPS, M. C. & ROTHBLAT, G. H. 1995. Cellular cholesterol efflux mediated by cyclodextrins. *Journal of Biological Chemistry*, 270, 17250-17256.
- KINSNER-OVASKAINEN, A., PRIETO, P., STANZEL, S. & KOPP-SCHNEIDER, A. 2013. Selection of test methods to be included in a testing strategy to predict acute oral toxicity: an approach based on statistical analysis of data collected in phase 1 of the ACuteTox project. *Toxicology in Vitro*, 27, 1377-1394.
- KIPRIANOVA, I., JUST, A., LEUCHS, B., ROMMELAERE, J. & ANGELOVA, A. L. 2020. Fluorescence In Situ Hybridization (FISH) Detection of Viral Nucleic Acids in Oncolytic H-1 Parvovirus-Treated Human Brain Tumors. *Oncolytic Viruses*. Springer.
- KRADY, J. K. & WARD, D. C. 1995. Transcriptional activation by the parvoviral nonstructural protein NS-1 is mediated via a direct interaction with Sp1. *Molecular and cellular biology*, 15, 524-533.
- KUHN, I., HARDEN, P., BAUZON, M., CHARTIER, C., NYE, J., THORNE, S., REID, T., NI, S., LIEBER, A. & FISHER, K. 2008. Directed evolution generates a novel oncolytic virus for the treatment of colon cancer. *PloS one*, 3, e2409.
- KULKARNI, A., FERREIRA, T., BRETSCHER, C., GREWENIG, A., EL-ANDALOUSSI, N., BONIFATI, S., MARTTILA, T., PALISSOT, V., HOSSAIN, J., AZUAJE, F., MILETIC, H., YSTAAS, L., GOLEBIEWSKA, A., NICLOU, S., ROETH, R., NIESLER, B., WEISS, A., BRINO, L. & MARCHINI, A. *in press*. Oncolytic H-1 parvovirus binds to sialic acid on laminins for cell attachment and entry. *Nature communications*.
- KUMARI, S., SWETHA, M. & MAYOR, S. 2010. Endocytosis unplugged: multiple ways to enter the cell. *Cell research*, 20, 256-275.
- KUROI, K., KAMIJO, M., UEKI, M., NIWA, Y., HIRAMATSU, H. & NAKABAYASHI, T. 2020. Time-resolved FTIR study on the structural switching of human galectin-1 by light-induced disulfide bond formation. *Physical Chemistry Chemical Physics*, 22, 1137-1144.
- KURUPPU, D. & TANABE, K. K. 2005. Viral oncolysis by herpes simplex virus and other viruses. *Cancer biology & therapy*, 4, 524-531.
- LACHMANN, S., ROMMELEARE, J. & NÜESCH, J. P. 2003. Novel PKC $\eta$  is required to activate replicative functions of the major nonstructural protein NS1 of minute virus of mice. *Journal of virology*, 77, 8048-8060.
- LACROIX, J., KIS, Z., JOSUPEIT, R., SCHLUND, F., STROH-DEGE, A., FRANK-STÖHR, M., LEUCHS, B., SCHLEHOFER, J. R., ROMMELAERE, J. & DINSART, C. 2018. Preclinical testing of an oncolytic parvovirus in Ewing

sarcoma: protoparvovirus H-1 induces apoptosis and lytic infection in vitro but fails to improve survival in vivo. *Viruses*, 10, 302.

- LACROIX, J., LEUCHS, B., LI, J., HRISTOV, G., DEUBZER, H. E., KULOZIK, A. E., ROMMELAERE, J., SCHLEHOFER, J. R. & WITT, O. 2010. Parvovirus H1 selectively induces cytotoxic effects on human neuroblastoma cells. *International journal of cancer*, 127, 1230-1239.
- LACROIX, J., SCHLUND, F., LEUCHS, B., ADOLPH, K., STURM, D., BENDER, S., HIELSCHER, T., PFISTER, S. M., WITT, O. & ROMMELAERE, J. 2014. Oncolytic effects of parvovirus H-1 in medulloblastoma are associated with repression of master regulators of early neurogenesis. *International journal of cancer*, 134, 703-716.
- LAWRENCE, M. S., STOJANOV, P., POLAK, P., KRYUKOV, G. V., CIBULSKIS, K., SIVACHENKO, A., CARTER, S. L., STEWART, C., MERMEL, C. H. & ROBERTS, S. A. 2013. Mutational heterogeneity in cancer and the search for new cancer-associated genes. *Nature*, 499, 214-218.
- LE CESNE, A., DUPRESSOIR, T., JANIN, N., SPIELMANN, M., LE CHEVALIER, T., SANCHO-GARNIER, H., PAOLETTI, C., ROMMELAERE, J., STEHELIN, D. & TURSZ, T. Intra-lesional administration of a live virus, parvovirus H-1 (PVH-1) in cancer patients: a feasibility study. Proc Ann Meet Am Soc Clin Oncol, 1993. 297.
- LEE, P.-H., LIU, C.-M., HO, T.-S., TSAI, Y.-C., LIN, C.-C., WANG, Y.-F., CHEN, Y.-L., YU, C.-K., WANG, S.-M. & LIU, C.-C. 2015. Enterovirus 71 virion-associated galectin-1 facilitates viral replication and stability. *PLoS One*, 10, e0116278.
- LEFFLER, H., CARLSSON, S., HEDLUND, M., QIAN, Y. & POIRIER, F. 2002. Introduction to galectins. *Glycoconjugate journal*, 19, 433-440.
- LEGENDRE, D. & ROMMELAERE, J. 1994. Targeting of promoters for trans activation by a carboxy-terminal domain of the NS-1 protein of the parvovirus minute virus of mice. *Journal of virology*, 68, 7974-7985.
- LEGRAND, C., ROMMELAERE, J. & CAILLET-FAUQUET, P. 1993. MVM (p) NS-2 protein expression is required with NS-1 for maximal cytotoxicity in human transformed cells. *Virology*, 195, 149-155.
- LEICHT, D. T., BALAN, V., KAPLUN, A., SINGH-GUPTA, V., KAPLUN, L., DOBSON, M. & TZIVION, G. 2007. Raf kinases: function, regulation and role in human cancer. *Biochimica et Biophysica Acta (BBA)-Molecular Cell Research*, 1773, 1196-1212.
- LEPUR, A., CARLSSON, M. C., NOVAK, R., DUMIĆ, J., NILSSON, U. J. & LEFFLER, H. 2012. Galectin-3 endocytosis by carbohydrate independent and dependent pathways in different macrophage like cell types. *Biochimica et Biophysica Acta (BBA)-General Subjects*, 1820, 804-818.

- LEUCHS, B., ROSCHER, M., MULLER, M., KURSCHNER, K. & ROMMELAERE, J. 2016. Standardized large-scale H-1PV production process with efficient quality and quantity monitoring. *J Virol Methods*, 229, 48-59.
- LEVADITI, C. & NICOLAU, S. 1922. Sur le culture du virus vaccinal dans les neoplasmes epithelieux. *CR Soc Biol*, 86, 928.
- LEVRONEY, E. L., AGUILAR, H. C., FULCHER, J. A., KOHATSU, L., PACE, K. E., PANG, M., GURNEY, K. B., BAUM, L. G. & LEE, B. 2005. Novel innate immune functions for galectin-1: galectin-1 inhibits cell fusion by Nipah virus envelope glycoproteins and augments dendritic cell secretion of proinflammatory cytokines. *The Journal of Immunology*, 175, 413-420.
- LI, F.-Y., WANG, S.-F., BERNARDES, E. S. & LIU, F.-T. 2020. Galectins in host defense against microbial infections. *Lectin in Host Defense Against Microbial Infections*. Springer.
- LI, J., BONIFATI, S., HRISTOV, G., MARTTILA, T., VALMARY-DEGANO, S., STANZEL, S., SCHNÖLZER, M., MOUGIN, C., APRAHAMIAN, M. & GREKOVA, S. P. 2013a. Synergistic combination of valproic acid and oncolytic parvovirus H-1PV as a potential therapy against cervical and pancreatic carcinomas. *EMBO molecular medicine*, 5, 1537-1555.
- LI, L., COTMORE, S. F. & TATTERSALL, P. 2013b. Parvoviral left-end hairpin ears are essential during infection for establishing a functional intranuclear transcription template and for efficient progeny genome encapsidation. *Journal of virology*, 87, 10501-10514.
- LI, X. & RHODE, S. 1990. Mutation of lysine 405 to serine in the parvovirus H-1 NS1 abolishes its functions for viral DNA replication, late promoter trans activation, and cytotoxicity. *Journal of virology*, 64, 4654-4660.
- LIANG, M. 2018. Oncorine, the world first oncolytic virus medicine and its update in China. *Current cancer drug targets*, 18, 171-176.
- LIN, S., NADEAU, P. E., WANG, X. & MERGIA, A. 2012. Caveolin-1 reduces HIV-1 infectivity by restoration of HIV Nef mediated impairment of cholesterol efflux by apoA-I. *Retrovirology*, 9, 1-16.
- LIU, B., ROBINSON, M., HAN, Z., BRANSTON, R., ENGLISH, C., REAY, P., MCGRATH, Y., THOMAS, S., THORNTON, M. & BULLOCK, P. 2003. ICP34. 5 deleted herpes simplex virus with enhanced oncolytic, immune stimulating, and anti-tumour properties. *Gene therapy*, 10, 292-303.
- LIU, J., RAN, Z. H., XIAO, S. D. & ROMMELAERE, J. 2005. Changes in gene expression profiles induced by parvovirus H-1 in human gastric cancer cells. *Chinese journal of digestive diseases*, 6, 72-81.
- LOCKER, J. K. & SCHMID, S. L. 2013. Integrated electron microscopy: super-duper resolution. *PLoS Biol*, 11, e1001639.

- LOMBARDO, E., RAMÍREZ, J. C., AGBANDJE-MCKENNA, M. & ALMENDRAL, J. M. 2000. A beta-stranded motif drives capsid protein oligomers of the parvovirus minute virus of mice into the nucleus for viral assembly. *Journal of Virology*, 74, 3804-3814.
- LOMBARDO, E., RAMÍREZ, J. C., GARCIA, J. & ALMENDRAL, J. M. 2002. Complementary roles of multiple nuclear targeting signals in the capsid proteins of the parvovirus minute virus of mice during assembly and onset of infection. *Journal of virology*, 76, 7049-7059.
- LÓPEZ-BUENO, A., RUBIO, M.-P., BRYANT, N., MCKENNA, R., AGBANDJE-MCKENNA, M. & ALMENDRAL, J. M. 2006. Host-selected amino acid changes at the sialic acid binding pocket of the parvovirus capsid modulate cell binding affinity and determine virulence. *Journal of virology*, 80, 1563-1573.
- LÓPEZ-BUENO, A., SEGOVIA, J. C., BUEREN, J. A., O'SULLIVAN, M. G., WANG, F., TATTERSALL, P. & ALMENDRAL, J. M. 2008. Evolution to pathogenicity of the parvovirus minute virus of mice in immunodeficient mice involves genetic heterogeneity at the capsid domain that determines tropism. *Journal of virology*, 82, 1195-1203.
- LORSON, C., PEARSON, J., BURGER, L. & PINTEL, D. 1998. An Sp1-binding site and TATA element are sufficient to support full transactivation by proximally bound NS1 protein of minute virus of mice. *Virology*, 240, 326-337.
- LUNARDI, C., TINAZZI, E., BASON, C., DOLCINO, M., CORROCHER, R. & PUCETTI, A. 2008. Human parvovirus B19 infection and autoimmunity. *Autoimmunity reviews*, 8, 116-120.
- MACEDO, N., MILLER, D. M., HAQ, R. & KAUFMAN, H. L. 2020. Clinical landscape of oncolytic virus research in 2020. *Journal for immunotherapy of cancer*, 8.
- MACHALA, E. A., AVDIC, S., STERN, L., ZAJONC, D. M., BENEDICT, C. A., BLYTH, E., GOTTLIEB, D. J., ABENDROTH, A., MCSHARRY, B. P. & SLOBEDMAN, B. 2019a. Restriction of human cytomegalovirus infection by galectin-9. *Journal of virology*, 93.
- MACHALA, E. A., MCSHARRY, B. P., ROUSE, B. T., ABENDROTH, A. & SLOBEDMAN, B. 2019b. Gal power: the diverse roles of galectins in regulating viral infections. *Journal of General Virology*, 100, 333-349.
- MAHONEY, D. J., LEFEBVRE, C., ALLAN, K., BRUN, J., SANAEI, C. A., BAIRD, S., PEARCE, N., GRÖNBERG, S., WILSON, B. & PRAKESH, M. 2011. Virus-tumor interactome screen reveals ER stress response can reprogram resistant cancers for oncolytic virus-triggered caspase-2 cell death. *Cancer cell*, 20, 443-456.
- MAITRA, R., GHALIB, M. H. & GOEL, S. 2012. Reovirus: a targeted therapeutic—progress and potential. *Molecular cancer research*, 10, 1514-1525.

- MALERBA, M., DAEFFLER, L., ROMMELAERE, J. & IGGO, R. 2003. Replicating parvoviruses that target colon cancer cells. *Journal of virology*, 77, 6683-6691.
- MANI, B., BALTZER, C., VALLE, N., ALMENDRAL, J. M., KEMPF, C. & ROS, C. 2006. Low pH-dependent endosomal processing of the incoming parvovirus minute virus of mice virion leads to externalization of the VP1 N-terminal sequence (N-VP1), N-VP2 cleavage, and uncoating of the full-length genome. *Journal of virology*, 80, 1015-1024.
- MANSOUR, M., PALESE, P. & ZAMARIN, D. 2011. Oncolytic specificity of Newcastle disease virus is mediated by selectivity for apoptosis-resistant cells. *Journal of virology*, 85, 6015-6023.
- MANTEUFEL, J. & TRUYEN, U. 2008. Animal bocaviruses: a brief review. *Intervirology*, 51, 328-334.
- MARCHINI, A., BONIFATI, S., SCOTT, E. M., ANGELOVA, A. L. & ROMMELAERE, J. 2015a. Oncolytic parvoviruses: from basic virology to clinical applications. *Virology journal*, 12, 6.
- MARCHINI, A., DAEFFLER, L., POZDEEV, V., ANGELOVA, A. & ROMMELAERE, J. 2019. Immune conversion of tumor microenvironment by oncolytic viruses: the protoparvovirus H-1PV case study. *Frontiers in immunology*, 10, 1848.
- MARCHINI, A., LI, J., SCHROEDER, L., ROMMELAERE, J. & GELETNEKY, K. 2015b. *Cancer therapy with a parvovirus combined with a Bcl-2 inhibitor*.
- MARCHINI, A., ROMMELAERE, J., EL-ANDALOUSSI, N., HRISTOV, G. & LI, J. 2013. *Cancer Therapy with a Parvovirus Combined with an HDAC Inhibitor*. Google Patents.
- MARCHINI, A., SCOTT, E. M. & ROMMELAERE, J. 2016. Overcoming barriers in oncolytic virotherapy with HDAC inhibitors and immune checkpoint blockade. *Viruses*, 8, 9.
- MAROTO, B., VALLE, N., SAFFRICH, R. & ALMENDRAL, J. M. 2004. Nuclear export of the nonenveloped parvovirus virion is directed by an unordered protein signal exposed on the capsid surface. *Journal of virology*, 78, 10685-10694.
- MARTINEZ-BOSCH, N., BARRANCO, L. E., OROZCO, C. A., MORENO, M., VISA, L., IGLESIAS, M., OLDFIELD, L., NEOPTOLEMOS, J. P., GREENHALF, W. & EARL, J. 2018. Increased plasma levels of galectin-1 in pancreatic cancer: potential use as biomarker. *Oncotarget*, 9, 32984.
- MARTÍNEZ-VÉLEZ, N., GARCIA-MOURE, M., MARIGIL, M., GONZÁLEZ-HUARRIZ, M., PUIGDELLOSES, M., PÉREZ-LARRAYA, J. G., ZALACAÍN, M., MARRODÁN, L., VARELA-GURUCEAGA, M. & LASPIDEA, V. 2019. The oncolytic virus Delta-24-RGD elicits an antitumor effect in pediatric glioma and DIPG mouse models. *Nature communications*, 10, 1-10.

- MATTHEWS, P. C., MALIK, A., SIMMONS, R., SHARP, C., SIMMONDS, P. & KLENERMAN, P. 2014. PARV4: an emerging tetraparvovirus. *PLoS pathogens*, 10.
- MAYLE, K. M., LE, A. M. & KAMEI, D. T. 2012. The intracellular trafficking pathway of transferrin. *Biochimica et Biophysica Acta*, 1820, 264-281.
- MCMAHON, H. T. & BOUCROT, E. 2011. Molecular mechanism and physiological functions of clathrin-mediated endocytosis. *Nature reviews Molecular cell biology*, 12, 517.
- MERCER, J., SCHELHAAS, M. & HELENIUS, A. 2010. Virus entry by endocytosis. *Annual review of biochemistry*, 79, 803-833.
- MERCIER, S., ST-PIERRE, C., PELLETIER, I., OUELLET, M., TREMBLAY, M. J. & SATO, S. 2008. Galectin-1 promotes HIV-1 infectivity in macrophages through stabilization of viral adsorption. *Virology*, 371, 121-129.
- MERRILL, M. K., BERNHARDT, G., SAMPSON, J. H., WIKSTRAND, C. J., BIGNER, D. D. & GROMEIER, M. 2004. Poliovirus receptor CD155-targeted oncolysis of glioma. *Neuro-oncology*, 6, 208-217.
- MÉSZÁROS, I., TÓTH, R., OLASZ, F., TIJSSEN, P. & ZÁDORI, Z. 2017. The SAT protein of porcine parvovirus accelerates viral spreading through induction of irreversible endoplasmic reticulum stress. *Journal of virology*, 91.
- MIEST, T. S. & CATTANEO, R. 2014. New viruses for cancer therapy: meeting clinical needs. *Nature reviews microbiology*, 12, 23-34.
- MILLER, C. L. & PINTEL, D. J. 2002. Interaction between parvovirus NS2 protein and nuclear export factor Crm1 is important for viral egress from the nucleus of murine cells. *Journal of virology*, 76, 3257-3266.
- MISINZO, G., DELPUTTE, P. L. & NAUWYNCK, H. J. 2008. Inhibition of endosome-lysosome system acidification enhances porcine circovirus 2 infection of porcine epithelial cells. *Journal of virology*, 82, 1128-1135.
- MIYAGAWA, Y., MARINO, P., VERLENGIA, G., UCHIDA, H., GOINS, W. F., YOKOTA, S., GELLER, D. A., YOSHIDA, O., MESTER, J. & COHEN, J. B. 2015. Herpes simplex viral-vector design for efficient transduction of nonneuronal cells without cytotoxicity. *Proceedings of the national academy of sciences*, 112, E1632-E1641.
- MOEHLER, M., BLECHACZ, B., WEISKOPF, N., ZEIDLER, M., STREMMEL, W., ROMMELAERE, J., GALLE, P. R. & CORNELIS, J. J. 2001. Effective infection, apoptotic cell killing and gene transfer of human hepatoma cells but not primary hepatocytes by parvovirus H1 and derived vectors. *Cancer gene therapy*, 8, 158-167.
- MOEHLER, M., SIEBEN, M., ROTH, S., SPRINGSGUTH, F., LEUCHS, B., ZEIDLER, M., DINSART, C., ROMMELAERE, J. & GALLE, P. R. 2011.



- Activation of the human immune system by chemotherapeutic or targeted agents combined with the oncolytic parvovirus H-1. *BMC cancer*, 11, 1-14.
- MOEHLER, M., ZEIDLER, M., SCHEDE, J., ROMMELAERE, J., GALLE, P. R., CORNELIS, J. J. & HEIKE, M. 2003. Oncolytic parvovirus H1 induces release of heat-shock protein HSP72 in susceptible human tumor cells but may not affect primary immune cells. *Cancer gene therapy*, 10, 477-480.
- MOEHLER, M. H., ZEIDLER, M., WILSBERG, V., CORNELIS, J. J., WOELFEL, T., ROMMELAERE, J., GALLE, P. R. & HEIKE, M. 2005. Parvovirus H-1-induced tumor cell death enhances human immune response in vitro via increased phagocytosis, maturation, and cross-presentation by dendritic cells. *Human gene therapy*, 16, 996-1005.
- MOISEEVA, E. P., JAVED, Q., SPRING, E. L. & DE BONO, D. P. 2000. Galectin 1 is involved in vascular smooth muscle cell proliferation. *Cardiovascular research*, 45, 493-502.
- MOISEEVA, E. P., WILLIAMS, B. & SAMANI, N. J. 2003. Galectin 1 inhibits incorporation of vitronectin and chondroitin sulfate B into the extracellular matrix of human vascular smooth muscle cells. *Biochimica et Biophysica Acta (BBA)-General Subjects*, 1619, 125-132.
- MUHARRAM, G., LE RHUN, E., LOISON, I., WIZLA, P., RICHARD, A., MARTIN, N., ROUSSEL, A., BEGUE, A., DEVOS, P. & BARANZELLI, M.-C. 2010. Parvovirus H-1 induces cytopathic effects in breast carcinoma-derived cultures. *Breast cancer research and treatment*, 121, 23-33.
- MUIK, A., KNEISKE, I., WERBIZKI, M., WILFLINGSSEDER, D., GIROGLOU, T., EBERT, O., KRAFT, A., DIETRICH, U., ZIMMER, G. & MOMMA, S. 2011. Pseudotyping vesicular stomatitis virus with lymphocytic choriomeningitis virus glycoproteins enhances infectivity for glioma cells and minimizes neurotropism. *Journal of virology*, 85, 5679-5684.
- MUÑOZ-FONTELA, C., MACIP, S., MARTÍNEZ-SOBRIDO, L., BROWN, L., ASHOUR, J., GARCÍA-SASTRE, A., LEE, S. W. & AARONSON, S. A. 2008. Transcriptional role of p53 in interferon-mediated antiviral immunity. *The Journal of experimental medicine*, 205, 1929-1938.
- NASO, M. F., TOMKOWICZ, B., PERRY, W. L. & STROHL, W. R. 2017. Adeno-associated virus (AAV) as a vector for gene therapy. *BioDrugs*, 31, 317-334.
- NOESCH, J. P., COTMORE, S. F. & TATTERSALL, P. 1992. Expression of functional parvoviral NS1 from recombinant vaccinia virus: effects of mutations in the nucleotide-binding motif. *Virology*, 191, 406-416.
- NÜESCH, J. 2006. *Regulation of non-structural protein functions by differential synthesis, modification and trafficking*, London: Hodder Arnold.
- NÜESCH, J. P., BÄR, S., LACHMANN, S. & ROMMELAERE, J. 2009. Ezrin-radixin-moesin family proteins are involved in parvovirus replication and spreading. *Journal of virology*, 83, 5854-5863.

- NÜESCH, J. P., CHRISTENSEN, J. & ROMMELAERE, J. 2001. Initiation of minute virus of mice DNA replication is regulated at the level of origin unwinding by atypical protein kinase C phosphorylation of NS1. *Journal of virology*, 75, 5730-5739.
- NÜESCH, J. P., LACHMANN, S., CORBAU, R. & ROMMELAERE, J. 2003. Regulation of minute virus of mice NS1 replicative functions by atypical PKC $\lambda$  in vivo. *Journal of virology*, 77, 433-442.
- NÜESCH, J. P., LACHMANN, S. & ROMMELAERE, J. 2005. Selective alterations of the host cell architecture upon infection with parvovirus minute virus of mice. *Virology*, 331, 159-174.
- NUESCH, J. P., LACROIX, J., MARCHINI, A. & ROMMELAERE, J. 2012. Molecular pathways: rodent parvoviruses--mechanisms of oncolysis and prospects for clinical cancer treatment. *Clin Cancer Res*, 18, 3516-23.
- NÜESCH, J. P., LACROIX, J., MARCHINI, A. & ROMMELAERE, J. 2012. Molecular pathways: rodent parvoviruses—mechanisms of oncolysis and prospects for clinical cancer treatment. *Clinical Cancer Research*, 18, 3516-3523.
- NÜESCH, J. P. & ROMMELAERE, J. 2007. A viral adaptor protein modulating casein kinase II activity induces cytopathic effects in permissive cells. *Proceedings of the National Academy of Sciences*, 104, 12482-12487.
- NÜESCH, J. P. & ROMMELAERE, J. 2014. Tumor suppressing properties of rodent parvovirus NS1 proteins and their derivatives. *Anticancer Genes*, 99-124.
- NÜESCH, J. P. & TATTERSALL, P. 1993. Nuclear targeting of the parvoviral replicator molecule NS1: evidence for self-association prior to nuclear transport. *Virology*, 196, 637-651.
- NYKKY, J., VUENTO, M. & GILBERT, L. 2014. Role of mitochondria in parvovirus pathology. *PLoS One*, 9, e86124.
- OHSHIMA, T., IWAMA, M., UENO, Y., SUGIYAMA, F., NAKAJIMA, T., FUKAMIZU, A. & YAGAMI, K.-I. 1998. Induction of apoptosis in vitro and in vivo by H-1 parvovirus infection. *Journal of General Virology*, 79, 3067-3071.
- OLOFSSON, S. & BERGSTRÖM, T. 2005. Glycoconjugate glycans as viral receptors. *Annals of medicine*, 37, 154-172.
- OUELLET, M., MERCIER, S., PELLETIER, I., BOUNOU, S., ROY, J., HIRABAYASHI, J., SATO, S. & TREMBLAY, M. J. 2005. Galectin-1 acts as a soluble host factor that promotes HIV-1 infectivity through stabilization of virus attachment to host cells. *The Journal of Immunology*, 174, 4120-4126.
- PACE, K. E., LEE, C., STEWART, P. L. & BAUM, L. G. 1999. Restricted receptor segregation into membrane microdomains occurs on human T cells during apoptosis induced by galectin-1. *The Journal of Immunology*, 163, 3801-3811.

- PAGLINO, J. C., ANDRES, W. & VAN DEN POL, A. N. 2014. Autonomous parvoviruses neither stimulate nor are inhibited by the type I interferon response in human normal or cancer cells. *Journal of virology*, 88, 4932-4942.
- PARATO, K. A., BREITBACH, C. J., LE BOEUF, F., WANG, J., STORBECK, C., ILKOW, C., DIALLO, J.-S., FALLS, T., BURNS, J. & GARCIA, V. 2012. The oncolytic poxvirus JX-594 selectively replicates in and destroys cancer cells driven by genetic pathways commonly activated in cancers. *Molecular Therapy*, 20, 749-758.
- PARATO, K. A., SENGER, D., FORSYTH, P. A. & BELL, J. C. 2005. Recent progress in the battle between oncolytic viruses and tumours. *Nature Reviews Cancer*, 5, 965.
- PARKER, J. S., MURPHY, W. J., WANG, D., O'BRIEN, S. J. & PARRISH, C. R. 2001. Canine and feline parvoviruses can use human or feline transferrin receptors to bind, enter, and infect cells. *Journal of Virology*, 75, 3896-3902.
- PARKER, J. S. & PARRISH, C. R. 2000. Cellular uptake and infection by canine parvovirus involves rapid dynamin-regulated clathrin-mediated endocytosis, followed by slower intracellular trafficking. *Journal of virology*, 74, 1919-1930.
- PERROS, M., DELEU, L., VANACKER, J.-M., KHERROUCHE, Z., SPRUYT, N., FAISST, S. & ROMMELAERE, J. 1995. Upstream CREs participate in the basal activity of minute virus of mice promoter P4 and in its stimulation in ras-transformed cells. *Journal of virology*, 69, 5506-5515.
- PHUANGSAB, A., LORENCE, R. M., REICHARD, K. W., PEEPLES, M. E. & WALTER, R. J. 2001. Newcastle disease virus therapy of human tumor xenografts: antitumor effects of local or systemic administration. *Cancer letters*, 172, 27-36.
- POPPERS, J., MULVEY, M., KHOO, D. & MOHR, I. 2000. Inhibition of PKR activation by the proline-rich RNA binding domain of the herpes simplex virus type 1 Us11 protein. *Journal of virology*, 74, 11215-11221.
- PORWAL, M., COHEN, S., SNOUSSI, K., POPA-WAGNER, R., ANDERSON, F., DUGOT-SENANT, N., WODRICH, H., DINSART, C., KLEINSCHMIDT, J. A. & PANTÉ, N. 2013. Parvoviruses cause nuclear envelope breakdown by activating key enzymes of mitosis. *PLoS pathogens*, 9.
- PRETA, G., CRONIN, J. G. & SHELDON, I. M. 2015. Dynasore-not just a dynamin inhibitor. *Cell Communication and Signaling*, 13, 24.
- PUZANOV, I., MILHEM, M. M., MINOR, D., HAMID, O., LI, A., CHEN, L., CHASTAIN, M., GORSKI, K. S., ANDERSON, A. & CHOU, J. 2016. Talimogene laherparepvec in combination with ipilimumab in previously untreated, unresectable stage IIIB-IV melanoma. *Journal of Clinical Oncology*, 34, 2619.

- QIN, Y., RODIN, S., SIMONSON, O. E. & HOLLANDE, F. Laminins and cancer stem cells: partners in crime? *Seminars in cancer biology*, 2017. Elsevier, 3-12.
- QIU, J., SÖDERLUND-VENERMO, M. & YOUNG, N. S. 2017. Human parvoviruses. *Clinical microbiology reviews*, 30, 43-113.
- QUATTROCCHI, S., RUPRECHT, N., BÖNSCH, C., BIELI, S., ZÜRCHER, C., BOLLER, K., KEMPF, C. & ROS, C. 2012. Characterization of the early steps of human parvovirus B19 infection. *Journal of virology*, 86, 9274-9284.
- RAFFELSBERGER, W., KRAUSE, Y., MOULINIER, L., KIEFFER, D., MORAND, A.-L., BRINO, L. & POCH, O. 2008. RReportGenerator: automatic reports from routine statistical analysis using R. *Bioinformatics*, 24, 276-278.
- RAJAPAKSHA, I., ANGUS, P. & HERATH, C. 2018. Adeno-associated virus (AAV)-mediated gene therapy for disorders of inherited and non-inherited origin. *In Vivo and Ex Vivo Gene Therapy for Inherited and Non-Inherited Disorders*. IntechOpen.
- RAN, Z.-H., RAYET, B., ROMMELAERE, J. & FAISST, S. 1999. Parvovirus H-1-induced cell death: influence of intracellular NAD consumption on the regulation of necrosis and apoptosis. *Virus research*, 65, 161-174.
- RAYKOV, Z., GREKOVA, S., GALABOV, A. S., BALBONI, G., KOCH, U., APRAHAMIAN, M. & ROMMELAERE, J. 2007. Combined oncolytic and vaccination activities of parvovirus H-1 in a metastatic tumor model. *Oncology reports*, 17, 1493-1499.
- RAYKOV, Z., GREKOVA, S., LEUCHS, B., APRAHAMIAN, M. & ROMMELAERE, J. 2008. Arming parvoviruses with CpG motifs to improve their oncosuppressive capacity. *International journal of cancer*, 122, 2880-2884.
- RHODE, S. 1985. trans-Activation of parvovirus P38 promoter by the 76K noncapsid protein. *Journal of virology*, 55, 886-889.
- RIBAS, A., DUMMER, R., PUZANOV, I., VANDERWALDE, A., ANDTBACKA, R. H., MICHIELIN, O., OLSZANSKI, A. J., MALVEHY, J., CEBON, J. & FERNANDEZ, E. 2017. Oncolytic virotherapy promotes intratumoral T cell infiltration and improves anti-PD-1 immunotherapy. *Cell*, 170, 1109-1119. e10.
- RIOLOBOS, L., VALLE, N., HERNANDO, E., MAROTO, B., KANN, M. & ALMENDRAL, J. M. 2010. Viral oncolysis that targets Raf-1 signaling control of nuclear transport. *Journal of virology*, 84, 2090-2099.
- ROBERTSON, M. J., DEANE, F. M., ROBINSON, P. J. & MCCLUSKEY, A. 2014. Synthesis of Dynole 34-2, Dynole 2-24 and Dyngo 4a for investigating dynamin GTPase. *Nature protocols*, 9, 851-870.

- ROMMELAERE, J. & CORNELIS, J. J. 1991. Antineoplastic activity of parvoviruses. *Journal of virological methods*, 33, 233-251.
- ROMMELAERE, J., GELETNEKY, K., ANGELOVA, A. L., DAEFFLER, L., DINSART, C., KIPRIANOVA, I., SCHLEHOFER, J. R. & RAYKOV, Z. 2010. Oncolytic parvoviruses as cancer therapeutics. *Cytokine & growth factor reviews*, 21, 185-195.
- ROS, C., BAYAT, N., WOLFISBERG, R. & ALMENDRAL, J. M. 2017. Protoparvovirus Cell Entry. *Viruses*, 9, 313.
- ROS, C., BURCKHARDT, C. J. & KEMPF, C. 2002. Cytoplasmic trafficking of minute virus of mice: low-pH requirement, routing to late endosomes, and proteasome interaction. *Journal of virology*, 76, 12634-12645.
- RUIZ, Z., D'ABRAMO JR, A. & TATTERSALL, P. 2006. Differential roles for the C-terminal hexapeptide domains of NS2 splice variants during MVM infection of murine cells. *Virology*, 349, 382-395.
- RUIZ, Z., MIHAYLOV, I. S., COTMORE, S. F. & TATTERSALL, P. 2011. Recruitment of DNA replication and damage response proteins to viral replication centers during infection with NS2 mutants of Minute Virus of Mice (MVM). *Virology*, 410, 375-384.
- RUSSELL, S. J., PENG, K.-W. & BELL, J. C. 2012. Oncolytic virotherapy. *Nature biotechnology*, 30, 658.
- SATO-DAHLMAN, M. & YAMAMOTO, M. 2018. The development of oncolytic adenovirus therapy in the past and future-for the case of pancreatic cancer. *Current cancer drug targets*, 18, 153-161.
- SCHERZ-SHOVAL, R. & ELAZAR, Z. 2007. ROS, mitochondria and the regulation of autophagy. *Trends in cell biology*, 17, 422-427.
- SCHULZ, H., SCHMOECKEL, E., KUHN, C., HOFMANN, S., MAYR, D., MAHNER, S. & JESCHKE, U. 2017. Galectins-1,-3, and-7 are prognostic markers for survival of ovarian cancer patients. *International journal of molecular sciences*, 18, 1230.
- SHAFREN, D. R., SYLVESTER, D., JOHANSSON, E. S., CAMPBELL, I. G. & BARRY, R. D. 2005. Oncolysis of human ovarian cancers by echovirus type 1. *International journal of cancer*, 115, 320-328.
- SHOEMAKER, R. H. 2006. The NCI60 human tumour cell line anticancer drug screen. *Nature Reviews Cancer*, 6, 813-823.
- SHORT, B. 2018. A cell-free screen of caveolae interactions. *The Journal of Cell Biology*, 217, 1883.
- SILVA, J. M., MARRAN, K., PARKER, J. S., SILVA, J., GOLDING, M., SCHLABACH, M. R., ELLEDGE, S. J., HANNON, G. J. & CHANG, K.

2008. Profiling essential genes in human mammary cells by multiplex RNAi screening. *science*, 319, 617-620.
- SIMMONS JR, G. E., TAYLOR, H. E. & HILDRETH, J. E. 2012. Caveolin-1 suppresses Human Immunodeficiency virus-1 replication by inhibiting acetylation of NF- $\kappa$ B. *Virology*, 432, 110-119.
- SINGH, B., FLEURY, C., JALALVAND, F. & RIESBECK, K. 2012. Human pathogens utilize host extracellular matrix proteins laminin and collagen for adhesion and invasion of the host. *FEMS microbiology reviews*, 36, 1122-1180.
- SINGH, M., JADHAV, H. R. & BHATT, T. 2017. Dynamin functions and ligands: classical mechanisms behind. *Molecular pharmacology*, 91, 123-134.
- SPRINGFELD, C., VON MESSLING, V., FRENZKE, M., UNGERECHTS, G., BUCHHOLZ, C. J. & CATTANEO, R. 2006. Oncolytic efficacy and enhanced safety of measles virus activated by tumor-secreted matrix metalloproteinases. *Cancer research*, 66, 7694-7700.
- STOJDL, D. F., LICHTY, B., KNOWLES, S., MARIUS, R., ATKINS, H., SONENBERG, N. & BELL, J. C. 2000. Exploiting tumor-specific defects in the interferon pathway with a previously unknown oncolytic virus. *Nature medicine*, 6, 821-825.
- SUIKKANEN, S., AALTONEN, T., NEVALAINEN, M., VÄLILEHTO, O., LINDHOLM, L., VUENTO, M. & VIHINEN-RANTA, M. 2003. Exploitation of microtubule cytoskeleton and dynein during parvoviral traffic toward the nucleus. *Journal of virology*, 77, 10270-10279.
- SUIKKANEN, S., SÄÄJÄRVI, K., HIRSIMÄKI, J., VÄLILEHTO, O., REUNANEN, H., VIHINEN-RANTA, M. & VUENTO, M. 2002. Role of recycling endosomes and lysosomes in dynein-dependent entry of canine parvovirus. *Journal of virology*, 76, 4401-4411.
- SWANSON, J. A. & WATTS, C. 1995. Macropinocytosis. *Trends in cell biology*, 5, 424-428.
- TATTERSALL, P., CAWTE, P., SHATKIN, A. & WARD, D. 1976. Three structural polypeptides coded for by minute virus of mice, a parvovirus. *Journal of Virology*, 20, 273-289.
- TOOLAN, H. W. 1961. A virus associated with transplantable human tumors. *Bulletin of the New York Academy of Medicine*, 37, 305.
- TOOLAN, H. W., DALLDORE, G., BARCLAY, M., CHANDRA, S. & MOORE, A. E. 1960. An unidentified, filtrable agent isolated from transplanted human tumors. *Proceedings of the National Academy of Sciences of the United States of America*, 46, 1256.

- TOOLAN, H. W., SAUNDERS, E. L., SOUTHAM, C. M., MOORE, A. E. & LEVIN, A. G. 1965. H-1 Virus Viremia in the Human. *Proceedings of the Society for Experimental Biology and Medicine*, 119, 711-715.
- UNGERECHTS, G., ENGELAND, C. E., BUCHHOLZ, C. J., EBERLE, J., FECHNER, H., GELETNEKY, K., HOLM, P. S., KREPPPEL, F., KUHNEL, F., LANG, K. S., LEBER, M. F., MARCHINI, A., MOEHLER, M., MUHLEBACH, M. D., ROMMELAERE, J., SPRINGFELD, C., LAUER, U. M. & NETTELBECK, D. M. 2017. Virotherapy Research in Germany: From Engineering to Translation. *Hum Gene Ther*, 28, 800-819.
- VAN DEN BRULE, F., CASTRONOVO, V., MENARD, S., GIAVAZZI, R., MARZOLA, M., BELOTTI, D. & TARABOLETTI, G. 1996. Expression of the 67 kD laminin receptor in human ovarian carcinomas as defined by a monoclonal antibody, MLuC5. *European Journal of Cancer*, 32, 1598-1602.
- VANLANDINGHAM, P. A. & CERESA, B. P. 2009. Rab7 regulates late endocytic trafficking downstream of multivesicular body biogenesis and cargo sequestration. *Journal of Biological Chemistry*, 284, 12110-12124.
- VASTA, G. R., AHMED, H., BIANCHET, M. A., FERNÁNDEZ-ROBLEDO, J. A. & AMZEL, L. M. 2012a. Diversity in recognition of glycans by F-type lectins and galectins: molecular, structural, and biophysical aspects. *Annals of the New York Academy of Sciences*, 1253, E14.
- VASTA, G. R., AHMED, H., NITA-LAZAR, M., BANERJEE, A., PASEK, M., SHRIDHAR, S., GUHA, P. & FERNÁNDEZ-ROBLEDO, J. A. 2012b. Galectins as self/non-self recognition receptors in innate and adaptive immunity: an unresolved paradox. *Frontiers in immunology*, 3, 199.
- VENDEVILLE, A., RAVALLEC, M., JOUSSET, F.-X., DEVISE, M., MUTUEL, D., LÓPEZ-FERBER, M., FOURNIER, P., DUPRESSOIR, T. & OGLIASTRO, M. 2009. Densovirus infectious pathway requires clathrin-mediated endocytosis followed by trafficking to the nucleus. *Journal of virology*, 83, 4678-4689.
- VERSCHUERE, T., VAN WOENSEL, M., FIEUWS, S., LEFRANC, F., MATHIEU, V., KISS, R., VAN GOOL, S. W. & DE VLEESCHOUWER, S. 2013. Altered galectin-1 serum levels in patients diagnosed with high-grade glioma. *Journal of neuro-oncology*, 115, 9-17.
- VIHINEN-RANTA, M., KALELA, A., MÄKINEN, P., KAKKOLA, L., MARJOMÄKI, V. & VUENTO, M. 1998. Intracellular route of canine parvovirus entry. *Journal of virology*, 72, 802-806.
- VIHINEN-RANTA, M., WANG, D., WEICHERT, W. S. & PARRISH, C. R. 2002. The VP1 N-terminal sequence of canine parvovirus affects nuclear transport of capsids and efficient cell infection. *Journal of virology*, 76, 1884-1891.

- VIHINEN-RANTA, M., YUAN, W. & PARRISH, C. R. 2000. Cytoplasmic trafficking of the canine parvovirus capsid and its role in infection and nuclear transport. *Journal of virology*, 74, 4853-4859.
- VIHINEN-RANTA, M., KAKKOLA, L., KALELA, A., VILJA, P. & VUENTO, M. 1997. Characterization of a nuclear localization signal of canine parvovirus capsid proteins. *European journal of biochemistry*, 250, 389-394.
- VON KLEIST, L., STAHLSCHMIDT, W., BULUT, H., GROMOVA, K., PUCHKOV, D., ROBERTSON, M. J., MACGREGOR, K. A., TOMILIN, N., PECHSTEIN, A. & CHAU, N. 2011. Role of the clathrin terminal domain in regulating coated pit dynamics revealed by small molecule inhibition. *Cell*, 146, 471-484.
- WANG, L.-H., ROTHBERG, K. G. & ANDERSON, R. 1993. Mis-assembly of clathrin lattices on endosomes reveals a regulatory switch for coated pit formation. *The Journal of cell biology*, 123, 1107-1117.
- WANG, W.-H., LIN, C.-Y., CHANG, M. R., URBINA, A. N., ASSAVALAPSAKUL, W., THITITHANYANONT, A., CHEN, Y.-H., LIU, F.-T. & WANG, S.-F. 2019. The role of galectins in virus infection-A systemic literature review. *Journal of Microbiology, Immunology and Infection*.
- WEISS, N., STROH-DEGE, A., ROMMELAERE, J., DINSART, C. & SALOMÉ, N. 2012. An in-frame deletion in the NS protein-coding sequence of parvovirus H-1PV efficiently stimulates export and infectivity of progeny virions. *Journal of virology*, 86, 7554-7564.
- WEITZMAN, M. D. 2006. The parvovirus life cycle: an introduction to molecular interactions important for infection. *Parvoviruses; Kerr, JR, Cotmore, SF, Bloom, ME, Linden, RM, Parrish, CR, Eds*, 143-156.
- WICKHAM, T. J., FILARDO, E. J., CHERESH, D. A. & NEMEROW, G. R. 1994. Integrin alpha v beta 5 selectively promotes adenovirus mediated cell membrane permeabilization. *The Journal of cell biology*, 127, 257-264.
- WICKHAM, T. J., MATHIAS, P., CHERESH, D. A. & NEMEROW, G. R. 1993. Integrins  $\alpha\beta 3$  and  $\alpha\beta 5$  promote adenovirus internalization but not virus attachment. *Cell*, 73, 309-319.
- WILDEN, H., FOURNIER, P., ZAWATZKY, R. & SCHIRRMACHER, V. 2009. Expression of RIG-I, IRF3, IFN- $\beta$  and IRF7 determines resistance or susceptibility of cells to infection by Newcastle Disease Virus. *International journal of oncology*, 34, 971-982.
- WILSON, G. M., JINDAL, H. K., YEUNG, D. E., CHEN, W. & ASTELL, C. R. 1991. Expression of minute virus of mice major nonstructural protein in insect cells: purification and identification of ATPase and helicase activities. *Virology*, 185, 90-98.
- WILSON, J. M., DE HOOP, M., ZORZI, N., TOH, B.-H., DOTTI, C. G. & PARTON, R. G. 2000. EEA1, a tethering protein of the early sorting endosome, shows a



- polarized distribution in hippocampal neurons, epithelial cells, and fibroblasts. *Molecular biology of the cell*, 11, 2657-2671.
- WILSON, T. G., FIRTH, M. N., POWELL, J. T. & HARRISON, F. L. 1989. The sequence of the mouse 14 kDa  $\beta$ -galactoside-binding lectin and evidence for its synthesis on free cytoplasmic ribosomes. *Biochemical Journal*, 261, 847-852.
- WU, R., WU, T., WANG, K., LUO, S., CHEN, Z., FAN, M., XUE, D., LU, H., ZHUANG, Q. & XU, X. 2018. Prognostic significance of galectin-1 expression in patients with cancer: a meta-analysis. *Cancer cell international*, 18, 108.
- YANG, M.-L., CHEN, Y.-H., WANG, S.-W., HUANG, Y.-J., LEU, C.-H., YEH, N.-C., CHU, C.-Y., LIN, C.-C., SHIEH, G.-S. & CHEN, Y.-L. 2011. Galectin-1 binds to influenza virus and ameliorates influenza virus pathogenesis. *Journal of virology*, 85, 10010-10020.
- YOSHIMORI, T., YAMAMOTO, A., MORIYAMA, Y., FUTAI, M. & TASHIRO, Y. 1991. Bafilomycin A1, a specific inhibitor of vacuolar-type H (+)-ATPase, inhibits acidification and protein degradation in lysosomes of cultured cells. *Journal of Biological Chemistry*, 266, 17707-17712.
- ZÁDORI, Z., SZELEI, J., LACOSTE, M.-C., LI, Y., GARIÉPY, S., RAYMOND, P., ALLAIRE, M., NABI, I. R. & TIJSSEN, P. 2001. A viral phospholipase A2 is required for parvovirus infectivity. *Developmental cell*, 1, 291-302.
- ZÁDORI, Z., SZELEI, J. & TIJSSEN, P. 2005. SAT: a late NS protein of porcine parvovirus. *Journal of virology*, 79, 13129-13138.
- ZHANG, Y.-N., LIU, Y.-Y., XIAO, F.-C., LIU, C.-C., LIANG, X.-D., CHEN, J., ZHOU, J., BALOCH, A. S., KAN, L. & ZHOU, B. 2018. Rab5, Rab7, and Rab11 are required for Caveola-dependent endocytosis of classical swine fever virus in porcine alveolar macrophages. *Journal of virology*, 92, e00797-18.
- ZHOU, Y., WEN, F., ZHANG, P., TANG, R. & LI, Q. 2016. Vesicular stomatitis virus is a potent agent for the treatment of malignant ascites. *Oncology reports*, 35, 1573-1581.

# Appendix

## Research article published (Appendix 1)

**Ferreira, T.**, Kulkarni, A., Bretscher, C., Richter, K., Ehrlich, M., & Marchini, A. (2020). Oncolytic H-1 Parvovirus Enters Cancer Cells through Clathrin-Mediated Endocytosis. *Viruses*, *12*(10), 1199.

## Review article published (Appendix 2)

Angelova, A., **Ferreira, T.**, Bretscher, C., Rommelaere, J., & Marchini, A. (2021). Parvovirus-based combinatorial immunotherapy: a reinforced therapeutic strategy against poor-prognosis solid cancers. *Cancers*, *13*(2), 342.

## Research article accepted for publication

Kulkarni, A., **Ferreira, T.**, Bretscher, C., Grewenig, A., El-Andaloussi, N., Bonifati, S., Marttila, T., Palissot, V., Hossain, J., Azuaje, F., Miletic, H., Ystaas, L., Golebiewska, A., Niclou, S., Roeth, R., Niesler, B., Weiss, A., Brino, L. & Marchini, A. (2021). Oncolytic H-1 parvovirus binds to sialic acid on laminins for cell attachment and entry. *Nature communications*. In press.

## Research article ready to be submitted

**Ferreira, T.**, Kulkarni, A., Bretscher, C., Hossain, J., Azuaje, F., Miletic, H., Ystaas, L. & Marchini, A. (2021). Galectin-1 Plays a Role in Oncolytic H-1 Parvovirus Infection. *To be submitted to a peer-reviewed journal*.



Article

# Oncolytic H-1 Parvovirus Enters Cancer Cells through Clathrin-Mediated Endocytosis

Tiago Ferreira <sup>1</sup>, Amit Kulkarni <sup>2</sup>, Clemens Bretscher <sup>1</sup>, Karsten Richter <sup>3</sup>, Marcelo Ehrlich <sup>4</sup> and Antonio Marchini <sup>1,2,\*</sup>

<sup>1</sup> Laboratory of Oncolytic Virus Immuno-Therapeutics, German Cancer Research Centre, Im Neuenheimer Feld 242, 69120 Heidelberg, Germany; t.ferreira@dkfz.de (T.F.); c.bretscher@dkfz.de (C.B.)

<sup>2</sup> Laboratory of Oncolytic Virus Immuno-Therapeutics, Luxembourg Institute of Health, 84 Val Fleuri, L-1526 Luxembourg, Luxembourg; amit.kulkarni@lih.lu

<sup>3</sup> Core Facility Electron Microscopy, German Cancer Research Centre, Im Neuenheimer Feld 280, 69120 Heidelberg, Germany; k.richter@dkfz-heidelberg.de

<sup>4</sup> Laboratory of Signal Transduction and Membrane Biology, The Shumins School for Biomedicine and Cancer Research, George S. Wise Faculty of Life Sciences, Tel Aviv University, 69978 Tel Aviv, Israel; marceloe@post.tau.ac.il

\* Correspondence: a.marchini@dkfz.de or antonio.marchini@lih.lu; Tel.: +49-6221-424969 or +352-26-970-856

Received: 8 October 2020; Accepted: 19 October 2020; Published: 21 October 2020



**Abstract:** H-1 protoparvovirus (H-1PV) is a self-propagating virus that is non-pathogenic in humans and has oncolytic and oncosuppressive activities. H-1PV is the first member of the *Parvoviridae* family to undergo clinical testing as an anticancer agent. Results from clinical trials in patients with glioblastoma or pancreatic carcinoma show that virus treatment is safe, well-tolerated and associated with first signs of efficacy. Characterisation of the H-1PV life cycle may help to improve its efficacy and clinical outcome. In this study, we investigated the entry route of H-1PV in cervical carcinoma HeLa and glioma NCH125 cell lines. Using electron and confocal microscopy, we detected H-1PV particles within clathrin-coated pits and vesicles, providing evidence that the virus uses clathrin-mediated endocytosis for cell entry. In agreement with these results, we found that blocking clathrin-mediated endocytosis using specific inhibitors or small interfering RNA-mediated knockdown of its key regulator, AP2M1, markedly reduced H-1PV entry. By contrast, we found no evidence of viral entry through caveolae-mediated endocytosis. We also show that H-1PV entry is dependent on dynamin, while viral trafficking occurs from early to late endosomes, with acidic pH necessary for a productive infection. This is the first study that characterises the cell entry pathways of oncolytic H-1PV.

**Keywords:** oncolytic viruses; rodent protoparvovirus H-1PV; virus entry; clathrin-mediated endocytosis

## 1. Introduction

The rodent H-1 protoparvovirus (H-1PV) belongs to the *Parvoviridae* family, genus *Protoparvovirus* [1]. This genus also includes *Rodent protoparvovirus 1* (H-1PV, Kilham rat virus, LuIII virus, minute virus of mice (MVM), mouse parvovirus, tumour virus X, rat minute virus), *Rodent protoparvovirus 2* (rat parvovirus 1), *Carnivore protoparvovirus 1* (canine parvovirus (CPV) and feline panleukopenia parvovirus (FPV)), *Primate protoparvovirus 1* (bufavirus) and *Ungulate parvovirus 1* (porcine parvovirus (PPV)) [2,3]. Protoparvoviruses (PtPVs) are single-stranded DNA viruses with an icosahedral capsid of about 25 nm diameter. Their genomes encompass the non-structural (NS) and the viral particle (VP) transcriptional units, whose expressions are regulated by the P4 and P38 promoters, respectively. The NS transcriptional unit encodes the NS1 and NS2 proteins, whereas the VP transcriptional unit encodes the VP1 and VP2 capsid proteins and the small alternatively translated protein [4].

Owing to their ability to specifically infect, replicate and kill human cancer cells, rodent PtPVs are under investigation as potential anticancer therapies. Pre-clinical studies have revealed that H-1PV in particular has remarkable oncolytic and oncosuppressive activity in a number of cell culture and animal models of cancers from different origins [5]. Notably, H-1PV-induced cancer cell death and lysis are immunogenic and stimulate the immune system to participate in the elimination of cancer cells [6]. NS1 is the major effector of H-1PV oncototoxicity [7].

Although viral oncolytic activity is shared between rodent PtPVs, H-1PV is the only member of the genus to have reached the clinic as an anticancer therapy. In a phase I/IIa clinical trial in patients with recurrent glioblastoma (ParvOryx01), H-1PV treatment was safe, well-tolerated and associated with first evidence of anticancer efficacy. This evidence included the ability of H-1PV to cross the blood–brain barrier after intravenous administration, its wide distribution in the tumour bed, the induction of tumour necrosis and immuno-conversion of the tumour microenvironment. As a result, virus treatment led to an improved progression-free survival and median overall survival of patients in comparison with historical controls [8]. A dose-escalation phase I/IIa pilot study in patients with metastatic pancreatic cancer recently confirmed the excellent safety and tolerability of H-1PV treatment. In accordance with the results of ParvOryx01, patients who responded to the treatment showed evident changes in the tumour microenvironment and induction of specific immune responses [9].

The PtPV life cycle is strictly dependent on host cellular factors for a productive infection, from cell surface attachment and entry to virus DNA replication, gene expression, multiplication and egress. Some of these factors are frequently overexpressed or dysregulated in cancer cells. The list includes cell cycle regulators, transcription factors, modulators of the DNA damage response, kinases and cytoskeleton components (reviewed in Reference [10]). However, unlike for other PtPVs, the early steps of H-1PV infection remain to be characterised.

The first interaction between PtPVs and the target cell occurs through binding to a specific surface receptor exposed on the host plasma membrane. Cellular receptors for some PtPVs have been described, such as the transferrin receptor for CPV and FPV. H-1PV, like MVM and PPV, uses sialic acid (SA) for cell surface attachment and entry. However, it is unclear whether SA itself acts as a functional viral receptor for the virus or is a component of an as yet unidentified receptor(s) or receptor complex [3,11,12].

After docking to the cellular membrane, viruses are internalised through different pathways [13]. Clathrin- and caveolae-mediated endocytosis are two dynamin-dependent pathways, whereas macropinocytosis, lipid-raft-mediated endocytosis and caveolae/clathrin-independent endocytosis are dynamin-independent pathways [14,15]. Clathrin-mediated endocytosis is the pathway commonly used by small viruses, including PtPVs [16–20]. The mechanism begins with the recruitment of adaptor protein 2 (AP-2) complexes on the plasma membrane, followed by the assembly of a three-dimensional clathrin coat that leads to a progressive invagination of the membrane. Dynamin self-assembles around the vesicle neck and mediates its scission, and the vesicle is subsequently released into the interior of the cell [21].

PtPVs also use alternative endocytic pathways. For instance, MVM prototype strain takes at least three different endocytic routes: clathrin-, caveolae- and clathrin-independent carrier-mediated endocytosis [22]. Even though endocytosis seems to be the default entry pathway for PtPVs, differences between members of the family may contribute to the tropism of these viruses.

As the PtPV is trafficked within the cellular endosome, its capsid undergoes slow structural changes. In particular, the acidic environment exposes the catalytic phospholipase 2 domain of VP1. This conformational change promotes the digestion of the endosomal membrane, resulting in the release of viral particles from the late endosome to the cytosol [3]. Thereafter, incoming PtPV particles are transported to the nucleus in a process that is dependent on the cytoskeleton and associated motor proteins [23].

In this study, we used electron microscopy (EM) and immunofluorescence (IF), together with a number of chemical inhibitors and siRNA-mediated knockdown, to identify which of these pathways H-1PV uses to enter cancer cells. We found that H-1PV cell uptake occurs preferentially through clathrin-mediated, but not caveolae-mediated, endocytosis in cervical carcinoma HeLa and glioma NCH125 cell lines. Entry was also dependent on dynamin activity. We show that after its internalisation, H-1PV, like other PtPVs, passes through early endosomes to late endosomes/lysosomes during its cytosolic trafficking. Productive infection relies heavily on the acidic pH in the endosomes.

## 2. Materials and Methods

### 2.1. Cells and Viruses

The cervical carcinoma-derived HeLa [7] and the glioblastoma-derived NCH125 cell lines [24] were cultured in Dulbecco's modified Eagle's medium (DMEM) supplemented with 10% FBS, 100 units/mL penicillin, 100 µg/mL streptomycin and 2 mM L-glutamine (all from Gibco, Thermo Fischer Scientific, Darmstadt, Germany) in a humidified incubator at 37 °C. Both cell lines were tested for mycoplasma contamination by PCR in a regular base.

Both wild-type H-1PV and recombinant H-1PV harbouring the green fluorescent protein-encoding gene (rech-1PV-EGFP) were produced, purified and titrated as previously described [25,26].

### 2.2. Electron Microscopy

HeLa cells were seeded on punched sheets of ACLAR-Fluoropolymer films (Electron Microscopy Sciences) at a density of  $8 \times 10^4$  cells/well in 24-well plates. On the following day, cells were infected with H-1PV at a multiplicity of infection (MOI) of 2000 plaque forming units (pfu) per cell in DMEM 5% FBS at 4 °C for 1 h to allow virus attachment to the cell surface and promote a synchronised infection. In order to catch the internalisation event, cells were shifted to 37 °C for 0, 5, 10, 20 and 30 min. After incubation, ACLAR-Fluoropolymer films were embedded in epoxy resin for ultrathin sectioning according to standard procedures. Briefly, chemical fixation was carried out in buffered aldehyde (4% formaldehyde, 2% glutaraldehyde, 1 mM CaCl<sub>2</sub>, 1 mM MgCl<sub>2</sub> in 100 mM Ca-cacodylate, pH 7.2), followed by post-fixation in buffered 1% osmium tetroxide and en bloc staining in 1% uranylacetate. Following dehydration in graded steps of ethanol, the adherent cells were flat-embedded in epoxy resin (mixture of glycid ether, methyladnic anhydride and dodeceny succinic-anhydride; Serva). Ultrathin sections of nominal thickness 60 nm and contrast-stained with lead-citrate and uranylacetate were analysed using a Zeiss EM 910 (Carl Zeiss, Oberkochen, Germany) at 120 kV and micrographs taken using a slow scan charge-coupled device camera (TRS, Olympus, Moorenweis, Germany).

### 2.3. Co-Localisation of H-1PV and Cellular Proteins by Confocal Microscopy

HeLa cells were seeded at a density of  $3.5 \times 10^3$  cells/spot on spot slides and grown in 50 µL of complete cellular medium. On the following day, cells were placed on ice for 15 min and then infected with wild-type H-1PV at a MOI of 500 (pfu/cell) in a total of 70 µL of 5% FCS-containing medium. At 1 h post-infection, cells were shifted to 37 °C for varied times depending on the experiment, before being fixed with 3.7% paraformaldehyde on ice for 15 min and permeabilised with 1% Triton X-100 for 10 min. Immunostaining was carried out with the following antibodies, all used at dilution 1:500 for 1 h: mouse monoclonal anti-H-1PV capsid (a conformational antibody kindly provided by Barbara Leuchs; DKFZ Virus Production and Development Unit, Heidelberg, Germany) [27], rabbit monoclonal anti-clathrin heavy chain (D3C6; Cell Signalling Technology, Leiden, Netherlands), rabbit monoclonal anti-EEA1 (3288; Cell Signalling Technology), rabbit monoclonal anti-Rab7 (93671; Cell Signalling Technology) and rabbit polyclonal anti-LAMP-1 (CD107a) (AB2971; Merck, Darmstadt, Germany). Anti-mouse Alexa Fluor 594 IgG (A11005; Thermo Fisher Scientific, Bleiswijk, Netherlands) or anti-rabbit Alexa Fluor 488 IgG (A11008; Thermo Fisher Scientific) were used as secondary antibodies. Nuclei were stained by 4',6-diamidin-2-phenylindol (DAPI). Images in the green channel (H-1PV), red channel

(varied cellular proteins) or blue channel (DAPI) were acquired with a confocal microscope (Leica TCS SP5 II, Wetzlar, Germany). Picture analysis was carried out using the Leica LAS X Software.

#### 2.4. Treatment with Inhibitors of Endocytosis Pathways

Hypertonic sucrose (Carl Roth), 0.40 M, chlorpromazine (Sigma-Aldrich Chemie GmbH, Steinheim, Germany), 2.5 µg/mL for HeLa or 5 µg/mL for NCH125, and pitstop 2 (Sigma-Aldrich Chemie GmbH), 30 µM, were used to inhibit clathrin-mediated endocytosis. Dynole™ Series Kit containing Dynole 31–2 (active drug) and 34–2 (negative control) (ab120474; Abcam, Cambridge, UK), 5 µM, were used to inhibit dynamin activity. Bafilomycin A1 (BafA1; Cell Signalling Technology), 10 nM, and ammonium chloride (NH<sub>4</sub>Cl; 1145, Merck), 25 mM, were used to prevent pH acidification. The concentrations of the aforementioned inhibitors were used at the highest doses before affecting the cellular proliferation. Nystatin (Sigma-Aldrich), 10 µg/mL, and methyl-β-cyclodextrin (MβCD; Sigma-Aldrich Chemie GmbH), 10 mM, were used to inhibit caveolae-mediated endocytosis. These concentrations were selected according to the literature [28,29] and also did not affect the proliferation of the cell lines used for the experiments.

Briefly, HeLa cells were seeded at a density of  $8 \times 10^4$  cells/well in 24-well plates and, on the following day, pre-treated for 45 min with the various inhibitors. Cells were then infected with recH-1PV-EGFP at a MOI of 0.2–0.3 transduction units (TU)/cell for 4 h, washed twice with PBS and grown in culture medium for an additional 20 h. At 24 h post-infection, cells were washed once with PBS, fixed with 3.7% paraformaldehyde on ice for 15 min, permeabilised with 1% Triton X-100 for 10 min and stained with DAPI. Fluorescence images of EGFP-positive cells were acquired with a BZ-9000 fluorescence microscope (Keyence Corporation, Osaka, Japan) with 4X or 10X objective. DAPI staining was used to visualise the nuclei (cells). At least two independent experiments, each performed in duplicate, were performed for every condition tested.

#### 2.5. Cell Proliferation Assay

Cell proliferation was monitored in real time through the xCELLigence system (ACEA Biosciences Inc., San Diego, CA, USA) according to the manufacturer's instructions. Briefly,  $8 \times 10^4$  HeLa or NCH125 cells per well were seeded in a 96-well E-plate (Roche) in a total volume of 100 µL of complete DMEM medium. On the following day, cells were treated with different inhibitors for 45 min, and subsequently washed with PBS. Cell proliferation was monitored every 30 min in real time over a period of 72 h. Data is expressed as "Normalised cell index", where all curves were normalised to an arbitrary value of 1.0 at the timepoint before treatment. Average values of each experimental condition assessed in triplicate are presented with the respective standard deviation (SD).

#### 2.6. siRNA-Mediated Knockdown

Cells were seeded at a density of  $4 \times 10^4$  cells/well in a 24-well plate and grown in 500 µL of normal growth medium. After 24 h, cells were transfected with 10 nM siRNA using Lipofectamine RNAiMAX (Thermo Fisher Scientific, Carlsbad, CA, USA) according to the manufacturer's instructions. For *AP2M1*, we used the *AP2M1* ON-TARGET plus Human siRNA SMARTpool (L-008170-00-0005) and, as a negative control, the plus Non-targeting pool (D-001810-10-05) (Dharmacon, Thermo Fisher Scientific). For *CAV-1*, we used two Silencer Select Validated siRNAs (s2446 and s2448; Life Technologies, Paisley, Scotland) and Silencer Select Negative Control #2 siRNA (4390846, Life Technologies) as a control. After 24 h, the medium was replaced, and cells were grown for an additional 24 h to allow efficient gene silencing. The cells were then infected for 24 h with recH-1PV-EGFP at 0.2–0.3 TU/cell. Cells were then washed once with PBS and processed as described above for fluorescence microscopy. At least two independent experiments, each performed in duplicate, were performed for every condition tested.

### 2.7. Western Blotting

Cells were harvested, washed in PBS, and then lysed on ice for 30 min in RIPA buffer (10 mM Tris-HCl pH 7.5, 150 mM NaCl, 1 mM EDTA pH 8, 1% NP-40, 0.5% Na-deoxycholate and 0.5% SDS supplemented with complete EDTA-free protease inhibitor (11697498001; Roche, Mannheim, Germany). Cellular debris was removed by centrifugation, and protein concentration in cell lysates was measured by bicinchoninic acid (BCA) assay (Thermo Fisher Scientific), according to manufacturer's instructions. SDS-PAGE analysis was performed on 50 µg of total protein extract. After separation, proteins were transferred to Hybond-P membrane (GE Healthcare, Freiburg, Germany). Immunoblotting was carried out with the following antibodies: mouse monoclonal anti-vinculin (sc-25336; Santa Cruz Biotechnology, Heidelberg, Germany) and rabbit monoclonal CAV-1 (D46G3; Cell Signalling Technology) at 1:1000 dilution. After incubation with horseradish peroxidase conjugated secondary antibodies (Santa Cruz Biotechnology) at 1:1000 dilution, proteins were revealed with Western Blot Chemiluminescence Reagent *Plus* (Perkin Elmer Life Sciences) and exposed to Hyperfilm™ ECL radiographic films (GE Healthcare).

## 3. Results

### 3.1. Electron Microscopy Analysis Reveals H-1PV within Clathrin-Coated Pits

In order to investigate the H-1PV internalisation pathway, we performed EM analysis of HeLa cells infected with H-1PV. Infection was carried out at 4 °C for 1 h to allow virus cell surface binding. Cells were then shifted back to 37 °C for various intervals to allow virus internalisation. EM analysis of infected cells at 4 °C showed the virus at the cell surface bound to thickened regions resembling clathrin-associated plasma membrane (Figure 1A) [30]. In the first 5 min after cells were shifted back to 37 °C, the invagination of clathrin-rich regions started with H-1PV particles remaining associated with these regions (Figure 1B). From 10 to 30 min, viral particles were detected both in clathrin-coated pits (Figure 1C) or in the cytosol inside completely invaginated vesicles (we found up to nine particles in a single vesicle) (Figure 1D). Furthermore, in the course of the experiment, no virus internalisation was found in vesicles with the small flask-shaped invaginations that are characteristic of caveolae-mediated endocytosis [31], which suggests that H-1PV is internalised mainly (if not exclusively) via clathrin-mediated endocytosis.

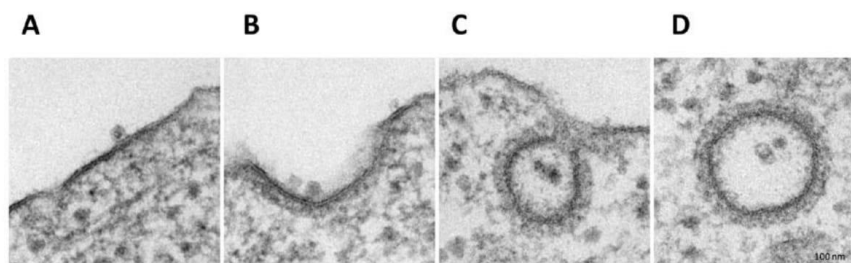


**Figure 1.** Endocytosis of H-1PV is clathrin-dependent. HeLa cells were infected with H-1PV for 1 h at 4 °C to allow H-1PV cell surface attachment but not entry. Cells were then shifted to 37 °C to allow H-1PV cell internalisation. Cells were collected every 5 min for a total of 30 min and processed for EM analysis. (A) At 4 °C, H-1PV particles are found attached to electro-dense (clathrin-rich) regions on the plasma membrane. (B) In the first 5 min after release at 37 °C, H-1PV particles are detected in early-forming clathrin-coated pits. (C) From 10 to 30 min, H-1PV particles moved into the cells within deeply invaginated clathrin-coated pits that were still connected to the plasma membrane, forming an hourglass-like membrane neck. (D) Later in the infection (10–30 min at 37 °C), H-1PV particles are seen being trafficked within the cell inside clathrin-coated vesicles.

### 3.2. H-1PV Co-Localises with Clathrin Upon Entry

The EM analysis provided first evidence that H-1PV uses clathrin-mediated endocytosis to enter cells. To confirm these results independently, we checked for possible co-localisation of H-1PV and clathrin-heavy chain (CHC). To this end, HeLa cells were infected with H-1PV for 1 h at 4 °C and then shifted back to 37 °C. After 30 min, a fraction of internalised H-1PV was clearly detected in association with CHC by confocal microscopy (Figure 2), providing further evidence that H-1PV is internalised through a clathrin-dependent pathway.

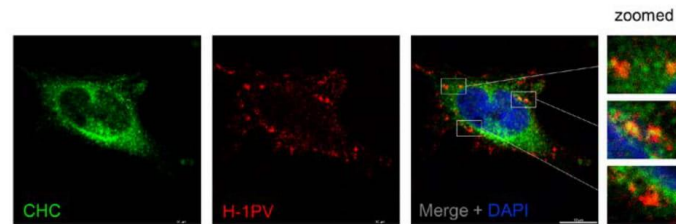


**Figure 2.** H-1PV co-localises with clathrin upon entry. HeLa cells were infected with H-1PV for 1 h at 4 °C and then shifted to 37 °C for 30 min before being processed for immunostaining using anti-H-1PV full capsid and anti-clathrin-heavy chain (CHC) antibodies. Cell nuclei were visualised by DAPI staining. Confocal microscopy analysis showed that H-1PV particles (Alexa Fluor 594, red) co-localised with CHC (Alexa Fluor 488, green) early upon infection. Three examples of regions where co-localisation is observed are framed by white boxes and shown zoomed in.

### 3.3. H-1PV Enters Cells Preferentially via Clathrin-Mediated Endocytosis

Next, we investigated whether targeting regulators of clathrin-mediated endocytosis would affect H-1PV infection. A recombinant H-1PV expressing the EGFP reporter gene (recH-1PV-EGFP) was used for the experiments. This non-replicative parvovirus shares the same capsid of the wild type but harbours the EGFP gene under the control of the natural P38 late promoter, whose activity is regulated by NS1 viral protein [25]. Therefore, the EGFP signal directly correlates to the ability of the virus to reach the nucleus and initiate its own gene transcription.

The effects of various inhibitors on H-1PV entry were assessed in HeLa and in glioma-derived NCH125 cell lines. The latter, like HeLa, is highly permissive to H-1PV infection. Pharmacological inhibitors included hypertonic sucrose, chlorpromazine (CPZ) and pitstop 2. Hypertonic sucrose is a classical inhibitor that traps clathrin in microcages [32]. CPZ is a cationic, amphiphilic drug that induces the misassembly of clathrin lattices at the cell surface and on endosomes [33]. Pitstop 2 interferes with the binding of proteins to the N-terminal domain of clathrin [34]. The internalisation of TexasRed-labelled transferrin, a protein known to be exclusively internalised through clathrin-mediated endocytosis, was monitored to check the effectiveness of each treatment [35]. At the concentrations used, the three inhibitors blocked transferrin uptake efficiently but did not affect cell proliferation (Supplementary Figure S1).

Pre-treatment with hypertonic sucrose decreased H-1PV transduction by more than 90% in HeLa and 80% in NCH125 cells compared to untreated cells (Figure 3A,B). When the compound was applied 3 h post-infection (by which time the virus is already internalised), no significant changes in H-1PV transduction were observed, indicating that the drug interferes with H-1PV transduction at the level of virus entry (Supplementary Figure S2). Strong inhibition of H-1PV transduction was also achieved by pre-treating cells with CPZ (approximately 90% reduction in both cell lines) or with pitstop 2 (60% reduction in HeLa and over 70% in NCH125 cells) compared to untreated cells.



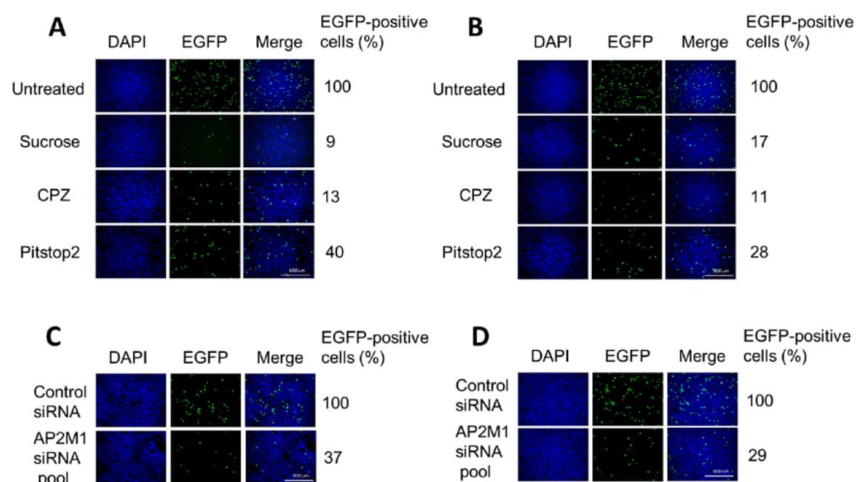


**Figure 3.** Blocking clathrin-mediated endocytosis results in a significant reduction of H-1PV transduction. (A) HeLa and (B) NCH125 cells were pre-treated with different clathrin-mediated endocytosis inhibitors (hypertonic sucrose, chlorpromazine (CPZ) or pitstop 2) or left untreated. Cells were then infected with recH-1PV-EGFP for 4 h in the presence of the inhibitor. At 20 h post-infection, cells were processed as described in the Materials and Methods (M&M) section. (C) HeLa and (D) NCH125 cells were transfected with a pool of siRNAs targeting either *AP2M1* or negative control. At 48 h post-transfection, cells were infected with recH-1PV-EGFP for 4 h and grown for an additional 20 h. Cells were then processed as described in the M&M section. Numbers represent the average percentage of EGFP-positive cells relative to the number of EGFP-positive cells observed in untreated or scrambled siRNA-transfected cells, which was arbitrarily set as 100%.

The AP-2 complex is a heterotetramer that plays an essential role in clathrin-mediated endocytosis [21]. To confirm the involvement of clathrin-mediated endocytosis in H-1PV cell entry, we silenced the expression of *AP2M1*, the gene encoding subunit  $\mu 1$  of AP-2 [36]. To this end, HeLa and NCH125 cells were transfected with either a siRNA pool targeting *AP2M1* or scrambled siRNA (negative control), and subsequently infected with recH-1PV-EGFP. Under conditions in which the silencing of *AP2M1* successfully reduced transferrin uptake, we observed a strong decrease in H-1PV transduction (over 60% compared to the scrambled siRNA-treated cells) in both cell lines (Figure 3C,D). Taken together, these results show that H-1PV uses clathrin-mediated endocytosis to enter HeLa and NCH125 cells.

#### 3.4. H-1PV Does Not Enter Cells via Caveolae-Dependent Endocytosis

To investigate whether H-1PV uses pathways other than clathrin-mediated endocytosis to enter HeLa and NCH125 cancer cells, we inhibited clathrin-independent endocytosis using nystatin and methyl- $\beta$ -cyclodextrin (M $\beta$ CD). Both drugs selectively disrupt lipid rafts (e.g., cholesterol), including those required for caveolae-dependent entry [28,29,37]. Yet, neither nystatin nor M $\beta$ CD decreased H-1PV transduction, providing evidence that the virus does not use this endocytic route to enter these cells (Figure 4A,B). Similar results were also obtained using the two drugs at lower or higher concentrations (0.1–100  $\mu$ g/mL for nystatin, 0.1–100  $\mu$ M for M $\beta$ CD). We also carried out siRNA-mediated knockdown of *CAV1* (which encodes for caveolin-1) by using two different siRNAs. Knock-down of *CAV1* gene expression did not decrease H-1PV transduction activity compared with scrambled siRNA-transfected cells, but instead increased it (Figure 4C,D). Together, these results indicate that caveolae-dependent endocytosis is not involved in H-1PV entry of HeLa and NCH125 cells.

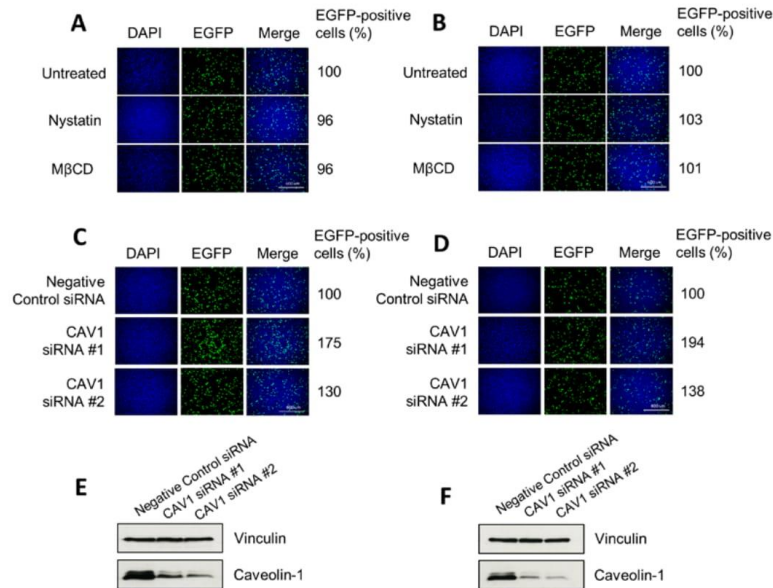


**Figure 4.** Disruption of clathrin-independent endocytosis does not decrease H-1PV transduction. (A) HeLa and (B) NCH125 cells were either pre-treated with cholesterol-sequestering drugs (nystatin or methyl- $\beta$  cyclodextrin (M $\beta$ CD)) for 45 min or left untreated. Cells were then infected with recH-1PV-EGFP for 4 h in the presence (or absence) of the inhibitor. At 20 h post-infection, cells were processed as described in the M&M section for immunofluorescence analysis. (C) HeLa and (D) NCH125 cells were transfected with siRNAs targeting *CAV1* or a negative control siRNA. At 48 h post-transfection, cells were infected with recH-1PV-EGFP for 4 h and grown for an additional 20 h. Cells were then processed as described in panel A. Numbers represent the average percentage of EGFP-positive cells relative to the number of EGFP-positive cells observed in untreated cells, which was arbitrarily set as 100%. The steady protein levels of caveolin-1 on lysates derived from (E) HeLa or (F) NCH125 siRNA-transfected cells were analysed by Western blotting. Vinculin was used as a loading control.

### 3.5. H-1PV Internalisation Is Dependent on Dynamin

Dynamin is a large GTPase with an essential role in cellular membrane fission for newly formed vesicles. It is therefore required for clathrin- and caveolae-mediated endocytosis but not for macropinocytosis [38]. We used the highly selective Dynole 34–2 to inhibit dynamin activity [39,40], and Dynole 31–2, its inactive form, as a negative control. At a concentration that blocked transferrin uptake, Dynole 34–2 drastically reduced virus transduction to just 8% in HeLa and 13% in NCH125 cells (Figure 5) compared to untreated cells. As expected, Dynole 31–2 did not have any significant effect on H-1PV transduction. These results demonstrate that dynamin plays an essential role in H-1PV infection.

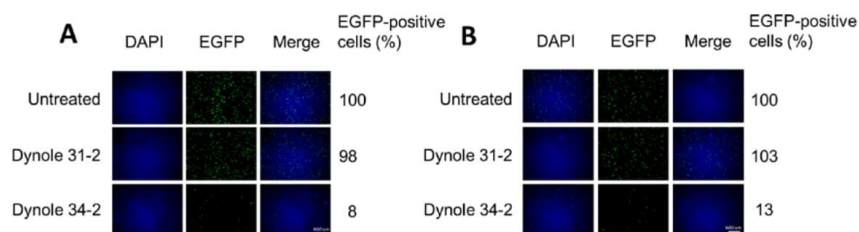


**Figure 5.** H-1PV requires dynamin activity for entry. (A) HeLa and (B) NCH125 cells were pre-treated with either Dynole 34-2 or its inactive form, Dynole 31-2. Cells were subsequently infected with reH-1PV-EGFP for 4 h in the presence of the inhibitor. At 20 h post-infection, cells were processed as described in Figure 4A. Numbers represent the average percentage of EGFP-positive cells relative to the number of EGFP-positive cells observed in untreated cells that was arbitrarily set as 100%.

### 3.6. H-1PV Hijacks Endosomes for Trafficking into the Cytosol and Acidic pH Is Required for Productive H-1PV Infection

The Rab family of proteins and their effectors play a key role in the formation, maintenance and trafficking of endosomes [41]. Early endosome antigen 1 (EEA1) is a Rab5 effector protein that is involved in sorting endocytic vesicles at the early endosome level [42]. Rab7 is considered to be the key regulator of late endosome trafficking. Lysosomal-associated membrane protein 1 (LAMP-1) is enriched in late endosomes and lysosomes, where, among other functions, it maintains lysosomal integrity and pH [43,44].

To provide direct evidence that H-1PV hijacks endocytosis for its intracellular trafficking, we infected HeLa cells with H-1PV for 1 h, fixed the cells, and then stained viral capsids as well as EEA1, Rab7 and LAMP-1 proteins with antibodies. Confocal microscopy analysis showed that H-1PV co-localised with EEA1, Rab7 and LAMP-1 markers during infection (Figure 6A).

Next, we hypothesised that the acidic pH in the endocytic compartments would provide the environmental conditions required for a productive H-1PV infection [3] (as it does for other P1PV infections), possibly triggering the conformational changes necessary for uncoating and nuclear translocation. To test whether low endosomal pH is required for H-1PV infection, we pre-treated HeLa and NCH125 cells with ammonium chloride ( $\text{NH}_4\text{Cl}$ ), a lysosomotropic weak base [45], or bafilomycin A1 (BafA1), a blocker of vacuolar  $\text{H}^+$ -ATPases [46]. Treatment with  $\text{NH}_4\text{Cl}$  resulted in a strong decrease of virus transduction in both HeLa and NCH125 cells (39% and 30%, respectively) (Figure 6B,C), while treatment with BafA1 completely abolished H-1PV transduction (Figure 6D,E), in comparison to untreated cells. Together, these results provide evidence that H-1PV, like other P1PVs, requires acidic endosomal pH for a productive infection.

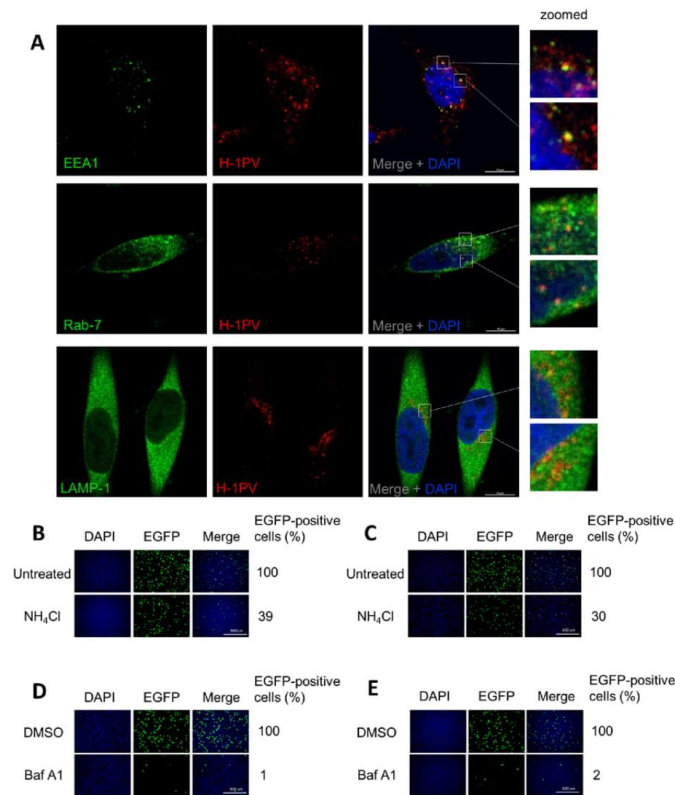


**Figure 6.** H-1PV trafficking occurs via the endosomal system with acidic pH being crucial for a productive infection. (A) HeLa cells were infected with H-1PV at MOI of 500 pfu/cell for 1 h at 4 °C and shifted to 37 °C for 30 min. Cells were then fixed, permeabilised and stained with DAPI and H-1PV capsid antibody, together with one of the endosomal markers (EEA1, Rab-7 or LAMP-1). Confocal microscopy analysis indicates that H-1PV particles (Alexa Fluor 594) co-localise with all three markers, EEA1, Rab-7 and LAMP-1 (Alexa Fluor 488), upon infection. Two examples of regions where co-localisation is observed are framed in white boxes and shown enlarged. (B,D) HeLa and (C,E) NCH125 cells were incubated with ammonium chloride (NH<sub>4</sub>Cl) or bafilomycin A1 (BafA1) respectively, for 45 min, or left untreated. Cells were subsequently infected with recH-1PV-EGFP for 4 h in the presence of the inhibitor. At 20 h post-infection, cells were processed as described in the M&M section. Numbers represent the average percentage of EGFP-positive cells relative to the number of EGFP-positive cells observed in untreated cells, which was arbitrarily set as 100%.

#### 4. Discussion

H-1PV is a promising oncolytic virus. Early-phase clinical studies show that virus treatment is safe, well-tolerated and associated with first signs of anticancer efficacy. The present study aimed to fill a gap in knowledge of H-1PV biology regarding the pathways used by this virus to enter cancer cells. We chose two cancer cell lines as models to investigate the early steps of H-1PV infection: the cervical carcinoma-derived HeLa cell line and the glioma-derived NCH125 cell line. Previous laboratory studies have shown that these two cell lines are highly permissive to H-1PV infection and susceptible to its oncolytic activity [7,24,47].

In our study, for the first time, we show that H-1PV exploits clathrin-mediated endocytosis to enter cancer cells. EM analysis of H-1PV-infected HeLa cells revealed virus particles associated with clathrin-coated pits and then internalised inside clathrin-coated vesicles (Figure 1). In agreement with this finding, confocal microscopy analysis showed co-localisation of H-1PV and clathrin (Figure 2). Furthermore, pharmacological inhibition of clathrin-mediated endocytosis using hypertonic sucrose, CPZ and pitstop 2, as well as siRNA-mediated silencing of *AP2M1*, a key regulator of clathrin-mediated endocytosis, confirmed the heavy dependence of H-1PV on this pathway for successful entry into both HeLa and NCH125 cancer cells (Figure 3).

Previous research has reported that other PtPVs use clathrin-mediated endocytosis to gain access to cells and progress the infection (reviewed in Reference [3]). Our results are therefore in agreement with the idea that clathrin-mediated endocytosis is the default entry pathway for PtPVs. However, a number of PtPVs have also been shown to hijack alternative endocytic pathways. For instance, MVMp uses at least three different endocytic routes, such as clathrin-, caveolae- and clathrin-independent carrier-mediated endocytosis [22]. Moreover, PPV uses both clathrin-dependent endocytosis and macropinocytosis [16]. FPV and CPV are taken up by cells via binding to the transferrin receptor, which is typically endocytosed by clathrin-mediated endocytosis. However, FPV may also enter cells through alternative internalisation mechanisms, as deletions or mutations in the internalisation motif of the transferrin receptor, while decreasing FPV cellular uptake, did not completely arrest viral infection [48]. Although we cannot completely rule out the possibility that H-1PV, like other PtPVs, can also use different pathways to enter HeLa and NCH125 cancer cells, our results seem to exclude caveolae-mediated endocytosis as a major entry pathway. Indeed, pre-treatment of cells with nystatin and M $\beta$ CD, two inhibitors of caveolae-mediated endocytosis, did not decrease H-1PV transduction levels, suggesting that these drugs did not modify H-1PV entry. These results are in agreement with previous studies showing that bovine parvovirus (BPV) [17] and PPV [16] do not use caveolae-mediated endocytosis for their cell internalisation. Surprisingly, *CAV1* siRNA-mediated knockdown increased H-1PV transduction (Figure 4), suggesting that caveolin-1 (the protein encoded by *CAV1*) interferes with H-1PV infection. Human immunodeficiency virus (HIV) infection is restricted by caveolin-1 in various ways, e.g., at the transcriptional level by suppressing NF- $\kappa$ B p65 acetylation in macrophages, or by interacting with HIV viral proteins to impair viral infectivity [49,50]. Similarly, abundant caveolin-1 levels prevent Influenza A virus from infecting mouse embryo fibroblasts, which is reversed by depleting caveolin-1 [51]. Further experiments are required to find out whether and at what level caveolin-1 represents a negative modulator of H-1PV infection. Along these lines, caveolin-1 antagonists or inhibitors could offer an interesting strategy to improve H-1PV efficacy in cancer with elevated levels of caveolin-1.

Our study also provides important evidence that dynamin is involved in H-1PV entry (Figure 5). Dynamin is also required for MVMp entry in murine A9 fibroblasts, a process that occurs through both clathrin- and caveolae-mediated endocytosis [22]. However, the same study showed that dynamin is not involved in MVMp entry into mouse mammary cells transformed with polyomavirus middle T antigen, which instead occurs via clathrin-independent carrier-mediated endocytosis [22].

Another cell entry route used by viruses is macropinocytosis, generally described as a dynamin-independent process [52,53]. Among PtPVs, PPV has been reported to use this route of entry [16]. However, we showed that inhibition of dynamin almost completely abolished H-1PV infection, which makes it unlikely that H-1PV uses macropinocytosis as an alternative pathway to enter HeLa and NCH125 cancer cells.

Numerous viruses are known to hijack Rab-dependent pathways to enter cells. Of these, Rab5 and Rab7 GTPases are the key regulators of transport to early and late endosomes, while LAMP-1 is present mainly in late endosomes/lysosomes [41,54]. In the present study, we show that H-1PV particles co-localise with EEA1, an early endosome marker, and with Rab7 and LAMP-1, two late endosome markers (Figure 6A), indicating that H-1PV, like other PtPVs [3], uses endosomes for its cytosolic trafficking into the cells. However, a fraction of H-1PV particles is most likely trapped

in LAMP1-positive lysosomes. This has been observed for other PtPVs such as MVM, for which sequestration in LAMP1-positive lysosomes limits the efficiency of its nuclear translocation [55], and CPV, which accumulates in perinuclear LAMP2-positive lysosomes [56].

Previous studies have shown that the acidic environment inside the endosomes changes in redox conditions, and acid proteases and phosphatases drive the conformational rearrangements in the catalytic phospholipase 2 domain of the VP1 protein [55,57,58]. These changes are required first for the release of PtPV particles from the late endosome to the cytosol, and then for translocation into the nucleus [23,57,59,60]. For instance, the endosomal acidic environment is required for a productive infection of B19V [20], CPV [18,61,62] and MVM [55,63], among other parvoviruses. In agreement with these observations, we also found that NH<sub>4</sub>Cl and BafA1 strongly hampered H-1PV transduction (Figure 6).

In summary, our study shows, for the first time, that H-1PV internalisation occurs via clathrin-mediated and dynamin-dependent endocytosis, while requiring endosomal acidification, with EEA1 and Rab7 involved in the infection process. However, we cannot rule out the possibility of H-1PV taking other pathways in other cell types. Important questions remain, namely which receptor H-1PV uses to initiate uptake and whether other co-receptors are involved. In addition, the exact mechanisms of endosomal escape and subsequent nuclear entry, and finally the site where the H-1PV genome becomes accessible for replication, need to be investigated [3]. A better understanding of the early steps of H-1PV (and, more generally, PtPV) infection is crucial not only to decipher viral tropism and inherent oncolytic properties, but also to improve the clinical potential of H-1PV in cancer virotherapy.

**Supplementary Materials:** The following are available online at <http://www.mdpi.com/1999-4915/12/10/1199/s1>, Figure S1: Entry pathway inhibitors did not alter cell proliferation. Figure S2: Sucrose, a classical inhibitor of clathrin-mediated endocytosis, has no impact on virus transduction if added 4 h after virus infection.

**Author Contributions:** Conceptualisation, T.F. and A.M.; methodologies, T.F., A.K., M.E. and K.R.; investigation, T.F., C.B. (confocal microscopy analysis) and K.R. (EM analysis); data curation, T.F. and A.M.; writing—original draft preparation, T.F. and A.M.; writing—review and editing, A.M.; visualisation, T.F., C.B. and A.M.; supervision, A.M.; funding acquisition, A.M. All authors have read and agreed to the published version of the manuscript.

**Funding:** This study has been partially funded by a research grant from the Cooperational Research Program of the Deutsches Krebsforschungszentrum, Heidelberg, and the Ministry of Science and Technology (MOST), Israel, to A.M. and M.E.

**Acknowledgments:** We are grateful to Barbara Leuchs (DKFZ, Heidelberg, Germany) for kindly providing the H-1PV capsid monoclonal antibody. We would also like to extend our acknowledgements to Tiina Marttila for producing both the H-1PV wild-type and the recH-1PV-EGFP viruses. We thank Caroline Hadley (INLEXIO) for critically reading the manuscript.

**Conflicts of Interest:** A.M. is co-inventor in several H-1PV-related patents. No other conflicts of interest are declared by the authors.

## References

1. Cotmore, S.F.; Tattersall, P. Parvoviral host range and cell entry mechanisms. *Adv. Virus Res.* **2007**, *70*, 183–232. [[PubMed](#)]
2. Cotmore, S.F.; Agbandje-McKenna, M.; Chiorini, J.A.; Mukha, D.V.; Pintel, D.J.; Qiu, J.; Soderlund-Venermo, M.; Tattersall, P.; Tijssen, P.; Gatherer, D. The family parvoviridae. *Arch. Virol.* **2014**, *159*, 1239–1247. [[CrossRef](#)] [[PubMed](#)]
3. Ros, C.; Bayat, N.; Wolfisberg, R.; Almendral, J.M.J.V. Protoparvovirus cell entry. *Viruses* **2017**, *9*, 313. [[CrossRef](#)] [[PubMed](#)]
4. Bretscher, C.; Marchini, A. H-1 parvovirus as a cancer-killing agent: Past, present, and future. *Viruses* **2019**, *11*, 562. [[CrossRef](#)] [[PubMed](#)]
5. Hartley, A.; Kavishwar, G.; Salvato, I.; Marchini, A. A roadmap for the success of oncolytic parvovirus-based anticancer therapies. *Annu. Rev. Virol.* **2020**, *7*, 537–557. [[CrossRef](#)]

6. Marchini, A.; Daeffler, L.; Pozdeev, V.I.; Angelova, A.; Rommelaere, J. Immune conversion of tumor microenvironment by oncolytic viruses: The protoparvovirus H-1PV case study. *Front. Immunol.* **2019**, *10*, 1848. [[CrossRef](#)]
7. Hristov, G.; Kramer, M.; Li, J.; El-Andaloussi, N.; Mora, R.; Daeffler, L.; Zentgraf, H.; Rommelaere, J.; Marchini, A. through its nonstructural protein NS1, parvovirus H-1 induces apoptosis via accumulation of reactive oxygen species. *J. Virol.* **2010**, *84*, 5909–5922. [[CrossRef](#)]
8. Geletneky, K.; Huesing, J.; Rommelaere, J.; Schlehofer, J.R.; Leuchs, B.; Dahm, M.; Krebs, O.; von Knebel Doeberitz, M.; Huber, B.; Hajda, J. Phase I/IIa study of intratumoral/intracerebral or intravenous/intracerebral administration of Parvovirus H-1 (ParvOryx) in patients with progressive primary or recurrent glioblastoma multiforme: ParvOryx01 protocol. *BMC Cancer* **2012**, *12*, 99. [[CrossRef](#)]
9. Hajda, J.; Lehmann, M.; Krebs, O.; Kieser, M.; Geletneky, K.; Jäger, D.; Dahm, M.; Huber, B.; Schöning, T.; Sedlaczek, O. A non-controlled, single arm, open label, phase II study of intravenous and intratumoral administration of ParvOryx in patients with metastatic, inoperable pancreatic cancer: ParvOryx02 protocol. *BMC Cancer* **2017**, *17*, 1–11. [[CrossRef](#)]
10. Nüesch, J.P.; Lacroix, J.; Marchini, A.; Rommelaere, J. Molecular pathways: Rodent parvoviruses—Mechanisms of oncolysis and prospects for clinical cancer treatment. *Clin. Cancer Res.* **2012**, *18*, 3516–3523. [[CrossRef](#)]
11. López-Bueno, A.; Rubio, M.-P.; Bryant, N.; McKenna, R.; Agbandje-McKenna, M.; Almendral, J.M. Host-selected amino acid changes at the sialic acid binding pocket of the parvovirus capsid modulate cell binding affinity and determine virulence. *J. Virol.* **2006**, *80*, 1563–1573. [[CrossRef](#)] [[PubMed](#)]
12. Allaupe, X.; El-Andaloussi, N.; Leuchs, B.; Bonifati, S.; Kulkarni, A.; Marttila, T.; Kaufmann, J.K.; Nettelbeck, D.M.; Kleinschmidt, J.; Rommelaere, J. Retargeting of rat parvovirus H-1PV to cancer cells through genetic engineering of the viral capsid. *J. Virol.* **2012**, *86*, 3452–3465. [[CrossRef](#)] [[PubMed](#)]
13. Harbison, C.E.; Chiorini, J.A.; Parrish, C.R. The parvovirus capsid odyssey: From the cell surface to the nucleus. *Trends Microbiol.* **2008**, *16*, 208–214. [[CrossRef](#)]
14. Doherty, G.J.; McMahon, H.T. Mechanisms of endocytosis. *Annu. Rev. Biochem.* **2009**, *78*, 857–902. [[CrossRef](#)] [[PubMed](#)]
15. Mercer, J.; Schelhaas, M.; Helenius, A. Virus entry by endocytosis. *Annu. Rev. Biochem.* **2010**, *79*, 803–833. [[CrossRef](#)]
16. Boisvert, M.; Fernandes, S.; Tijssen, P. Multiple pathways involved in porcine parvovirus cellular entry and trafficking toward the nucleus. *J. Virol.* **2010**, *84*, 7782–7792. [[CrossRef](#)]
17. Dudleemajil, E.; Lin, C.-Y.; Dredge, D.; Murray, B.K.; Robison, R.A.; Johnson, F.B. Bovine parvovirus uses clathrin-mediated endocytosis for cell entry. *J. Gen. Virol.* **2010**, *91*, 3032–3041. [[CrossRef](#)]
18. Parker, J.S.; Parrish, C.R. Cellular uptake and infection by canine parvovirus involves rapid dynamin-regulated clathrin-mediated endocytosis, followed by slower intracellular trafficking. *J. Virol.* **2000**, *74*, 1919–1930. [[CrossRef](#)]
19. Vendeville, A.; Ravallec, M.; Jousset, F.-X.; Devise, M.; Mutuel, D.; López-Ferber, M.; Fournier, P.; Dupressoir, T.; Ogliastro, M. Densovirus infectious pathway requires clathrin-mediated endocytosis followed by trafficking to the nucleus. *J. Virol.* **2009**, *83*, 4678–4689. [[CrossRef](#)]
20. Quattrocchi, S.; Ruprecht, N.; Bönsch, C.; Bieli, S.; Zürcher, C.; Boller, K.; Kempf, C.; Ros, C. Characterization of the early steps of human parvovirus B19 infection. *J. Virol.* **2012**, *86*, 9274–9284. [[CrossRef](#)]
21. McMahon, H.T.; Boucrot, E. Molecular mechanism and physiological functions of clathrin-mediated endocytosis. *Nat. Rev. Mol. Cell Biol.* **2011**, *12*, 517. [[CrossRef](#)] [[PubMed](#)]
22. Garcin, P.O.; Panté, N. The minute virus of mice exploits different endocytic pathways for cellular uptake. *Virology* **2015**, *482*, 157–166. [[CrossRef](#)] [[PubMed](#)]
23. Suikkanen, S.; Aaltonen, T.; Nevalainen, M.; Väililehto, O.; Lindholm, L.; Vuento, M.; Vihinen-Ranta, M. Exploitation of microtubule cytoskeleton and dynein during parvoviral traffic toward the nucleus. *J. Virol.* **2003**, *77*, 10270–10279. [[CrossRef](#)] [[PubMed](#)]
24. Di Piazza, M.; Mader, C.; Geletneky, K.; y Calle, M.H.; Weber, E.; Schlehofer, J.; Deleu, L.; Rommelaere, J. Cytosolic activation of cathepsins mediates parvovirus H-1-induced killing of cisplatin and TRAIL-resistant glioma cells. *J. Virol.* **2007**, *81*, 4186–4198. [[CrossRef](#)]

25. El-Andaloussi, N.; Endeke, M.; Leuchs, B.; Bonifati, S.; Kleinschmidt, J.; Rommelaere, J.; Marchini, A. Novel adenovirus-based helper system to support production of recombinant parvovirus. *Cancer Gene Ther.* **2011**, *18*, 240–249. [[CrossRef](#)]
26. El-Andaloussi, N.; Leuchs, B.; Bonifati, S.; Rommelaere, J.; Marchini, A. Efficient recombinant parvovirus production with the help of adenovirus-derived systems. *J. Vis. Exp.* **2012**, *62*, e3518. [[CrossRef](#)]
27. Leuchs, B.; Roscher, M.; Muller, M.; Kurschner, K.; Rommelaere, J. Standardized large-scale H-1PV production process with efficient quality and quantity monitoring. *J. Virol. Methods* **2016**, *229*, 48–59. [[CrossRef](#)]
28. Rodal, S.K.; Skretting, G.; Garred, Ø.; Vilhardt, F.; Van Deurs, B.; Sandvig, K. Extraction of cholesterol with methyl- $\beta$ -cyclodextrin perturbs formation of clathrin-coated endocytic vesicles. *Mol. Biol. Cell* **1999**, *10*, 961–974. [[CrossRef](#)]
29. Anderson, H.; Chen, Y.; Norkin, L. Bound simian virus 40 translocates to caveolin-enriched membrane domains, and its entry is inhibited by drugs that selectively disrupt caveolae. *Mol. Biol. Cell* **1996**, *7*, 1825–1834. [[CrossRef](#)]
30. Locker, J.K.; Schmid, S.L. Integrated electron microscopy: Super-duper resolution. *PLoS Biol.* **2013**, *11*, e1001639.
31. Short, B. A cell-free screen of caveolae interactions. *J. Cell Biol.* **2018**, *217*, 1883. [[CrossRef](#)]
32. Heuser, J.E.; Anderson, R. Hypertonic media inhibit receptor-mediated endocytosis by blocking clathrin-coated pit formation. *J. Cell Biol.* **1989**, *108*, 389–400. [[CrossRef](#)]
33. Wang, L.-H.; Rothberg, K.G.; Anderson, R. Mis-assembly of clathrin lattices on endosomes reveals a regulatory switch for coated pit formation. *J. Cell Biol.* **1993**, *123*, 1107–1117. [[CrossRef](#)]
34. Von Kleist, L.; Stahlschmidt, W.; Bulut, H.; Gromova, K.; Puchkov, D.; Robertson, M.J.; MacGregor, K.A.; Tomilin, N.; Pechstein, A.; Chau, N. Role of the clathrin terminal domain in regulating coated pit dynamics revealed by small molecule inhibition. *Cell* **2011**, *146*, 471–484. [[CrossRef](#)] [[PubMed](#)]
35. Mayle, K.M.; Le, A.M.; Kamei, D.T. The intracellular trafficking pathway of transferrin. *Biochim. Biophys. Acta* **2012**, *1820*, 264–281. [[CrossRef](#)] [[PubMed](#)]
36. Kadlecova, Z.; Spielman, S.J.; Loerke, D.; Mohanakrishnan, A.; Reed, D.K.; Schmid, S.L. Regulation of clathrin-mediated endocytosis by hierarchical allosteric activation of AP2. *J. Cell Biol.* **2017**, *216*, 167–179. [[CrossRef](#)] [[PubMed](#)]
37. Kilsdonk, E.P.; Yancey, P.G.; Stoudt, G.W.; Bangerter, F.W.; Johnson, W.J.; Phillips, M.C.; Rothblat, G.H. Cellular cholesterol efflux mediated by cyclodextrins. *J. Biol. Chem.* **1995**, *270*, 17250–17256. [[CrossRef](#)] [[PubMed](#)]
38. Singh, M.; Jadhav, H.R.; Bhatt, T. Dynamin functions and ligands: Classical mechanisms behind. *Mol. Pharmacol.* **2017**, *91*, 123–134. [[CrossRef](#)]
39. Hill, T.A.; Gordon, C.P.; McGeachie, A.B.; Venn-Brown, B.; Odell, L.R.; Chau, N.; Quan, A.; Mariana, A.; Sakoff, J.A.; Chircop, M. Inhibition of dynamin mediated endocytosis by the *Dynoles*—Synthesis and functional activity of a family of indoles. *J. Med. Chem.* **2009**, *52*, 3762–3773. [[CrossRef](#)]
40. Robertson, M.J.; Deane, F.M.; Robinson, P.J.; McCluskey, A. Synthesis of Dynole 34-2, Dynole 2-24 and Dyngo 4a for investigating dynamin GTPase. *Nat. Protoc.* **2014**, *9*, 851–870. [[CrossRef](#)]
41. Jordens, I.; Marsman, M.; Kuij, C.; Neeffjes, J. Rab proteins, connecting transport and vesicle fusion. *Traffic* **2005**, *6*, 1070–1077. [[CrossRef](#)] [[PubMed](#)]
42. Wilson, J.M.; De Hoop, M.; Zorzi, N.; Toh, B.-H.; Dotti, C.G.; Parton, R.G. EEA1, a tethering protein of the early sorting endosome, shows a polarized distribution in hippocampal neurons, epithelial cells, and fibroblasts. *Mol. Biol. Cell* **2000**, *11*, 2657–2671. [[CrossRef](#)] [[PubMed](#)]
43. Eskelinen, E.-L.; Tanaka, Y.; Saftig, P. At the acidic edge: Emerging functions for lysosomal membrane proteins. *Trends Cell Biol.* **2003**, *13*, 137–145. [[CrossRef](#)]
44. Eskelinen, E.-L. Roles of LAMP-1 and LAMP-2 in lysosome biogenesis and autophagy. *Mol. Asp. Med.* **2006**, *27*, 495–502. [[CrossRef](#)]
45. Misinzo, G.; Delputte, P.L.; Nauwynck, H.J. Inhibition of endosome-lysosome system acidification enhances porcine circovirus 2 infection of porcine epithelial cells. *J. Virol.* **2008**, *82*, 1128–1135. [[CrossRef](#)]
46. Yoshimori, T.; Yamamoto, A.; Moriyama, Y.; Futai, M.; Tashiro, Y. Bafilomycin A1, a specific inhibitor of vacuolar-type H<sup>(+)</sup>-ATPase, inhibits acidification and protein degradation in lysosomes of cultured cells. *J. Biol. Chem.* **1991**, *266*, 17707–17712.



47. Li, J.; Bonifati, S.; Hristov, G.; Marttila, T.; Valmary-Degano, S.; Stanzel, S.; Schnolzer, M.; Mougin, C.; Aprahamian, M.; Grekova, S.P.; et al. Synergistic combination of valproic acid and oncolytic parvovirus H-1PV as a potential therapy against cervical and pancreatic carcinomas. *EMBO Mol. Med.* **2013**, *5*, 1537–1555. [[CrossRef](#)]
48. Hueffer, K.; Palermo, L.M.; Parrish, C.R. Parvovirus infection of cells by using variants of the feline transferrin receptor altering clathrin-mediated endocytosis, membrane domain localization, and capsid-binding domains. *J. Virol.* **2004**, *78*, 5601–5611. [[CrossRef](#)]
49. Simmons, G.E., Jr.; Taylor, H.E.; Hildreth, J.E. Caveolin-1 suppresses Human Immunodeficiency virus-1 replication by inhibiting acetylation of NF- $\kappa$ B. *Virology* **2012**, *432*, 110–119. [[CrossRef](#)]
50. Lin, S.; Nadeau, P.E.; Wang, X.; Mergia, A. Caveolin-1 reduces HIV-1 infectivity by restoration of HIV Nef mediated impairment of cholesterol efflux by apoA-I. *Retrovirology* **2012**, *9*, 1–16. [[CrossRef](#)]
51. Bohm, K.; Sun, L.; Thakor, D.; Wirth, M. Caveolin-1 limits human influenza A virus (H1N1) propagation in mouse embryo-derived fibroblasts. *Virology* **2014**, *462*, 241–253. [[CrossRef](#)] [[PubMed](#)]
52. Swanson, J.A.; Watts, C. Macropinocytosis. *Trends Cell Biol.* **1995**, *5*, 424–428. [[CrossRef](#)]
53. Preta, G.; Cronin, J.G.; Sheldon, I.M. Dynasore-not just a dynamin inhibitor. *Cell Commun. Signal.* **2015**, *13*, 24. [[CrossRef](#)]
54. Zhang, Y.-N.; Liu, Y.-Y.; Xiao, F.-C.; Liu, C.-C.; Liang, X.-D.; Chen, J.; Zhou, J.; Baloch, A.S.; Kan, L.; Zhou, B. Rab5, Rab7, and Rab11 are required for Caveola-dependent endocytosis of classical swine fever virus in porcine alveolar macrophages. *J. Virol.* **2018**, *92*, e00797-18. [[CrossRef](#)] [[PubMed](#)]
55. Mani, B.; Baltzer, C.; Valle, N.; Almendral, J.M.; Kempf, C.; Ros, C. Low pH-dependent endosomal processing of the incoming parvovirus minute virus of mice virion leads to externalization of the VP1 N-terminal sequence (N-VP1), N-VP2 cleavage, and uncoating of the full-length genome. *J. Virol.* **2006**, *80*, 1015–1024. [[CrossRef](#)]
56. Suikkanen, S.; Sääjärvi, K.; Hirsimäki, J.; Väililehto, O.; Reunanen, H.; Vihinen-Ranta, M.; Vuento, M. Role of recycling endosomes and lysosomes in dynein-dependent entry of canine parvovirus. *J. Virol.* **2002**, *76*, 4401–4411. [[CrossRef](#)]
57. Zádori, Z.; Szelei, J.; Lacoste, M.-C.; Li, Y.; Gariépy, S.; Raymond, P.; Allaire, M.; Nabi, I.R.; Tijssen, P. A viral phospholipase A2 is required for parvovirus infectivity. *Dev. Cell* **2001**, *1*, 291–302. [[CrossRef](#)]
58. Farr, G.A.; Zhang, L.-g.; Tattersall, P. Parvoviral virions deploy a capsid-tethered lipolytic enzyme to breach the endosomal membrane during cell entry. *Proc. Natl. Acad. Sci. USA* **2005**, *102*, 17148–17153. [[CrossRef](#)]
59. Canaan, S.; Zádori, Z.; Ghomashchi, F.; Bollinger, J.; Sadilek, M.; Moreau, M.E.; Tijssen, P.; Gelb, M.H. Interfacial enzymology of parvovirus phospholipases A2. *J. Biol. Chem.* **2004**, *279*, 14502–14508. [[CrossRef](#)] [[PubMed](#)]
60. Vihinen-Ranta, M.; Wang, D.; Weichert, W.S.; Parrish, C.R. The VP1 N-terminal sequence of canine parvovirus affects nuclear transport of capsids and efficient cell infection. *J. Virol.* **2002**, *76*, 1884–1891. [[CrossRef](#)] [[PubMed](#)]
61. Vihinen-Ranta, M.; Kalela, A.; Mäkinen, P.; Kakkola, L.; Marjomäki, V.; Vuento, M. Intracellular route of canine parvovirus entry. *J. Virol.* **1998**, *72*, 802–806. [[CrossRef](#)] [[PubMed](#)]
62. Basak, S.; Turner, H. Infectious entry pathway for canine parvovirus. *Virology* **1992**, *186*, 368–376. [[CrossRef](#)]
63. Ros, C.; Burckhardt, C.J.; Kempf, C. Cytoplasmic trafficking of minute virus of mice: Low-pH requirement, routing to late endosomes, and proteasome interaction. *J. Virol.* **2002**, *76*, 12634–12645. [[CrossRef](#)] [[PubMed](#)]



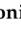


**Publisher's Note:** MDPI stays neutral with regard to jurisdictional claims in published maps and institutional affiliations.



© 2020 by the authors. Licensee MDPI, Basel, Switzerland. This article is an open access article distributed under the terms and conditions of the Creative Commons Attribution (CC BY) license (<http://creativecommons.org/licenses/by/4.0/>).

Review

# Parvovirus-Based Combinatorial Immunotherapy: A Reinforced Therapeutic Strategy against Poor-Prognosis Solid Cancers

Assia Angelova <sup>1,\*</sup> , Tiago Ferreira <sup>2</sup> , Clemens Bretscher <sup>2</sup> , Jean Rommelaere <sup>1</sup>  and Antonio Marchini <sup>2,3</sup> 

<sup>1</sup> German Cancer Research Center (DKFZ), Research Program Infection, Inflammation and Cancer, Clinical Cooperation Unit Virotherapy, Im Neuenheimer Feld 242, 69120 Heidelberg, Germany; j.rommelaere@dkfz-heidelberg.de

<sup>2</sup> German Cancer Research Center (DKFZ), Laboratory of Oncolytic-Virus-Immunotherapeutics (LOVIT), Im Neuenheimer Feld 242, 69120 Heidelberg, Germany; t.ferreira@dkfz-heidelberg.de (T.F.); c.bretscher@gmx.de (C.B.); antonio.marchini@lih.lu (A.M.)

<sup>3</sup> Luxembourg Institute of Health (LIH), Laboratory of Oncolytic-Virus-Immunotherapeutics (LOVIT), 84 rue Val Fleuri, L-1526 Luxembourg, Luxembourg

\* Correspondence: a.angelova@dkfz-heidelberg.de; Tel.: +49-6221-42-4960

**Simple Summary:** Oncolytic virotherapy using oncolytic viruses with natural or engineered cancer-destroying capacities has emerged as a promising treatment concept in modern oncology. Rodent protoparvoviruses, in particular the rat H-1 parvovirus (H-1PV), have demonstrated their broad-range tumor-suppressive properties in both preclinical models and clinical studies. In addition to inducing selective tumor cell death, these viruses are also able to exert immunostimulating effects and reverse tumor-driven immune suppression. Parvovirotherapy holds therefore a potential for enhancing the efficacy of other cancer immunotherapies. The aim of this review is to provide an overview of all H-1PV-based combinatorial immunotherapeutic approaches against poor-prognosis human solid cancers that have been tested so far. Current challenges and future prospects of parvoviro-immunotherapy, notably parvovirus inclusion into various immunotherapeutic protocols against glioblastoma, pancreatic cancer, among other standard therapy-refractory solid malignancies, are also discussed in the light of H-1PV further clinical development.

**Abstract:** Resistance to anticancer treatments poses continuing challenges to oncology researchers and clinicians. The underlying mechanisms are complex and multifactorial. However, the immunologically “cold” tumor microenvironment (TME) has recently emerged as one of the critical players in cancer progression and therapeutic resistance. Therefore, TME modulation through induction of an immunological switch towards inflammation (“warming up”) is among the leading approaches in modern oncology. Oncolytic viruses (OVs) are seen today not merely as tumor cell-killing (oncolytic) agents, but also as cancer therapeutics with multimodal antitumor action. Due to their intrinsic or engineered capacity for overcoming immune escape mechanisms, warming up the TME and promoting antitumor immune responses, OVs hold the potential for creating a proinflammatory background, which may in turn facilitate the action of other (immunomodulating) drugs. The latter provides the basis for the development of OV-based immunostimulatory anticancer combinations. This review deals with the smallest among all OVs, the H-1 parvovirus (H-1PV), and focuses on H-1PV-based combinatorial approaches, whose efficiency has been proven in preclinical and/or clinical settings. Special focus is given to cancer types with the most devastating impact on life expectancy that urgently call for novel therapies.

**Keywords:** parvovirus; oncolytic; tumor microenvironment; immunotherapy; combination therapy; glioblastoma; pancreatic cancer; colorectal cancer; melanoma



**Citation:** Angelova, A.; Ferreira, T.; Bretscher, C.; Rommelaere, J.; Marchini, A. Parvovirus-Based Combinatorial Immunotherapy: A Reinforced Therapeutic Strategy against Poor-Prognosis Solid Cancers. *Cancers* **2021**, *13*, 342. <https://doi.org/10.3390/cancers13020342>

Received: 17 December 2020

Accepted: 15 January 2021

Published: 19 January 2021

**Publisher's Note:** MDPI stays neutral with regard to jurisdictional claims in published maps and institutional affiliations.



**Copyright:** © 2021 by the authors. Licensee MDPI, Basel, Switzerland. This article is an open access article distributed under the terms and conditions of the Creative Commons Attribution (CC BY) license (<https://creativecommons.org/licenses/by/4.0/>).

## 1. Introduction

The rodent H-1 protoparvovirus (H-1PV) (for an overview of H-1PV classification and biology, we redirect the readers to a recent review by Bretscher and Marchini [1]) was first discovered as a contaminating agent in xeno-transplanted human tumor cell lines [2]. Originally identified as a pathogen, which lethally affects rat fetuses and newborn rats by causing cerebellar hypoplasia and hepatitis [3], H-1PV was later found to preferentially replicate in rat- and in human-transformed or tumor-derived cell cultures, while sparing their non-malignant counterparts [4,5]. H-1PV intrinsic oncotropism and oncoselectivity are a complex phenomenon based on multiple molecular determinants, which are underrepresented in normal cells, but characteristic of tumor cells [6]. Importantly, humans are not naturally infected with this virus, and no association between H-1PV and human disease has been observed [7]. Two early clinical studies of virus administration to cancer patients—dating back to the 1960s and 1990s of last century—demonstrated the lack of H-1PV pathogenic effects and the feasibility of the approach [8,9], thus laying the groundwork for the development of parvovirus (PV)-based oncolytic virotherapy. Three decades of laboratory efforts brought about extensive preclinical evidence of H-1PV broad tumor-suppressive potential [5,10]. Furthermore, it became increasingly apparent that in addition to directly inducing cancer cell death (oncolysis), H-1PV was also capable of exerting immuno-stimulating effects in various preclinical cancer models [11,12].

PV induced immune system stimulation results from multiple infection-associated immunogenic events. Depending on the tumor model, virus dose, route of administration and the immunological status of the host, one or another immunogenic stimulus may prevail [11]. Regardless of the particular mechanism involved, PV-mediated immunomodulation contributes to the “warming up” of the tumor microenvironment (TME) (Figure 1), increases tumor visibility and enhances immune cell reactivity [13]. H-1PV infection-associated immunogenic events and their impact on the immune system are reviewed in detail elsewhere [12,13], and briefly summarized below.

- Immunogenic cell death (ICD) of H-1PV-infected tumor cells (indirect immune cell stimulation): PVs are potent triggers of immunogenic stimuli through tumor cell ICD induction. Infected tumor cells release a spectrum of proinflammatory mediators, in particular chemo- and cyto-kines, and pathogen- and danger-associated molecular patterns (PAMPs, DAMPs), which are in turn capable of boosting the maturation and reactivity of distinct immune cell populations. This can be exemplified by H-1PV-infected human melanoma cells, which activate dendritic cell (DC) maturation through the release of heat shock protein 72 [14]. In line with this observation, H-1PV-infected pancreatic and colorectal carcinoma cells were shown to stimulate natural killer (NK) cell tumor-killing capacity through both the overexpression of ligands specific for NK cell activation receptors and the downregulation of MHC I on infected tumor cells [15,16]. Notably, productive infection of tumor cells is not required for immune stimulation. This was demonstrated by co-incubating H-1PV-infected semi-permissive pancreatic carcinoma cells with peripheral blood mononuclear cells (PBMC), under which conditions induction of Th1 signature and release of interferon-gamma (IFN- $\gamma$ ) and tumor necrosis factor-alpha (TNF- $\alpha$ ) were detected in the PBMC population [17].
- H-1PV infection of immune cells (direct immune cell stimulation): H-1PV infection of human immune cell subpopulations has been documented in various preclinical settings. Virus entry may take place in T, B, NK, DC and monocytic populations; however, infection is aborted at subsequent virus intracellular replication steps [18]. Abortive infection can nevertheless exert multiple immuno-stimulating effects, such as expression of IFN-stimulated genes and proinflammatory cytokine production [17,18]. On the other hand, H-1PV is able to inhibit the immune suppressive activity of regulatory T (Treg) cells [18].
- H-1PV impact on tumor vasculature: It has been demonstrated that endothelial (precursor) cells may constitute direct targets for parvovirus-mediated toxicity. These cells sustain an abortive H-1PV infection in vitro. In animal models, virus treatment

inhibits the growth of lymphatic endothelium-derived tumors (Kaposi's sarcoma). Furthermore, recombinant propagation-deficient parvoviral vectors armed with angiostatic chemokines achieve significant reduction of vascular endothelial growth factor (VEGF) expression in Kaposi's sarcoma cells [19]. Given the control exerted by the vasculature of tumors over their infiltration with immune cells, these effects are likely to contribute to H-1PV immuno-stimulating activity, as further discussed below. Altogether, these data warrant validation of H-1PV as a tool against highly vascularized cancers, e.g., glioblastoma, one of the most angiogenic human tumors.

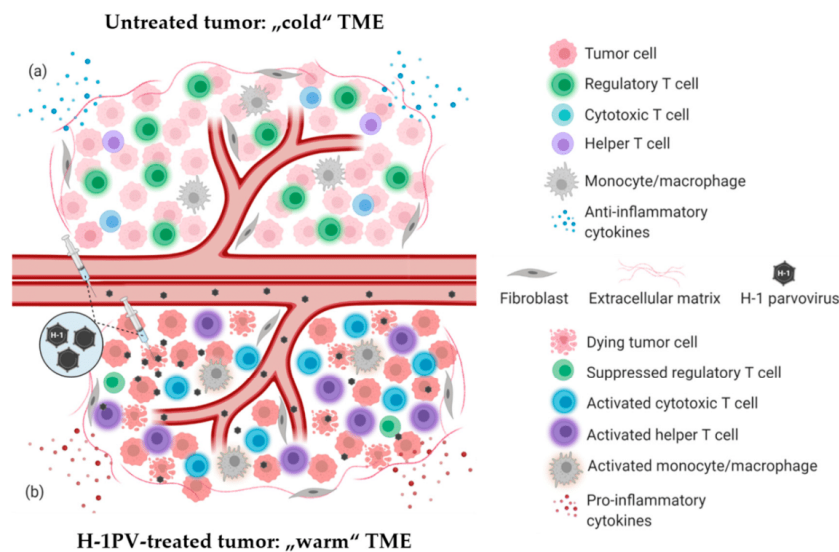


**Figure 1.** H-1PV-induced modulation of tumor microenvironment immune landscape. (a) Immunosuppressive (“cold”) tumor microenvironment (TME) of a solid tumor. The tumor is often infiltrated with abundant immunosuppressive regulatory T cells (Treg)/myeloid-derived suppressor cells (MDSC). Tumor-infiltrating lymphocytes (TILs) (CD8+ CTLs, CD4+ Th cells) are scarce and/or anergic. Tumor and various TME cells produce anti-inflammatory cytokines to maintain immune suppression and facilitate tumor growth and dissemination. (b) Tumor infection with H-1PV results in immunogenic tumor cell death leading to the release proinflammatory cytokines, pathogen- and danger-associated molecular patterns (PAMPs and DAMPs), which alarm the immune system. The infection of tumor cells does not necessarily have to be productive for this immuno-stimulating effect to be achieved. Furthermore, abortive infection of immunocytes (CTLs, Th cells, monocytes/macrophages) with H-1PV can also lead to their activation. In contrast, H-1PV inhibits the immune suppressive functions of Treg cells. An immunological switch takes place and converts the “cold” TME into a “warmed up” (inflamed) one. Virus-mediated immuno-conversion of TME favors the mounting of enhanced antitumor immune responses.

The above-outlined H-1PV potential for creating a proinflammatory immune environment and alerting the immune system to the presence of a tumor opens prospects for combining the virus with various immunomodulators or other therapeutic agents endowed with immuno-stimulating properties. This combinatorial approach is in particular promising for the treatment of human tumors that remain presently incurable and pose continuing research and clinical challenges. Pancreatic ductal adenocarcinoma (PDAC), glioblastoma, colorectal cancer (CRC) and melanoma are among those cancers, which are urgently calling for novel therapeutic strategies. H-1PV-based immunotherapeutic combinations are reviewed below, which aim at targeting these devastating malignancies.

## 2. Parvovirus-Based Combinatorial Immunotherapy against Pancreatic Cancer

PDAC is the most common neoplasm of the pancreas and one of the most aggressive human cancers. It is characterized by quick progression, broad intraperitoneal dissemination (peritoneal carcinomatosis) and frequent resistance to conventional treatments. PDAC is usually diagnosed at advanced stages, when surgical resection is either not feasible or inefficient, as most patients eventually suffer from local recurrence and metachronous metastasis [20]. Current chemotherapy regimens achieve only minor improvements of PDAC dismal prognosis: the median survival time and overall 5-year survival remain as low as <12 months and approximately 5%, respectively [21]. Gemzar (gemcitabine) is the standard drug used to treat PDAC patients after surgery. Yet, gemcitabine only prolongs the survival of the majority (82%) of the patients by less than two-fold. On the same line, pathway-specific targeted therapies showed little efficacy against PDAC [22]. Therefore, new treatment paradigms need to be urgently explored in order to extend PDAC patient life expectancy and offer better quality of life.

H-1PV is among the oncolytic viruses (OVs), which have promising potential for efficiently targeting pancreatic cancer. PDAC sensitivity to H-1PV-induced oncolysis was demonstrated in various preclinical models [23,24]. Infection of human PDAC-derived cells leads to their killing, which is mediated at least in part by cathepsins [24]. Importantly, H-1PV sensitivity is preserved in gemcitabine-resistant cultures [23], thus opening up prospects to circumvent PDAC resistance to current standard death inducers.

### 2.1. H-1PV + Nucleoside Analogues (Gemcitabine)

As gemcitabine is currently considered the gold chemotherapeutic standard in PDAC clinical management, the therapeutic efficacy of gemcitabine in combination with H-1PV was tested in a rat syngeneic orthotopic PDAC model. H-1PV administration to gemcitabine-pretreated animals led to significant tumor suppression and survival prolongation in comparison with the mock-infected or gemcitabine-only treated groups [23]. These *in vivo* findings could not be straightforwardly ascribed to synergistic tumor cell death enhancement only. Indeed, *in vitro* studies showed that the cytotoxic effects of the combination, while allowing effective dose reduction for both agents, did not result in complete PDAC culture elimination. This prompted the investigation of the immunological effects exerted by the H-1PV + gemcitabine combination as an added value to direct tumor cell killing. Markers of ICD induction were analyzed in various PDAC cell lines, treated with either virus (or gemcitabine) alone or with H-1PV + gemcitabine. It was demonstrated that the release of high-mobility group box 1 protein (HMGB1) is a strikingly robust feature of H-1PV-infected PDAC cells [24]. Furthermore, H-1PV-triggered HMGB1 release did not require lytic infection, in line with the above-described PBMC activation by non-productively infected PDAC cells [17]. Gemcitabine alone was unable to induce HMGB1 secretion, yet H-1PV-induced HMGB1 release remained unaffected in gemcitabine-treated cells. Gemcitabine, on the other hand, was able to induce—albeit not in all cell lines tested—mature interleukin 1-beta (IL-1 $\beta$ ) accumulation in culture supernatants. Taken together, these data show that H-1PV and gemcitabine complement each other in the induction of immunogenic signals. The compatibility of H-1PV-induced alarmin (HMGB1) secretion with other (ICD-inducing) chemotherapeutic regimens warrants the consideration of PV inclusion into various multimodal anti-PDAC treatment protocols [24]. The therapeutic promise of H-1PV administration in gemcitabine-treated pancreatic cancer patients is further supported by several reports in the literature showing that, unlike most nucleoside analogues, gemcitabine is lacking immunosuppressive properties. On the contrary, gemcitabine may be beneficial not only to the cytotoxic but also to the pro-immune outcome of H-1PV infection, as assumed from the findings below.

- One study conducted in gemcitabine-treated PDAC patients revealed the ability of the drug to enhance T cell-mediated and DC-dependent host immune responses [25].

- In keeping with the aforementioned data, it was documented that gemcitabine therapy may promote naïve T cell activation in PDAC patients and enhance their responsiveness to specific vaccination or to other forms of immunotherapy [26].
- The understanding of gemcitabine immunoregulating effects as a complementary constituent of tumor cell toxicity was extended by the demonstration that this drug alleviates pancreatic cancer immune escape through NK cell cytotoxicity enhancement [27].
- Studies conducted in murine orthotopic PDAC models provided yet another insight into gemcitabine-mediated immuno-stimulation, namely by indicating that low chemotherapeutic doses selectively deplete effector/memory Treg cell populations. The latter has a strong impact on PDAC microenvironment, as Tregs usually form large intra-tumoral infiltrates and trigger local immune suppression [28,29].
- Last but not least, in cancer models other than PDAC, gemcitabine enhances the efficacy of OV (e.g., reovirus) therapy. This complementation is achieved through gemcitabine-mediated inhibition of myeloid-derived suppressor cell (MDSC) recruitment to the TME and acceleration of reovirus-induced antitumor T cell immune responses [30].

Based on favorable preclinical data hinting at the potentiation of OV-induced antitumor effects in the presence of gemcitabine, a clinical trial, ParvOryx02 (NCT02653313), was designed and conducted with the aim to provide a clinical proof-of-principle of the safety (and efficacy) of H-1PV + gemcitabine co-treatment. Patients with inoperable metastatic (at least one hepatic metastasis) pancreatic cancer were treated with H-1PV. The virus was first administered intravenously (40% of the total virus dose on four consecutive days), and the remaining virus dose was then given intra-metastatically as single hepatic injection, followed by gemcitabine treatment [31]. Partial response and extended overall survival were observed in two out of seven trial patients, and immunological signatures most likely contributed to this improved outcome. The ParvOryx02 study therefore provided the first clinical indication that immune mechanisms underlie PV-mediated tumor suppression [32].

## 2.2. H-1PV + Histone Deacetylase Inhibitors (Valproic Acid)

Preclinical proof-of-concept was also obtained for another treatment combining H-1PV with the histone deacetylase (HDAC) inhibitor (HDACi) valproic acid (VPA) [33]. HDACis hold significant promise in cancer therapy, due to their ability to cause malignant cell growth inhibition, re-differentiation and death [34]. Most interestingly, HDAC inhibition was also found to potentiate the oncotoxicity of various OVs, including vesicular stomatitis [35], herpes- [36], adeno- [37] and parvo [33]-viruses (for a review, see Reference [38]). The synergism between HDACi and H-1PV was first demonstrated by Li et al., who conducted preclinical testing of this combination in cervical carcinoma and PDAC models [33]. VPA proved to synergize with H-1PV in inducing DNA damage, oxidative stress and death in PDAC-derived cell lines. This cooperation was traced back, at least in part, to the ability of VPA to stimulate the acetylation and, in consequence, the oncotoxic activity of the viral protein NS1. Interestingly, VPA-induced hyperacetylation of NS1 was also associated with enhanced H-1PV DNA replication and viral gene transcription, ultimately boosting virus multiplication in tumor cells. The VPA-dependent increase in both H-1PV intrinsic oncotoxicity and multiplication was reflected in the potentiation of tumor suppression in animal models. In order to establish a clinically relevant animal model of PDAC, patient-derived material was xeno-transplanted in non-obese diabetic/severe combined immunodeficiency disease (NOD/SCID) mice. Alternatively, the human AsPC-1 cell line was implanted into nude rats. Tumors were subjected to mono versus combinatorial treatment and tumor growth parameters were comparatively evaluated. In line with the *in vitro* observations, H-1PV + VPA administration resulted in enhanced NS1 and H-1PV intra-tumoral accumulation, correlating with an increase in oxidative stress and subsequent apoptosis in co-treated tumors. The combination achieved complete AsPC-1 tumor eradication. Patient-derived xenografts were also responsive, yet to a somewhat

lesser extent, probably due to the characteristic PDAC intra-tumoral heterogeneity and prominent presence of stroma.

It is noteworthy that besides its effects on tumor cell growth and OV oncotoxicity, VPA was reported to modulate the immune system, providing an additional possible interface for cooperation with OVs at the level of their intrinsic immuno-stimulating activity. VPA was indeed shown to:

- Exert epigenetic regulation of various immune functions, e.g., attenuation of MDSC immunosuppressive effects [39].
- Induce the expression of MHC I-related chain A (MICA) and B (MICB) molecules, as well as of UL16-binding proteins (ULBPs) in human tumor cells, thereby triggering their enhanced recognition by NK cells [40], like H-1PV does (see above [15,16]).
- Mediate the inhibition of macrophage migration inhibitory factor (MIF) expression through local chromatin deacetylation-based transcription targeting [41].

As a whole, the above data speak for the high translational relevance of VPA to the future development of PV-based combinatorial (immuno) therapies.

In conclusion, two drugs that are available on the pharmaceutical market, i.e., gemcitabine (cytostatic) and VPA (antiepileptic), proved to be efficient in synergizing with H-1PV to suppress pancreatic cancer (Figure 2).

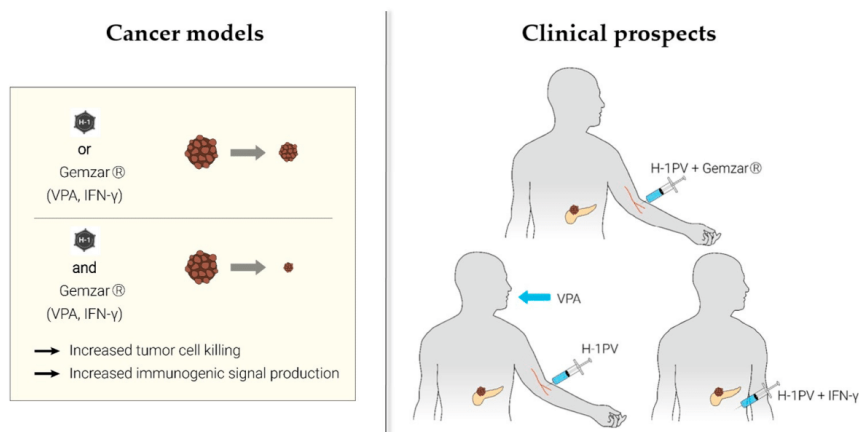


**Figure 2.** Parvovirus-based viro-immunotherapeutic combinations under development against pancreatic ductal adenocarcinoma (PDAC). H-1PV-induced tumor cell lysis cooperates with gemcitabine-triggered programmed tumor cell death, valproic acid (VPA)-dependent epigenetic transcription regulation or interferon (IFN)- $\gamma$ -induced immuno-stimulation to suppress PDAC. Preclinical data suggest that the immune system mediates, at least in part, this cooperation. H-1PV infection of tumor cells leads to the release of PAMPs/DAMPs, such as high-mobility group box 1 protein (HMGB1), which in turn alert the immune system to danger and mobilize an inflammatory antitumor immune response. Various aspects of H-1PV-, gemcitabine-, VPA- and IFN- $\gamma$ -exerted immunomodulation may converge and synergize upon exposure of the host immune system to the respective combinations. The underlying mechanisms remain to be elucidated in detail by gathering extensive clinical experience. For details and references, see main text.

### 2.3. H-1PV + Proinflammatory Cytokines (Interferon-Gamma)

Another combination with substantial potential for clinical development relies on the mutual complementation of H-1PV- and IFN- $\gamma$ -mediated immune stimulation. It was shown that IFN- $\gamma$  improves the vaccination potential of the virus and diminishes the development of peritoneal carcinomatosis in preclinical PDAC models. Concomitant intraperitoneal administration of both H-1PV and IFN- $\gamma$  in these models led to extended an-

imal survival correlating with enhanced peritoneal macrophage and splenocyte responses against tumor cells [42].

### 3. Parvovirus-Based Combinatorial Immunotherapy against Glioblastoma

Glioblastoma multiforme (GBM) is the most common and aggressive human primary brain tumor. Similar to PDAC, GBM patients experience a very poor outcome. The 5-year overall survival rate is very low, around 5.1% [43]. GBM treatment faces a unique challenge: the presence of the blood–brain barrier (BBB), which largely prevents drugs, including small-molecule ones, from entering the central nervous system [44]. Current therapeutic approaches therefore include surgical resection of the tumor—to the largest extent feasible and safe—followed by radiotherapy and concomitant chemotherapy [45]. Unfortunately, despite all clinical efforts, tumor progression and recurrence typically occur, calling for alternative therapeutic solutions [46].

Based on the so far unmet need for novel, more efficient treatments, GBM was among the preclinical tumor models most extensively studied in our laboratory. H-1PV capacity for selectively killing glioma cells through cytosolic activation of lysosomal proteases was first demonstrated *in vitro* [47]. These results were validated in animal models, namely in immunocompetent rats bearing orthotopic autologous RG-2 tumors and in immunodeficient rats bearing xeno-transplanted human U87 gliomas. In these models, tumor regression after local, intravenous or intranasal virus administration was observed [47–49]. H-1PV treatment was not associated with any significant off-target toxicities; accordingly, virus transcription and NS1 protein accumulation could be detected in regressing tumor remnants and not in the surrounding normal tissues [48]. Interestingly, the therapeutic effect was potentiated in the presence of an intact host immune system. T cell depletion impaired H-1PV-induced glioma suppression; conversely, the presence of T cell only, in the absence of PV treatment, was not sufficient to inhibit tumor growth [11]. These preclinical observations provided the first hints of host T cell response involvement in PV-mediated glioma regression, hence the rationale for the development of PV-based immunotherapies against glioblastoma.

Pursuant to the above-described preclinical findings, the ParvOryx01 trial (NCT01301430) in recurrent glioblastoma patients delivered the first clinical proof-of-concept for tumor-infiltrating lymphocytes (TILs) playing substantial role in H-1PV-mediated immunomodulation of GBM TME. Although ParvOryx01 primary objectives were to determine virus safety, tolerability, pharmacokinetics, shedding and maximum tolerated dose, the analysis of post-virus-treatment resected tumor tissues revealed the presence of prominent immune cell infiltrates [50]. These infiltrates were comprised of CD45+CD3+CD4+ and CD45+CD3+CD8+ TILs. The latter contained both perforin and granzyme B-positive secretory granules, which is indicative of CTL cytolytic activity. TILs proved, in addition, to be CD25 (IL2 receptor alpha chain)-positive. Only a minor fraction of these cells expressed FOXP3, indicating the scarcity of Treg cells within the intra-tumoral immune infiltrates. Intra-tumoral production of proinflammatory cytokines (IFN- $\gamma$ , IL-2) was also detected, together with inducible nitric oxide synthase (iNOS) expression in CD68+ tumor-associated microglia/macrophage cells [50,51]. Interestingly, tumor cells expressed the CD40 ligand (CD40L), a positive prognostic factor in glioblastoma [52]. Co-expression of CD40L and CD40, considered as a negative prognostic factor, was not seen [50,51]. Taken together, these first clinical findings indicated that H-1PV has the capacity to exert immunostimulating effects on glioblastoma TME. This makes the virus a worthwhile partner in therapeutic combinations, which aim at warming up the intrinsically immunosuppressive and immune-evasive environment of brain tumors.

#### 3.1. H-1PV + Ionizing Radiation

We have previously shown that radiotherapy, one of the conventional first-line treatments in glioblastoma patients, sensitizes low-passage glioma cultures to H-1PV oncolysis. Pre-irradiation increases the susceptibility of these cells to virus infection. Interestingly,



H-1PV achieves killing both radiation-sensitive and resistant glioma cells [53]. Apart from triggering enhanced tumor cytolysis, the irradiation followed by H-1PV treatment holds, in addition, the potential—although not yet validated in animal models—of acting as combinatorial immunotherapy. Indeed, although irradiation was long regarded as a local anticancer therapy, the first reports on radiotherapy interactions with the host immune system can be traced back to the 1970s of the last century. In 1979, Slone et al. were the first to report that the radiation dose required to control 50% of mouse fibrosarcomas was twice as high in immunocompromised animals as in immunocompetent hosts [54]. Furthermore, tumor regression at sites distant to radiation fields, the so-called abscopal effect, has been systematically observed [55]. Radiation-triggered immunomodulation encompasses, among other effects, ICD induction, T and NK cell activation and MDSC suppression. These observations prompted the development of various combination therapy regimens based on radiation and other immunomodulating agents [56,57], including OVAs (e.g., adeno-, herpes simplex-, measles- and vaccinia-viruses) against glioma [58].

### 3.2. H-1PV + Tumor Angiogenesis Inhibitors (Bevacizumab)

Another promising approach is the combination of H-1PV with bevacizumab (Avastin®). This co-treatment was evaluated in a series of compassionate virus uses in recurrent glioblastoma patients. Bevacizumab is an anti-VEGF-A monoclonal antibody available in Europe since 2005 for the treatment of breast, lung, kidney, colon, ovarian and endometrial carcinomas. In 2009, bevacizumab was approved by the Food and Drug Administration (FDA) for application in glioblastoma patients [59]. While achieving a steroid-sparing effect and alleviation of edema, bevacizumab monotherapy has, however, not demonstrated significant survival benefits [60]. On the other hand, scientists and clinicians have gathered an extensive—and yet to grow—knowledge of bevacizumab's mode of action. In particular, bevacizumab was found to exert immunomodulating activity by counteracting VEGF-induced negative effects on DC maturation, antigen presentation and lymphocytic trafficking [61]. These bevacizumab properties, together with the ParvOryx01 trial experience showing H-1PV treatment-associated immunogenic changes in glioblastoma TME, have opened up prospects for novel anti-glioma combinatorial immunotherapy development, i.e., H-1PV + bevacizumab (Figure 3). A compassionate use proof-of-concept program was conducted in five GBM patients, who developed a second or third recurrence after being treated in the ParvOryx01 trial. The patients underwent tumor resection, followed by local H-1PV administration and bevacizumab. The mean survival after treatment was extended to 15.4 months. Moreover, in three out of the five patients, striking remission of the recurrence was observed, providing first clinical hints of synergistic glioblastoma suppression through parvoviro-immunotherapy [62].

### 3.3. H-1PV + PD-1 Immune Checkpoint Inhibitors (Nivolumab)

Checkpoint blockade, a strategy which aims at overcoming immune system tolerance towards the tumor through the release from negative regulators of immune activation (immune checkpoints), is presently at the leading edge of cancer immunotherapy. Although efficient in controlling various other solid tumors, immune checkpoint inhibitors (ICIs) frequently fail to achieve a significant response in glioblastoma patients [63]. Several preclinical studies and clinical trials have therefore been initiated, in order to determine the optimal ICI-based combinations and redefine the future standards of care for this deadly disease [64].

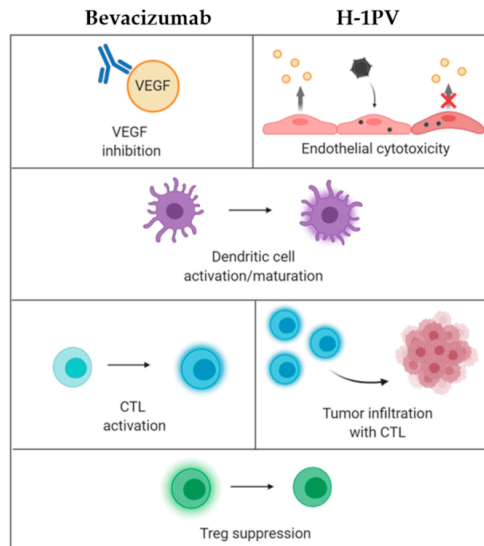


**Figure 3.** Rationale for combining H-1PV administration with bevacizumab treatment in patients with recurrent glioblastoma multiforme (GBM). Bevacizumab antibody and H-1PV infection share the capacity for inhibiting vascular endothelial growth factor (VEGF) (production) (upper row) and triggering distinct immuno-modulations (lower rows), raising hopes to improve antitumor immunity by combining both treatments. In support of this strategy, bevacizumab and H-1PV were found to jointly achieve significant clinical improvement in GBM patients at second or third recurrence, leading to remission of the recurrent tumor. The precise mechanisms of this therapeutic potentiation remain to be determined. However, the establishment by H-1PV of an immunologically “improved” proinflammatory background, which facilitates bevacizumab-mediated immuno-stimulating effects, is a likely scenario. For details and references, see the main text.

First clinical hints of improved antitumor effects of H-1PV virotherapy upon combination with checkpoint blockade were obtained through compassionate virus uses. A series of three patients with rapidly progressing recurrent glioblastoma were treated with H-1PV (two were irradiated prior to virus administration), followed by bevacizumab and the programmed cell death protein 1 (PD-1) inhibitor nivolumab. In addition, all patients received the HDACi VPA. This innovative PV-based multimodal strategy led to radiologically confirmed tumor regression accompanied by clinical improvement in all subjects 4 to 8 weeks after virus injection [65]. An objective tumor response was also seen in another group of primary or recurrent glioblastoma patients, who received H-1PV in combination with bevacizumab and checkpoint blockade. Complete to partial tumor remission was documented in 78% of the cases, which is a significantly higher response rate than the one reported in the literature for bevacizumab- and ICI-based monotherapies [66].

Altogether, the above data provide a strong impetus for further clinical development of H-1PV combinations with radiation and/or immunomodulators (in particular bevacizumab and ICIs) in the fight against glioblastoma.

#### 4. Parvovirus-Based Combinatorial Immunotherapy against Colorectal Cancer

CRC is another major cause of cancer-related deaths worldwide. Although the implementation of early-detection screening programs has substantially improved the 5-year overall survival, prognosis for CRC patients with stage 4 metastatic disease remains poor [67]. Immunotherapy, in particular checkpoint blockade, has proved efficient against

heavily mutated colorectal tumors. However, it fails to elicit sufficiently strong therapeutic responses in carcinomas, which are mismatch-repair-proficient (pMMR) and possess low levels of microsatellite instability (MSI-L). Low mutational burden, together with the lack of immune cell infiltration, contribute to pMMR-MSI-L immune resistance [68]. Novel approaches are therefore needed for the treatment of patients with advanced metastatic or low mutational burden CRC. One such approach, combinatorial immunotherapy, holds much potential for extending the scope of checkpoint blockade so as to bring benefit also to CRC patients with unfavorable prognosis.

#### *H-1PV + CTLA-4 Immune Checkpoint Blockade (Tremelimumab)*

Many tumor types, including CRC, overexpress the immune checkpoint cytotoxic T-lymphocyte-associated protein 4 (CTLA-4) and thus transmit inhibitory signals to T cells [69]. This immune evasion strategy creates an immunosuppressive environment, which allows the tumor to escape immune recognition and destruction. The anticancer effects of tremelimumab, a CTLA-4-specific human antibody, applied either alone or in combination with H-1PV, were studied by Heinrich et al. [70] in a human in vitro CRC model. H-1PV infection alone was found to reduce the viability of SW480 CRC cells and enhance extracellular CTLA-4 expression. SW480 cells and immature DCs (iDCs) co-culture experiments demonstrated that the expression of DC maturation and activation markers, namely CD83, CD80 and CD86, sharply increased when the tumor cells were infected with H-1PV. Notably, additional treatment of H-1PV-infected SW480 cells with tremelimumab resulted in IFN- $\gamma$  enrichment of the co-culture supernatant [70].

#### **5. Parvovirus-Based Combinatorial Immunotherapy against Melanoma**

Cutaneous melanoma, also known as black skin cancer, is an aggressive tumor arising from the melanocytes. Over the past 10 years, melanoma has become a prototype for testing novel targeted therapies, first and foremost, immune checkpoint blockade. PD-1 inhibition has shown significant clinical success in controlling locoregional melanoma [71]. However, metastatic melanoma is a severe life-threatening condition for which reinforcement of current treatment tools and approaches is still needed.

#### *H-1PV + CTLA-4 (Ipilimumab)/PD-1 (Nivolumab) Immune Checkpoint Blockade*

In order to investigate the immunological effects of H-1PV in combination with ipilimumab and/or nivolumab, a human ex vivo melanoma model was used by Goepfert et al. Similar to the observations made in CRC-derived cells [70], upregulation of immune checkpoints, CTLA-4, PD-1 and PD-L1 in particular, was seen in H-1PV-infected melanoma cells. Yet, the virus potentiated the capacity of melanoma cells to induce iDC maturation in co-culture experiments. Nivolumab and ipilimumab, when added to the treatment scheme, triggered a further increase in the release into the co-culture supernatant of IFN- $\gamma$  and TNF- $\alpha$ , respectively. Further to this, upon combination with H-1PV, the two ICIs induced stronger CTL activation, compared to virus alone [72]. Combining PV-induced immunogenic oncolysis with CTLA-4 and/or PD-1 blockade allows achieving a double goal, i.e., tumor cell killing and activation of the immune system against the tumor. This triggering of complementary events, centered on tumor destruction and immune-mediated elimination, renders the H-1PV + ICI approach promising for melanoma and other solid tumors' treatment.

#### **6. Conclusions**

Preclinical research and clinical experience have demonstrated the multimodal anti-cancer activity of the oncolytic parvovirus H-1PV. Two essential facets of H-1PV-induced tumor suppression consist of direct killing of malignant cells (oncolysis) and activation of cellular immune responses against the tumor. H-1PV infection, oncolysis and immune stimulation are interconnected, coordinated events, which cooperate towards multisided tumor elimination.

Glioblastoma and pancreatic adenocarcinoma are among the most devastating human malignancies, characterized by resistance to current therapies, tendency to recurrence and an overall poor outcome. H-1PV has undergone clinical testing in two recently conducted trials, ParvOryx01 in glioblastoma and ParvOryx02 in pancreatic carcinoma. Virus excellent safety and tolerability, together with the capacity for gentle TME immune landscape proinflammatory modulation, provide a strong impetus for further H-1PV clinical development. It should, however, be noted that in the clinical setting, various patient-dependent factors may result in suboptimal antitumor effects. Large intra-tumoral tissue heterogeneity, emergence of tumor cells resistant to virus infection/killing, dominance of the highly immunosuppressive TME, hampered virus spreading, off-target infection and virus neutralization by antiviral antibodies are among the major barriers to efficient H-1PV-induced tumor elimination. While various other approaches (capsid modification, chimera generation, fitness mutant selection, armed vector construction) to H-1PV treatment optimization are currently under investigation, PV-based combinatorial therapies are considered as a particularly promising avenue that holds the potential of enhancing both oncolysis and immune-mediated tumor destruction. Combinations of the virus with other anticancer approaches, namely irradiation, chemotherapy (gemcitabine), epigenetic modulation (HDACi), angiogenesis regulation (bevacizumab) or immunotherapy (immune checkpoint blockade), were evaluated in both preclinical models and in cancer patients. The combinatorial H-1PV-based viro(immuno)therapeutic strategy was proven to achieve greater anticancer effects compared to individual agents alone. The synergistic boost was particularly pronounced in combinations including the HDACi VPA, bevacizumab or the PD-1 inhibitor nivolumab. Glioblastoma patients treated with this combination showed striking tumor remission and extended survival, notably after second or even third recurrence. These early clinical observations speak in favor of considering H-1PV inclusion into various immunotherapeutic protocols against glioblastoma and other poor-prognosis solid tumors (Figure 4).

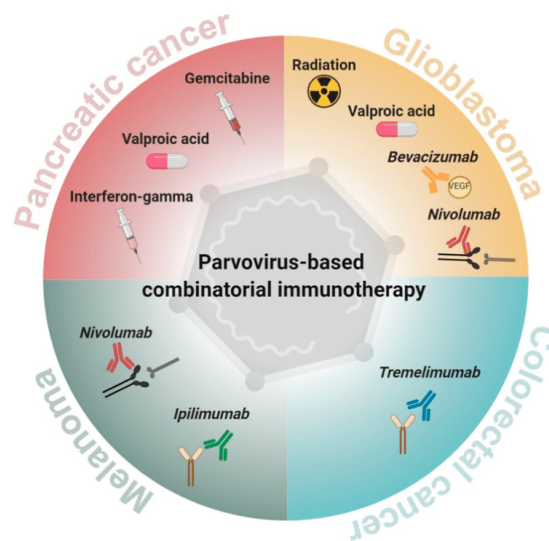


**Figure 4.** H-1PV inclusion into combinatorial anticancer immunotherapy regimens. The development of H-1PV combinations with ionizing radiation, chemotherapeutics, histone deacetylase inhibitors (HDACis), angiogenesis inhibitors and immunomodulators holds significant promise for the future of poor-prognosis solid cancer treatment.

**Author Contributions:** Writing—original draft preparation, A.A., T.F. and C.B.; writing—review and editing, A.A., J.R. and A.M. All authors have read and agreed to the published version of the manuscript.

**Funding:** The parvovirus research described in this review was partially funded by research grants from the Luxembourg Cancer Foundation and Télévie to A.M., and from ORYX GmbH & Co. KG to A.A., J.R. and A.M.

**Acknowledgments:** The authors wish to thank all members and collaborators of the former Tumor Virology Division at the German Cancer Research Center, for their contribution to the work described in this review. We are deeply indebted to the clinical trial and compassionate use program participants and their families, for their contribution to gathering clinical experience and knowledge. We are grateful to K. Geletneky for helpful discussions of the glioblastoma compassionate parvovirus use program.

**Conflicts of Interest:** A.A., T.F., J.R. and A.M. are holders of patents or patent applications related to H-1PV use for cancer therapeutic purposes. The parvovirus clinical trials (ParvOryx01, ParvOryx02) and compassionate H-1PV uses were financially supported by ORYX GmbH & Co. KG (Baldham, Germany). The funders had no role in the writing of the manuscript or in the decision to submit it for publication.

## References

- Bretscher, C.; Marchini, A. H-1 parvovirus as a cancer-killing agent: Past, present, and future. *Viruses* **2019**, *11*, 562. [[CrossRef](#)] [[PubMed](#)]
- Toolan, H.W.; Dalldore, G.; Barclay, M.; Chandra, S.; Moore, A.E. An unidentified, filtrable agent isolated from transplanted human tumors. *Proc. Natl. Acad. Sci. USA* **1960**, *46*, 1256–1258. [[CrossRef](#)] [[PubMed](#)]
- Besselsen, D.G.; Besch-Williford, C.L.; Pintel, D.J.; Franklin, C.L.; Hook, R.R.; Riley, L.K. Detection of H-1 parvovirus and Kilham rat virus by PCR. *J. Clin. Microbiol.* **1995**, *33*, 1699–1703. [[CrossRef](#)] [[PubMed](#)]
- Rommelaere, J.; Giese, N.; Cziepluch, C.; Cornelis, J.J. Parvoviruses as anticancer agents. In *Viral Therapy of Human Cancers*; Sinkovics, J.G., Horvath, J.C., Eds.; Marcel Dekker: New York, NY, USA, 2005; pp. 627–675.
- Rommelaere, J.; Geletneky, K.; Angelova, A.L.; Daeffler, L.; Dinsart, C.; Kiprianova, I.; Schlehofer, J.R.; Raykov, Z. Oncolytic parvoviruses as cancer therapeutics. *Cytokine Growth Factor Rev.* **2010**, *21*, 185–195. [[CrossRef](#)]
- Angelova, A.L.; Geletneky, K.; Nüesch, J.P.F.; Rommelaere, J. Tumor selectivity of oncolytic parvoviruses: From in vitro and animal models to cancer patients. *Front. Bioeng. Biotechnol.* **2015**, *3*, 55. [[CrossRef](#)]
- Newman, S.J.; McCallin, P.F.; Sever, J.L. Attempts to isolate H-1 virus from spontaneous human abortions: A negative report. *Teratology* **1970**, *3*, 279–281. [[CrossRef](#)]
- Toolan, H.W.; Saunders, E.L.; Southam, C.M.; Moore, A.E.; Levin, A.G. H-1 virus viremia in the human. *Exp. Biol. Med.* **1965**, *119*, 711–715. [[CrossRef](#)]
- Le Cesne, A.; Dupressoir, T.; Janin, N.; Spielmann, M.; Le Chevalier, T.; Sancho-Garnier, H.; Paoletti, C.; Rommelaere, J.; Stehelin, D.; Tursz, T.; et al. Intralesional administration of a live virus, parvovirus H1 (PVH1) in cancer patients: A feasibility study. *Proc. Am. Soc. Clin. Oncol.* **1993**, *12*, 297.
- Hartley, A.; Kavishwar, G.; Salvato, I.; Marchini, A. A roadmap for the success of oncolytic parvovirus-based anticancer therapies. *Annu. Rev. Virol.* **2020**, *7*, 537–557. [[CrossRef](#)]
- Geletneky, K.; Nüesch, J.P.; Angelova, A.L.; Kiprianova, I.; Rommelaere, J. Double-faceted mechanism of parvoviral oncosuppression. *Curr. Opin. Virol.* **2015**, *13*, 17–24. [[CrossRef](#)]
- Angelova, A.L.; Rommelaere, J. Immune System Stimulation by Oncolytic Rodent Protoparvoviruses. *Viruses* **2019**, *11*, 415. [[CrossRef](#)] [[PubMed](#)]
- Marchini, A.; Daeffler, L.; Pozdeev, V.I.; Angelova, A.; Rommelaere, J. Immune conversion of tumor microenvironment by oncolytic viruses: The protoparvovirus H-1PV case study. *Front. Immunol.* **2019**, *10*, 1848. [[CrossRef](#)] [[PubMed](#)]
- Moehler, M.; Zeidler, M.; Schede, J.; Rommelaere, J.; Galle, P.R.; Cornelis, J.J.; Heike, M. Oncolytic parvovirus H1 induces release of heat-shock protein HSP72 in susceptible human tumor cells but may not affect primary immune cells. *Cancer Gene Ther.* **2003**, *10*, 477–480. [[CrossRef](#)] [[PubMed](#)]
- Bhat, R.; Dempe, S.; Dinsart, C.; Rommelaere, J. Enhancement of NK cell antitumor responses using an oncolytic parvovirus. *Int. J. Cancer* **2010**, *128*, 908–919. [[CrossRef](#)]
- Bhat, R.; Rommelaere, J. NK-cell-dependent killing of colon carcinoma cells is mediated by natural cytotoxicity receptors (NCRs) and stimulated by parvovirus infection of target cells. *BMC Cancer* **2013**, *13*, 367. [[CrossRef](#)]
- Grekova, S.P.; Aprahamian, M.; Giese, N.; Schmitt, S.; Giese, T.; Falk, C.S.; Daeffler, L.; Cziepluch, C.; Rommelaere, J.; Raykov, Z. Immune cells participate in the oncosuppressive activity of parvovirus H-1PV and are activated as a result of their abortive infection with this agent. *Cancer Biol. Ther.* **2010**, *10*, 1280–1289. [[CrossRef](#)]

18. Moralès, O.; Richard, A.; Martin, N.; Mrizak, D.; Sénéchal, M.; Miroux, C.; Pancré, V.; Rommelaere, J.; Caillet-Fauquet, P.; De Launoit, Y.; et al. Activation of a Helper and Not Regulatory Human CD4+ T Cell Response by Oncolytic H-1 Parvovirus. *PLoS ONE* **2012**, *7*, e32197. [CrossRef]
19. Lavie, M.; Struyf, S.; Stroh-Dege, A.; Rommelaere, J.; Van Damme, J.; Dinsart, C. Capacity of wild-type and chemokine-armed parvovirus H-1PV for inhibiting neo-angiogenesis. *Virology* **2013**, *447*, 221–232. [CrossRef]
20. Felsenstein, M.; Hruban, R.H.; Wood, L.D. New developments in the molecular mechanisms of pancreatic tumorigenesis. *Adv. Anat. Pathol.* **2018**, *25*, 131–142. [CrossRef]
21. Siegel, R.L.; Mph, K.D.M.; Jemal, A. Cancer statistics, 2017. *CA A Cancer J. Clin.* **2017**, *67*, 7–30. [CrossRef]
22. Neoptolemos, J.; Kleeff, J.; Michl, P.; Costello, E.; Greenhalf, W.; Palmer, D.H. Therapeutic developments in pancreatic cancer: Current and future perspectives. *Nat. Rev. Gastroenterol. Hepatol.* **2018**, *15*, 333–348. [CrossRef] [PubMed]
23. Angelova, A.L.; Aprahamian, M.; Grekova, S.P.; Hajri, A.; Leuchs, B.; Giese, N.A.; Dinsart, C.; Herrmann, A.; Balboni, G.; Rommelaere, J.; et al. Improvement of Gemcitabine-Based Therapy of Pancreatic Carcinoma by Means of Oncolytic Parvovirus H-1PV. *Clin. Cancer Res.* **2009**, *15*, 511–519. [CrossRef] [PubMed]
24. Angelova, A.L.; Grekova, S.P.; Heller, A.; Kuhlmann, O.; Soyka, E.; Giese, T.; Aprahamian, M.; Bour, G.; Rüffer, S.; Cziepluch, C.; et al. Complementary Induction of Immunogenic Cell Death by Oncolytic Parvovirus H-1PV and Gemcitabine in Pancreatic Cancer. *J. Virol.* **2014**, *88*, 5263–5276. [CrossRef] [PubMed]
25. Plate, J.M.D.; Harris, J.E. Effects of gemcitabine treatment on immune cells and functions in pancreatic cancer patients. *Cancer Res.* **2004**, *64* (Suppl. 7), 500.
26. Plate, J.M.D.; Plate, A.E.; Shott, S.; Bograd, S.; Harris, J.E. Effect of gemcitabine on immune cells in subjects with adenocarcinoma of the pancreas. *Cancer Immunol. Immunother.* **2005**, *54*, 915–925. [CrossRef] [PubMed]
27. Lin, X.; Huang, M.; Xie, F.; Zhou, H.; Yang, J.; Huang, Q. Gemcitabine inhibits immune escape of pancreatic cancer by down regulating the soluble ULBP2 protein. *Oncotarget* **2016**, *7*, 70092–70099. [CrossRef]
28. Shevchenko, I.; Karakhanova, S.; Soltek, S.; Link, J.; Bayry, J.; Werner, J.; Umansky, V.; Bazhin, A.V. Low-dose gemcitabine depletes regulatory T cells and improves survival in the orthotopic Panc02 model of pancreatic cancer. *Int. J. Cancer* **2013**, *133*, 98–107. [CrossRef] [PubMed]
29. Homma, Y.; Taniguchi, K.; Nakazawa, M.; Matsuyama, R.; Mori, R.; Takeda, K.; Ichikawa, Y.; Tanaka, K.; Endo, I. Changes in the immune cell population and cell proliferation in peripheral blood after gemcitabine-based chemotherapy for pancreatic cancer. *Clin. Transl. Oncol.* **2014**, *16*, 330–335. [CrossRef]
30. Gujar, S.A.; Clements, D.A.; Dielschneider, R.; Helson, E.; Marcato, P.S.; Lee, P.W. Gemcitabine enhances the efficacy of reovirus-based oncotherapy through anti-tumour immunological mechanisms. *Br. J. Cancer* **2014**, *110*, 83–93. [CrossRef]
31. Hajda, J.; Lehmann, M.; Krebs, O.; Kieser, M.; Geletneký, K.; Jäger, D.; Dahm, M.; Huber, B.; Schöning, T.; Sedlacek, O.; et al. A non-controlled, single arm, open label, phase II study of intravenous and intratumoral administration of ParvOryx in patients with metastatic, inoperable pancreatic cancer: ParvOryx02 protocol. *BMC Cancer* **2017**, *17*, 1–11. [CrossRef]
32. ParvOryx02: A Phase II Trial of Intravenous and Intratumoral Administration of H-1 Parvovirus in Patients with Metastatic Pancreatic Cancer. Available online: [http://oryx-medicine.com/fileadmin/user\\_upload/uploads/News/Publications/201910\\_JOVC\\_Ungerechts\\_ParvOryx02.pdf](http://oryx-medicine.com/fileadmin/user_upload/uploads/News/Publications/201910_JOVC_Ungerechts_ParvOryx02.pdf) (accessed on 16 November 2020).
33. Li, J.; Bonifati, S.; Hristov, G.; Marttila, T.; Valmary-Degano, S.; Stanzel, S.; Schnölzer, M.; Mougín, C.; Aprahamian, M.; Grekova, S.P.; et al. Synergistic combination of valproic acid and oncolytic parvovirus H-1 PV as a potential therapy against cervical and pancreatic carcinomas. *EMBO Mol. Med.* **2013**, *5*, 1537–1555. [CrossRef] [PubMed]
34. Minucci, S.; Pelicci, P.G. Histone deacetylase inhibitors and the promise of epigenetic (and more) treatments for cancer. *Nat. Rev. Cancer* **2006**, *6*, 38–51. [CrossRef] [PubMed]
35. Alvarez-Breckenridge, C.A.; Yu, J.; Price, R.L.; Wei, M.; Wang, Y.; Nowicki, M.O.; Ha, Y.P.; Bergin, S.M.; Hwang, C.; Fernandez, S.A.; et al. The histone deacetylase inhibitor valproic acid lessens NK cell action against oncolytic virus-infected glioblastoma cells by inhibition of STAT5/T-BET signaling and generation of gamma interferon. *J. Virol.* **2012**, *86*, 4566–4577. [CrossRef] [PubMed]
36. Otsuki, A.; Patel, A.; Kasai, K.; Suzuki, M.; Kurozumi, K.; Chiocca, E.A.; Saeki, Y. Histone Deacetylase Inhibitors Augment Antitumor Efficacy of Herpes-based Oncolytic Viruses. *Mol. Ther.* **2008**, *16*, 1546–1555. [CrossRef]
37. VanOosten, R.L.; Earel, J.K., Jr.; Griffith, T.S. Histone deacetylase inhibitors enhance Ad5-TRAIL killing of TRAIL-resistant prostate tumor cells through increased caspase-2 activity. *Apoptosis* **2006**, *12*, 561–571. [CrossRef]
38. Marchini, A.; Scott, E.M.; Rommelaere, J. Overcoming barriers in oncolytic virotherapy with HDAC inhibitors and immune checkpoint blockade. *Viruses* **2016**, *8*, 9. [CrossRef]
39. Xie, Z.; Ago, Y.; Okada, N.; Tachibana, M. Valproic acid attenuates immunosuppressive function of myeloid-derived suppressor cells. *J. Pharmacol. Sci.* **2018**, *137*, 359–365. [CrossRef]
40. Armeanu, S.; Bitzer, M.; Lauer, U.M.; Venturelli, S.; Pathil, A.; Krusch, M.; Kaiser, S.; Jobst, J.; Smirnow, I.; Wagner, A.; et al. Natural Killer Cell-Mediated Lysis of Hepatoma Cells via Specific Induction of NKG2D Ligands by the Histone Deacetylase Inhibitor Sodium Valproate. *Cancer Res.* **2005**, *65*, 6321–6329. [CrossRef]
41. Lugrin, J.; Ding, X.C.; Le Roy, D.; Chanson, A.-L.; Sweep, F.C.; Calandra, T.; Roger, T. Histone deacetylase inhibitors repress macrophage migration inhibitory factor (MIF) expression by targeting MIF gene transcription through a local chromatin deacetylation. *Biochim. Biophys. Acta BBA Bioenerg.* **2009**, *1793*, 1749–1758. [CrossRef]

42. Grekova, S.P.; Aprahamian, M.; Daeffler, L.; Leuchs, B.; Angelova, A.; Giese, T.; Galabov, A.; Heller, A.; Giese, N.A.; Rommelaere, J.; et al. Interferon  $\gamma$  improves the vaccination potential of oncolytic parvovirus H-1PV for the treatment of peritoneal carcinomatosis in pancreatic cancer. *Cancer Biol. Ther.* **2011**, *12*, 888–895. [[CrossRef](#)]
43. Ostrom, Q.T.; Gittleman, H.; Truitt, G.; Boscia, A.; Kruchko, C.; Barnholtz-Sloan, J.S. CBTRUS statistical report: Primary brain and other central nervous system tumors diagnosed in the United States in 2011–2015. *Neuro Oncol.* **2018**, *20*, iv1–iv86. [[CrossRef](#)] [[PubMed](#)]
44. Xu, Y.-Y.; Gao, P.; Sun, Y.; Duan, Y. Development of targeted therapies in treatment of glioblastoma. *Cancer Biol. Med.* **2015**, *12*, 223–237. [[PubMed](#)]
45. Davis, M.E. Glioblastoma: Overview of Disease and Treatment. *Clin. J. Oncol. Nurs.* **2016**, *20*, S2–S8. [[CrossRef](#)] [[PubMed](#)]
46. Gallego, O. Nonsurgical treatment of recurrent glioblastoma. *Curr. Oncol.* **2015**, *22*, 273–281. [[CrossRef](#)] [[PubMed](#)]
47. Di Piazza, M.; Mader, C.; Geletneky, K.; Calle, M.H.Y.; Weber, E.; Schlehofer, J.; Deleu, L.; Rommelaere, J. Cytosolic Activation of cathepsins mediates parvovirus H-1-induced killing of cisplatin and trail-resistant glioma cells. *J. Virol.* **2007**, *81*, 4186–4198. [[CrossRef](#)]
48. Geletneky, K.; Kiprianova, I.; Ayache, A.; Koch, R.; Herrero y Calle, M.; Deleu, L.; Sommer, C.; Thomas, N.; Rommelaere, J.; Schlehofer, J.R. Regression of advanced rat and human gliomas by local or systemic treatment with oncolytic parvovirus H-1 in rat models. *Neuro Oncol.* **2010**, *12*, 804–814. [[CrossRef](#)]
49. Kiprianova, I.; Thomas, N.; Ayache, A.; Fischer, M.; Leuchs, B.; Klein, M.; Rommelaere, J.; Schlehofer, J.R. Regression of glioma in rat models by intranasal application of parvovirus H-1. *Clin. Cancer Res.* **2011**, *17*, 5333–5342. [[CrossRef](#)]
50. Geletneky, K.; Hajda, J.; Angelova, A.L.; Leuchs, B.; Capper, D.; Bartsch, A.J.; Neumann, J.-O.; Schöning, T.; Hüsing, J.; Beelte, B.; et al. Oncolytic H-1 parvovirus shows safety and signs of immunogenic activity in a first phase I/IIa glioblastoma trial. *Mol. Ther.* **2017**, *25*, 2620–2634. [[CrossRef](#)]
51. Angelova, A.L.; Barf, M.; Geletneky, K.; Unterberg, A.; Rommelaere, J. Immunotherapeutic potential of oncolytic H-1 parvovirus: Hints of glioblastoma microenvironment conversion towards immunogenicity. *Viruses* **2017**, *9*, 382. [[CrossRef](#)]
52. Chonan, M.; Saito, R.; Shoji, T.; Shibahara, I.; Kanamori, M.; Sonoda, Y.; Watanabe, M.; Kikuchi, T.; Ishii, N.; Tominaga, T. CD40/CD40L expression correlates with the survival of patients with glioblastomas and an augmentation in CD40 signaling enhances the efficacy of vaccinations against glioma models. *Neuro Oncol.* **2015**, *17*, 1453–1462. [[CrossRef](#)]
53. Geletneky, K.; Hartkopf, A.D.; Krempien, R.; Rommelaere, J.; Schlehofer, J.R. Improved killing of human high-grade glioma cells by combining ionizing radiation with oncolytic parvovirus H-1 infection. *J. Biomed. Biotechnol.* **2010**, *2010*, 1–9. [[CrossRef](#)] [[PubMed](#)]
54. Slone, H.B.; Peters, L.J.; Milas, L. Effect of host immune capability on radiocurability and subsequent transplantability of a murine fibrosarcoma. *J. Natl. Cancer Inst.* **1979**, *63*, 1229–1235. [[CrossRef](#)]
55. Reynders, K.; Illidge, T.; Siva, S.; Chang, J.Y.; De Ruyscher, D. The abscopal effect of local radiotherapy: Using immunotherapy to make a rare event clinically relevant. *Cancer Treat. Rev.* **2015**, *41*, 503–510. [[CrossRef](#)] [[PubMed](#)]
56. Van Limbergen, E.J.; De Ruyscher, D.K.; Pimentel, V.O.; Marcus, D.; Berbee, M.; Hoeben, A.; Rekers, N.H.; Theys, J.; Yaromina, A.; Dubois, L.J.; et al. Combining radiotherapy with immunotherapy: The past, the present and the future. *Br. J. Radiol.* **2017**, *90*, 20170157. [[CrossRef](#)]
57. Zhao, X.; Shao, C. Radiotherapy-Mediated Immunomodulation and Anti-Tumor Abscopal Effect Combining Immune Checkpoint Blockade. *Cancers* **2020**, *12*, 2762. [[CrossRef](#)]
58. Toucheffu, Y.; Vassaux, G.; Harrington, K.J. Oncolytic viruses in radiation oncology. *Radiother. Oncol.* **2011**, *99*, 262–270. [[CrossRef](#)]
59. Garcia, J.; Hurwitz, H.I.; Sandler, A.B.; Miles, D.; Coleman, R.L.; Deurloo, R.; Chinot, O.L. Bevacizumab (Avastin®) in cancer treatment: A review of 15 years of clinical experience and future outlook. *Cancer Treat. Rev.* **2020**, *86*, 102017. [[CrossRef](#)]
60. Gilbert, M.R.; Dignam, J.J.; Armstrong, T.S.; Wefel, J.S.; Blumenthal, D.T.; Vogelbaum, M.A.; Colman, H.; Chakravarti, A.; Pugh, S.; Won, M.; et al. A randomized trial of bevacizumab for newly diagnosed glioblastoma. *N. Engl. J. Med.* **2014**, *370*, 699–708. [[CrossRef](#)]
61. Brown, N.F.; Carter, T.J.; Ottaviani, D.; Mulholland, P. Harnessing the immune system in glioblastoma. *Br. J. Cancer* **2018**, *119*, 1171–1181. [[CrossRef](#)]
62. Geletneky, K.; Angelova, A.; Leuchs, B.; Bartsch, A.; Capper, D.; Hajda, J.; Rommelaere, J. ATNT-07. Favorable response of patients with glioblastoma at second or third recurrence to repeated injection of oncolytic parvovirus H-1 in combination with bevacicumab. *Neuro Oncol.* **2015**, *17*, v11. [[CrossRef](#)]
63. Reardon, D.A.; Omuro, A.; Brandes, A.A.; Rieger, J.; Wick, A.; Sepulveda, J.; Phuphanich, S.; De Souza, P.; Ahluwalia, M.S.; Lim, M.; et al. OS10.3 randomized phase 3 study evaluating the efficacy and safety of nivolumab vs bevacizumab in patients with recurrent glioblastoma: CheckMate 143. *Neuro Oncol.* **2017**, *19*, iii21. [[CrossRef](#)]
64. Desai, K.; Hubben, A.; Ahluwalia, M. The role of checkpoint inhibitors in glioblastoma. *Target. Oncol.* **2019**, *14*, 375–394. [[CrossRef](#)] [[PubMed](#)]
65. Geletneky, K.; Weiss, C.; Bernhard, H.; Capper, D.; Leuchs, B.; Marchini, A.; Rommelaere, J. ATIM-29. First clinical observation of improved anti-tumor effects of viro-immunotherapy with oncolytic parvovirus H-1 in combination with PD-1 checkpoint blockade and bevacicumab in patients with recurrent glioblastoma. *Neuro Oncol.* **2016**, *18*, vi24. [[CrossRef](#)]

66. Geletneký, K.; Bartsch, A.; Weiss, C.; Bernhard, H.; Marchini, A.; Rommelaere, J. ATIM-40. High rate of objective anti-tumor response in 9 patients with glioblastoma after viro-immunotherapy with oncolytic parvovirus H-1 in combination with bevacicunab and PD-1 checkpoint blockade. *Neuro Oncol.* **2018**, *20*, vi10. [[CrossRef](#)]
67. Siegel, R.L.; DeSantis, C.; Jemal, A. Colorectal cancer statistics, 2014. *CA A Cancer J. Clin.* **2014**, *64*, 104–117. [[CrossRef](#)]
68. Le, D.T.; Durham, J.N.; Smith, K.N.; Wang, H.; Bartlett, B.R.; Aulakh, L.K.; Lu, S.; Kemberling, H.; Wilt, C.; Lubner, B.S.; et al. Mismatch repair deficiency predicts response of solid tumors to PD-1 blockade. *Science* **2017**, *357*, 409–413. [[CrossRef](#)]
69. Mazzolini, G. Immunotherapy and immunoescape in colorectal cancer. *World J. Gastroenterol.* **2007**, *13*, 5822–5831. [[CrossRef](#)]
70. Heinrich, B.; Goepfert, K.; Delic, M.; Galle, P.R.; Moehler, M. Influence of the oncolytic parvovirus H-1, CTLA-4 antibody tremelimumab and cytostatic drugs on the human immune system in a human in vitro model of colorectal cancer cells. *OncoTargets Ther.* **2013**, *6*, 1119–1127. [[CrossRef](#)]
71. Huang, A.C.; Orlovski, R.J.; Xu, X.; Mick, R.; George, S.M.; Yan, P.K.; Manne, S.; Kraya, A.A.; Wubbenhorst, B.; Dorfman, L.; et al. A single dose of neoadjuvant PD-1 blockade predicts clinical outcomes in resectable melanoma. *Nat. Med.* **2019**, *25*, 454–461. [[CrossRef](#)]
72. Goepfert, K.; Dinsart, C.; Rommelaere, J.; Foerster, F.; Moehler, M. Rational combination of parvovirus h1 with ctla-4 and pd-1 checkpoint inhibitors dampens the tumor induced immune silencing. *Front. Oncol.* **2019**, *9*, 425. [[CrossRef](#)]